VNIVER$ITAT ĞͰ VALÈNCIA

Test del Modelo Estándar
a energías bajas

Martín González Alonso

IFIC, Departamento de Física Teórica

Tesis doctoral, Julio 2010

Director de tesis:
Antonio Pich

ANTONIO PICH ZARDOYA, Catedrático del Departamento de Física Teórica de la Universitat de València,

CERTIFICA:

Que la presente memoria "TEST DEL MODELO ESTÁNDAR A ENER-GÍAS BAJAS" ha sido realizada bajo su dirección en el Departamento de Física Teórica de la Universitat de València, por MARTÍN GONZÁLEZ ALONSO y constituye su Tesis para optar al grado de Doctor en Física.

Y para que así conste, en cumplimiento de la legislación vigente, presenta en el Departamento de Física Teórica de la Universitat de València la referida Tesis Doctoral, y firma el presente certificado.

Valencia, a 18 de Mayo de 2010.

Antonio Pich Zardoya

To Luz María, of course.

Contents

Introducción

La física de partículas está sin lugar a dudas en un momento histórico. Casi cuarenta años después de que se formularan las bases teóricas del llamado Modelo Estándar de las interacciones electrodébiles y fuertes, estamos a punto de dar un paso más y ver qué nos tiene reservado la Naturaleza. Nuevas simetrías, nuevas interacciones o incluso nuevas dimensiones podrían ser descubiertas en los próximos años.

Este paso adelante en nuestra comprensión del mundo microscópico es un proyecto que involucra a toda la comunidad de física de altas energías. Será el resultado de años de duro trabajo llevado a cabo por nuestros compañeros experimentales en el Gran Colisionador de Hadrones (LHC) en el CERN, construyendo el más potente acelerador de partículas, que ha comenzado a funcionar hace tan solo unos meses. Y no sólo en el LHC sino también en otras increíbles instalaciones experimentales, como laboratorios subterráneos o detectores instalados en satélites. Será el producto de décadas de trabajo teórico, aprendiendo a realizar cálculos precisos dentro del Modelo Estándar, absolutamente necesarios para desentrañar la eventual señal de Nueva Física de entre los millones y millones de datos que se recogerán, y también el resultado del trabajo de todos esos físicos teóricos que decidieron no esperar la información experimental y ya han explorado todo tipo de posibles escenarios de Nueva Física.

El primer objetivo de este proyecto global es encontrar una explicación dinámica de las masas de las partículas, o lo que es lo mismo, averiguar cuál es mecanismo que rompe la simetría electrodébil. De acuerdo con el Modelo Estándar, el responsable es un campo escalar conocido como campo de Higgs. Si esta descripción es correcta, las medidas experimentales realizadas hasta la fecha nos dicen que la partícula de Higgs estaba sólo un poco más allá del alcance de LEP y que será encontrada en el LHC tras algunos años de colisiones y análisis de datos. Diversas alternativas a este sencillo mecanismo han sido propuestas, aunque todas ellas presentan algún defecto que no las hace convincentes. Huelga decir que tanto el descubrimiento del bosón de Higgs estándar como de cualquier mecanismo alternativo representará un descubrimiento de enorme importancia en la historia de la física de partículas. Se tratará de la última pieza del Modelo Estándar o de la primera pieza del próximo paradigma teórico.

En el supuesto caso en el que el bosón de Higgs sea encontrado, uno debe preguntarse por qué el Modelo Estándar no puede ser la descripción final del mundo microscópico. No puede serlo esencialmente por las mismas razones por las que la tabla periódica de Mendeleev no podía ser toda la historia: porque hay hechos expe-

rimentales que el actual modelo no puede responder (la simetría materia-antimateria, qué partícula constituye la materia oscura, la explicación de la energía oscura, la gravedad cuántica, las masas de los neutrinos, ...) y porque incluso en el sector en el que el las predicciones del modelo se ajustan perfectamente a los datos, la filosofía de la ciencia nos obliga a buscar un modelo más simple (¿por qué tres generaciones de partículas? ¿por qué estas masas para las partículas? ¿por qué hay tres constantes de acoplo? etc.).

Pero aún así, incluso tras esta respuesta afirmativa, uno debe hacerse la pregunta concreta de por qué el actual Modelo Estándar de la Física de Partículas debe fallar en la descripción de los datos experimentales que serán medidos *en la próxima generación de experimentos*. La respuesta es que podría no fallar. Pero en cierto sentido esto sería un gran descubrimiento, porque implicaría que no hemos comprendido algo profundo sobre la Teoría Cuántica de Campos, el marco teórico que describe el mundo microscópico, donde los efectos cuánticos y relativistas están presentes. El escenario conocido como "gran desierto" donde sólo un Higgs ligero es observado y nada nuevo se encuentra en el rango del teraelectronvoltio (TeV) genera con total seguridad más preguntas que respuestas.

Como ya hemos señalado, la carrera para descubrir la Nueva Física no está monopolizada por el LHC, sino que hay por todo el mundo otros experimentos tremendamente sofisticados que escudriñarán direcciones en las que el LHC es completamente ciego. Es realmente increíble que midiendo por ejemplo kaones y piones en experimentos donde la energía de las partículas es mucho más pequeña que en el Tevatrón o el LHC, uno sea sensible a escalas mucho más altas que el TeV. Este hecho anti-intuitivo es en parte sólo otra consecuencia de las propiedades cuánticas del mundo microscópico que estamos explorando, y donde las partículas de gran masa (aún por descubrir) contribuyen a procesos de energías bajas a través de correcciones cuánticas. De este tipo de experimentos hemos aprendido en las últimas décadas que la estructura de sabor de la nueva teoría que reemplazará al Modelo Estándar es altamente no genérica, hecho que permanece sin explicación por el momento. La próxima generación de experimentos en el sector de sabor (las llamadas fábricas de B's, los experimentos con kaones, ...) alcanzarán sensibilidades sin precedentes y por tanto explorarán energías aún más altas.

Esta interacción entre experimentos de energías altas y bajas es absolutamente necesaria y va más allá de la primera observación de una señal de Nueva Física. En la probable situación donde la primera discrepancia con el Modelo Estándar aparezca en el LHC, será muy difícil interpretar esta señal y discernir entre la enorme cantidad de posibles modelos teóricos, principalmente debido al hecho de que el LHC es un colisionador de hadrones, donde los efectos de la interacción fuerte son omnipresentes. La complementariedad con otros experimentos será crucial en la comprensión de la estructura completa de la nueva teoría.

El esfuerzo hecho por la comunidad científica en todo el mundo ha sido enorme y hay mucho en juego. Las apuestas están ya hechas, aunque como siempre en la ciencia, la Naturaleza tendrá la última palabra.

En esta tesis doctoral abordaremos dos aspectos diferentes de la parte teórica

de este gran proyecto. Por una parte trataremos con las interacciones fuertes y con su naturaleza no-perturbativa, un marco teórico extremadamente complejo que representa el mayor obstáculo hoy día en la obtención de predicciones precisas para los distintos observables. Por otra parte, iremos más allá del Modelo Estándar y analizaremos el impacto fenomenológico de la Nueva Física en los observables de energías bajas (procesos con kaones, física del tau, desintegración del neutrón, ...) donde la precisión experimental es tan alta que pueden extraerse fuertes cotas. A continuación desarrollamos estos dos puntos.

El Modelo Estándar: cuando predecir es el reto

Realizar cálculos precisos en el Modelo Estándar no es una tarea fácil en absoluto. La Teoría Cuántica de Campos, el lenguaje matemático en el que las leyes de las física de partículas están escritas, es una teoría tremendamente complicada y la extracción de soluciones precisas a las ecuaciones es literalmente un reto para la comunidad de físicos teóricos. Los métodos perturbativos disponibles en el sector electrodébil del Modelo Estándar pierden su validez en la descripción del mundo hadrónico de energías bajas, y nos vemos obligados a buscar herramientas alternativas.

En las últimas décadas diversas propuestas se han aplicado con éxito para mejorar nuestra capacidad para realizar cálculos teóricos en el sector hadrónico (Teoría de Perturbaciones Quirales, Reglas de Suma de QCD, ...), mientras que al mismo tiempo el estudio de las ecuaciones de la teoría formulada en el retículo (*lattice* QCD) y su solución numérica se ha desarrollado considerablemente, y para muchas cantidades es ya la fuente de información más precisa.

Lattice QCD es una disciplina muy prometedora y en el futuro, los métodos analíticos alternativos podrían no ser capaces de competir con ella. Uno podría ingenuamente pensar por tanto que la mejor estrategia es sentarse y esperar el desarrollo de los cálculos en el retículo, y olvidarse de los enfoques analíticos. Pero por una parte hay que tener en cuenta que hay observables para los que los cálculos en el retículo están muy lejos de ser competitivos y el avance científico no puede simplemente congelarse durante décadas. Por otra parte, *lattice* QCD es una disciplina en pleno desarrollo y necesita de los enfoques alternativos para comprobar sus resultados y detectar posibles errores sistemáticos. Es más, la combinación de *lattice* QCD con la Teoría de Perturbaciones Quirales es de crucial importancia desde un punto de vista práctico, ya que permite trabajar con masas de quarks no físicas y extrapolar los resultados a los valores físicos, lo que es muy útil para reducir el tiempo de cálculo necesario.

Nos centraremos en esta tesis en las llamadas Reglas de Suma de QCD, que representan un método analítico para trabajar con las interacciones fuertes. Este método ha sido muy útil desde su formulación a finales de los setenta, pero tal y como veremos hay aspectos teóricos que aún merecen un cuidadoso estudio. Formularemos el método desde sus principios básicos, analizando con visión crítica los diversos elementos e incertidumbres asociadas, para posteriormente aplicarlo en la

determinación de diversos parámetros a partir de los datos de las desintegraciones hadrónicas del leptón τ, medidos principalmente por las Colaboraciones ALEPH y OPAL en el CERN.

En la parte final de la tesis iremos más allá de la desintegración del leptón τ y repasaremos el estado actual de las diferentes determinaciones de los elementos V_{ud} y V_{us} de la matriz de Cabibbo-Kobayashi-Maskawa (CKM), lo que nos conducirá al estudio de las desintegraciones semileptónicas de kaones y piones, de la desintegración del muón y de los procesos nucleares. En estas extracciones, veremos la interacción y la complementariedad de los distintos enfoques. Necesitaremos la Teoría de Perturbaciones Quiral para realizar cálculos teóricos con kaones y piones, cálculos perturbativos con varios loops para tener en cuenta los efectos electrodébiles y *lattice* QCD para extraer el valor de ciertos parámetros hadrónicos.

Más allá de las leyes conocidas: buscando en la oscuridad

Desde la misma formulación del Modelo Estándar a finales de los años sesenta y principio de los setenta, los físicos teóricos han intentado encontrar una extensión convincente de él (o una alternativa), que pudiera explicar al menos algunas de las cuestiones todavía no resueltas. El espectro de posibilidades es enorme, desde pequeñas extensiones del Modelo Estándar donde sólo una partícula es añadida (como por ejemplo el axión, asociado al problema con la simetría CP en las interacciones fuertes) hasta teorías tremendamente ambiciosas que pretenden unificar no sólo las interacciones electrodébiles y fuertes, sino también la gravedad, como por ejemplo la teoría de cuerdas.

Quizás podemos señalar supersimetría como la extensión más popular, que siguiendo el camino de los avances teóricos que desembocaron en el Modelo Estándar usa la simetría como referente. Supersimetría sería una nueva simetría de la Naturaleza, que relaciona bosones y fermiones y que conlleva la existencia de un super-compañero por cada partícula conocida. Al igual que ocurre con la simetría electrodébil, tiene que existir un mecanismo que la rompe a una energía muy alta para que las masas de estas super-partículas queden por encima de los límites experimentales actuales. Esta teoría representa una extensión del Modelo Estándar muy atractiva desde un punto de vista teórico y además parece encajar de manera natural en el contexto de la teoría de cuerdas (de hecho fue formulada por primera vez en este marco) y podría resolver diversos problemas, como por ejemplo la existencia de un candidato para la materia oscura (la partícula supersimétrica más ligera). En cualquier caso, la motivación original y principal de supersimetría fue la solución al problema de la jerarquía, ya que las contribuciones cuánticas de las super-partículas pueden cancelar las contribuciones de sus partículas compañeras, estabilizando la masa del bosón de Higgs. De esta manera sería posible tener un campo escalar fundamental con una masa que no necesita un ajuste no-natural de su valor (*fine-tuning*). Esta búsqueda de *naturalidad* ha sido la principal fuente de inspiración para los teóricos

en la búsqueda de posibles extensiones del Modelo Estándar. Sin embargo, las medidas realizadas por LEP en el CERN y por otros experimentos de gran precisión han arrinconado las teorías supersimétricas hasta una posición no-natural, donde algún tipo de *fine-tuning* parece inevitable. De esta forma, la principal motivación para la teoría parece haberse casi desvanecido.

Esto ha incentivado la exploración de otras posibles soluciones y nos ha conducido a nuevos escenarios, algunos de ellos realmente exóticos e interesantes, con dimensiones adicionales de tamaño macroscópico y pequeños agujeros negros en el LHC. También ha provocado un renovado interés por antiguas teorías alternativas, como por ejemplo technicolor, donde la simetría electrodébil está rota por una nueva dinámica fuertemente acoplada *à la* QCD. En cualquier caso, las investigaciones realizadas hasta la fecha parecen indicar que todas las posibilidades requieren *fine-tuning* en alguna medida.

Existe una perspectiva alternativa que puede seguirse en el estudio de la Nueva Física, basada en el concepto de Teorías de Campos Efectivas. Esta metodología no escoge ningún modelo en particular sino que parte tan solo de un contenido de partículas a energías bajas y de unas ciertas simetrías de la teoría, lo cual permite un estudio casi independiente del modelo. Por tanto, en este enfoque el Modelo Estándar representa una buena descripción de la Naturaleza hasta una cierta escala de energías que es muy superior a la masa de la partícula estándar más pesada (quark top o bosón de Higgs), salvo por ciertas correcciones que pueden ser parametrizadas en términos de operadores de dimensiones más altas.

De esta forma es posible analizar la información experimental disponible en un marco teórico general y concluir qué operadores están más o menos suprimidos. Los resultados de este análisis indicarán qué experimentos pueden ser interesantes para estudiar aquellos operadores menos acotados y qué experimentos son en cierto sentido redundantes ya que explorarían regiones que ya han sido excluidas por otras medidas.

La interacción de estos estudios independientes del modelo y de los análisis realizados dentro de una extensión concreta del Modelo Estándar es muy necesaria. El primer enfoque puede indicar nuevas direcciones que no están acotadas por los datos y estimular nuevas ideas entre los teóricos para la construcción de modelos, mientras que el segundo es necesario para evitar trabajar con un número infinito de parámetros y también para indicar posibles canales de detección directa de las nuevas partículas.

En la segunda parte de esta tesis seguiremos este análisis independiente del modelo de Nueva Física, repasando la derivación del Lagrangiano más general compatible con la conservación del número leptónico y bariónico, que fue realizada hace ya más de veinte años, y donde el Modelo Estándar es el término dominante y la Nueva Física a la escala del teraelectronvoltio aparece como una corrección. Aplicaremos este marco teórico al estudio de la desintegración del muón y de las desintegraciones semileptónicas de los quarks ligeros, poniendo las bases para un análisis sistemático de los efectos de Nueva Física en los procesos de energías bajas, y manteniendo pleno contacto con la física del TeV. De esta forma puede evaluarse, en un marco

general que no prioriza ningún modelo concreto de Nueva Física, la relevancia de las medidas experimentales de energías bajas para la restricción de las extensiones del Modelo Estándar.

Más concretamente analizaremos con gran detalle los test de unitariedad de la primera fila de la matriz CKM, y mostraremos como la enorme precisión alcanzada tanto a nivel experimental como teórico en los observables asociados pone esta cota al mismo nivel de relevancia que aquellas que vienen de colisionadores u otras medidas electrodébiles de gran precisión.

De esta forma, comprobaremos de manera explícita cómo los experimentos de bajas energías exploran regiones de la física desconocidas hasta hoy, aportando una información de gran valor sobre la estructura de la nueva teoría que reemplazará al Modelo Estándar. Por lo tanto, estos experimentos podrían adelantarse al LHC y ser los primeros en encontrar una señal experimental que no pueda explicarse sin dar un paso más allá de las leyes conocidas. Tras décadas de enorme trabajo teórico y experimental, este capítulo de la historia de la física de partículas se encuentra en su momento más álgido y ya sólo nos queda esperar.

Chapter 1

The New Physics Quest

The real benefit of science is to know, deep inside,
that you are following the narrow path which has
lead humanity out of the dark ages, and which might
make us reach goals which are unthinkable now.
T. Dorigo

Particle physics is certainly living a historical moment. Almost forty years after the foundation of the theoretical basis of the so-called Standard Model (SM) of electroweak and strong interactions we are about to go one step beyond it and see what Nature has in store for us. New symmetries, new interactions or even new dimensions can be just around the corner.

This step beyond our current understanding of the microscopic world is an enterprise of the whole high-energy physics community. It will be the result of years of hard work performed by our experimental colleagues at the Large Hadron Collider (LHC) at CERN, building the most powerful particle accelerator, that has just started to operate, and also at other amazing experimental facilities, like underground laboratories or detectors assembled in satellites. It will be the product of decades of theoretical work, learning to perform precise calculations within the Standard Model, absolutely necessary to disentangle the eventual New Physics (NP) signals from billions and billions of data, and also the result of the work of all those theoreticians that could not wait for the experimental information and have already explored all kinds of possible New Physics scenarios.

The first goal of this global enterprise is to find a dynamical explanation of the particle masses, that is, to find out which is exactly the mechanism that breaks the electroweak symmetry. According to the Standard Model, a scalar field known as Higgs field is responsible for it. If this description is right the data collected so far in different experiments tell us that the Higgs particle was just a bit beyond the LEP reach and that it will be found at the LHC, after some years of collisions and data analysis. Different alternatives to this simple mechanism for the origin of mass have been proposed, although none of them is free of flaws. Needless to say that both the discovery of the standard Higgs boson or of any alternative mechanism would

represent a major discovery in the history of particle physics. It would be either the final piece of the Standard Model or the first piece of the next theoretical paradigm.

Assuming the Higgs boson is found, one must wonder why the Standard Model cannot be the final description of the microscopic world. Essentially for the same reasons that the Mendeleev periodic table could not be the whole story: because there are some experimental facts that the current model cannot answer (matter-antimatter asymmetry, dark matter constituent, dark energy explanation, quantum gravity, neutrino masses ...) and because even in the sector where the model fits perfectly the data the philosophy of science forces us to search a more simple model (why 3 generations? why these values for the masses? why three coupling constants? etc.).

But still, even with this affirmative answer, one must ask the precise question of why the current Standard Model of Particle Physics must fail in the description of the data collected *in the next generation of experiments*. Well, the answer is that it might not fail. But in a certain sense this would be a huge discovery, since it would mean that we have not understood something deep about Quantum Field Theory, the theoretical framework that describes the microscopic world, where the quantum and relativistic effects are present. The scenario known as "big desert" where only a light Higgs particle is observed and nothing new is found in the TeV range would certainly provide more questions than answers.

As we have already pointed out, the race for the discovery of New Physics is not an LHC monopoly. There are other very sophisticated experiments all around the world looking at corners where the LHC is absolutely blind. It is really amazing that measuring for example kaons and pions in experiments where the energy of the particles is very much smaller than in Tevatron or the LHC, one is sensitive to energy scales beyond the TeV range. This counterintuitive fact is in part just another consequence of the quantum properties of the microscopic world that we are exploring, and where the heavy particles (still to be discovered) contribute to low-energy process through quantum corrections. From these kind of experiments we have learned in the last decades that the flavor structure of the new theory that supersedes the Standard Model is highly non-generic, something that remains unexplained so far. The next generation of experiments in the flavor sector (B factories, kaon experiments, ...) will achieve unprecedented sensitivities and therefore will explore even higher energy scales.

This interplay between low- and high-energy experiments is absolutely necessary and goes beyond the first observation of a New Physics signal. In the probable scenario where the first discrepancy with the SM appears at the LHC, it will be very difficult to interpret this signal and to distinguish among the plethora of possible theoretical models, essentially due to the fact the LHC is a hadron collider, where the strong interaction effects are omnipresent. The complementarity with other experiments will be crucial in the comprehension of the complete structure of the new theory.

The effort made by the scientific community all over the world has been enormous. The stakes are quite high. As always in science, Nature will have the final

word.

In this PhD thesis we address two different aspects of the theoretical part of this enterprise. On one hand we will deal with the strong interactions and their non-perturbative nature, an extremely difficult theoretical framework that represents the main obstacle nowadays for obtaining precise predictions for the different observables in the Standard Model. On the other hand we will take a look at the physics that can lie beyond it, and its phenomenological impact on low-energy processes (kaon processes, tau physics, neutron decay, ...), where the experimental accuracy is so high that very strong bounds can be obtained. Now we develop these two points.

1.1 The Standard Model: when predicting is the challenge

Performing accurate calculations within the Standard Model is not an easy task at all. Quantum Field Theory, the mathematical language in which particle physics is written, is a very complicated subject and the extraction of precise solutions to the equations is literally a challenge for the theoretical community. The perturbative methods available in the electroweak sector of the SM cannot help us in the description of the low-energy hadronic world from the Quantum Chromodynamics (QCD) Lagrangian, and we are forced to search for other tools.

In the last decades different analytical approaches have been successfully used in order to improve our capabilities to perform theoretical calculations in the hadronic sector (Chiral Perturbation Theory, QCD Sum Rules, ...), whereas at the same time the study of the equations of the theory formulated on a lattice and their numerical solutions has developed considerably, and for several quantities is already the most reliable source of information.

The lattice approach seems to be very promising and in the future the alternative analytical approaches might not be able to compete with it. One could naively think that therefore the best strategy is to sit and wait for the lattice development and forget about analytical methods, but things are not that simple. First of all, there are observables where the lattice calculations are very far from being competitive and one cannot simply freeze the scientific advance for decades. Secondly, Lattice QCD is a developing discipline and needs the alternative approaches to check results and detect possible systematic errors. And moreover, the combination of the lattice methods with for example Chiral Perturbation Theory is of crucial importance from a practical point of view, since it allows to work with non-physical quark masses and extrapolate the results to the physical points, what is very useful reducing the computational time needed.

We will concentrate in the first part of this thesis in the so-called QCD Sum Rules, that represent an analytical method to deal with the strong interactions. This method has been very useful since its modern formulation in the late seventies, but as we will see there are theoretical aspects that still deserve a careful study. We will formulate the method from its very basis, analyzing critically the different

elements and uncertainties. And later we will apply it for the extraction of different parameters from the precise hadronic τ decay data collected principally by the OPAL and ALEPH Collaborations at CERN.

In the final part of the thesis we will go beyond the τ decays and we will review the current status of the different determinations of V_{ud} and V_{us}, elements of the Cabibbo-Kobayashi-Maskawa (CKM) matrix, what will lead us to the study of semileptonic kaon and pion decay, muon decay and nuclear processes. In these extractions, we will see the interplay and complementarity of the different approaches. We will need Chiral Perturbation Theory to perform theoretical calculations with pions and kaons, perturbative multi-loops calculations to take into account the electroweak effects and Lattice QCD to extract the value of certain hadronic parameters.

1.2   Going beyond: searching in the darkness

Since the very foundation of the Standard Model in the late sixties and early seventies, the theoreticians have been trying to find a convincing theoretical extension of it (or an alternative to it), such that it could explain at least part of the so far unsolved questions. The spectrum of possibilities is huge, from small extensions of the SM where only one particle is added (like e.g. the axion, associated to the strong CP problem) to very ambitious frameworks that aim to unify not only strong and electroweak interactions but also gravity, like string theory.

We can maybe point supersymmetry as the most popular extension. It follows the path of the theoretical discoveries that ended with the formulation of the SM and uses the symmetry as the guiding principle. Supersymmetry would be a new symmetry of the world that relates bosons and fermions and entails the existence of a super-partner for every known particle. As the electroweak symmetry it has to be spontaneously broken at a very high scale in order to push the masses of these super-partners above the experimental limits. It is a nice theoretical extension of the SM that moreover seems to arise naturally in the context of string theory (indeed it was first formulated in that context!) and that could solve several problems, like for example the existence of a dark matter candidate (the lightest supersymmetric particle). In any case the original and main motivation for supersymmetry was the solution of the hierarchy problem, since the super-partners quantum contributions in the loops can cancel the other quantum contributions, stabilizing the mass of the Higgs boson. In this way one could have a fundamental scalar with a mass that does not need an *unnatural* fine-tuning. This search of *naturalness* has been the main source of inspiration for model-builders when looking for possible extensions of the SM. However, the measurements performed by LEP at CERN and by other precision experiments have cornered supersymmetry to an unnatural place where some fine-tuning seems to be necessary. In this way, the main motivation for the theory seems to have been almost lost.

This has triggered the exploration of other possible solutions and has led to new scenarios, some of them very exotic and exciting, with large additional spatial

dimensions and microscopic black holes that could be found at the LHC. It has also led to a revival interest in old alternatives like technicolor theories, where the electroweak symmetry is broken by new strong interacting dynamics *à la* QCD. In any case, the investigations made so far indicate that all the known possibilities require some degree of fine-tuning.

There is an alternative perspective that can be taken for the study of New Physics, based on the concept of Effective Field Theory. In this approach one does not commit with any particular model but only assumes the low-energy particle content and the symmetries of the theory, what allows a quite model-independent study. Therefore one has that the Standard Model (or a certain modification of it) represents a good description of Nature up to a certain scale that is well above the heaviest SM particle (top quark or Higgs), but for small corrections that can be parameterized in terms of higher dimensional operators.

In this way one can analyze the current experimental information in a general framework and conclude which operators are more or less suppressed, revealing which experiments can be interesting in order to probe those operators less constrained and which experiments are somehow redundant since they will explore regions already excluded by other measurements.

The interplay of these model-independent studies and the analyses performed within particular New Physics scenarios is very necessary, since the former can point at unconstrained new directions and trigger new ideas among the model-builder community, whereas the later are needed in order to avoid working with an infinite number of parameters and also in order to indicate possible direct detection channels of the new particles.

In the second part of this thesis we will follow this model-independent approach, reviewing the twenty years old derivation of the most general effective Lagrangian assuming only lepton and baryon number conservation, where the SM is the first term and the New Physics at the TeV scale appears as corrections to the SM dominant contribution. We will apply this framework to the study of the muon decay and the semileptonic decays of light quarks, putting the basis for a systematic analysis of New Physics effects in low-energy processes, keeping full contact with the TeV physics. In this way one can assess in a model-independent framework the relevance of the current experimental measurements constraining the extensions of the Standard Model.

In particular, we will analyze with great detail the unitarity test of the first row of the CKM matrix, and we will show how the achieved experimental and theoretical precision in the associated observables puts this constraint at the same level of relevance than those coming from colliders or other electroweak precision measurements.

Chapter 2

Hadronic tau decays: a QCD laboratory

> *(In this respect,) it would have been much nicer*
> *if the tau-lepton had had a mass of 5 GeV!*
> *R. D. Peccei & J. Solà [1]*

2.1 Introduction

The τ particle is a lepton of the third generation of the Standard Model, that has negative charge and a mass of 1776.99 ± 0.29 MeV. During the three decades passed since its discovery it has been deeply studied with different accelerators and detectors.

The τ lepton is the only lepton massive enough to decay into hadrons what makes it a very interesting object for the study of the strong interaction, given its relative simplicity compared with the purely hadronic processes. Its mass is such that gives us access to the low and intermediate energy regions where the non-perturbative effects are very important (resonances), but where the perturbative calculations can be still used within the appropriate framework that will be explained in the next chapter. In this way it offers many interesting, and sometimes unique, possibilities for testing the Standard Model and learning about QCD, both in the perturbative and non-perturbative regimes.

We can classify the τ-decays in leptonic and semileptonic (or hadronic) decays. There are two leptonic channels

$$\tau \rightarrow \nu_\tau + W \rightarrow \nu_\tau + \bar{\nu}_l + l, \qquad l = \mu, e, \tag{2.1}$$

and for them the SM prediction, including the electroweak corrections and neglecting the neutrino masses is [2]

$$\Gamma_{\tau \rightarrow l} \equiv \Gamma(\tau^- \rightarrow \nu_\tau l^- \bar{\nu}_l) = \frac{G_F^2 m_\tau^5}{192\pi^3} f\left(\frac{m_l^2}{m_\tau^2}\right) r_{EW}, \tag{2.2}$$

where $f(x) = 1 - 8x + 8x^3 - x^4 - 12x^2 \log x$, and the factor $r_{EW} = 0.99986$ takes into account the small radiative corrections and the non-local structure of the W-propagator.

The hadronic decays take place when the W-boson couples to a pair of quarks (see Fig. 2.1), that after the hadronization process give rise to the experimentally observed hadrons. We can divide in turn these decays in those where the total strange charge in the final state is zero and those where it is not-zero, that at first order in the strong interaction are given by

$$\tau \rightarrow \nu_\tau + W \rightarrow \nu_\tau + d + \overline{u}, \tag{2.3}$$

$$\tau \rightarrow \nu_\tau + W \rightarrow \nu_\tau + s + \overline{u}, \tag{2.4}$$

respectively.
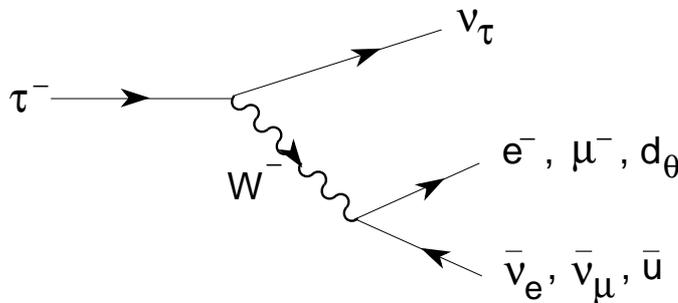
Figure 2.1: Feynman diagram at tree-level for the τ-decay.

Another well-known process where the strong interaction effects can be studied in simple conditions is the process $e^+ e^- \rightarrow \gamma \rightarrow$ hadrons. But notice that whereas in that process only the electromagnetic vector current $J^\mu = \sum_q Q_q \bar{q} \gamma^\mu q$ is examined, the hadronic τ decays offer the possibility of studying the properties of both the vector $V_{ij}^\mu = \bar{q}_j \gamma^\mu q_i$ and the axial-vector $A_{ij}^\mu = \bar{q}_j \gamma^\mu \gamma_5 q_i$ (con $q_j, q_i = u, d, s$) currents, in such a way that these two processes are complementary.

2.2 Experimental overview

Tau physics in the last decades has been dominated by two different and complementary experimental facilities: on one hand the LEP experiments ALEPH, DELPHI, L3 and OPAL, operating at the Z resonance at center-or-mass energies of 91.2 GeV, and on the other hand CLEO at CESR running at the $\Upsilon(4S)$ resonance (10.6 GeV). Up to 1.6×10^5 τ pairs have been recorded by each of the LEP experiments between 1990 and 1995, and in CLEO one has even larger statistics, although with less precision.

Given a specific channel $\tau \rightarrow \nu_\tau n$, where n stands for a certain hadronic system, one measures the number of events $N_n(s)$ where this hadronic system is emitted

with a total invariant mass $\sqrt{s}$. In this way one can construct the so-called spectral function that gives the associated probability of that event

$$\rho_{\tau \to \nu_\tau n}(s) \sim \frac{1}{N_n} \times \frac{\mathrm{dN_n}}{\mathrm{ds}}, \tag{2.5}$$

where we have omitted for simplicity the different factors usually included in the definition.

Although experimentally one observes the individual events, i.e. the exclusive decays, we will work with the following inclusive observables in this work:

- non-strange vector contribution to the total τ hadronic width, i.e. the sum over all the decays that have zero strangeness in the final state, and that are mediated by the vector current. It can be shown that these modes are those with an even number of pions[1]. The corresponding spectral function is precisely defined as

$$v_{ud}^{(1)}(s) \equiv \frac{1}{N_V} \frac{dN_V}{ds} \frac{m_\tau^2}{12\pi^2 |V_{ud}|^2 S_{\mathrm{EW}}} \frac{B(\tau^- \to V^- \nu_\tau)}{B(\tau^- \to e^- \overline{\nu}_e \nu_\tau)} \frac{1}{\left(1 - \frac{s}{m_\tau^2}\right)^2 \left(1 + \frac{2s}{m_\tau^2}\right)} \tag{2.6}$$

where V^- stands for a strangeless hadronic system with an even number of pions and where the different factors added to $1/N_V \times \mathrm{dN_V/ds}$ have been included for later convenience;

- non-strange axial-vector contribution to the total τ hadronic width, i.e. the sum over all those decays that have zero strangeness in the final state and an odd number of pions. In this case we define the spectral function as

$$a_{ud}^{(1)}(s) \equiv \frac{1}{N_A} \frac{dN_A}{ds} \frac{m_\tau^2}{12\pi^2 |V_{ud}|^2 S_{\mathrm{EW}}} \frac{B(\tau^- \to A^- \nu_\tau)}{B(\tau^- \to e^- \overline{\nu}_e \nu_\tau)} \frac{1}{\left(1 - \frac{s}{m_\tau^2}\right)^2 \left(1 + \frac{2s}{m_\tau^2}\right)} \tag{2.7}$$

where A^- stands for a strangeless hadronic system with an odd number of pions, except the one-pion state that is excluded. This exclusion of the $\tau \to \pi \nu_\tau$ and the different factors will be understood in the next section;

- strange contribution to the total τ hadronic width, i.e. sum over all the decays that involve non-zero total strange charge in the final state. In this case the separation in vector and axial-vector mediated decays is not possible.

The measurements of these spectral functions performed by ALEPH [3] are the most precise available and they are shown in Fig. 2.2.

---

[1]Modes with a $K\bar{K}$ pair contributes both to the V and A channel, what generates a certain error that will be taken into account.
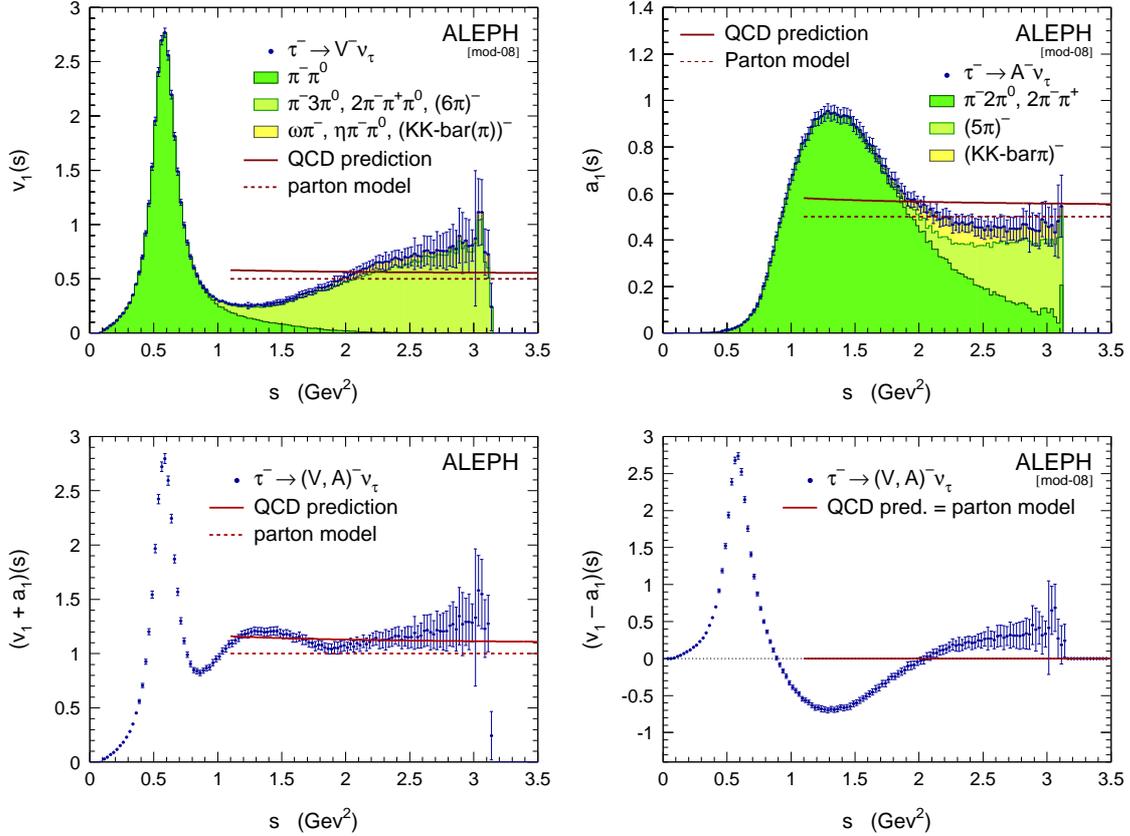
Figure 2.2: Vector (V), axial-vector (A), $V + A$ and $V - A$ τ hadronic spectral functions measured by ALEPH [3]. The shaded areas indicate the main contributing exclusive τ decay channels. The curves show the predictions from the parton model (dotted) and from massless perturbative QCD using $\alpha_S(M_Z) = 0.120$ (solid).

2.3   Theoretical calculation

From the electroweak Lagrangian

$$\mathcal{L}_{SM}(x) = -\frac{G_F}{\sqrt{2}} V_{ij} \ell_\mu h_{ij}^\mu \; , \tag{2.8}$$

where $\ell_\mu = \bar{\tau}\gamma_\mu(1 - \gamma_5)\nu_\tau$ and $h_{ij}^\mu = \bar{u}_i\gamma^\mu(1 - \gamma_5)d_j$, it can be formally calculated any exclusive tau decay $\tau \to \nu_\tau n$ (where n stands for a certain hadronic system) in terms of the hadronic matrix element $\langle n|h_{ij}^\mu(0)|0\rangle$ that cannot be calculated from first principles due to its non-perturbative nature.

If we consider an inclusive tau decay defined as the sum over all the possible channels mediated by a certain quark-current $\mathcal{J}_{ij}^\mu(x)$, then we end up with the

following objects

$$
\rho^{\mu\nu}_{ij,\mathcal{JJ}}(p) \equiv (2\pi)^3 \sum_n \langle 0|\mathcal{J}^{\mu}_{ij}(0)|n\rangle \langle n|\mathcal{J}^{\mu}_{ij}(0)^{\dagger}|0\rangle \, \delta^{(4)}(p - p_n) \tag{2.9}
$$

$$
= (-g^{\mu\nu}q^2 + q^{\mu}q^{\nu})\, \rho^{(1)}_{ij,\mathcal{JJ}}(p^2) + q^{\mu}q^{\nu}\, \rho^{(0)}_{ij,\mathcal{JJ}}(p^2)\,, \tag{2.10}
$$

where we have shown their Lorentz decomposition. In particular we will find the following result for the inclusive strange and non-strange decay widths mediated by the quark-currents $\mathcal{J}^{\mu}_{ud}(x)$ and $\mathcal{J}^{\mu}_{us}(x)$

$$
R^{S=0}_{\tau,\mathcal{J}} = 12\pi S_{\mathrm{EW}} \cos^2\theta_c \int_{m^2_\pi}^{m^2_\tau} \frac{ds}{m^2_\tau} \times
$$
$$
\left(1 - \frac{s}{m^2_\tau}\right)^2 \left[\left(1 + 2\frac{s}{m^2_\tau}\right)\rho^{(0+1)}_{ud,\mathcal{JJ}}(s) + \rho^{(0)}_{ud,\mathcal{JJ}}(s)\right]\,, \tag{2.11}
$$

$$
R^{S=1}_{\tau,\mathcal{J}} = 12\pi S_{\mathrm{EW}} \sin^2\theta_c \int_{m^2_K}^{m^2_\tau} \frac{ds}{m^2_\tau} \times
$$
$$
\left(1 - \frac{s}{m^2_\tau}\right)^2 \left[\left(1 + 2\frac{s}{m^2_\tau}\right)\rho^{(0+1)}_{us,\mathcal{JJ}}(s) + \rho^{(0)}_{us,\mathcal{JJ}}(s)\right]\,, \tag{2.12}
$$

where $s = p^2_h$ is the invariant mass of the final hadronic state, $S_{\mathrm{EW}} = 1.0194$ [2] is an electroweak correction factor and θ_C is the Cabibbo angle.

We focus now on the non-strange case. The (0)-component of both currents is well known theoretically: in the isospin limit the vector part $\rho^{(0)}_{ud,VV}(s)$ vanishes due to the conservation of the vector current (CVC), whereas the axial-vector part $\rho^{(0)}_{ud,AA}(s)$ is almost saturated by the pion pole contribution, fully calculable within χPT. Therefore we have

$$
\rho^{(0)}_{ud,AA}(s) \approx 2\, f^2_\pi\, \delta(s - \mathrm{m}^2_\pi)\,, \tag{2.13}
$$

and therefore

$$
R^{S=0}_{\tau,V} = 12\pi S_{\mathrm{EW}} \cos^2\theta_c \int_{s_0}^{m^2_\tau} \frac{ds}{m^2_\tau} \left(1 - \frac{s}{m^2_\tau}\right)^2 \left(1 + 2\frac{s}{m^2_\tau}\right)\rho^{(1)}_{ud,VV}(s) \tag{2.14}
$$

$$
R^{S=0}_{\tau,A} = 12\pi S_{\mathrm{EW}} \cos^2\theta_c \int_{s_0}^{m^2_\tau} \frac{ds}{m^2_\tau} \times
$$
$$
\left(1 - \frac{s}{m^2_\tau}\right)^2 \left[\left(1 + 2\frac{s}{m^2_\tau}\right)\rho^{(1)}_{ud,AA}(s) + 2\, f^2_\pi\, \delta(s - \mathrm{m}^2_\pi)\right]\,. \tag{2.15}
$$

From these results we can easily see that the $\rho^{(1)}_{ud,VV/AA}(s)$ functions are nothing but the spectral functions $v_1/a_1(s)$ that we have defined in Eqs. (2.6) and (2.7) but for a $2\pi^2$ factor

$$
\rho^{(1)}_{ud,VV}(s) = \frac{1}{2\pi^2}v_1(s)\,, \qquad \rho^{(1)}_{ud,AA}(s) = \frac{1}{2\pi^2}a_1(s)\,. \tag{2.16}
$$

These spectral functions are not calculable from first principles, at least not in the whole integration range from $s = 0$ to $s = m_\tau^2$ since our perturbative calculations are valid only at high energies. And so it seems that we cannot calculate either the exclusive or the inclusive decay widths.

But in the next chapter we will explain a theoretical framework that will allow us to re-write this kind of integrals of the inclusive spectral functions as contour integrals calculable within QCD. And therefore we will able to connect the QCD calculations with the hadronic tau decays. Thanks to this framework and depending on the goal, it may be interesting to study the integrals of one spectral function or other. Here we give some examples:

- The non-strange vector and axial-vector spectral function (and its sum) are well suited to study the perturbative physics and can be used to determine the strong coupling constant [4];

- The non-strange difference $v_1(s) - a_1(s)$ is well suited to study the non-perturbative physics, as we will see in Chapters 4 and 5;

- The difference between the strange and non-strange spectral function can be used to determine the value of the strange quark mass and the element V_{us} of the CKM matrix [5,6];

The spectral functions embody both the rich hadronic structure seen at low energy, and the quark behavior relevant in the higher energy regime and play an important role in the understanding of hadronic dynamics in the intermediate energy range. They represent the basic input for QCD studies and for evaluating low-energy contributions from hadronic vacuum polarization.

Chapter 3

QCD Sum Rules: derivation and dissection

Not only God knows, I know,
and by the end of the semester,
you will know.
Sidney R. Coleman

As we already emphasized in the Chapter 1, due to the non–perturbative character of the strong interaction described by the QCD Lagrangian, it is extremely difficult to cover the path that goes from the quarks and gluons to the observable hadrons. In this Chapter we will present a method that has been very useful during the last thirty years to help us in covering at least part of this path.

This method is known under the name of QCD Sum Rules and it was introduced in its modern form in 1979 [7] by Shifman, Vainshtein and Zakharov[1]. These QCD Sum Rules [7–9] are the result of the combination of the operator-product expansion developed by Wilson in 1969 [10] with the old dispersion relations known since the fifties [11] and with low-energy theorems. So as we see the bases of the QCD Sum Rules are even older than the Lagrangian of Quantum Chromodynamics, and this is so because the method is based on very general principles of Quantum Field Theory like causality and unitarity, that govern the analytic behavior of the two-point correlation functions, that will be introduced later. But the knowledge of the fundamental QCD Lagrangian is also an essential ingredient of the QCD Sum Rules for the exact calculation of the operator-product expansion and in order to prove the low-energy theorems that may be needed.

The QCD Sum Rules go far beyond the perturbative QCD calculations and take into account the highly non-perturbative nature of the QCD vacuum, a very complicated and unknown entity where the operators of the theory have in general non-vanishing expectation values. Non-perturbative effects are parameterized in terms of these vacuum expectation values, that we will consider free parameters

---

[1]Due to this work, carried out at the Institute for Theoretical and Experimental Physics (ITEP) in Moscow, this method is also known as SVZ (or ITEP) sum rules.

in the absence of an analytic way of calculating them from first principles (lattice determinations cannot compete still with phenomenological methods), and in this way the QCD Sum Rules start from the perturbative calculations and the QCD vacuum and connect them with hadronic observables. This is what makes the method so interesting. It goes from pure QCD to the hadronic resonances.

As we will see the QCD Sum Rules do not represent a method that can be refined indefinitely to any desired precision, like a Taylor expansion of a function, but has some systematic limits that it is important to understand. Given that the strong interaction is usually the main culprit of the SM uncertainties, it is crucial to be able to assign realistic errors to any QCD prediction in such a way that we can be in a position of claiming the eventual discovery of New Physics or discard it. So it is necessary to evaluate the different sources of error of a given sum rule prediction and to evaluate also the possible improvements of this prediction and the limits of this method for that particular calculation. This kind of analyses are extremely important in order to know which experiments must be undertaken in the near future and which are not useful since the theoretical knowledge is still poor.

The central objects of the QCD Sum Rules are the two-point correlation functions (correlators) $\Pi_{AB}(q^2)$, that will be introduced in the next section. We would like to keep the derivation and the discussion as general as possible and with this purpose we will work with a general correlator $\Pi_{AB}(q^2)$. But at the end of every section we will particularize to the case

$$\Pi_{AB}(q^2) \to \Pi_{LR}(q^2) \ , \tag{3.1}$$

where $\Pi_{LR}(q^2)$ will be defined in the next section. We do this with the intention of making the derivation more pedagogical and because this correlator will be the central object of the next two Chapters

3.1 Correlation Function

A two–point correlation function of two operators $A(x)$ and $B(x)$ is the vacuum expectation value of their T-ordered product

$$K(x - y) = \langle 0|T(A(x)B(y)^\dagger)|0\rangle \ , \tag{3.2}$$

where we have explicitly shown that the correlation function only depends on the relative distance $x - y$, due to the homogeneity of the vacuum. We will work in the momentum space

$$\Pi_{AB}(q) \ \equiv i \int d^4x \ e^{iqx} \langle 0|T(A(x)B(0)^\dagger)|0\rangle \ , \tag{3.3}$$

and the operators $A(x)$ and $B(x)$ will be two-quark currents with the generic form $\bar{q}^i \Gamma^n q^j$, where $\Gamma^n = 1, \gamma_5, \gamma^\mu, \gamma^\mu\gamma_5, \sigma^{\mu\nu}$ (or any linear combination of them) and $q^{i,j} = u, d, s..$

We will extract the Lorentz structure of the correlators in such a way that we end up working with scalar objects that contains the dynamical information and that only depend on q^2. For the sake of simplicity and in an abuse of terminology we will call them also correlators.

Depending on the phenomenology that one wants to study it is interesting to work with one correlator or another. We will be interested during the next Chapters in the LR correlator, and so we move on now to its rigorous definition.

3.1.1   The LR correlator

The vector and axial-vector quark currents $V_{ij}^\mu(x) = \overline{q}^i \gamma^\mu q^j$ and $A_{ij}^\mu = \overline{q}^i \gamma^\mu \gamma_5 q^j$ are specially interesting because they are realized in nature through the electroweak vector bosons W, Z and γ and there is a very rich associated phenomenology. Because of that, the sum rules generated by the corresponding correlators can be used to connect the hadronic world with the QCD Lagrangian.

In Chapters 4 and 5 we will pay special attention to the non-strange (or Cabibbo-allowed) left- and right-handed currents

$$
\begin{aligned}
L_{ud}^\mu(x) &\equiv V_{ud}^\mu(x) - A_{ud}^\mu(x) = \overline{u}\gamma^\mu(1-\gamma_5)d \ , & (3.4)\\
R_{ud}^\mu(x) &\equiv V_{ud}^\mu(x) + A_{ud}^\mu(x) = \overline{u}\gamma^\mu(1+\gamma_5)d \ , & (3.5)
\end{aligned}
$$

and the associated LR correlator

$$
\begin{aligned}
\Pi_{ud,LR}^{\mu\nu}(q) &\equiv i\int \mathrm{d}^4x\ \mathrm{e}^{iqx} \langle 0|T\left(L_{ud}^\mu(x)R_{ud}^\nu(0)^\dagger\right)|0\rangle \\
&= \left(-g^{\mu\nu}q^2 + q^\mu q^\nu\right)\Pi_{ud,LR}^{(1)}(q^2) + q^\mu q^\nu\, \Pi_{ud,LR}^{(0)}(q^2)\, , & (3.6)
\end{aligned}
$$

where we have shown the Lorentz decomposition. This two-point function is also called $V-A$ correlator because[2]

$$
\Pi_{ud,LR}^{\mu\nu}(s) = \Pi_{ud,VV}^{\mu\nu}(s) - \Pi_{ud,AA}^{\mu\nu}(s) \ , \tag{3.7}
$$

since the VA (and AV) correlation function vanishes due to parity invariance of the vacuum. More specifically we will be working with the following object

$$
\Pi_{ud,LR}^{(0+1)}(s) \equiv \Pi_{ud,LR}^{(0)}(s) + \Pi_{ud,LR}^{(1)}(s) \ , \tag{3.8}
$$

that abusing of the terminology and notation we will call LR correlator and denote by $\Pi_{LR}(s)$ for the sake of brevity.

3.1.2   Analytic structure of the correlators

Although the correlators are defined in principle for real values of q^2, the definition is formally valid also for complex values, in such a way that we can consider them

---

[2]In the literature, when the currents $A(x) = B(x)$, as in the VV or AA case, the subindex of the correlator is commonly reduced to just V or A.

complex functions of a complex variable q^2. The QCD Sum Rules take advantage of their analytic properties in the complex plane to relate different regions and connect the hadronic data with the QCD calculations.

It is always assumed that the correlators are analytic functions of q^2 in the whole complex plane except in the positive real axis, where they have a cut and maybe also some poles before the beginning of the cut[3]. This mathematical assumption comes from very general physical requirements, like causality and unitarity [12] and it is known since the times of the S-matrix theory.

It is usually said that the correlator satisfy the Schwarz reflection property across the real axis[4]

$$\Pi_{AB}((q^2)^*) = [\Pi_{AB}(q^2)]^* \ , \tag{3.9}$$

and that consequently the correlator takes real values for real q^2 and the discontinuity in the positive real axis associated to the cut is suffered only by the imaginary part.

It is obvious that mathematically this property cannot be true for arbitrary currents $A(x)$ and $B(x)$, since one can always redefine $A(x) \rightarrow e^{i\theta}A(x)$ and then the reflection property will not be satisfied. And indeed the property can in principle be false for the correlator even if we allow this rephasing.

But it is the physics that tells us that our correlators will satisfy this property up to a factor i that can appear due to conventions. In order to prove it for a particular pair of currents, the standard procedure is to demonstrate it in the deep euclidean region where QCD perturbation theory is reliable and, because of the analytic structure of the correlator, analytically continue this result to the rest of the complex plane.

In this way it can be proved that the LR correlator satisfy the Schwarz reflection principle and that is why we did not extract any factor i in the Lorentz decomposition (3.6). On the contrary, in the explicit analysis of the VT correlator of Ref. [13] we can see that it is necessary to extract a factor i from the definition of the correlator in order to satisfy the reflection property and therefore to have a real spectral function (see section 3.3).

3.2   General derivation of a QCD Sum Rule

Let us consider the general correlator $\Pi_{AB}(q^2)$ defined in Eq. (3.3) (we will omit in this section the AB subindex for brevity), a weight function $w(q^2)$, that must be analytic in the whole complex plane but for a possible pole at the origin[5], and the

---

[3]There is a subtlety that must be noticed. This property of analyticity affects the whole correlator, but once we Lorentz-decompose it, the remaining pieces may have a different analytic structure at the origin. In the case of the LR correlator (3.6) this happens for the (0)- and (1)-components, but not for the objects $\Pi_{LR}^{(0+1)}(s)$ and $s \cdot \Pi_{LR}^{(0)}(s)$ that must be analytic at $s = 0$. Due to this we will use this second decomposition.

[4]We discuss this issue for completeness, although it is not necessary to use this property at any moment to formulate the QCD Sum Rules.

[5]It is also assumed the weight function takes real values for real q^2. The derivation can be generalized in a straightforward way to weight functions with poles also out of the origin, but here
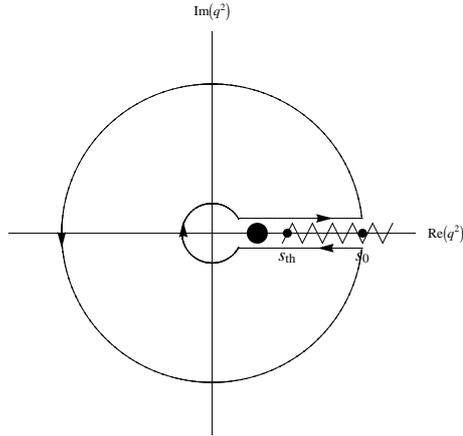
Figure 3.1: Circuit of integration in the q^2-complex plane. The radius of the inner circle is ϵ, the radius of the outer one is s_0 and the separation between the horizontal parts of the circuit is proportional to ϵ. We indicate the possible pole of the correlator at $q^2 \leq s_{th}$ and the cut starting at $q^2 = s_{th}$. The possible pole of the weight function at the origin is not marked.

circuit C in the q^2-complex plane that is shown in the Fig. 3.1. Taking into account the discussed analytic properties of the correlator and the weight function inside this circuit C we have by the Cauchy's theorem

$$\oint_C \Pi(z)w(z)dz = 0 \ , \tag{3.10}$$

where we have already used the notation $z = q^2$ that emphasizes that we are working in the complex plane. We can divide this integral in three contributions as it is shown diagrammatically in Fig. 3.2 finding

$$\int_{C_{out}} \Pi(z)w(z)dz + \int_{C_{in}} \Pi(z)w(z)dz + \int_{C_{cut}} \Pi(z)w(z)dz = 0 \ , \tag{3.11}$$

where C_{in}, C_{out} and C_{cut} referred to the circuits of Fig. 3.2. Taking the limit $\epsilon \to 0$ we have the *exact* relation

$$\oint_{C_{out}} \Pi(z)w(z)dz - 2\pi i \operatorname*{Res}_{s=0} (\Pi(z)w(z)) + \int_0^{s_0} \mathrm{Disc}\Pi(s)w(s)ds = 0 \ , \tag{3.12}$$

where $\operatorname*{Res}_{s=0} [F(s)]$ is the residue of $F(s)$ at $s = 0$ and $\mathrm{Disc}\Pi(s) \equiv \Pi(s+i\epsilon) - \Pi(s-i\epsilon)$, that is, the discontinuity of the correlator at the positive real axis. These three pieces are the main ingredients of a QCD Sum Rule, although we must make still some changes to arrive to its final form. Let us now explain the main features of the three contributions to (3.12) and in the following sections we will analyze them carefully:

---

we restrict ourselves to this case to simplify the equations and the discussion.
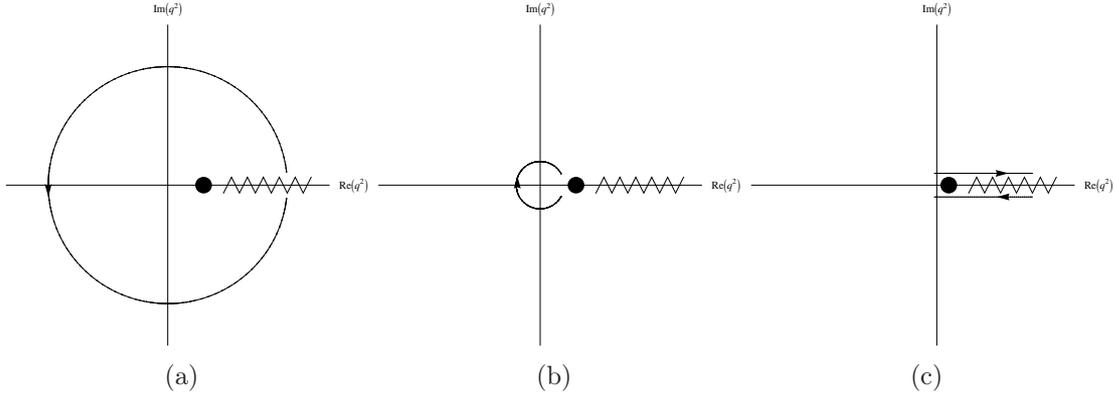
Figure 3.2: Diagrams that represent the different contributions to the integral (3.10) (see Eq. (3.12)).

- If s_0 is high enough, we can calculate within QCD the first integral of (3.12) (Fig. 3.2a) making use of the **Operator-Product Expansion**, a useful tool that will be explained in Section 3.4. Therefore we have

$$\oint_{C_{out}} \Pi(z)w(z)dz = \oint_{C_{out}} \Pi^{\text{OPE}}(z)w(z)dz + 2\pi i \ \text{DV}[w(z), s_0] \ , \qquad (3.13)$$

  where $\text{DV}[w(z), s_0]$ is the error associated to this OPE-substitution in a circuit of finite radius s_0. This error is called quark-hadron duality violation (DV) and will be analyzed carefully in Section 3.5.

- If $w(s)$ has a pole at the origin we will have the second term of (3.12) (Fig. 3.2b) and then we will need to know the structure of the correlator near the origin. This can be rigorously calculated using **Chiral Perturbation Theory**, the effective theory of QCD in the low-energy regime (see Section 4.1).

- **Spectral functions**.- In the third term of (3.12) (Fig. 3.2c), we have the discontinuity of the correlator at the positive real axis, that as we will show in Section 3.3, is related to the measurable spectral functions introduced in the previous Chapter in the following way

$$\Pi(q^2 + i\epsilon) - \Pi(q^2 - i\epsilon) = 2\pi i \rho(q^2) \ . \qquad (3.14)$$

  This is where the hadronic observables enter in our analysis.

Therefore, we can re-write our general expression of a QCD Sum Rule (3.12) in the following way

$$\int_0^{s_0} \rho(s)w(s)ds = \operatorname*{Res}_{z=0} \Pi^{\chi\text{PT}}(z)w(z) - \oint_{C_{out}} \frac{dz}{2\pi i}\Pi^{\text{OPE}}(z)w(z) - \text{DV}[w, s_0]. \qquad (3.15)$$

This *exact* expression represents a non-trivial constraint for the hadronic integral, that is nothing but a sum over hadronic states. This is why they are called *sum rules*. Notice that given a correlator we still have freedom in the choice of the weight and the value of the Cauchy's radius s_0, what will generate a plethora of sum rules for the same correlator, each with some problems and virtues.

Eq. (3.15) is the main result of this Chapter. In the following sections we will explain thoroughly the different ingredients that we have already introduced: the spectral functions, the operator-product expansion and the duality violation.

3.3 Spectral representation of a general correlator

Assuming just translation invariance and unitarity it can be shown that the correlators satisfy the so-called dispersion relation[6]

$$\Pi_{AB}(q^2) = \int dt \, \frac{\rho_{AB}(t)}{t - q^2 - i\epsilon} \, , \tag{3.16}$$

where $\rho_{AB}(t)$ is the spectral function, defined by

$$\rho_{AB}(q^2) \equiv (2\pi)^3 \sum_n \langle 0|A(0)|n\rangle \langle n|B(0)^\dagger|0\rangle \, \delta^{(4)}(q - p_n) \, , \tag{3.17}$$

where we see that in the case $A(x) = B(x)$ the spectral function is by construction a real and non–negative function.

The original proof was made more than fifty years ago by Källen and Lehmann [11] for the case $A(x) = B(x)$ and still today this is the standard assumption. We show in the Appendix A the demonstration for the general case where $A(x)$ and $B(x)$ are different.

From the dispersion relation (3.16) and using the identity

$$\frac{1}{t - q^2 \mp i\epsilon} = \mathrm{PP}\left(\frac{1}{t - q^2}\right) \pm i\,\pi\,\delta(t - q^2) \, , \tag{3.18}$$

one finds that the discontinuity of $\Pi_{AB}(q^2)$ across the real axis is related to the spectral function $\rho_{AB}(q^2)$ by:

$$\Pi_{AB}(q^2 + i\epsilon) - \Pi_{AB}(q^2 - i\epsilon) = 2\,\pi\,i\,\rho_{AB}(q^2) \, , \tag{3.19}$$

that was the pursued result that we used in the preceding section for the derivation of the QCD Sum Rule (3.15). We see then that the dispersion relation (3.16) connects the correlator evaluated at an euclidean point with the discontinuity in the opposite part of the real axis, that is, the timelike region.

Now we take a careful look to the LR spectral function and how it can be extracted from τ-data.

---

[6]We work for the moment with an unsubtracted dispersion relation, where the integral at the r.h.s. of (3.16) converges and one does not have to add any arbitrary polynomial. We will come back to this issue later.

3.3.1   LR spectral function: connection with data

In the previous Chapter we introduced the non-strange VV and AA spectral functions with their Lorentz decomposition

$$\rho^{\mu\nu}_{ud,\mathcal{J}\mathcal{J}}(p) \;\equiv\; (2\pi)^3 \sum_n \langle 0|\mathcal{J}^{\mu}_{ud}(0)|n\rangle\langle n|\mathcal{J}^{\mu}_{ud}(0)^{\dagger}|0\rangle\, \delta^{(4)}(p - p_n) \;, \qquad (3.20)$$

$$=\; (-g^{\mu\nu}q^2 + q^{\mu}q^{\nu})\, \rho^{(1)}_{ud,\mathcal{J}\mathcal{J}}(p^2) + q^{\mu}q^{\nu}\, \rho^{(0)}_{ud,\mathcal{J}\mathcal{J}}(p^2) \;. \qquad (3.21)$$

and we explained that they are measurable quantities that can be obtained from the leptonic tau decay. We focus now on the V-A difference

$$\rho^{(j)}_{ud,LR}(s) = \rho^{(j)}_{ud,VV}(s) - \rho^{(j)}_{ud,AA}(s) \;. \qquad (3.22)$$

As we explained in the previous Chapter the (0)-component is well known theoretically, with only the pion pole contribution in the axial-vector channel. Therefore

$$\rho^{(0)}_{ud,LR}(s) \;\approx\; -2\, f_{\pi}^2\, \delta(s - \mathrm{m}_{\pi}^2) \;, \qquad (3.23)$$

$$\rho^{(0+1)}_{ud,LR}(s) \;\approx\; -2\, f_{\pi}^2\, \delta(s - \mathrm{m}_{\pi}^2) + \rho^{(1)}_{ud,LR}(s)\, \theta(s - 4\mathrm{m}_{\pi}^2) \;, \qquad (3.24)$$

where the $\theta(s)$ function has been introduced just to emphasize that $\rho^{(1)}_{ud,LR}(s < 4\mathrm{m}_{\pi}^2)$ is zero. This spectral function $\rho^{(1)}_{ud,LR}(s)$ is the part that we are not able to predict from first principles, but we know it experimentally (for $s < m_{\tau}^2$). We will work with it during the next two Chapters, and sometimes we will call it just **LR spectral function** for brevity and denote it by $\rho_{LR}(s)$ or even $\rho(s)$ if the context allows us to do it without confusion.

    The determination of this spectral function by the ALEPH Collaboration is shown in the Fig. 3.3.
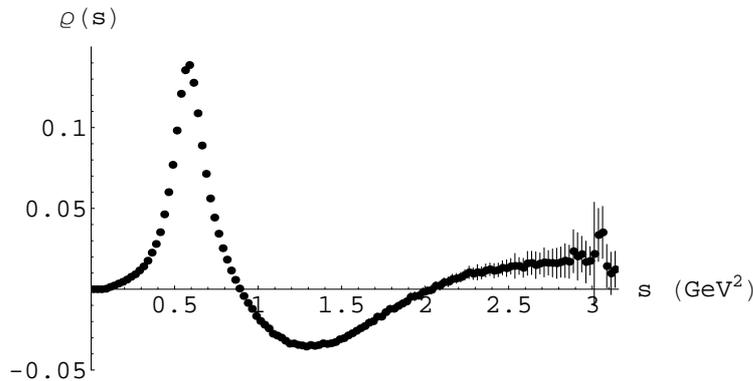

Figure 3.3: V-A spectral function measured by ALEPH [3].

3.4   The operator-product expansion

> *We are going to rely on the operator expansion*
> *beyond perturbation theory. Every step here is a*
> *new one and by no means evident.*
>   *M. Shifman, A. Vainshtein, V. Zakharov [7].*

3.4.1   Definition

In the operator-product expansion proposed by Wilson in 1969 [10] the product of operators, say $A(x)$ and $B(x)$, is expanded in a series of well defined local operators $O_i(x)$ with singular c-number coefficients $C_i(x)$.

$$A(x)B(y) = \sum_{i=0}^{\infty} C_i(x-y)O_i\left(\frac{x+y}{2}\right) \tag{3.25}$$

The local operator $O_i(x)$ is regular in the sense that the singularity of the product $A(x)B(y)$ for $x = y$ is fully contained in the coefficient functions $C_i(x-y)$. In Eq. (3.25) we have arranged each term in the order of decreasing singularity. Hence $C_0(x-y)$ is the most singular as $y \to x$, the next one is $C_1(x-y)$ and so on.

Applied to a two-point correlation function in the momentum space the OPE is equivalent to the assumption that at large external momentum q the following operator expansion is valid:

$$\begin{aligned}
\Pi_{AB}(-q^2) &\equiv i \int d^4x \ e^{iqx} \langle 0|T(A(x)B(0)^\dagger|0\rangle \\
&= \sum_n C_n^{AB}(q^2)\langle 0|O_n|0\rangle \equiv \sum_n C_n^{AB}(q^2)\langle O_n \rangle \ ,
\end{aligned} \tag{3.26}$$

where $C_n^{AB}(q^2)$ are coefficients and O_n are gauge-invariant local operators constructed from quarks and gluon fields. We will consider only spin-zero operators since only these contribute to the vacuum expectation value.

As we said, the operators O_n are conveniently classified according to their dimension n. An increase in dimension implies extra powers of $M^2/(-q^2)$ for the corresponding contribution, where M is some typical hadronic mass entering through the matrix element of O_n, and therefore even at intermediate $(-q^2) \sim 1$ GeV^2, the expansion can safely be truncated after a few terms. So we list now all the gauge-invariant operators with zero Lorentz spin and $n \leq 6$

$$\begin{aligned}
O_0 &= 1 & (3.27)\\
O_3 &= \bar{q}q & (3.28)\\
O_4 &= G_{\mu\nu}^a G^{a\mu\nu} & (3.29)\\
O_5 &= \bar{q}\sigma_{\mu\nu}\frac{\lambda^a}{2}G^{a\mu\nu}q\,, & (3.30)\\
O_6^\psi &= (\bar{q}\Gamma_r q)(\bar{q}\Gamma_s q)\,, & (3.31)\\
O_6^G &= f_{abc}G_{\mu\nu}^a G_\sigma^{b\,\nu} G^{c\sigma\mu}\,, & (3.32)
\end{aligned}$$

where $\Gamma_{r,s}$ denote various combination of Lorentz and color matrices. The unit operator is associated with the perturbative contribution that enters through its Wilson coefficient $C_0^{AB}(q^2)$. The corresponding vacuum averages of O_3 and O_4 are known as quark and gluon condensates, respectively, and as quark-gluon, four-quark and three-gluon condensates the rest of them. Notice that there are no colorless operators in QCD with dimension $d = 1, 2$. So we see that the non–perturbative contributions are suppressed by large powers of $M^2/(-q^2)$.

The OPE has been proved rigorously by Zimmermann [14] within the framework of perturbation theory, but there exist no non–perturbative proof of the OPE except for illustrations in some model field theories. We will assume the validity of the expansion also beyond perturbation theory as far as the first few terms are concerned, since explicit instanton solutions show that in higher orders in $(-q^2)$ the operator expansion becomes invalid [7].

3.4.2 Physical picture

The physical meaning of the operator expansion is the separation of scales. The OPE assumes the possibility of separating short and large distance effects and indeed being precise we must have written

$$\Pi_{AB}(-q^2) = \sum_n C_n^{AB}(q^2; \mu)\langle O_n \rangle(\mu) \ , \tag{3.33}$$

where μ is an arbitrary scale that defines what will be consider short-distance and large-distance physics. Of course, this dependence is non-physical and will not appear in any observable.

The interactions at momenta $p^2 > \mu^2$ (short distances) are included in the coefficients $C_n^{AB}(q^2; \mu)$, and if we take μ large enough we can calculate them perturbatively, thanks to asymptotic freedom[7]. In the free field theory we can extract the singularity structure of them just from dimensional arguments. In QCD and for high values of $-q^2$ we expect the corrections to this free field behavior to be small (logarithmic) thanks again to the asymptotic freedom. According to this we have

$$\Pi_{AB}(q^2) \approx \sum_n \frac{\tilde{C}_n^{AB}}{(-q^2)^{n/2}} \langle O_n \rangle \ , \tag{3.34}$$

up to logarithmic corrections, that only in the case of the perturbative contributions will be important. On the other hand, the large-distance contribution ($p^2 < \mu^2$) is accounted for phenomenologically, through the vacuum-to-vacuum matrix elements.

---

[7]In practice, using the standard methods of the Feynman-diagram technique, an explicit separation of distances is impossible in the quark-loop diagrams. One is forced to take into account both the soft parts of perturbative diagrams and the long-distance condensate effects simultaneously. This yields a certain amount of double counting, which is, fortunately, in many cases numerically insignificant, because the condensate contributions turn out to be much larger than the soft tails of perturbative diagrams.
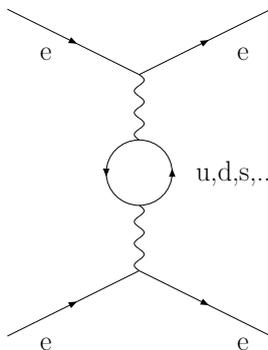
Figure 3.4: Quark-antiquark creation and annihilation by the virtual photon in the electron-electron scattering.

It is clear then that the contribution of the large-size fluctuations (independent of q^2) of the vacuum fields, can be consistently kept within the framework of the operator expansion, whereas the small-scale fluctuations cannot be included into the operator expansion, at least in its present form.

We can try to visualize the correlator and this separation of scales. The creation of quark-antiquark pair by the external current at one point and its absorption at another point by another current (see Fig. 3.4) is the physical process behind the formal definition of $\Pi_{AB}(q^2)$. It is clear that this quark-antiquark pair interacts with the vacuum fields, and that this interaction is beyond QCD perturbation theory and has to be taken into account separately. The vacuum fields in QCD are very complicated objects, with their origin in the nonlinear nature of the QCD Lagrangian. Let us just say about it that various non–perturbative approaches (instanton models, lattice simulation of QCD, etc.) indicate that these vacuum fields fluctuate with typical long-distance scales $\Lambda_{vac} \sim \Lambda_{QCD}$.

We explain now qualitatively how the contributions to the correlators coming from the vacuum fields can be performed. It can be shown that at large $-q^2 \gg \Lambda_{QCD}^2$ the average distance between the emission and absorption of the quark-antiquark pair is smaller than the scale of the vacuum fluctuations and so the quark-antiquark pair behaves as a short-distance probe of long-distance fields, being sensitive to averaged characteristics of these fields. Therefore quarks with large momenta interact with external static fields composed of soft vacuum gluons and quarks, as it is diagrammatically shown in Fig. 3.5.

It is important to say that, in addition to these mild effects of the quark scattering over the vacuum fields, there are specific vacuum fluctuations at short distances $\sim 1/\sqrt{-q^2}$, which absorb the whole momentum of the external quark current, and that violate the condensate expansion (direct instantons).
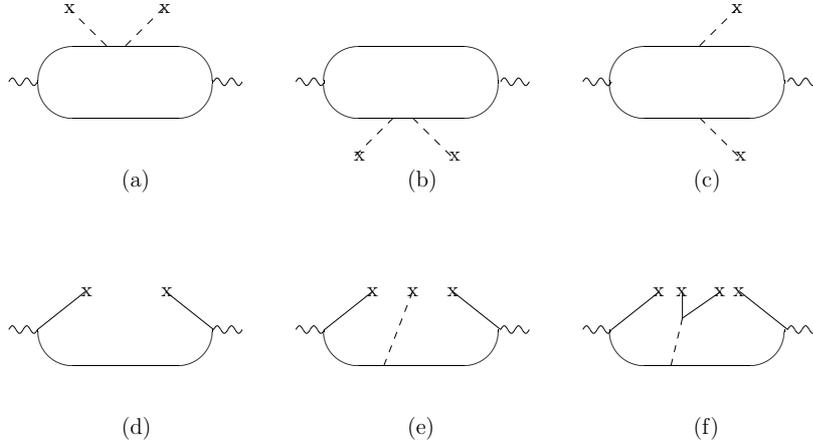
Figure 3.5: Diagrams corresponding to the gluon (a,b,c), quark (d), quark-gluon (e) and four-quark (f) condensate contributions to the OPE of a correlation function.

3.4.3 OPE of the LR correlator

In the Ref. [4] can be found a detailed analysis of the operator-product expansion of the VV and AA correlators. There we see that in the chiral limit ($m_u = m_d = 0$) these two correlators coincide to all orders in perturbation theory, and consequently the LR correlator vanishes in perturbation theory, what makes it a purely non-perturbative quantity.

Still in the chiral limit the first term of the OPE of the LR correlator is that of dimension $d = 6$, that have the three gluon (3.32) and the four-quark component (3.31). In Ref. [4] we can see that at leading order in the α_S expansion of their Wilson coefficients we can neglect the three-gluon contribution and we have

$$(-q^2)^3 \left[\Pi_{LR}^{(0+1)}(q^2) \right]^{(D=6)} = -8\pi\alpha_S \Big(\ \langle \bar{u}\gamma_\mu T^a d \cdot \bar{u}\gamma^\mu T^a d \rangle$$
$$-\langle \bar{u}\gamma_\mu\gamma_5 T^a d \cdot \bar{u}\gamma^\mu\gamma_5 T^a d \rangle \Big) \ . \qquad (3.35)$$

The nonzero up and down quark masses induce tiny corrections with dimensions two and four, which are negligible at $q^2 << 0$. Therefore we will have

$$\begin{aligned} \Pi_{LR}(q^2) &= C_2^{LR}(q^2;\mu)\langle O_2(\mu)\rangle + C_4^{LR}(q^2;\mu)\langle O_4(\mu)\rangle + C_6^{LR}(q^2;\mu)\langle O_6(\mu)\rangle + \dots \\ &\approx \frac{\tilde{C}_6^{LR}(\mu)}{(-q^2)^3}\langle O_6(\mu)\rangle + \frac{\tilde{C}_8^{LR}(\mu)}{(-q^2)^4}\langle O_8(\mu)\rangle + \dots \ , \\ &\equiv -\frac{\mathcal{O}_6^{LR}}{q^6} + \frac{\mathcal{O}_8^{LR}}{q^8} + \dots \ , \end{aligned} \qquad (3.36)$$

where we have introduced the objects $\mathcal{O}_n^{LR}$ that are μ-independent and approximately q^2-independent and that will be extracted from the data in the next Chapter. We will call them LR (or V-A) condensates.

3.5 Violation of the quark-hadron duality

In Section 3.2, when deriving the general expression of a QCD Sum Rule, we have followed the standard procedure of any sum rule analysis of replacing the correlator for its OPE expression in the whole circumference of radius s_0, see (3.13), in order to be able to calculate theoretically the associated contour integral

$$\oint_{|z|=s_0} dz\, \Pi(z)w(z)dz \;\rightarrow\; \oint_{|z|=s_0} dz\, \Pi^{\text{OPE}}(z)w(z)dz \;. \tag{3.37}$$

As we explained in the previous section the OPE of $\Pi(q^2)$ has been defined for $q^2 \ll 0$, and in this integral we are using it for any complex value such that $|q^2| = s_0$.

But one cannot perform this analytic continuation in the whole circuit and obtain the right expression of the correlator $\Pi(q^2)$ in the positive real axis, since that would mean that we could calculate then the associated spectral function, something that it is not possible, since the OPE is written in terms of quarks and gluons and cannot predict the production thresholds of hadrons and resonances, and indeed it will have production thresholds of pairs of quarks, that we know are confined. One says that there is no local quark-hadron duality if s_0 is finite, i.e.

$$\Pi(q^2 > 0) \neq \Pi^{\text{OPE}}(q^2 > 0) \;. \tag{3.38}$$

Therefore the OPE substitution of the correlator in (3.37) introduces an error, known as quark-hadron duality violation $\text{DV}[w(z), s_0]$ formally defined by

$$\text{DV}[w(z), s_0] = \frac{1}{2\pi i} \oint_{|z|=s_0} dz\, \left(\Pi(z) - \Pi^{\text{OPE}}(z) \right) w(z)dz \;, \tag{3.39}$$

where it is explicitly shown that the DV of a given sum rule depends crucially on the weight function $w(s)$ and the value of the Cauchy radius s_0.

The duality violation is older than the SVZ sum rules themselves and was discussed in the seventies in the context of the calculation of the process $e^+e^- \rightarrow$ hadrons [15, 16]. It was conjectured by Poggio, Quinn and Weinberg [16] in 1976 that the OPE represents a good approximation in the whole complex plane except in the region close to the positive real axis. This is equivalent to say that we cannot use the OPE to predict the value of the spectral function $\rho(s)$ at a given point s, but it can predict the average of the spectral function over a wide enough interval of energies.

This DV has been commonly disregarded in the sum rules analyses and indeed its definition has not been clear in the literature during decades. Let us remind that there are two kinds of errors in any practical OPE of a correlator. On one hand there is the fact that the OPE does probably not represent a perfect approximation of the real correlator, as simple instanton models show [7], since there are small effects that cannot be included in the OPE. And on the other hand, the OPE itself cannot be calculated with infinite precision, since we have to truncate the calculation of the Wilson coefficients at a certain order in α_S and also the condensates series.

Therefore we can calculate the correlator in the euclidean region with a certain error ϵ and the key point is that this error is enhanced during the analytic continuation to the positive real axis, generating there an error qualitatively bigger than ϵ, and this is what we call DV [17][8].

It is very instructive to work on a certain model (e.g. an instanton-based model) [17, 19–21] where the appearance of the DV can be seen explicitly in the analytic continuation of the OPE. We refer the interested reader to the nice reviews of M. Shifman [17].

During the first years of application of the SVZ sum rules the DV was usually disregarded, under the assumption of being negligible. Later it received more attention, and different authors started to assign it a certain error, extracted from an analysis of the stability of the results under changes in the Cauchy's radius s_0, since if the DV is negligible then there should not be any s_0-dependence[9]. Only in the last years a different approach has been followed to estimate the DV [17, 19–26], based on the use of simple models and general parametrizations, as we will explain with detail in Chapter 5.

3.5.1   An alternative expression for the DV

Now we want to perform some manipulations in (3.15) in order to derive an alternative expression for the DV. If we define $\rho^{\text{OPE}}(s) \equiv \frac{1}{\pi}\text{Im}\Pi^{\text{OPE}}(s)$, i.e. the prediction for the spectral function obtained assuming local duality, we have that (3.15) takes the form

$$\int_0^{s_0} \left(\rho(s) - \rho^{\text{OPE}}(s)\right) w(s)ds - \underset{s=0}{\text{Res}} \left(\Pi^{\chi\text{PT}}(z)w(z)\right) + \text{DV}[w(z), s_0] = 0 \ . \quad (3.40)$$

If we evaluate the expression for s_0 and $\tilde{s}_0 > s_0$, and compare the l.h.s. we find

$$\text{DV}[w(z), s_0] - \text{DV}[w(s), \tilde{s}_0] = \int_{s_0}^{\tilde{s}_0} \left(\rho(s) - \rho^{\text{OPE}}(s)\right) w(s)ds \ . \quad (3.41)$$

Setting $\tilde{s}_0 \to \infty$ and taking into account that $\text{DV}[w(z), \tilde{s}_0 = \infty] = 0$ one can write the DV in the following form [17, 19, 21, 22]

$$\text{DV}[w(z), s_0] = \int_{s_0}^{\infty} \left(\rho(s) - \rho^{\text{OPE}}(s)\right) w(s)ds \ , \quad (3.42)$$

that is the expression that we wanted to find. This result gives us a very different perspective of the meaning of the quark-hadron duality violation, expressing it

---

[8]The DV has been studied from this more mathematical perspective related to the stability of the analytic continuation in some works. We refer the interested reader to Ref. [18].

[9]We are discussing here QCD Sum Rules were the Cauchy's radius s_0 is finite. In the Borel sum rules, the exponential weight suppressed strongly the high-energy region and consequently one can take in practice an infinite Cuchy's radius. One is only moving the error from one place to another, since the exponential weights generate an infinite series of condensates that will be neglected.

in terms of the difference between the real spectral function and the OPE prediction for it beyond the upper integration limit. Let us emphasize again the explicit dependence of the DV on the weight function $w(s)$ and the Cauchy's radius s_0.

This expression is much simpler in the case of the LR correlator, where the perturbative contribution vanishes. If we neglect the logarithmic dependence of the Wilson coefficient the condensate contribution to the spectral function also vanishes and we have

$$\boxed{\mathrm{DV}_{LR}[w(z), s_0] = \int_{s_0}^{\infty} ds\ \rho_{LR}(s) w(s) ,} \tag{3.43}$$

that expresses the DV as the part of the integral of the spectral function that we have not included in the sum rule. Therefore while the expression (3.39) relates the DV to the break-down of $\Pi_{LR}^{\mathrm{OPE}}(z)$ (a quark-gluon quantity) near $z = s_0$, this last expression relates it to the hadronic spectral function $\rho_{LR}(s > s_0)$.

3.5.2   WSRs: measuring the DV

In 1967 Weinberg [27] conjectured that the LR spectral function satisfy the following relations

$$\int_0^{\infty} ds\ \rho_{LR}^{(1)}(s) = 2\ f_\pi^2 \tag{3.44}$$

$$\int_0^{\infty} ds\ \rho_{LR}^{(1)}(s)s = 0 , \tag{3.45}$$

known as first and second Weiberg Sum Rules (WSRs) respectively. Later they were proven to hold within QCD in the chiral limit [28], as can be deduced from the fact that the operator-product expansion of the LR correlator starts with the dimension-six condensate in the absence of quark masses (see Section 3.4.3). Indeed the first WSR holds also for massive quarks, whereas for the second WSR we have

$$\int_0^{s_0} ds\ \rho_{LR}^{(1)}(s)s = 2\ f_\pi^2\ m_\pi^2\ + \mathcal{O}(m_q^2 \alpha_S s_0), \tag{3.46}$$

where we see that for an infinite upper limit the integral diverges, although if we do not work with large values of s_0 this divergence can be neglected. These sum rules are extremely interesting because we can take a finite upper integration limit s_0 and then we can *measure* the DV

$$\mathrm{DV}[1, s_0] = -\int_0^{s_0} ds\ \rho_{LR}^{(1)}(s) + 2\ f_\pi^2 \tag{3.47}$$

$$\mathrm{DV}[s, s_0] = -\int_0^{s_0} ds\ \rho_{LR}^{(1)}(s)\ s + 2\ f_\pi^2\ m_\pi^2 , \tag{3.48}$$

neglecting again the corrections of the form $m_q^2 \alpha_S$. The results of these *measurements* are shown in Figs. 3.6, where we can see that the DV can be very important even at energies like $s_0 \sim 3\ \mathrm{GeV}^2$.

Of course, we cannot use these relations to estimate directly the DV of any other sum rule, since it depends crucially on the weight function. However, this does not mean that they cannot be useful. In the Fig. 3.6 we can see that the DV vanishes at some finite points

$$s_0 \sim 1.5 \text{ GeV}^2 \ , \qquad s_0 \sim 2.5 \text{ GeV}^2 \ , \qquad (3.49)$$

known as **duality points**, that coincide approximately for both sum rules. This fact has been used to suggest that these points are optimal to evaluate other sum rules and minimize their DV. It is reasonable to think that the duality points of two sum rules with similar weight functions will not be very different, but once we change substantially the weight function there is no sense in assuming that the duality points will still be close to each other. Therefore this strategy based on the use of duality points must be taken with great care, something that has not been done sometimes in the literature. We can safely believe the duality-point-based prediction if it does not depend on which duality point (3.49) is taken. Otherwise one must assign an error such that covers the prediction of both duality points.

These points are nothing but values of s_0 such that there is a numerical cancellation of the contributions that are ahead of them

$$\int_{s_0}^{\infty} ds \ \rho_{LR}^{(1)}(s) \ w(s) = 0 \ , \qquad (3.50)$$

and so it is clear that the highest duality point of (3.49) must be more stable under the change of the weight function than the smallest one, since the cancellation needed is smaller. Anyway, as we have emphasized, the use of the duality points must be taken with care and the systematic error of the method will be probably quite large.
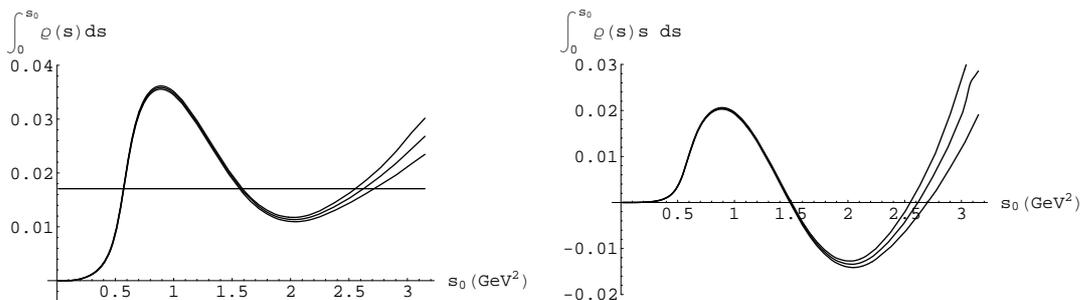
Figure 3.6: The first and second WSRs as a function of the upper integration variable s. The central curve corresponds to the central values of [3] while the upper and lower curve are the one sigma errors.

3.5.3   Pinched weights

During decades it has been assumed that the use of the so-called *pinched weights* (polynomial weights that vanish at $s = s_0$) minimizes the DV [29–35], since they

suppress the contribution from the most problematic region in the contour integral (3.39)

$$\mathrm{DV}[w(z), s_0] \; \equiv \; \frac{1}{2\pi i} \; \oint_{|s|=s_0} \mathrm{d}s \; w(s) \left(\Pi(s) - \Pi^{\mathrm{OPE}}(s) \right) \; . \tag{3.51}$$

But the alternative definition of the DV that expresses it in terms of the spectral function (3.43)

$$\mathrm{DV}[w(z), s_0] \; = \; \int_{s_0}^{\infty} \mathrm{d}s \; w(s) \, \rho(s) \; , \tag{3.52}$$

shows that things are not that simple and the assumption is not necessarily true, since a pinched-weight (PW) function will indeed suppressed the first part of this hadronic integral but at the same time may enhance the high-energy tail that can become important. If the final balance is positive and the weight function does its job minimizing the DV contribution with respect to the normal weight is something that depends on the particular weight used and on how fast the spectral function goes to zero, something that is not known theoretically.

This question about the convenience of the use of these PW is very entangled with the more general question of how to estimate the duality violation of a given sum rule. The observation of a more stable plateau in the final part of the data is the standard requirement to check if the weight improves the situation, and the deviations from the plateau the standard way of estimating the remaining DV. But it is important to notice that the existence of the plateau is a necessary but not sufficient condition, because it could be temporary. This is particularly plausible because the PWs produce curves that have derivative zero in the second duality point ($s_0 \sim 2.6 \text{ GeV}^2$), that is very near of the end of the data. That is, they produce a fake plateau, that can induce to the wrong conclusion that the DV is negligible for that weight and that value of s_0.

In principle one can know if the plateau is false or real performing a fit to a straight line. The correlations of the experimental points take into account if the plateau is real or it has been artificially created by the weight function. But in practice this fit is not always possible. The available window for the fit allows only a small range and if the correlations between points in that range are very large[10], then the standard χ^2-fit cannot be used, as explained in [36].

It must be emphasized that the PW functions are also useful because they are expected to minimize the experimental errors, since they suppress the region near the kinematical end point.

We will use these weights in the next Chapter, will give explicit examples of how they can fail in the Appendix B and will re-analyze them with the framework that we will explain in Chapter 5 to answer the question of their convenience in certain sum rules.

---

[10]This situation was found e.g. in the determination of the V-A condensates in Refs. [30, 31].

3.6   Conclusions

In this Chapter we have derived from very general first principles like analyticity and unitarity the expression of a generic QCD Sum Rule

$$\int_0^{s_0} \rho(s)w(s)ds = \operatorname*{Res}_{s=0}\left(\Pi^{\chi\mathrm{PT}}(z)w(z)\right) - \oint_{C_{out}} \frac{dz}{2\pi i}\Pi^{\mathrm{OPE}}(z)w(z) - \mathrm{DV}[w(z),s_0]. \quad (3.53)$$

This is a very important result, since it connects the hadronic observables with the quark-gluon calculations without making any assumption or working with any model. We have introduced and thoroughly explained the different elements that appear in this relation: the Wilson operator-product expansion that allows a QCD calculation of the correlator in the deep euclidean region, the spectral functions that are directly related with the experiment and the often disregarded duality violation, that will be carefully analyzed in Section 3.5. We postpone the discussion of the χPT contribution to the next Chapter, where it will be carefully studied.

To finish this Chapter with a more specific result and see the power of the sum rules, we particularize the general expression to the $\Pi_{LR}^{(0+1)}(q^2)$ correlator with the weight function $w(s) = s^2$. From expressions (3.36) and (3.23) we have

$$\int_0^{s_0} \rho_{LR}^{(1)}(s)\ s^2\ ds = 2f_\pi^2 m_\pi^4 + \mathcal{O}_6 - \mathrm{DV}[z^2, s_0]\ . \quad (3.54)$$

It can be seen that we can use this sum rule to extract from the hadronic tau data the value of $\mathcal{O}_6$, a purely non-perturbative QCD quantity. As we will see in Chapter 5 this is indeed the most precise source of information about the value of this quantity.

In the literature, given a certain correlator one can found a lot of different choices for the weight functions and the value of s_0. The Borel or Laplace Sum Rules employ weights of the form $e^{-\tau s}$ (e.g. [7,37,38]) that suppress strongly the high-energy region and therefore the DV, but at the same time they entail the appearance of an infinite number of condensates. The gaussian sum rules [39], with weight functions of the form $e^{-(s-\hat{s})/\sigma^2}$ have been used to study the violation of local duality. The Finite Energy Sum Rules [29–31,40,41] (FESRs) take a polynomial weight and a finite value of s_0 and have the advantage of involving just a small number of condensates. The finite value of s_0 generates potential problems with the DV, and there are different strategies available in the literature to minimize this problem (WSRs duality points, pinched weights, etc.). The sum rules that employ weights of the form $1/s^m$ being m a positive integer are sometimes called inverse finite energy sum rules and they are specially good behaved because the high-energy region contribution is small and the condensates do not appear.

In the next Chapters we are going to focus on the FESR and inverse FESR, but conceptually the others are very similar and our arguments and conclusions can be extended easily to those cases.

Chapter 4

Extracting Chiral LECs from tau decays

> *I was just guessing*
> *at numbers and figures,*
> *pulling the puzzles apart.*
> *Coldplay*

Thanks to the theoretical framework developed in the previous chapter, the precise hadronic τ-decay data provided in Refs. [3, 42–46] are a very important source of information, both on perturbative and non-perturbative QCD parameters.

The theoretical analysis of the inclusive τ decay width into hadrons (QCD Sum Rule with the Π_{LL} correlator) allows to perform an accurate determination of the QCD coupling $\alpha_s(M_\tau)$ [4, 29, 34, 47–50],which becomes the most precise determination of $\alpha_s(M_Z)$ after QCD running. In this case, non-perturbative QCD effects parameterized by power corrections are strongly suppressed.

Another example of the use of hadronic τ-decay data is the study of SU(3)– breaking corrections to the strangeness-changing two-point functions [5,6,35,51].The separate measurement of the $|\Delta S| = 0$ and $|\Delta S| = 1$ tau decay widths (associated to the correlators $\Pi_{ud/us,LL}$) provides accurate determinations of fundamental parameters of the Standard Model, such as the strange quark mass and the Cabibbo-Kobayashi-Maskawa quark-mixing $|V_{us}|$.

Very important phenomenological hadronic matrix elements and non-perturbative QCD quantities can also be obtained from τ-decay data. Of special interest is the difference of the vector and axial-vector spectral functions, because in the chiral limit the corresponding $V - A$ correlator (or LR correlator) is exactly zero in perturbation theory. The τ-decay measurement of the $V - A$ spectral function has been used to perform phenomenological tests of the Weinberg Sum Rules [52–54], to compute the electromagnetic mass difference between the charged and neutral pions [53], and to determine several QCD vacuum condensates (see Chapter 5). From the same spectral function one can also determine the $\Delta I = 3/2$ contribution of the $\Delta S = 1$ four-quark operators Q_7 and Q_8 to $\varepsilon'_K/\varepsilon_K$, in the chiral limit [30, 41, 54–57].

In this Chapter we will see how using Chiral Perturbation Theory (χPT) [58–60], the effective field theory of QCD at very low energies, the hadronic τ-decay data can also be related to order parameters of the spontaneous chiral symmetry breaking (SχSB) of QCD [61]. χPT describes the SχSB Nambu-Goldstone boson physics through an expansion in external momenta and quark masses and the coefficients of that expansion are related to order parameters of SχSB.

There has been a lot of recent activity to determine the value of these low-energy constant (LECs) from theory, using as much as possible QCD information [62–77]. This strong effort is motivated by the precision required in present phenomenological applications, which makes necessary to include corrections of $\mathcal{O}(p^6)$, where the huge number of unknown couplings is the major source of theoretical uncertainty.

In this Chapter we present an accurate determination of the χPT couplings L_{10}^r and C_{87}^r, using the most recent experimental data on hadronic τ decays [78, 79]. Previous work on L_{10}^r using τ-decay data can be found in Refs. [32, 33, 53, 54, 80]. Our analysis is the first one which includes the known two-loop χPT contributions and, therefore, provides also the $\mathcal{O}(p^6)$ coupling C_{87}^r.

4.1   Chiral Perturbation Theory

Chiral Perturbation Theory [58–60] (see e.g. [81] for a pedagogical introduction) is the effective field theory (EFT) of the strong interactions at low energies. The central idea of the EFT approach was formulated by Weinberg as follows [58]: "... if one writes down the most general possible Lagrangian, including *all* terms consistent with assumed symmetry principles, and then calculates matrix elements with this Lagrangian to any given order of perturbation theory, the result will simply be the most general possible S–matrix consistent with analyticity, perturbative unitarity, cluster decomposition and the assumed symmetry principles."[1]

In the context of QCD these ideas have been applied to the interactions among the Goldstone bosons associated with the spontaneous chiral symmetry breaking. In this case, the effective theory is formulated in terms of the asymptotically observed states instead of the degrees of freedom of the underlying QCD Lagrangian (quarks and gluons).

A successful EFT program requires both the knowledge of the most general Lagrangian up to a given order as well as an expansion scheme for observables. Due to the small Goldstone boson masses and their vanishing interactions in the zero-energy limit, a derivative and quark-mass expansion is a natural scenario for the corresponding EFT. At present, in the mesonic sector the Lagrangian is known up to and including $\mathcal{O}(p^6)$, where p denotes a small quantity such as a four momentum or a pion mass.

---

[1]This procedure will be applied in the construction of the effective Lagrangian of Chapter 6

4.1.1 The effective Lagrangian

The starting point of mesonic Chiral Perturbation Theory is the QCD Lagrangian for N_l massless (light) quarks:

$$\mathcal{L}_{\mathrm{QCD}}^0 = \sum_{l=1}^{N_l} (\bar{q}_{R,l} i\slashed{D}\, q_{R,l} + \bar{q}_{L,l} i\slashed{D}\, q_{L,l}) - \frac{1}{4}\mathcal{G}_{\mu\nu,a}\mathcal{G}_a^{\mu\nu} , \tag{4.1}$$

where $q_{L/R,l}$ denote the left/right-handed components of the light quark fields, $D_\mu q_{L/R,l}$ is the covariant derivative and $\mathcal{G}_{\mu\nu,a}$ are the corresponding gluonic field strengths. Here, we will be concerned with the cases $N_l = 2, 3$ referring to (u, d) or (u, d, s) quarks, respectively. This Lagrangian is invariant under separate global $\mathrm{SU}(N_l)_{L/R}$ transformations of the left- and right-handed fields and, in addition, it has an overall $\mathrm{U}(1)_V$ symmetry. Different empirical facts give rise to the assumption that this chiral symmetry is spontaneously broken down to its vectorial subgroup $\mathrm{SU}(N_l)_V \times \mathrm{U}(1)_V$. For example, the low-energy hadron spectrum seems to follow multiplicities of the irreducible representations of the group $\mathrm{SU}(N_l)$ instead of $\mathrm{SU}(N_l)_L \times \mathrm{SU}(N_l)_R$, as indicated by the absence of degenerate multiplets of opposite parity. Besides, the lightest mesons form a pseudoscalar octet with masses much smaller than those of the corresponding vector mesons. According to Coleman's theorem [82], the symmetry pattern of the spectrum reflects the invariance of the vacuum state. Therefore, as a result of Goldstone's theorem [83], one would expect 3 (8) massless Goldstone bosons for $N_l = 2$ (3) with vanishing interactions as their energies tend to zero. The explicit symmetry breaking due to small but finite u, d and s quark masses, that will be treated perturbatively, generates also small masses for these Goldstone bosons.

The QCD symmetries and its symmetry breaking pattern —due to the quark masses— are mapped onto the most general effective Lagrangian for the interaction of the Goldstone bosons. This Lagrangian is organized in the number of derivatives and quark mass terms [58–60, 84–87]

$$\mathcal{L}_{\chi\mathrm{PT}}(x) = \mathcal{L}_2 + \mathcal{L}_4 + \mathcal{L}_6 + \cdots , \tag{4.2}$$

where the lowest-order Lagrangian is given by[2]

$$\mathcal{L}_2 = \frac{f^2}{4}\mathrm{Tr}\Big[D_\mu U (D^\mu U)^\dagger + \chi U^\dagger + U\chi^\dagger\Big]. \tag{4.3}$$

Here,

$$U(x) = \exp\left(i\frac{\sqrt{2}\,\phi}{f}\right), \quad \phi = \begin{pmatrix} \frac{1}{\sqrt{2}}\pi^0 + \frac{1}{\sqrt{6}}\eta_8 & \pi^+ & K^+ \\ \pi^- & -\frac{1}{\sqrt{2}}\pi^0 + \frac{1}{\sqrt{6}}\eta_8 & K^0 \\ K^- & \bar{K}^0 & -\frac{2}{\sqrt{6}}\eta_8 \end{pmatrix},$$

is a matrix containing the Goldstone boson fields and f denotes the pion decay constant in the chiral limit: $f_\pi = f[1 + \mathcal{O}(m_{u,d})] = 92.4$ MeV. Under a chiral

---

[2]In the following, we will give equations for the three-flavor case.

transformation $q_{R,L} \rightarrow g_{R,L}\, q_{R,L}$, where $(g_L, g_R) \in SU(3)_L \times SU(3)_R$, the matrix U transforms as $U \rightarrow g_R\, U\, g_L^\dagger$.

When including external sources in the QCD Lagrangian, the covariant derivative is defined as[3]

$$
\begin{aligned}
D_\mu U &= \partial_\mu U - ir_\mu U + iU\ell_\mu \,, &\text{(4.5)}\\
D_\mu U^\dagger &= \partial_\mu U^\dagger + iU^\dagger r_\mu - i\ell_\mu U^\dagger \,. &\text{(4.6)}
\end{aligned}
$$

The small quark masses are contained in $\chi = 2B_0\mathcal{M}$, where $\mathcal{M} = \mathrm{diag}(m_u, m_d, m_s)$ is the quark mass matrix and B_0 is related to the quark condensate $\langle \bar{q}q \rangle_0$ in the chiral limit.

The next-to-leading-order Lagrangian contains 10 low-energy constants L_i [60]

$$
\begin{aligned}
\mathcal{L}_4(x) =\;& L_1 \langle D_\mu U^\dagger D^\mu U \rangle^2 + L_2 \langle D_\mu U^\dagger D_\nu U \rangle \langle D^\mu U^\dagger D^\nu U \rangle \\
&+ L_3 \langle D_\mu U^\dagger D^\mu U D_\nu U^\dagger D^\nu U \rangle + L_4 \langle D_\mu U^\dagger D^\mu U \rangle \langle U^\dagger \chi + \chi^\dagger U \rangle \\
&+ L_5 \langle D_\mu U^\dagger D^\mu U \left(U^\dagger \chi + \chi^\dagger U \right) \rangle + L_6 \langle U^\dagger \chi + \chi^\dagger U \rangle^2 \\
&+ L_7 \langle U^\dagger \chi - \chi^\dagger U \rangle^2 + L_8 \langle \chi^\dagger U \chi^\dagger U + U^\dagger \chi U^\dagger \chi \rangle \\
&- iL_9 \langle F_R^{\mu\nu} D_\mu U D_\nu U^\dagger + F_L^{\mu\nu} D_\mu U^\dagger D_\nu U \rangle + L_{10} \langle U^\dagger F_R^{\mu\nu} U F_{L\mu\nu} \rangle \\
&+ H_1 \langle F_{R\mu\nu} F_R^{\mu\nu} + F_{L\mu\nu} F_L^{\mu\nu} \rangle + H_2 \langle \chi^\dagger \chi \rangle \,, &\text{(4.7)}
\end{aligned}
$$

where the field strength tensors are defined by

$$
\begin{aligned}
F_L^{\mu\nu} &= \partial^\mu \ell^\nu - \partial^\nu \ell^\mu - i[\ell^\mu, \ell^\nu] \,, &\text{(4.8)}\\
F_R^{\mu\nu} &= \partial^\mu r^\nu - \partial^\nu r^\mu - i[r^\mu, r^\nu] \,. &\text{(4.9)}
\end{aligned}
$$

The terms proportional to H_1 and H_2 do not contain the pseudoscalar fields and are therefore not directly measurable

At $\mathcal{O}(p^6)$, 90 (23) additional low-energy constant $C_{i=1,\cdots,90}$ appear in the even (odd) intrinsic parity sector [84–86]. We show here just one of the terms

$$
\mathcal{L}_6(x) = C_{87} \langle \nabla_\rho f_{-\mu\nu} \nabla^\rho f_-^{\mu\nu} \rangle + \dots \qquad\text{(4.10)}
$$

for illustration and because we will determine in this chapter the value of this C_{87} parameter.

The low-energy constants f_π, B, $L_{i=1,\cdots,10}$ and $C_{i=1,\cdots,90}$ are not fixed by symmetry requirements alone and have to be determined phenomenologically or using non-perturbative techniques. The $\mathcal{O}(p^2)$ and $\mathcal{O}(p^4)$ couplings have been determined in the past to an acceptable accuracy (a recent compilation can be found in Ref. [88]) but the $\mathcal{O}(p^6)$ couplings C_i are much less well determined.

---

[3] Here $r_\mu \equiv v_\mu + a_\mu$ and $\ell_\mu \equiv v_\mu - a_\mu$ are defined as the external sources added to the symmetric Lagrangian (4.1)

$$
\mathcal{L}_{QCD} = \mathcal{L}_{QCD}^0 + \bar{q}\gamma^\mu (v_\mu + \gamma_5 a_\mu)q - \bar{q}(s - i\gamma_5 p)q \,. \qquad\text{(4.4)}
$$

This formalism is used to incorporate the explicit breaking of chiral symmetry through the quark masses (making $s = \mathcal{M}$) and also to incorporate the electromagnetic and weak interactions.

4.1.2 Weinberg's power counting scheme

In addition to the most general Lagrangian, one needs a method to assess the importance of the various diagrams calculated from the effective Lagrangian. Using Weinberg's power counting scheme [58], one may analyze the behavior of a given diagram calculated in the framework of Eq. (4.2) under a linear re-scaling of all *external* momenta, $p_i \mapsto t p_i$, and a quadratic re-scaling of the light quark masses, $\hat{m} \mapsto t^2 \hat{m}$. The chiral dimension D of a given diagram with amplitude $\mathcal{M}(p_i, \hat{m})$ is defined by

$$\mathcal{M}(t p_i, t^2 \hat{m}) = t^D \mathcal{M}(p_i, \hat{m}), \tag{4.11}$$

where, in n dimensions,

$$D = 2 + (n-2)N_L + \sum_{k=1}^{\infty} 2(k-1)N_{2k}^\pi \geq 2 \text{ in 4 dimensions}, \tag{4.12}$$

where N_L is the number of independent loop momenta and N_{2k}^π the number of vertices originating from $\mathcal{L}_{2k}(x)$. A diagram with chiral dimension D is said to be of order $\mathcal{O}(p^D)$. Clearly, for small enough momenta and masses diagrams with small D, such as $D = 2$ or $D = 4$, should dominate[4]. Note that, for $n = 4$, loop diagrams are always suppressed due to the term $2N_L$ in Eq. (4.12) and therefore we have a perturbative scheme in terms of external momenta and masses which are small compared to some scale (here $4\pi f \approx 1$ GeV).

It can be shown that, when calculating one-loop graphs, using vertices from $\mathcal{L}_2$ of Eq. (4.3), one generates ultraviolet divergences that can be absorbed into the redefinition of the fields and the parameters of the most general Lagrangian. Since $\mathcal{L}_2$ of Eq. (4.3) is not renormalizable in the traditional sense, the infinities cannot be absorbed by a renormalization of the coefficients f and B. According to Weinberg's power counting of Eq. (4.12), one-loop graphs with vertices from $\mathcal{L}_2$ are of $\mathcal{O}(p^4)$ and therefore one needs to renormalize the parameters of $\mathcal{L}_4$ to cancel one-loop infinities. So we see that the theory is renormalizable order by order.

4.2 Theoretical Framework

During this chapter we will work with the LR correlator $\Pi(q^2) \equiv \Pi_{ud,LR}^{(0+1)}(q^2)$ defined in (3.6) that we repeat here

$$\Pi_{ud,LR}^{\mu\nu}(s) = i \int d^4x \, e^{iqx} \langle 0 | T \left(L_{ud}^\mu(x) R_{ud}^\nu(0)^\dagger \right) | 0 \rangle$$

$$= (-g^{\mu\nu}q^2 + q^\mu q^\nu) \, \Pi_{ud,LR}^{(0+1)}(q^2) + g^{\mu\nu}q^2 \, \Pi_{ud,LR}^{(0)}(q^2), \tag{4.13}$$

---

[4]The re-scaling of Eq. (4.11) must be viewed as a mathematical tool. While external three-momenta can, to a certain extent, be made arbitrarily small, the re-scaling of the quark masses is a theoretical instrument only.

where $L_{ud}^{\mu}(x) \equiv \bar{u}\gamma^{\mu}(1-\gamma_5)d$ and $R_{ud}^{\mu}(x) \equiv \bar{u}\gamma^{\mu}(1+\gamma_5)d$. It is convenient to make explicit the contribution of the pion pole to the correlator

$$\Pi(s) = \frac{2f_{\pi}^2}{s - m_{\pi}^2} + \overline{\Pi}(s) . \tag{4.14}$$

We will work in the isospin limit $m_u = m_d$ where $\Pi_{ud,V}^{(0)}(q^2) = 0$. In particular we will concentrate in this chapter in the QCD Sum Rules that are obtained for this correlator and the weights $w(s) = s^{-2}, s^{-1}$, so that we only have to take our general formula (3.15) derived in the previous chapter and particularize it to this situation. In this way we have the exact relation

$$\int_{s_{\rm th}}^{s_0}\frac{{\rm d}s}{s^m}\, \rho(s) \;+\; \frac{1}{2\pi i}\oint_{|s|=s_0}\frac{{\rm d}s}{s^m}\Pi^{\rm OPE}(s) + {\rm DV}[s^{-m}, s_0] = \frac{2f_{\pi}^2}{m_{\pi}^{2m}} + \operatorname*{Res}_{s=0}\frac{\Pi(s)}{s^m} . \tag{4.15}$$

For positive values of m the OPE does not give any contribution to the integration along the circle $|s| = s_0$ if we neglect the logarithmic corrections to the Wilson coefficients. In order to calculate the residue at the origin of $\Pi(s)/s^m$ we expand the V-A correlator in his Taylor series[5]

$$\overline{\Pi}(s) = \overline{\Pi}(0) + \overline{\Pi}'(0)\cdot s + \frac{1}{2}\overline{\Pi}''(0)\cdot s^2 + \dots , \tag{4.16}$$

and one gets then:

$$\int_{s_{\rm th}}^{s_0}\frac{{\rm d}s}{s^m}\,\rho(s) + {\rm DV}[s^{-m}, s_0] \;=\; \frac{2f_{\pi}^2}{m_{\pi}^{2m}} + \frac{\Pi^{(m-1)}(0)}{(m-1)!} \;=\; \frac{\overline{\Pi}^{(m-1)}(0)}{(m-1)!} , \tag{4.17}$$

where $\overline{\Pi}^{(m-1)}(0)$ denotes the $(m-1)$th derivative of $\overline{\Pi}(s)$ at $s = 0$. Therefore we have the following two sum rules for the $m = 1, 2$ cases

$$\int_{s_{\rm th}}^{s_0}{\rm d}s\,\frac{1}{s^2}\,\rho(s) + {\rm DV}[1/s^2, s_0] \;=\; \overline{\Pi}'(0) , \tag{4.18}$$

$$\int_{s_{\rm th}}^{s_0}{\rm d}s\,\frac{1}{s}\,\rho(s) + {\rm DV}[1/s, s_0] \;=\; \overline{\Pi}(0) . \tag{4.19}$$

The interest of this relation stems from the fact that at low values of s the correlator can be rigourously calculated within χPT. At present $\Pi(s)$ is known up to $\mathcal{O}(p^6)$ [89], in terms of the LECs that we want to determine[6]. The choices $m = 1$ and $m = 2$ allow us then to relate the spectral function measured in τ decays with the theoretical expressions of $\overline{\Pi}(0)$ and $\overline{\Pi}'(0)$

$$\overline{\Pi}(0) \;=\; -8\,{\rm L}_{10}^r(\mu) + {\rm corrections} , \tag{4.20}$$

$$\overline{\Pi}'(0) \;=\; 16\,{\rm C}_{87}^r(\mu) \;+\; \frac{1}{480\,\pi^2}\left(\frac{1}{m_K^2} + \frac{2}{m_{\pi}^2}\right) + {\rm corrections} , \tag{4.21}$$

---

[5]In principle one should perform the Laurent expansion of the V-A correlator, but we have taken into account its analytic properties near the origin.

[6]See Appendix C for the complete expression of $\Pi(s)$ at order $\mathcal{O}(p^6)$.

where the corrections will be calculated in Section 4.4. Here $L_{10}^r(\mu)$ and $C_{87}^r(\mu)$ are the renormalized low-energy constants at the scale μ and, as any μ-dependent quantity, they are not directly observable. We define now the effective parameters

$$
L_{10}^{\text{eff}} \equiv -\frac{1}{8}\overline{\Pi}(0) = L_{10}^r(\mu) + \text{corrections}\,, \tag{4.22}
$$

$$
C_{87}^{\text{eff}} \equiv \frac{1}{16}\overline{\Pi}'(0) = C_{87}^r(\mu) + \frac{1}{7680\,\pi^2}\left(\frac{1}{m_K^2}+\frac{2}{m_\pi^2}\right) + \text{corrections}\,, \tag{4.23}
$$

that are μ-independent and directly observable as the sum rules (4.19) and (4.18) show clearly. In the next section we will extract their value from the hadronic τ-decay measurements, whereas in Section 4.4 we will calculate their exact relation with the corresponding χPT parameters and derive numerical values for those LECs.

4.3 Determination of Effective Couplings

We will use the 2005 ALEPH data on semileptonic τ decays [3], shown in Fig. 3.3, which provide the most recent and precise measurement of the $V - A$ spectral function. As we have seen the effective chiral couplings can be directly extracted from the following integrals over the hadronic spectrum:

$$
-8\,L_{10}^{\text{eff}} \equiv \overline{\Pi}(0) = \frac{1}{\pi}\int_{s_{th}}^{s_0}\frac{\mathrm{d}s}{s}\,\rho(s)\,, \tag{4.24}
$$

$$
16\,C_{87}^{\text{eff}} \equiv \overline{\Pi}'(0) = \frac{1}{\pi}\int_{s_{th}}^{s_0}\frac{\mathrm{d}s}{s^2}\,\rho(s)\,. \tag{4.25}
$$

These relations are exactly satisfied at $s_0 \to \infty$, whereas at finite values of s_0 we will have a contribution from the quark-hadron duality violation, that we have not explicitly written. Therefore (4.24) and (4.25) assume that the OPE approximates well the correlator $\Pi(s)$ over the entire complex circle $|s| = s_0$, or equivalently, that that the integrals on the real axis from s_0 to infinite are negligible (compared with the experimental errors), what is expected to be true only for high enough values of s_0 and for accidental "duality points". The kinematics of τ decay restrict the upper limit of integration to the range $0 \leq s_0 \leq m_\tau^2$ and therefore we are forced to work with a finite value of s_0.

If the cutoff $s_0 = m_\tau^2$ is high enough to neglect the DV error is something that we have to conclude *a posteriori*, from the study of the sensitivity to s_0 of the integrals (4.24) and (4.25), although the particular weights of these sum rules are likely to generate a small DV, since they suppress the high-energy region.

In Fig. 4.1, we plot the value of L_{10}^{eff} and C_{87}^{eff} obtained from Eq. (4.24) and Eq. (4.25) for different values of s_0 using the ALEPH data. The band between the continuous lines shows the corresponding experimental uncertainties (at one sigma). As expected, the result is far from an horizontal line at low values of s_0, where the applicability of the OPE is suspect. The oscillatory behavior stabilizes quite fast reaching a rather stable and flat result at values of s_0 between 2 and 3 GeV^2. The
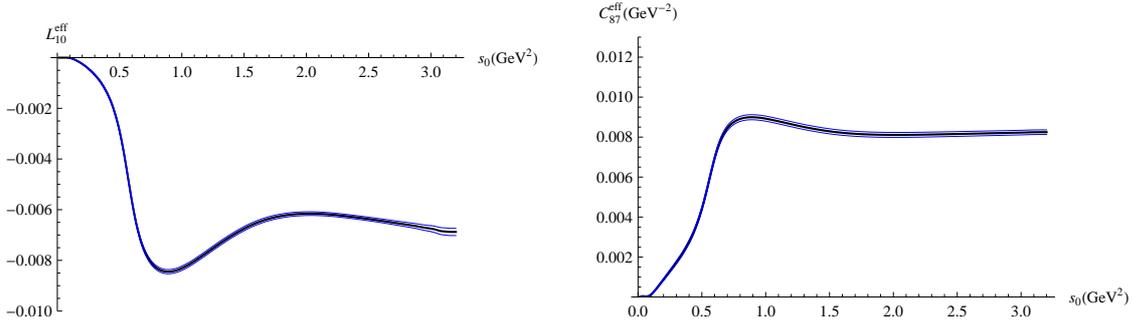
Figure 4.1: Results obtained for the effective parameter using the relations (4.24) and (4.25) with the tau decay data and taking different values for s_0.

weight factor $1/s^m$ decreases the impact of the high-energy region, minimizing the size of quark-hadron duality violations, and the integrals appear then to be much better behaved than the corresponding FESRs with s^n ($n \geq 0$) weights, as we will explicitly check in the next chapter.

In the case of L_{10}^{eff} if we look close enough (see Fig. 4.2) we find that the current experimental data are sufficiently accurate to appreciate that the plateau is only approximate, that is, the small DV is still larger than the experimental error. In the case of C_{87}^{eff} the DV is smaller and the experimental error band is compatible with a perfect plateau, that is to say, the DV is smaller than the experimental errors (or at most it is of the same order).
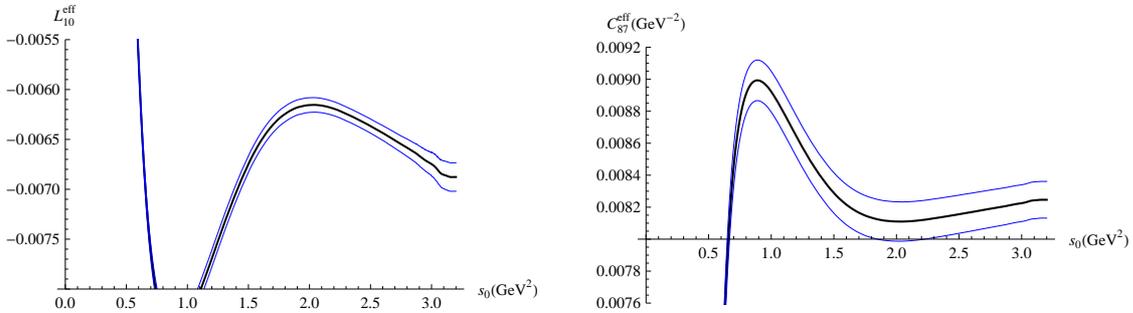
Figure 4.2: Enlargements of the curves shown in the Fig. 4.1.

Consequently the choice of a specific value of s_0 will not be relevant for C_{87}^{eff}, but it will be for L_{10}^{eff}, where different values of s_0 will produce incompatible values of L_{10}^{eff}. Of course, one can just assign an overestimated error compatible with any value s_0 of the plateau, let's say

$$L_{10}^{\text{eff}} = -(6.6 \pm 0.3) \cdot 10^{-3} , \tag{4.26}$$
$$C_{87}^{\text{eff}} = +(8.15 \pm 0.20) \cdot 10^{-3} \, \text{GeV}^{-2} , \tag{4.27}$$

but as we have said this is an overestimated error (especially in the case of L_{10}^{eff}) and we have theoretical information (the WSRs) that can be used to improve this

determination. In order to exploit this theoretical information about the behavior of the DV and estimate the central value for L_{10}^{eff} and its error, there are different strategies available in the literature. We review them here with a critical analysis:

- **Maximum value of** s_0.- The naive choice is to take s_0 as large as possible [42, 44, 53], that is $s_0 = m_\tau^2$, in order to minimize the DV error. Although in principle one expects that the larger is s_0 the smaller is the DV, the WSRs teach us that this reasoning can be too naive due to the oscillatory behavior of the spectral function. Assuming than the lessons learned from the WSRs can be applied to these sum rules (that is, that the weights are not dramatically different), we know that the cancellations make $s_0 \sim 2.5$ GeV^2 a much better choice. Besides, the maximum s_0 entails a big experimental error. Because of these reasons we will not take this point.

- **Representative-plateau point**.- In order to minimize the DV (that decreases with s_0) and the experimental error (that grows with s_0) one can take a point approximately in the middle of the plateau, that will be large but not the maximum [33]

$$L_{10}^{\text{eff}}(s_0 = 2.7 \text{ GeV}^2) = -(6.51 \pm 0.08) \cdot 10^{-3} \qquad (4.28)$$
$$C_{87}^{\text{eff}}(s_0 = 2.7 \text{ GeV}^2) = +(8.18 \pm 0.12) \cdot 10^{-3} \text{ GeV}^{-2}, \qquad (4.29)$$

  where the errors are purely experimental and do not contain any estimation of the DV contribution, that as we have seen in the figures is not negligible, at least in the case of L_{10}^{eff}.

- **Duality points**.- Another possibility is to give the predictions fixing s_0 at the so-called duality points, where the first and second WSRs happen to be satisfied (see Section 3.5.2). At the highest "duality point", which is more reliable, we obtain $L_{10}^{\text{eff}} = -(6.45 \pm 0.09) \cdot 10^{-3}$, where the quoted error only includes the experimental uncertainty. Being conservative, one could also take into account the first "duality point"; performing a weighted average of both results, we get $L_{10}^{\text{eff}} = -(6.50 \pm 0.13) \cdot 10^{-3}$, where the uncertainty covers the values obtained at the two duality points.

- **Oscillations**.- We know that the V-A spectral function should go to zero as s_0 increases and the expected behavior is oscillatory. Therefore assuming that the integral (4.24) oscillates around his asymptotic value with decreasing oscillations, one can get another estimate performing an average between the maxima and minima of the successive oscillations. This procedure gives a value $L_{10}^{\text{eff}} = -(6.5 \pm 0.2) \cdot 10^{-3}$, that is perfectly compatible with the previous results based on the duality points.

- **Continuing the spectral function**.- Using appropriate oscillating functions defined in [22] which mimic the real quark-hadron oscillations above the data[7]

---

[7]We will develop this idea with great detail in the next Chapter.

we can get another estimate. These functions are defined such that they match the data at ~ 3 GeV^2, go to zero with decreasing oscillations and satisfy the first and second WSRs. We find in this way $L_{10}^{\text{eff}} = -(6.50 \pm 0.12) \cdot 10^{-3}$, where the error spans the range generated by the different functions used. This result agrees well with our previous estimates.

- **Pinched weights**[8].- We can take advantage of the WSRs to construct modified sum rules with weight factors proportional to $(1 - s/s_0)$, in order to suppress numerically the role of the suspect region around $s \sim s_0$:

$$-8\,L_{10}^{\text{eff}} = \frac{1}{\pi} \int_{s_{th}}^{s_0} \frac{\mathrm{d}s}{s} \left(1 - \frac{s}{s_0}\right) \rho(s) + \Delta_1(s_0), \tag{4.30}$$

$$= \frac{1}{\pi} \int_{s_{th}}^{s_0} \frac{\mathrm{d}s}{s} \left(1 - \frac{s}{s_0}\right)^2 \rho(s) + 2\Delta_1(s_0) - \Delta_2(s_0). \tag{4.31}$$

The factors $\Delta_1(s_0) = \left(2f_\pi^2 + \tilde{C}_2^{LR}\right)/s_0$ and $\Delta_2(s_0) = \left(2f_\pi^2 m_\pi^2 - \tilde{C}_4^{LR}\right)/s_0^2$ are small corrections dominated by the f_π^2 term, since $\tilde{C}_{2,4}^{LR}$ vanish in the chiral limit (see the OPE in Eq. (3.34) to see the definition of $\tilde{C}_n^{LR}$). The sum rule (4.31) has been previously used in Refs. [32,33]. The dashed and dot-dashed lines in Fig. 4.3 show the results obtained from Eqs. (4.30) and (4.31), respectively. As already found in Refs. [32,33], these PW minimize the theoretical uncertainties in a sizable way, giving rise to very stable results over a quite wide range of s_0 values. One gets then $L_{10}^{\text{eff}} = -(6.51 \pm 0.06) \cdot 10^{-3}$ using Eq. (4.30), and $L_{10}^{\text{eff}} = -(6.45 \pm 0.06) \cdot 10^{-3}$ from Eq. (4.31).

Taking into account all the previous discussion, we quote as our final result:

$$L_{10}^{\text{eff}} = -(6.48 \pm 0.06) \cdot 10^{-3}. \tag{4.32}$$

We have made a completely analogous analysis to determine the effective coupling C_{87}^{eff}. The results are shown in Fig. 4.4. The continuous lines, obtained from Eq. (4.25), are much more stable than the corresponding results for L_{10}^{eff}, owing to the $1/s^2$ factor in the integrand. The dashed and dot-dashed lines correspond to the results obtained from the modified sum rules:

$$16\,C_{87}^{\text{eff}} = \frac{1}{\pi} \int_{s_{th}}^{s_0} \frac{\mathrm{d}s}{s^2} \left(1 - \frac{s^2}{s_0^2}\right) \rho(s) + \frac{\Delta_1(s_0)}{s_0}, \tag{4.33}$$

$$= \frac{1}{\pi} \int_{s_{th}}^{s_0} \frac{\mathrm{d}s}{s^2} \left(1 - \frac{s}{s_0}\right)^2 \left(1 + 2\frac{s}{s_0}\right) \rho(s) + \frac{3\Delta_1(s_0) - 2\Delta_2(s_0)}{s_0}. \tag{4.34}$$

---

[8] As was explained in Section 3.5.3 the use of the PW is not always beneficial and they can generate an underestimation of the errors. Due to this we have not based our analysis entirely on them, but we have used other methods to check the compatibility of their results. In Appendix B we analyze the use of the PW in these sum rules and in the next chapter we will prove (within our parameterization) that they indeed minimize the experimental and DV error.
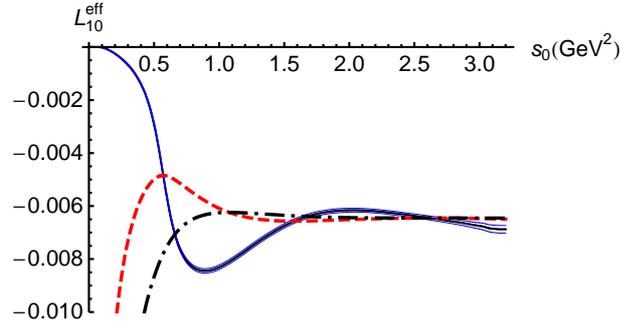
Figure 4.3: Determinations of L_{10}^{eff} at different values of s_0, using the modified expressions of Eqs. (4.30) (dashed line) and (4.31) (dot-dashed line). For clarity, we do not include their corresponding error bands. We left the result obtained with the standard weight Eq. (4.24) (solid line) for comparison.

The agreement among the different estimates is quite remarkable. We quote as our final conservative result,

$$C_{87}^{\text{eff}} = (8.18 \pm 0.13) \cdot 10^{-3}\,\text{GeV}^{-2}\,. \tag{4.35}$$
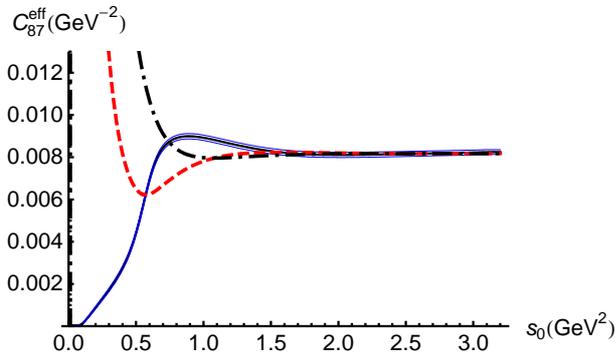
Figure 4.4: Determinations of C_{87}^{eff} at different values of s_0. The continuous lines show the results obtained from Eq. (4.25). The modified expressions in Eqs. (4.33) and (4.34) give rise to the dashed and dot-dashed lines, respectively. For clarity, we do not include their corresponding error bands.

4.4   χPT results

In this section we will calculate the behavior near the origin of the V-A correlator with χPT and therefore we will relate the effective parameters to the LECs of the theory (at a certain renormalization scale). In particular we need to calculate the value of $\Pi(s)$ and his derivative in the origin.

4.4.1   Calculation at order p^4

Before going on to the $\mathcal{O}(p^6)$ calculation it is interesting to present the more simple $\mathcal{O}(p^4)$ calculation, that it is equivalent conceptually but does not involve so long expressions. Therefore we start from the well-known result [60]

$$\Pi(s) = \frac{2f_\pi^2}{s - m_\pi^2} - 8L_{10}^r - 8B_V^{\pi\pi}(s) - 4B_V^{KK}(s) \tag{4.36}$$

where

$$B_V^{ii}(s) \equiv \frac{1}{192\pi^2}\sigma^2(\sigma \log \frac{\sigma-1}{\sigma+1} + 2) - \frac{1}{32\pi^2}(\log \frac{m_i^2}{\mu^2} + 1) + \frac{1}{288\pi^2} , \tag{4.37}$$

$$\sigma \equiv \sqrt{1 - \frac{4m_i^2}{s}} . \tag{4.38}$$

From this expression we have

$$
\begin{aligned}
\frac{-1}{8}\,\overline{\Pi}\,(0) &= L_{10}^r + \lim_{s\to 0} B_V^{\pi\pi}(s) + \frac{1}{2}\lim_{s\to 0} B_V^{KK}(s) \\
&= L_{10}^r + \frac{1 + \log \frac{m_\pi^2}{\mu^2}}{192\pi^2} + \frac{1 + \log \frac{m_K^2}{\mu^2}}{384\pi^2} \\
&= L_{10}^r + \frac{1}{384\pi^2} \log \frac{m_K^2}{m_\pi^2} + \frac{1 + \log \frac{m_\pi^2}{\mu^2}}{128\pi^2} ,
\end{aligned}
\tag{4.39}
$$

and we can see that the effective parameter L_{10}^{eff} (l.h.s.) correspond to the low-energy constant $L_{10}^r(\mu)$ but for a correction that cancels the χPT renormalization scale dependence of $L_{10}^r(\mu)$ (and hence the name of L_{10}^{eff}). We extend this notation and define in the same way C_{87}^{eff}, although in this case C_{87}^r may not be the largest contribution, since there is another contribution at order p^4

$$
\begin{aligned}
\frac{1}{16}\,\overline{\Pi}'(0) &= \frac{-1}{16}\left(8\lim_{s\to 0}\frac{d}{ds}B_V^{\pi\pi}(s) - 4\lim_{s\to 0}\frac{d}{ds}B_V^{KK}(s) \right) \\
&= \frac{1}{16}\frac{1}{480\pi^2}\left(\frac{1}{m_K^2} + \frac{2}{m_\pi^2} \right) .
\end{aligned}
\tag{4.40}
$$

Of course at this order we cannot extract C_{87}^r from C_{87}^{eff} because we do not have still C_{87}^r in the χPT Lagrangian, but we can just see how important is the $\mathcal{O}(p^4)$ contribution to C_{87}^{eff}.

4.4.2   Calculation at order p^6

In this section we will start from the following result for the V-A correlator [89]

$$
\begin{aligned}
\Pi(s) \;=\;\; & \frac{2f_\pi^2}{s - \mathrm{m}_\pi^2} - 8\mathrm{L}_{10}^r - 8B_V^{\pi\pi}(s) - 4B_V^{KK}(s) && (4.41) \\
& + 16\; \mathrm{C}_{87}^r\; s && (4.42) \\
& - 32\; \mathrm{m}_\pi^2\; (C_{61}^r - C_{12}^r - C_{80}^r) && (4.43) \\
& - 32\; (\mathrm{m}_\pi^2 + 2\mathrm{m}_K^2)\; (C_{62}^r - C_{13}^r - C_{81}^r) && (4.44) \\
& + 16\left((2\mu_\pi + \mu_K)(\mathrm{L}_9^r + 2\mathrm{L}_{10}^r) - (2B_V^{\pi\pi}(s) + B_V^{KK}(s))\; \mathrm{L}_9^r\; \frac{s}{f_\pi^2} \right) && (4.45) \\
& - 8\; G_{2L}(\mu, s)\;, && (4.46)
\end{aligned}
$$

where the functions $B_V^{ii}(s)$ were defined in (4.37), $G_{2L}(s)$ represents the 2-loop contributions (the explicit expression can be found in Appendix C , but we will work with this notation in order to avoid endless expressions) and

$$
\mu_i = \frac{m_i^2}{32\pi^2 f_\pi^2} \log \frac{m_i^2}{\mu^2}\;. \tag{4.47}
$$

It is convenient to analyze the different terms of this expression, looking not only to their importance in the chiral expansion but also in the expansion in the number of quark colors N_c [90]:

- (4.41) is the contribution of order p^2 and p^4. Notice that the one-loop corrections given by the $B_V^{ii}(s)$ functions are suppressed by one power of $1/N_C$ with respect to the $\mathrm{L}_{10}^r(\mu)$ contact term;

- (4.42) is the s-dependent part of the $\mathcal{O}(p^6)$ counterterms;

- (4.43) is a counterterm contribution suppressed by the factor m_π^2;

- (4.44) is a counterterm contribution that is enhanced by $\mathrm{m}_K^2/\mathrm{m}_\pi^2$ with respect to (4.43), but has a $1/N_c$ suppression factor because these LECs are associated to operators with two traces [63, 85];

- (4.45) is the one-loop contribution of the order p^4 χPT Lagrangian and therefore is also suppressed by a factor $1/N_c$ with respect to (4.43). It contains LECs of order p^4;

- (4.46) is the two-loop contribution, does not depend on any LEC, and it is suppressed by a factor $(1/N_c)^2$ with respect to (4.43).

From this expression we can calculate the value of the correlator and his derivative in the origin, finding

$$
\begin{aligned}
\mathrm{L}_{10}^{\mathrm{eff}} \;\equiv\; & -\frac{1}{8}\,\overline{\Pi}(0) \\
=\; & \mathrm{L}_{10}^r(\mu) + \frac{1}{128\,\pi^2}\left[1 - \log\left(\frac{\mu^2}{m_\pi^2}\right) + \frac{1}{3}\log\left(\frac{m_K^2}{m_\pi^2}\right)\right] \\
& +\; 4m_\pi^2\,(C_{61}^r - C_{12}^r - C_{80}^r)(\mu) \\
& +\; 4\left(2m_K^2 + m_\pi^2\right)(C_{62}^r - C_{13}^r - C_{81}^r)(\mu) \\
& -\; 2\,(2\mu_\pi + \mu_K)\,(\mathrm{L}_9^r + 2\mathrm{L}_{10}^r)(\mu) \\
& +\; G_{2L}(\mu, s{=}0) + \mathcal{O}(p^8)\,,
\end{aligned}
\tag{4.48}
$$

$$
\begin{aligned}
\mathrm{C}_{87}^{\mathrm{eff}} \;\equiv\; & \frac{1}{16}\,\overline{\Pi}\,'(0) \\
=\; & \mathrm{C}_{87}^r(\mu) + \frac{1}{7680\,\pi^2}\left(\frac{1}{m_K^2} + \frac{2}{m_\pi^2}\right) \\
& -\; \frac{1}{64\,\pi^2 f_\pi^2}\left[1 - \log\left(\frac{\mu^2}{m_\pi^2}\right) + \frac{1}{3}\log\left(\frac{m_K^2}{m_\pi^2}\right)\right]\mathrm{L}_9^r(\mu) \\
& -\; \frac{1}{2}\,G_{2L}'(\mu, s{=}0) + \mathcal{O}(p^8)\,,
\end{aligned}
\tag{4.49}
$$

where $G_{2L}'(\mu, s) \equiv \frac{d}{ds}G_{2L}(\mu, s)$.

The derivative operation, when acting over the one-loop contribution to $\Pi(s)$, generates the terms proportional to inverse powers of the pion and kaon masses in the second line. For simplicity, we relegate the explicit analytic forms of $G_{2L}(\mu)$ and $G_{2L}'(\mu)$, which are very lengthy and not too enlightening to Appendix C.

4.5   Determination of L_{10}^r and C_{87}^r

In this section we want to use the relations (4.48) and (4.49) and the values of the effective parameters $\mathrm{L}_{10}^{\mathrm{eff}}$ and $\mathrm{C}_{87}^{\mathrm{eff}}$ obtained in Section 4.3 to determine the χPT couplings L_{10}^r and C_{87}^r at a certain value of the scale μ.

At $\mathcal{O}(p^4)$ the determination of L_{10}^r is straightforward, since one only needs to subtract from $\mathrm{L}_{10}^{\mathrm{eff}}$ the term $\left[1 - \log\left(\mu^2/m_\pi^2\right) + \frac{1}{3}\log\left(m_K^2/m_\pi^2\right)\right]/(128\pi^2)$. Taking $\mu = M_\rho$ as the reference value for the χPT renormalization scale, one gets

$$
\mathrm{L}_{10}^r(M_\rho) = -(5.22 \pm 0.06)\cdot 10^{-3}\,.
\tag{4.50}
$$

At order p^6, the numerical relation is more subtle because it gets small corrections from other LECs. As we have seen, it is useful to classify the $\mathcal{O}(p^6)$ contributions through their ordering within the $1/N_C$ expansion. The tree-level term $4m_\pi^2(C_{61}^r - C_{12}^r - C_{80}^r)$, which is the only $\mathcal{O}(p^6)$ correction in the large–N_C limit, is numerically

small because it appears suppressed by a factor m_π^2. The three relevant couplings have been determined phenomenologically with a moderate accuracy:

$$
\begin{aligned}
C_{61}^r(M_\rho) &= (1.24 \pm 0.44) \cdot 10^{-3}\,\mathrm{GeV}^{-2}\ (\text{from }\Pi_{ud,V}^{(0+1)}(0) - \Pi_{us,V}^{(0+1)}(0))\ [66,67], \\
C_{12}^r(M_\rho) &= (0.4 \pm 6.3) \cdot 10^{-5}\,\mathrm{GeV}^{-2}\quad (\text{from the }K\pi\text{ scalar form factor})\ [71]\ , \\
C_{80}^r(M_\rho) &= (2.1 \pm 0.5) \cdot 10^{-3}\,\mathrm{GeV}^{-2}\quad (\text{from }a_1/K_1\text{ mass and} \\
&\qquad\qquad\qquad\qquad\qquad\qquad\text{width differences})\ [72]\ .
\end{aligned}
$$

These determinations agree reasonably well with published meson-exchange estimates [65, 89] and lead to a total contribution

$$
4m_\pi^2(C_{61}^r - C_{12}^r - C_{80}^r)(M_\rho) = -(6.7 \pm 5.2) \cdot 10^{-5}\ . \tag{4.51}
$$

The scale dependence of this combination of $\mathcal{O}(p^6)$ couplings [84–86] between $\mu = 0.6$ GeV and $\mu = 1.1$ GeV is within its quoted uncertainty.

At NLO in $1/N_C$ we need to consider the tree-level contribution proportional to the combination of LECs $(C_{62}^r - C_{13}^r - C_{81}^r)$. We are not aware of any published estimate of these $1/N_C$ suppressed couplings, beyond the trivial statement that they do not get any tree-level contribution from resonance exchange [63, 65]. We will adopt the conservative range

$$
|C_{62}^r - C_{13}^r - C_{81}^r|(M_\rho) \le |C_{61}^r - C_{12}^r - C_{80}^r|(M_\rho)/3\ , \tag{4.52}
$$

which gives a contribution

$$
4(2m_K^2 + m_\pi^2)(C_{62}^r - C_{13}^r - C_{81}^r)(M_\rho) = (0.0 \pm 5.8) \cdot 10^{-4}\ . \tag{4.53}
$$

The scale dependence between $\mu = 0.6$ GeV and $\mu = 1.1$ GeV of this combination of $\mathcal{O}(p^6)$ couplings [84–86] is within its quoted uncertainty. The uncertainty on this term will dominate our final error on the $L_{10}^r(M_\rho)$ determination. At the same NLO in $1/N_C$, there is also a one-loop correction proportional to $L_9^r(M_\rho)$; using the $\mathcal{O}(p^6)$ determination $L_9^r(M_\rho) = (5.93 \pm 0.43) \cdot 10^{-3}$ [74], this contribution gives

$$
2(2\mu_\pi + \mu_K)\,L_9^r(M_\rho) = -(1.56 \pm 0.11) \cdot 10^{-3}\ . \tag{4.54}
$$

Finally, the $1/N_C^2$ suppressed two-loop function which collects the non-analytic contributions takes the value $G_{2L}(M_\rho) = -0.52 \cdot 10^{-3}$, one order of magnitude smaller than L_{10}^{eff}, but still eight times larger than the uncertainty quoted for L_{10}^{eff} in (4.32). Taking all these contributions into account, we finally get the wanted $\mathcal{O}(p^6)$ result:

$$
\begin{aligned}
L_{10}^r(M_\rho) &= -(4.06 \pm 0.04_{L_{10}^{\mathrm{eff}}} \pm 0.39_{\mathrm{LECs}}) \cdot 10^{-3} \\
&= -(4.06 \pm 0.39) \cdot 10^{-3}\ , \tag{4.55}
\end{aligned}
$$

where the uncertainty has been split into its two main components. The final error is completely dominated by our ignorance on the $1/N_C$ suppressed LECs of $\mathcal{O}(p^6)$.

The determination of C_{87}^r from C_{87}^{eff} at this order in the chiral expansion does not involve any unknown LEC (like the determination of L_{10}^r at order p^4). The contribution of order p^4 in the relation (4.49) is

$$\frac{-1}{7680\,\pi^2}\left(\frac{1}{m_K^2}+\frac{2}{m_\pi^2}\right)=-1.41\cdot10^{-3}\ \text{GeV}^{-2}\ ,\qquad(4.56)$$

whereas the one-loop correction from $\mathcal{L}_4(x)$, which depends on $L_9^r(M_\rho)$, gives $-(1.75\pm0.13)\cdot10^{-3}\ \text{GeV}^{-2}$ and the two-loop contributions $G_{2L}'(M_\rho)=-0.28\cdot10^{-3}\ \text{GeV}^{-2}$. In spite of the chiral and $1/N_C$ suppression, the different contributions go in the same direction and the final correction is very sizable, decreasing the final value of the $\mathcal{O}(p^6)$ LEC:

$$\begin{aligned}
C_{87}^r(M_\rho) &= (4.89\pm0.13_{C_{87}^{\text{eff}}}\pm0.13_{\text{LECs}})\cdot10^{-3}\ \text{GeV}^{-2}\\
&= (4.89\pm0.18)\cdot10^{-3}\ \text{GeV}^{-2}\ ,
\end{aligned}\qquad(4.57)$$

where we see that in this case the error is equally shared by the experimental and LECs uncertainties.

4.6   From L_{10}^r to L_9^r

A recent reanalysis of the decay $\pi^+\to e^+\nu\gamma$ [72], using new experimental data, has provided quite accurate values for the combination of LECs L_9+L_{10},

$$L_9^r(M_\rho)+L_{10}^r(M_\rho)=\begin{cases}(1.32\pm0.14)\cdot10^{-3}\ ,&\mathcal{O}(p^4),\\(1.44\pm0.08)\cdot10^{-3}\ ,&\mathcal{O}(p^6),\end{cases}\qquad(4.58)$$

that can be used in combination with our results for $L_{10}^r(M_\rho)$ to extract the value of $L_9^r(M_\rho)$:

$$L_9^r(M_\rho)=\begin{cases}(6.54\pm0.15)\cdot10^{-3}\ ,&\mathcal{O}(p^4),\\(5.50\pm0.40)\cdot10^{-3}\ ,&\mathcal{O}(p^6),\end{cases}\qquad(4.59)$$

in perfect agreement with the $\mathcal{O}(p^4)$ result $L_9^r(M_\rho)=(6.9\pm0.7)\cdot10^{-3}$ of Ref. [88] and the $\mathcal{O}(p^6)$ result $L_9^r(M_\rho)=(5.93\pm0.43)\cdot10^{-3}$ of Ref. [74]. This last comparison represents an indirect check (in fact the only possible one for the moment) of our $\mathcal{O}(p^6)$ result for L_{10}^r.

4.7   SU(2) χPT

Up to now, we have discussed the low-energy constants of SU(3) χPT. It is useful to consider also the effective low-energy theory with only two flavors of light quarks to perform high-accuracy phenomenological determinations of the corresponding LECs at NLO. Moreover, recent lattice calculations with two dynamical quarks are already

able to obtain the SU(2) LECs with high precision and this is an important check for them.

In SU(2) χPT, there are ten LECs, $l_{i=1,..7}$ and $h_{1,2,3}$, at $\mathcal{O}(p^4)$ [59]. Using the $\mathcal{O}(p^6)$ relation between $l_5^r(\mu)$ and $L_{10}^r(\mu)$, recently obtained in Ref. [91] we get

$$
\begin{aligned}
\bar{l}_5 &= -192\pi^2 \, L_{10}^{\text{eff}} + 1 + \log\left(\frac{m_K}{\hat{m}_K}\right) \\
&+ 768\,\pi^2 \, m_\pi^2 (C_{61}^r + C_{62}^r - C_{12}^r - C_{13}^r - C_{80}^r - C_{81}^r)(\mu) \\
&+ 1536\,\pi^2 (m_K^2 - \hat{m}_K^2)(C_{62}^r - C_{13}^r - C_{81}^r)(\mu) \\
&- 384\,\pi^2 (2\mu_\pi + \mu_K - \hat{\mu}_K)(L_9^r + 2L_{10}^r)(\mu) \\
&- x_K \left[-\frac{67}{48} + \frac{21}{16}\rho_1 + \frac{5}{8}\log\left(\frac{4}{3}\right) - \frac{17}{4}\log\left(\frac{\mu^2}{\hat{m}_K^2}\right) + \frac{3}{4}\log^2\left(\frac{\mu^2}{\hat{m}_K^2}\right) \right] \\
&+ 192\,\pi^2 \, G_{2L}(\mu) + \mathcal{O}(p^8)\,,
\end{aligned}
\tag{4.60}
$$

where $\hat{m}_K^2 = m_K^2 - m_\pi^2/2$ is the kaon mass squared in the limit $m_u = m_d = 0$, $x_K = \hat{m}_K^2/(16\pi^2 f_\pi^2)$, $\hat{\mu}_K = \hat{m}_K^2 \log(\hat{m}_K/\mu)/(16\pi^2 f_\pi^2)$ and $\rho_1 \simeq 1.41602$. The invariant coupling $\bar{l}_5$ is defined by [59]

$$
\bar{l}_5 \equiv -192\pi^2 l_5^r - \log\frac{M_\pi^2}{\mu^2}\,,
\tag{4.61}
$$

$$
\bar{l}_6 \equiv -96\pi^2 l_6^r - \log\frac{M_\pi^2}{\mu^2}\,,
\tag{4.62}
$$

where we have defined also $\bar{l}_6$ for future convenience.

The first line in (4.60) contains the $\mathcal{O}(p^4)$ contributions; the determination of $\bar{l}_5$ at this order is then straightforward. The full $\mathcal{O}(p^6)$ result, with the different tree-level, one-loop and two-loop corrections, is given in the other lines. Following the same procedure as in the SU(3) case, we get the results

$$
\bar{l}_5 = \begin{cases} 13.30 \pm 0.11\,, & \mathcal{O}(p^4), \\ 12.24 \pm 0.21\,, & \mathcal{O}(p^6). \end{cases}
\tag{4.63}
$$

From a phenomenological analysis of the radiative decay $\pi \to l\nu\gamma$ within SU(2) χPT, the authors of Ref. [73] obtained

$$
\bar{l}_6 - \bar{l}_5 = \begin{cases} 2.57 \pm 0.35\,, & \mathcal{O}(p^4), \\ 2.98 \pm 0.33\,, & \mathcal{O}(p^6). \end{cases}
\tag{4.64}
$$

Using these results and our determinations for $\bar{l}_5$ one gets[9]

$$
\bar{l}_6 = \begin{cases} 15.80 \pm 0.29\,, & \mathcal{O}(p^4), \\ 15.22 \pm 0.39\,, & \mathcal{O}(p^6). \end{cases}
\tag{4.65}
$$

---

[9]Actually, at order p^4, the most precise value of the combination $\bar{l}_6 - \bar{l}_5$ is obtained if we calculate it from the $SU(3)$ combination $L_9 + L_{10}$ of Ref. [72], that is Eq. (4.58). In this way we have obtained a prediction for $\bar{l}_6$ that supersedes that of Ref. [78].

Making use of the recent results obtained in Ref. [92] we can also rewrite our result for C_{87}^r in the SU(2) χPT language, getting the first determination of c_{50}^r

$$c_{50}^r(M_\rho) = (4.95 \pm 0.18) \cdot 10^{-3} \text{ GeV}^{-2} \ . \tag{4.66}$$

4.8   Summary and comparisons

Using the most recent hadronic τ-decay data [3] on the $V - A$ spectral function, and general properties of QCD such as analyticity, the OPE and χPT, we have determined very accurately the chiral low-energy constants $L_{10}^r(M_\rho)$, $\bar{l}_5$, $C_{87}^r(M_\rho)$ and $c_{50}^r(M_\rho)$, working both at $\mathcal{O}(p^4)$ and $\mathcal{O}(p^6)$ in the chiral expansion. Taking into account the results of Refs. [72,73] we have also extracted the values of $L_9^r(M_\rho)$ and $\bar{l}_6$. The results are summarized in Tables 4.1 and 4.2.

χPT$_2$	χPT$_3$
$\bar{l}_5 = 13.30 \pm 0.11$	$L_{10}^r(M_\rho) = -(5.22 \pm 0.06) \cdot 10^{-3}$
$\bar{l}_6 = 15.80 \pm 0.29$	$L_9^r(M_\rho) = (6.54 \pm 0.15) \cdot 10^{-3}$

Table 4.1: Results for the χPT LECs obtained at $\mathcal{O}(p^4)$.

χPT$_2$	χPT$_3$
$\bar{l}_5 = 12.24 \pm 0.21$	$L_{10}^r(M_\rho) = -(4.06 \pm 0.39) \cdot 10^{-3}$
$\bar{l}_6 = 15.22 \pm 0.39$	$L_9^r(M_\rho) = (5.50 \pm 0.40) \cdot 10^{-3}$
$c_{50}^r = (4.95 \pm 0.18) \cdot 10^{-3} \text{ GeV}^{-2}$	$C_{87}^r(M_\rho) = (4.89 \pm 0.18) \cdot 10^{-3} \text{ GeV}^{-2}$

Table 4.2: Results for the χPT LECs obtained at $\mathcal{O}(p^6)$.

Our error estimate includes a careful analysis of the theoretical uncertainties associated with the use of the OPE in the dangerous region close to the physical cut. Moreover, in (4.55) and (4.57) we have explicitly separated the error into its two main components, showing that our present ignorance on the $1/N_C$ suppressed LECs dominates the final uncertainty of the $L_{10}^r(M_\rho)$ determination at $\mathcal{O}(p^6)$, whereas in the C_{87}^r case the error is equally shared by the experimental and LECs uncertainties.

We can find different determinations of these LECs in the literature, that we can divide in phenomenological, theoretical and lattice determinations.

Phenomenological determinations.- Before the existence of τ-data L_{10}^r was extracted from the form factors of radiative pion decay (where the combination $L_{10}^r + L_9^r$ appears) together with the knowledge of L_9^r. Once τ-data was available from DORIS at DESY [93] and PEP at SLAC [94] it was possible to perform the first sum rule determination of L_{10}^r [80]. This determination used data-interpolated functions extracted from [1] and did not assign any error to the result.

With the good quality τ-data coming from LEP at CERN several authors repeated this analysis, although in most of the cases they just got the effective parameter and did not extract the L_{10}^r value. Due to this, we show in Table 4.3 the different values obtained for the effective parameter.

$L_{10}^{\text{eff}} \cdot 10^3$	Ref.	Data
-6.0	[80]	Argus Coll. (1986) [93]
-6.36 ± 0.19	[53]	ALEPH Coll. (1998) [42, 43]
-5.80 ± 0.20	[54]	ALEPH Coll. (1998) [42, 43]
-6.43 ± 0.08	[32]	ALEPH Coll. (1998) [42, 43]
-6.45 ± 0.06	[33]	ALEPH Coll. (2005) [3]
-6.48 ± 0.06	This work [78]	ALEPH Coll. (2005) [3]

Table 4.3: Different determinations of L_{10}^{eff}.

The determination of Ref. [53] was done through a simultaneous fit of this parameter and the OPE corrections of dimensions six and eight to several spectral moments of the hadronic distribution with the older 1998 ALEPH data [42, 43], in good agreement with us, although obviously less precise.

The value of Ref. [54] is the only one that disagrees with ours, being 3.2 σ smaller. It was extracted from τ data using the first "duality point" of the WSRs and the older ALEPH τ-data. The difference comes from underestimated theoretical uncertainties in this reference, as can be easily seen by choosing instead the second duality point or varying slightly the value of the first duality point. In fact the same Ref. [54] (see Eq. (10) therein) presents also a different estimate of L_{10}^{eff} that is in very good agreement with our result.

In Ref. [32] L_{10}^{eff} was determined using the older ALEPH τ-data and an updated re-analysis with the new data was given in [33]. We see that they are in good agreement with our result, but their analysis relies completely on the use of the pinched weights whereas ours includes a more detailed assessment of the theoretical uncertainties, that discards a possible failure of the PW (see Appendix B).

Only in Ref. [53] the value of the chiral parameter L_{10}^r was extracted (at order p^4), finding

$$L_{10}^r(M_\rho) = -(5.13 \pm 0.19) \cdot 10^{-3}, \ \mathcal{O}(p^4) , \tag{4.67}$$

obviously also in good agreement with our $\mathcal{O}(p^4)$ result. We can perform an indirect check through the comparison of our $\mathcal{O}(p^4)$ result for L_9^r with the value $L_9^r(M_\rho) = (6.9 \pm 0.7) \cdot 10^{-3}$ obtained from the charge radius of the pion [88]. We see a very good agreement and a clear improvement in the precision[10].

Our determination of L_{10}^r ($\bar{l}_5$) is the first one at $\mathcal{O}(p^6)$, although again we can make an indirect and interesting check comparing our $\mathcal{O}(p^6)$ result for L_9^r ($\bar{l}_6$) with the value $L_9^r(M_\rho) = (5.93 \pm 0.43) \cdot 10^{-3}$ ($\bar{l}_6 = 16.0 \pm 0.5 \pm 0.7$) obtained from the charge radius of the pion [74] ([75]). The agreement is once more very good and the improvement in the numerical value of $\bar{l}_6$ is remarkable.

Our determination of C_{87}^r (c_{50}^r) is the first one performed phenomenologically, although in Ref. [32] the value of $\overline{\Pi}'(0)$ was extracted using the same QCD Sum

---

[10]This is equivalent to use the old extraction of L_{10}^r based on the use of the relation $L_{10}^{\text{eff}} = \frac{-1}{12} f_\pi^2 \langle r_\pi^2 \rangle + \frac{1}{4} F_A$.

Rule that we have used (with the old ALEPH) data, and from there we can extract the value $C_{87}^{\text{eff}} = (8.12 \pm 0.13) \cdot 10^{-3} \, \text{GeV}^{-2}$ that is in good agreement with ours.

Theoretical determinations.- Our determinations of $L_{10}^r(\mu)$ and $C_{87}^r(\mu)$ at $\mu = M_\rho$ agree within errors with the large–N_C estimates based on lowest-meson dominance [62–64, 76, 89]:

$$
\begin{aligned}
L_{10} &= -\frac{F_V^2}{4M_V^2} + \frac{F_A^2}{4M_A^2} \approx -\frac{3f_\pi^2}{8M_V^2} \approx -5.4 \cdot 10^{-3}, \\
C_{87} &= \frac{F_V^2}{8M_V^4} - \frac{F_A^2}{8M_A^4} \approx \frac{7f_\pi^2}{32M_V^4} \approx 5.3 \cdot 10^{-3} \, \text{GeV}^{-2}.
\end{aligned}
$$

They are also in good agreement with the result of Refs. [68, 69] for C_{87} based on Padé Approximants. These predictions, however, are unable to fix the scale dependence which is of higher-order in $1/N_C$. More recently, the resonance chiral theory Lagrangian [63, 64, 95] has been used to analyze the LR correlator at NLO order in the $1/N_C$ expansion [70]. Matching the effective field theory description with the short-distance QCD behavior, the two LECs are determined, keeping full control of their μ dependence. The theoretically predicted values [70]

$$
\begin{aligned}
L_{10}^r(M_\rho) &= -(4.4 \pm 0.9) \cdot 10^{-3}, & (4.68) \\
C_{87}^r(M_\rho) &= (3.6 \pm 1.3) \cdot 10^{-3} \, \text{GeV}^{-2}, & (4.69)
\end{aligned}
$$

are in perfect agreement with our determinations, although less precise.

Lattice determinations.- The most recent lattice calculations find the following results (order p^4):

$$
\begin{aligned}
L_{10}^r(M_\rho) &= \begin{cases} -(5.2 \pm 0.5) \cdot 10^{-3} & [96], \\ -(5.7 \pm 1.1 \pm 0.7) \cdot 10^{-3} & [97], \end{cases} \\
\bar{l}_6 &= \begin{cases} 14.9 \pm 1.2 \pm 0.7 & [98], \\ 11.9 \pm 0.7 \pm 1.0 & [99]. \end{cases}
\end{aligned}
\qquad (4.70)
$$

They are in good agreement with our determinations (although still far from the phenomenological precision), but for the last one that is slightly smaller. As discussed in Ref. [99], this is partly due to the deviation of the lattice determination of the pion decay constant from the χPT one.

Therefore we can conclude that the different analytical approaches and the various lattice calculations agree very well with our precise phenomenological values.

As a final remark let us say that the L_{10} parameter has a conceptual importance that goes beyond the framework of χPT, since the analogous parameter in strongly coupled extensions of the Standard Model (e.g. technicolor theories) is equal to the S Peskin-Takeuchi parameter [100] but for a minus sign and some factors. It has been suggested that a QCD-like theory will generate a positive value of S, what makes very interesting its determination. Some works [101] indicated that the electroweak data entailed $S < 0$, what led to the assertion that the electroweak symmetry breaking does not mimic QCD, but more recent works showed that a positive S is still allowed by the current experimental data [102].

Chapter 5

Estimating the Duality Violation

There is no such thing as a
theoretical uncertainty.
All there is is theoretical stupidity.
Guido Altarelli

The basic assumption behind the QCD Sum Rules is that the quark and hadron degrees of freedom provide two dual descriptions of the same strong interaction dynamics. This quark-hadron duality is a consequence of the assumed confinement of QCD. In more technical terms, a sum rule is a dispersion relation relating the value of a given two-point correlation function at some Euclidean value of Q^2 with an integral over the corresponding spectral function in the Minkowskian domain. Quark-hadron duality allows us to calculate this Minkowskian integral in terms of hadrons, using the available experimental data. Ideally, the resulting QCD Sum Rule is an exact mathematical relation arising from analyticity and confinement (duality). In practice, however, as we have explained in Chapter 3 a series of approximations need unavoidably to be adopted in its specific numerical implementation (OPE truncation, cutoff in the hadronic integral, etc.).

The associated violation of quark-hadron duality is difficult to estimate, because of our inability to make reliable QCD calculations at low and intermediate energies. The normal way to assess the theoretical uncertainties of QCD Sum Rules consists in estimating the OPE truncation error and testing the stability of the results with variations of s_0. However, this method is too naive (see Appendix B) and can underestimate the DV.

Violations of QCD quark-hadron duality [17] have been poorly studied and often disregarded. Its importance in Finite Energy Sum Rules (FESRs) has attracted some attention recently [21–24], owing to the phenomenological need for higher accuracies. To estimate the size of these effects is of course of maximal importance, if we want to master the strong interaction at all energies and be able to perform precision QCD calculations. This importance extends to all particle physics when one realizes that those calculations are often necessary to disentangle New Physics from the Standard Model. Moreover, duality violations will also be present in NP scenarios characterized by a strongly-interacting dynamics. A better knowledge

of duality violations in QCD would help to understand their role in more exotic theories.

In the following, we present a detailed analysis of the possible numerical impact of duality violations in the description of the LR correlator [25, 26]. Let us repeat that this is a very good laboratory to test the problem because this correlator is an order parameter of chiral-symmetry breaking: in the massless quark limit it vanishes to all orders in perturbation theory, i.e. its operator product expansion only contains power-suppressed contributions, starting with dimension six. In the absence of any theory of duality violations, we will use a generic, but theoretically motivated, model [17, 20] to assess the phenomenological relevance of these effects.

The theoretical ingredients of our analysis are presented in the next section. Section 5.2 contains a detailed discussion of the behavior of the physical spectral function at high energies. Using the most recent experimental data, we generate a large number of "acceptable" spectral functions which satisfy all known QCD constraints. Our numerical results, obtained through a careful statistical analysis of the whole set of possible spectral functions, are given in section 5.3. Section 5.6 summarizes our findings.

5.1   Theoretical Framework

In this chapter we will work again with the LR correlator $\Pi(q^2) \equiv \Pi_{LR}^{(0+1)}(q^2)$. As we have explained carefully in the previous chapter, its analytic properties allow us to derive the exact relation (3.15), that we show now for a weight function of the form $w(s) = s^n$, being n an integer number that can be positive or negative

$$\int_{s_{\rm th}}^{s_0} {\rm d}s\, s^n\, \rho(s) \;+\; \frac{1}{2\pi i} \oint_{|s|=s_0} {\rm d}s\, s^n\, \Pi(s) \;=\; 2 f_\pi^2\, m_\pi^{2n} + \operatorname*{Res}_{s=0}\left[s^n\, \Pi(s)\right], \qquad (5.1)$$

Integrals of the chiral spectral function $\rho(s)$ times the weight function s^n from the continuum threshold $s_{\rm th}$ up to s_0 are usually called spectral chiral moments $M_n(s_0)$; when $s_0 \to \infty$ we will denote them M_n for brevity.

As was extensively explained in Chapter 3, in order to evaluate the contour integral of (5.1), one approximates $\Pi(s)$ with its OPE expression

$$\Pi^{\rm OPE}(s) \;=\; \sum_{k=3} \frac{C_{2k}(\nu)\,\langle O_{2k}\rangle(\nu)}{(-s)^k} \;\equiv\; \sum_{k=3} \frac{\mathcal{O}_{2k}}{(-s)^k}\,, \qquad (5.2)$$

where $\mathcal{O}_{2k}$ are the so-called V-A condensates. So we can rewrite Eq. (5.1) as

$$\int_{s_{\rm th}}^{s_0} {\rm d}s\, s^n\, \rho(s) \;+\; \frac{1}{2\pi i} \oint_{|s|=s_0} {\rm d}s\, s^n\, \Pi^{\rm OPE}(s) \;+\; {\rm DV}[s^n, s_0]$$
$$= 2 f_\pi^2\, m_\pi^{2n} \;+\; \operatorname*{Res}_{s=0}\left[s^n\, \Pi(s)\right], \quad (5.3)$$

where

$$\mathrm{DV}[s^n, s_0] \;\equiv\; \frac{1}{2\pi i} \oint_{|s|=s_0} {\rm d}s\, s^n\, \left(\Pi(s) - \Pi^{\rm OPE}(s)\right) \qquad (5.4)$$

parameterizes the violation of quark-hadron duality that we are interested in. The relation (5.3) contains all the elements of a standard QCD Sum Rule, with the hadronic contribution (integral of the $V - A$ non-strange spectral function), the OPE contour integral at $|s| = s_0$ and the possible residue at the origin calculable with Chiral Perturbation Theory.

In order to analyse duality violation effects in different sum rules, we will use the weights $w(s) = s^n$, with $n = -2, -1, 2, 3$, that generate the following four FESRs:[1]

$$M_{-2}(s_0) \equiv \int_{s_{\mathrm{th}}}^{s_0} ds \, \frac{1}{s^2} \, \rho(s) = 16 \, C_{87}^{\mathrm{eff}} - \mathrm{DV}[1/s^2, s_0] \,, \qquad (5.5)$$

$$M_{-1}(s_0) \equiv \int_{s_{\mathrm{th}}}^{s_0} ds \, \frac{1}{s} \, \rho(s) = -8 L_{10}^{\mathrm{eff}} - \mathrm{DV}[1/s, s_0] \,, \qquad (5.6)$$

$$M_2(s_0) \equiv \int_{s_{\mathrm{th}}}^{s_0} ds \, s^2 \, \rho(s) = 2 f_\pi^2 m_\pi^4 + \mathcal{O}_6 - \mathrm{DV}[s^2, s_0] \,, \qquad (5.7)$$

$$M_3(s_0) \equiv \int_{s_{\mathrm{th}}}^{s_0} ds \, s^3 \, \rho(s) = 2 f_\pi^2 m_\pi^6 - \mathcal{O}_8 - \mathrm{DV}[s^3, s_0] \,, \qquad (5.8)$$

where the effective parameters $L_{10}^{\mathrm{eff}} \equiv -\frac{1}{8} \overline{\Pi}(0)$ and $C_{87}^{\mathrm{eff}} \equiv \frac{1}{16} \overline{\Pi}'(0)$ were introduced in the previous chapter, while $\mathcal{O}_{6,8}$ are defined in Eq. (5.2). These four sum rules have been used in the past [30–33, 41, 42, 53, 61, 78, 104] to extract the values of either the χPT couplings L_{10}^r and C_{87}^r, or the vacuum expectation values of the dimension six and eight operators appearing in the OPE. In those works the DV effects were just inferred from the s_0-stability (if not just neglected), that as we will see can be a misleading method. Here we want to analyze the effect of DV on these four observables using a different approach that will be explained in the following sections.

For the computation of the hadronic integral representation of the moments $M_n(s_0)$ we will use the 2005 ALEPH data on semileptonic τ decays [3], shown in Fig. 3.3, which provide the most recent and precise measurement of the $V - A$ spectral function $\rho(s)$.

5.1.1   Theoretically known spectral moments

In the four sum rules introduced in the previous section, we use the experimental data to extract theoretical information, namely the value of the corresponding parameters or, equivalently, the value of the spectral moments for $s_0 \to \infty$, M_n. There exist a few additional sum rules where we know theoretically the value of the spectral moments when $s_0 \to \infty$. These sum rules will play a special role in our analysis because they give us very valuable information on the spectral function $\rho(s)$

---

[1]Here we neglect the logarithmic corrections to the Wilson coefficients in the OPE. The error associated to this approximation is expected to be smaller than the other errors involved in the analysis, as was found e.g. in Refs. [31, 103].

for $s \geq s_0$. The three sum rules that we will use are:

$$M_0 \;=\; \int_{s_{\text{th}}}^{\infty} \mathrm{d}s \, \rho(s) \;=\; 2f_\pi^2 \,, \tag{5.9}$$

$$M_1 \;=\; \int_{s_{\text{th}}}^{\infty} \mathrm{d}s \, s \, \rho(s) \;=\; 2f_\pi^2 m_\pi^2 \,, \tag{5.10}$$

$$\int_{s_{\text{th}}}^{\infty} \mathrm{d}s \, s \, \log\!\left(\frac{s}{\lambda^2}\right) \rho(s)\big|_{m_q=0} \;=\; (m_{\pi^0}^2 - m_{\pi^+}^2)_{\text{EM}} \, \frac{8\pi}{3\alpha} f_0^2 \,. \tag{5.11}$$

The relations (5.9) and (5.10) are the first and second Weinberg sum rules that were already introduced in Section 3.5.2, while the third identity is the pion sum rule (πSR) that gives the electromagnetic pion mass splitting in the chiral limit [105]. In the second WSR there are contributions of the form $\mathcal{O}(m_q^2 \alpha_S s_0)$ [28], where s_0 is the upper limit of the integral, but they are negligible for the values of s_0 that we are considering.

5.1.2   Duality violation

To get vanishing DV in sum rules like (5.3) and (5.5–5.8) one could think working with an infinite Cauchy radius s_0, but this is clearly not an option because the spectral function $\rho(s)$ is only known up to $s_{\text{max}} = m_\tau^2$. We can predict the value of $\rho(s)$ at high-enough energies using perturbative QCD, but there is an intermediate region above s_{max} where perturbation theory is still not reliable. Therefore we have to deal with this DV unavoidably, and it is important to keep in mind that at $s_0 \sim 3$ GeV^2 it can represent a sizable contribution to the sum rules, as the WSRs show clearly (see Section 3.5.2).

Since the solution to QCD is not known yet, DV is almost by definition a non-calculable quantity and that is the reason why it has been taken to be negligible very often. But in order to make precise and reliable predictions one must worry about the size of this effect.

In our analysis we will study the DV from the perspective that gives us the expression (3.43)

$$\text{DV}[w(s), s_0] \;=\; \int_{s_0}^{\infty} \mathrm{d}s \, w(s) \, \rho(s) \,, \tag{5.12}$$

that shows the DV effect as a hadronic integral that can be analyzed phenomenologically.

We know from QCD that the spectral function $\rho(s)$ has to vanish at high values of s and, consequently, we expect the region right above s_0 to be the most relevant in (5.12). This makes the "pinched weights" (polynomial weight functions with a zero at $s = s_0$) an interesting tool to minimize the DV. However, in (5.12) we can see something that is hidden in (5.4), namely that one has to worry also about the possible enhancement of the contribution from the high-energy part of the integral ($s \gg s_0$) produced by the "pinched weights". And thus, we see that the use of these

weights can worsen the situation. Another direct consequence from (5.12), unless accidental cancelations occur, is that by weighting less the high-energy part of the spectral integral one can get smaller DV. In particular, for our spectral moments $M_n(s_0)$, one expects the DV effects to increase with increasing values of n. Thus, the size of the DV will be smaller in the determination of L_{10}^{eff} than in the determination of the chiral moment M_2.

To quantify the DV uncertainties of a given sum rule we must then estimate the possible behavior of the spectral function beyond s_0. The DV is an estimate of the freedom in the behavior of the spectral function above s_0, once all the theoretical and phenomenological knowledge on that spectral function and on its moments has been taken into account. For instance, QCD tells us that $\rho(s)$ must go *quickly* enough to zero when $s \to \infty$. This is a valuable information, but one can still imagine infinite possible shapes for the spectral function and, therefore, the limits imposed on DV effects are poor and not good enough for most phenomenological analyses.

Some theoretically motivated models for the DV were advocated in Refs. [17, 19, 20]. We will adopt a simple parameterization of the spectral function at high energies, based in the resonance model proposed and studied in Refs. [17, 20, 21]. Following the discussion above, we add more physical constraints to the behaviour of $\rho(s)$ and require that it satisfies the WSRs and the πSR [22]. Our goal is to generate a bunch of physically acceptable spectral functions and translate this information into DV limits.

A similar work has been done in [23] to estimate the DV uncertainties associated with the determination of α_s from hadronic τ decay data. An important difference of our present study with those works is that they make separate analyses for the vector and axial-vector channels, without imposing the constraints from the WSRs and πSR. In fact, one can easily check that those sum rules are not satisfied for the vast majority of the generated spectral functions used in [23] (as can be seen in Fig. 2 of Ref. [24]). So the results found there cannot be applied to the $V - A$ channel that we want to study here.

5.2 Acceptable $V - A$ Spectral Functions

5.2.1 Spectral-function parameterization

We split the integral of the spectral function $\rho(s)$ in two parts. For the low-energy part of the integral we will use the ALEPH data, whereas in the rest of the integration range we will work under the assumption that the spectral function is well described by the following parameterization

$$\rho(s \geq s_z) \quad = \quad \kappa \, e^{-\gamma s} \sin(\beta(s - s_z)) \, , \tag{5.13}$$

that has κ, γ, β and s_z as free parameters. From the ALEPH data we know that the $V - A$ spectral function $\rho(s)$ has a second zero around 2 GeV^2 (see Fig. 3.3), which is represented in our parameterization through the s_z parameter. We will take this zero as the separation point between the use of the data and the use of the model.

At high values of s this parameterization appears naturally in the equidistant resonance-based model with finite widths introduced in Refs. [17, 20] and has also been used in Refs. [21, 23] to study the DV of sum rules with different correlators.

In the region $2.0 \text{ GeV}^2 \leq s \leq 3.3 \text{ GeV}^2$ the proposed parameterization is compatible with the ALEPH data; the corresponding χ^2 fit gives the result

$$\chi^2_{\min}(\kappa, \gamma, \beta, s_z) = \chi^2(1.00, 1.05, 0.40, 2.03) = 4.4 \ll \text{ d.o.f.} = 41 . \qquad (5.14)$$

In fact the compatibility appears to be too good, in the sense that the minimum χ^2 is much smaller than the number of degrees of freedom (d.o.f.): $41 = 45$ points - 4 parameters. This low value of $\chi^2_{\min}$ was also found in Refs. [23, 50].

5.2.2 Imposing constraints

As we have already said, the WSRs and the πSR in (5.9), (5.10) and (5.11) are an important source of information on $\rho(s)$, for s values beyond the range of the τ data. In the literature, the use of this information has been mostly limited to define the so-called "duality points", values of s_0 for which the WSRs are satisfied, i.e. $\text{DV}[s^n, s^0] = 0$ ($n = 0, 1$). These duality points are frequently used to evaluate the other FESRs, but this introduces an unknown systematic error and several ambiguities, like which duality point is the best option.

We will fully use that information by imposing that the spectral function $\rho(s)$, given by the latest ALEPH data below $s_z \sim 2 \text{ GeV}^2$ and Eq. (5.13) for $s > s_z$, fulfils the two WSRs and the πSR within uncertainties. This requirement constrains the regions in the parameter space of model (5.13) that are compatible with both QCD and the data. We will find all possible tuples[2] $(\kappa, \gamma, \beta, s_z)$ which are compatible with such constraints by fitting the model. In this way, we analyse how much freedom is left for the shape of the spectral function after imposing all we know on $\rho(s)$ from data plus QCD. We will also require the compatibility between model and data in the region[3] $1.7 \text{ GeV}^2 \leq s \leq 3.15 \text{ GeV}^2$.

---

[2]We will talk about "tuple" referring to a set of values $(\kappa, \gamma, \beta, s_z)$.

[3]Although we are assuming that the model describes correctly the spectral function beyond $s_z \sim 2 \text{ GeV}^2$, we impose the compatibility with the data from 1.7 GeV^2 to ensure the continuity of the spectral function in the matching region between the data and the model.

The four imposed conditions can be written quantitatively in the following form:[4]

$$\int_0^{s_z} \rho(s)^{\text{ALEPH}} \, ds + \int_{s_z}^{\infty} \rho(s; \kappa, \gamma, \beta, s_z) ds = 2f_\pi^2 = (17.1 \pm 0.4) \cdot 10^{-3} \text{ GeV}^2, \quad (5.15)$$

$$\int_0^{s_z} \rho(s)^{\text{ALEPH}} s \, ds + \int_{s_z}^{\infty} \rho(s; \kappa, \gamma, \beta, s_z) \, s \, ds = 2f_\pi^2 m_\pi^2 = (0.3 \pm 0.8) \cdot 10^{-3} \text{ GeV}^4, \quad (5.16)$$

$$\int_0^{s_z} \rho(s)^{\text{ALEPH}} s \, \log\left(\frac{s}{1 \text{ GeV}^2}\right) \, ds + \int_{s_z}^{\infty} \rho(s; \kappa, \gamma, \beta, s_z) \, s \, \log\left(\frac{s}{1 \text{ GeV}^2}\right) \, ds$$

$$= (m_{\pi^0}^2 - m_{\pi^+}^2)_{\text{EM}} \frac{8\pi}{3\alpha} f_0^2 = -(10.9 \pm 1.5) \cdot 10^{-3} \text{ GeV}^4, \quad (5.17)$$

$$\chi^2(\kappa, \gamma, \beta, s_z) < \chi_{\text{crit}}^2 = \text{d.o.f.} = 54. \quad (5.18)$$

5.2.3 Selection process of acceptable models

After defining the minimal conditions that a tuple has to satisfy in order to be accepted, we perform a scanning over the 4-dimensional parameter space, looking for physically acceptable tuples. We emphasize the importance of taking properly into account the data correlations. For instance, if one analyses the compatibility of a null spectral function with the ALEPH data in the region $(2, 3.15)$ GeV^2, the resulting minimum χ^2 is very sensitive to these correlations:

$$\chi^2(0.0, \gamma, \beta, s_z)/\text{d.o.f.} = 0.99 \quad \text{(correlations included)}, \quad (5.19)$$
$$\chi^2(0.0, \gamma, \beta, s_z)/\text{d.o.f.} = 4.58 \quad \text{(correlations excluded)}. \quad (5.20)$$

To perform the parameter-space scanning process, we adopt the following procedure. First, we define a rectangular region such that it contains the four-dimensional ellipsoid defined by $\chi^2(\kappa, \gamma, \beta, s_z) = \text{d.o.f.}$, and we create a lattice with $20^4 = 16 \cdot 10^4$ points, that is, $16 \cdot 10^4$ tuples (or functions). We find that 1789 of them satisfy our set of minimal conditions; i.e., 1789 of them represent possible shapes of the physical spectral function beyond 2 GeV^2. Fig. 5.1 shows the statistical distribution of the parameters of our model after the selection process. In Fig. 5.2 we show the distribution of the quantity $\chi^2(\kappa, \gamma, \beta, s_z)$ for those tuples that have passed the selection process. We find that all accepted tuples generate values of χ^2 larger than 10.0; i.e., tuples following the central values of the experimental points do not pass

---

[4] The quoted errors in Eqs. (5.15) and (5.16) are just data errors, whereas in (5.17) the main uncertainty comes from the fact that quark masses do not vanish in nature and we are using real data (not chiral-limit data). We estimate this uncertainty taking for the pion decay constant the value $f_0 = 87 \pm 5$ MeV, that covers a range that includes the physical value and the different estimates of the chiral limit value [106, 107]. We also include a small uncertainty coming from the residual scale dependence of the logarithm, which is proportional to the second WSR. We consider $\lambda \sim 1$ GeV a good choice of scale because higher values would suppress the high-energy part of the integral (the information that we want to use), while smaller values would generate larger τ-data errors in (5.17), losing also information about the high-energy region.
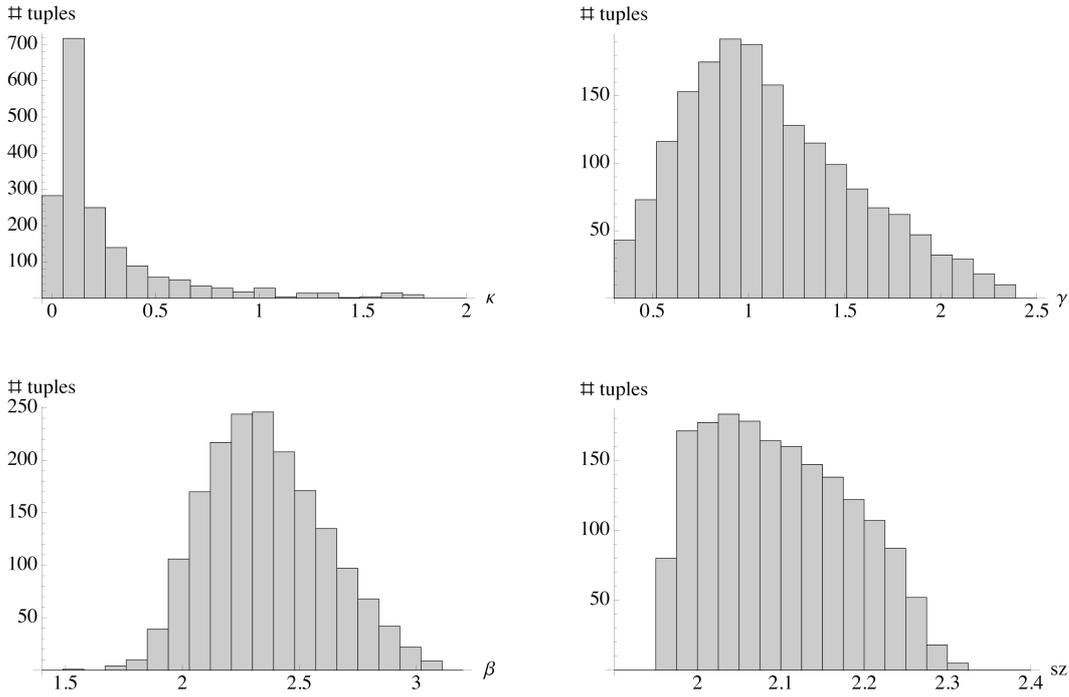
Figure 5.1: Statistical distribution of acceptable models in the parameter space κ (upper-left), γ (upper-right), β (lower-left) and s_z (lower-right).

the selection process; neither do the tuples that go above the central values. Thus our model indicates clearly that the third bump of the spectral function should be smaller than what the ALEPH data suggest (see Fig. 3.3). The size of this third bump is an important issue that future high-quality τ decay data could clarify. For illustrative purposes, Fig. 5.3 shows one of the hundreds of functions that satisfy our set of conditions.
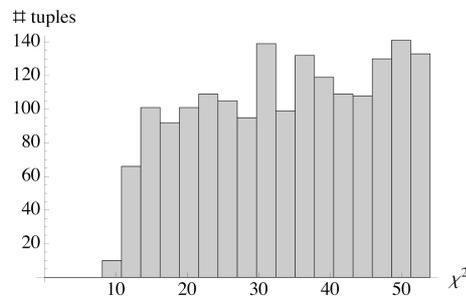
Figure 5.2: Distribution of $\chi^2(\kappa, \gamma, \beta, s_z)$ values for acceptable tuples between 0 and $\chi^2_{\text{crit}} = \text{d.o.f.} = 54$.
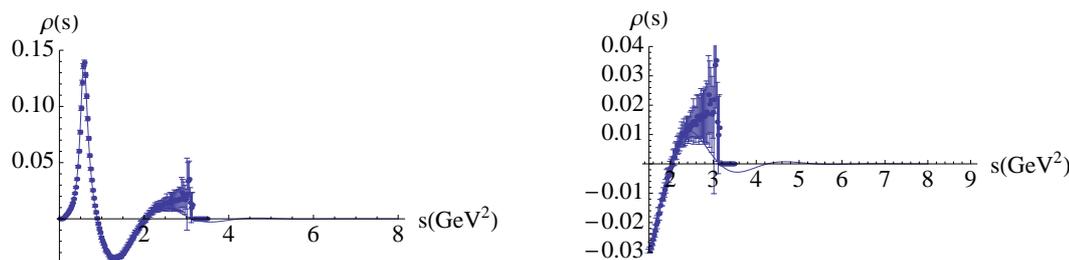
Figure 5.3: Spectral function $\rho(s)$ generated with $(\kappa, \gamma, \beta, s_z) = (0.24, 1.23, 2.82, 2.03)$, together with the experimental ALEPH data [3]. $\chi^2 = 38.7$ for this tuple.

5.3   Numerical Results

For each one of the hundreds of functions that have passed our selection process, we can calculate the associated values of C_{87}^{eff}, L_{10}^{eff}, $\mathcal{O}_6$ and $\mathcal{O}_8$, simply carrying out the integrals of Eqs. (5.5–5.8) with $s_0 \to \infty$. The results of this analysis are summarized in Fig. 5.4, which shows the statistical distribution of the calculated parameters[5]. From these distributions, one gets the final numbers:

$$C_{87}^{\mathrm{eff}} = \left(8.167\,^{+\,0.007}_{-\,0.002} \pm 0.12\right) \cdot 10^{-3} \ \mathrm{GeV}^{-2} = (8.17 \pm 0.12) \cdot 10^{-3} \ \mathrm{GeV}^{-2}, \quad (5.21)$$

$$L_{10}^{\mathrm{eff}} = \left(-6.46\,^{+\,0.03}_{-\,0.01} \pm 0.07\right) \cdot 10^{-3} \quad = \quad \left(-6.46\,^{+\,0.08}_{-\,0.07}\right) \cdot 10^{-3}, \quad (5.22)$$

$$\mathcal{O}_6 = \left(-5.4\,^{+\,3.4}_{-\,1.0} \pm 1.2\right) \cdot 10^{-3} \ \mathrm{GeV}^6 = \left(-5.4\,^{+\,3.6}_{-\,1.6}\right) \cdot 10^{-3} \ \mathrm{GeV}^6, \quad (5.23)$$

$$\mathcal{O}_8 = \left(-8.9\,^{+\,12.4}_{-\,7.1} \pm 2.1\right) \cdot 10^{-3} \ \mathrm{GeV}^8 = \left(-8.9\,^{+\,12.6}_{-\,7.4}\right) \cdot 10^{-3} \ \mathrm{GeV}^8, \quad (5.24)$$

where the first error is that associated to the high-energy region (integral from s_z to infinity), that we compute from the dispersion of the histograms of Fig. 5.4, and the second error is that associated to the low-energy region (integral from zero to s_z), that we compute in a standard way from the ALEPH data. These results correspond to the 68% probability region (one sigma). Since the first error is not gaussian we show also now the 95% probability results (95% of the acceptable spectral functions give a result within the quoted interval):

$$C_{87}^{\mathrm{eff}} = \left(8.167\,^{+\,0.011}_{-\,0.007} \pm 0.24\right) \cdot 10^{-3} \ \mathrm{GeV}^{-2} = (8.17 \pm 0.24) \cdot 10^{-3} \ \mathrm{GeV}^{-2} \quad (5.25)$$

$$L_{10}^{\mathrm{eff}} = \left(-6.46\,^{+\,0.04}_{-\,0.03} \pm 0.14\right) \cdot 10^{-3} \quad = \quad \left(-6.46\,^{+\,0.15}_{-\,0.14}\right) \cdot 10^{-3}, \quad (5.26)$$

$$\mathcal{O}_6 = \left(-5.4\,^{+\,4.2}_{-\,2.7} \pm 2.4\right) \cdot 10^{-3} \ \mathrm{GeV}^6 = \left(-5.4\,^{+\,4.8}_{-\,3.6}\right) \cdot 10^{-3} \ \mathrm{GeV}^6, \quad (5.27)$$

$$\mathcal{O}_8 = \left(-8.9\,^{+\,16.9}_{-\,15.1} \pm 4.2\right) \cdot 10^{-3} \ \mathrm{GeV}^8 = \left(-8.9\,^{+\,17.4}_{-\,15.7}\right) \cdot 10^{-3} \ \mathrm{GeV}^8. \quad (5.28)$$

---

[5]We can see in Fig. 5.4 that $\mathcal{O}_6$ is negative for all the spectral functions, as expected from the condition $q^2\Pi(q^2) \geq 0$ for $-\infty \geq q^2 \geq 0$, proven by Witten [108].
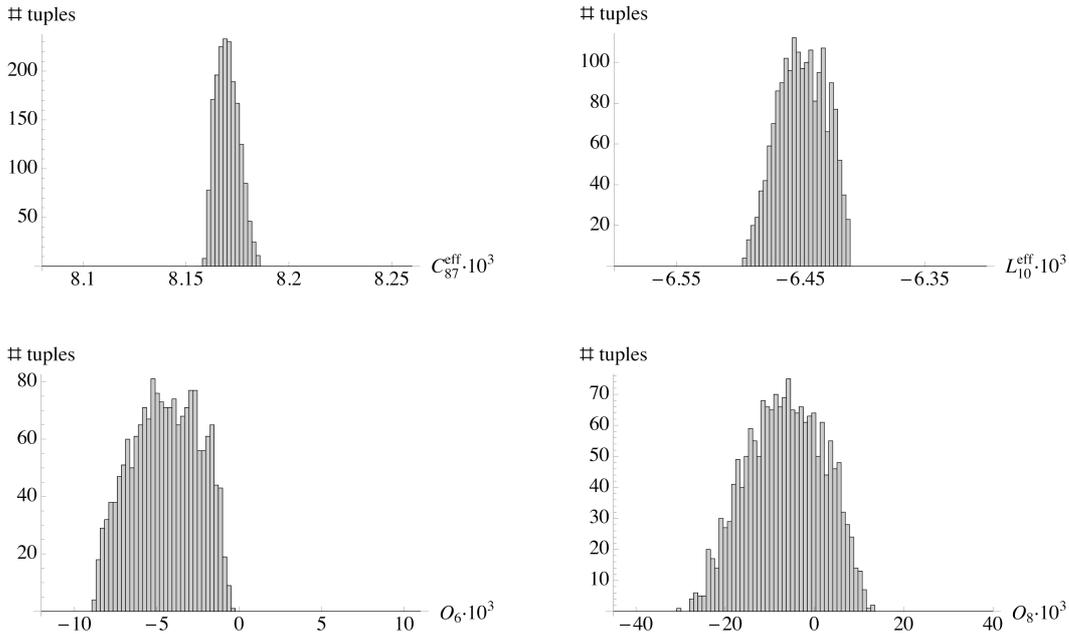
Figure 5.4: Statistical distribution of values of C_{87}^{eff} (upper-left), L_{10}^{eff} (upper-right), $\mathcal{O}_6$ (lower-left) and $\mathcal{O}_8$ (lower-right) for acceptable models. The parameters are expressed in GeV elevated to the corresponding power.

Our calculations have been done with a very simple, but physically motivated, parameterization of DV [17]. Most likely this parameterization does not represent the actual shape of the $V - A$ spectral function, but it accounts for the possible freedom of the function $\rho(s)$ beyond 2 GeV^2 and its consequences on the observables. Our statistical analysis translates the present ignorance on the high-energy behaviour of $\rho(s)$ into a clear quantitative assessment on the uncertainties of the phenomenologically extracted parameters.

As expected, the DV effects have very little impact on the values of C_{87}^{eff} and L_{10}^{eff}, because the corresponding FESRs (5.5) and (5.6) are dominated by the low-energy region where the available data sits. Our results are in excellent agreement with the most recent determination of these parameters, using the same ALEPH τ data, performed in Ref. [78] and explained in the previous chapter: $C_{87}^{\text{eff}} = (8.18 \pm 0.14) \cdot 10^{-3}$ GeV^{-2} and $L_{10}^{\text{eff}} = -(6.48 \pm 0.06) \cdot 10^{-3}$. The smaller uncertainties quoted in [78] are due to the use of the pinched weights (as we will see in the next section).

The situation is not so good for the moments M_2 and M_3 (or equivalently $\mathcal{O}_6$ and $\mathcal{O}_8$), which are sensitive to the high-energy behaviour of the spectral function. The present ALEPH data, together with the constraints from the WSRs and the πSR, are not good enough to determine the sign of $\mathcal{O}_8$ using the sum rule (5.8); the DV uncertainties turn out to be too large in this case. Our results are slightly better for $\mathcal{O}_6$, where there is no doubt in the sign, but again the effects of DV imply larger uncertainties than what was estimated in previous works based on the relation (5.7).

5.4 Using pinched weights

The above-explained approach to the calculation of the quark-hadron duality violation through the study of the freedom of the spectral function in the high-energy region allows us to address the question of the convenience of the use of the pinched weights (see Section 3.5.3 and Appendix B) and how to estimate the associated DV [26]. We are interested in PW functions that do not generate new unknown quantities (condensates of higher dimension), since in that case a clean analysis is not possible anymore.

As we have explained in the Appendix B, in the case of the condensates the pinched weights with a double zero at $s = s_0$ are expected to minimize the DV with respect to the standard weights s^n, although the question of how large is the remaining DV is still not clear[6]. In the case of the chiral parameters, the pinched weights will be better or worse than the standard weights depending essentially on how fast the spectral function goes to zero, in order to suppress the enhancement that the pinched weights produce in the high-energy region (see Eq. (5.12)). In other words, the key point is thfe value of the γ parameter, that as we have seen is around one. Our simple calculations of the Appendix B indicate that this is high enough to suppress the high-energy tail and so to benefit from the use of the PW. Now we want to check it explicitly with our hundreds of spectral functions.

Let us remind that in addition to the DV error (estimated from the dispersion of the histograms) we have the experimental ALEPH error, and both depend on the used weight. In principle one expects the PW to minimize also the experimental uncertainties, since they suppress the region near the kinematical end point.

We have repeated all our analysis with pinched weights $w(s)$ that have a double zero in $s = s_{pw}$, that is

$$
\begin{aligned}
P_{-2}(s_0) &\equiv \int_{s_{\text{th}}}^{s_0} \mathrm{d}s\, \frac{\rho(s)}{s^2} \left(1 - \frac{s}{s_{pw}}\right)^2 \left(1 + 2\frac{s}{s_{pw}}\right) \\
&= 16\, C_{87}^{\text{eff}} - 6\frac{f_\pi^2}{s_{pw}^2} + 4\frac{f_\pi^2 m_\pi^2}{s_{pw}^3} - \mathrm{DV}[w(z), s_0]\,, \quad (5.29)
\end{aligned}
$$

$$
\begin{aligned}
P_{-1}(s_0) &\equiv \int_{s_{\text{th}}}^{s_0} \mathrm{d}s\, \frac{\rho(s)}{s} \left(1 - \frac{s}{s_{pw}}\right)^2 \\
&= -8L_{10}^{\text{eff}} - 4\frac{f_\pi^2}{s_{pw}} + 2\frac{f_\pi^2 m_\pi^2}{s_{pw}^2} - \mathrm{DV}[w(z), s_0]\,, \quad (5.30)
\end{aligned}
$$

$$
\begin{aligned}
P_2(s_0) &\equiv \int_{s_{\text{th}}}^{s_0} \mathrm{d}s\, \rho(s)\, (s - s_{pw})^2 \\
&= 2f_\pi^2 s_{pw}^2 - 4f_\pi^2 m_\pi^2 s_{pw} + 2f_\pi^2 m_\pi^4 + \mathcal{O}_6 - \mathrm{DV}[w(z), s_0]\,, \quad (5.31)
\end{aligned}
$$

$$
\begin{aligned}
P_3(s_0) &\equiv \int_{s_{\text{th}}}^{s_0} \mathrm{d}s\, \rho(s)\, (s - s_{pw})^2 (s + 2s_{pw}) \\
&= -6f_\pi^2 m_\pi^2 s_{pw}^2 + 4f_\pi^2 s_{pw}^3 + 2f_\pi^2 m_\pi^6 - \mathcal{O}_8 - \mathrm{DV}[w(z), s_0]\,. \quad (5.32)
\end{aligned}
$$

---

[6]This was also analyzed in Ref. [21] in the particular context of a resonance-based model.
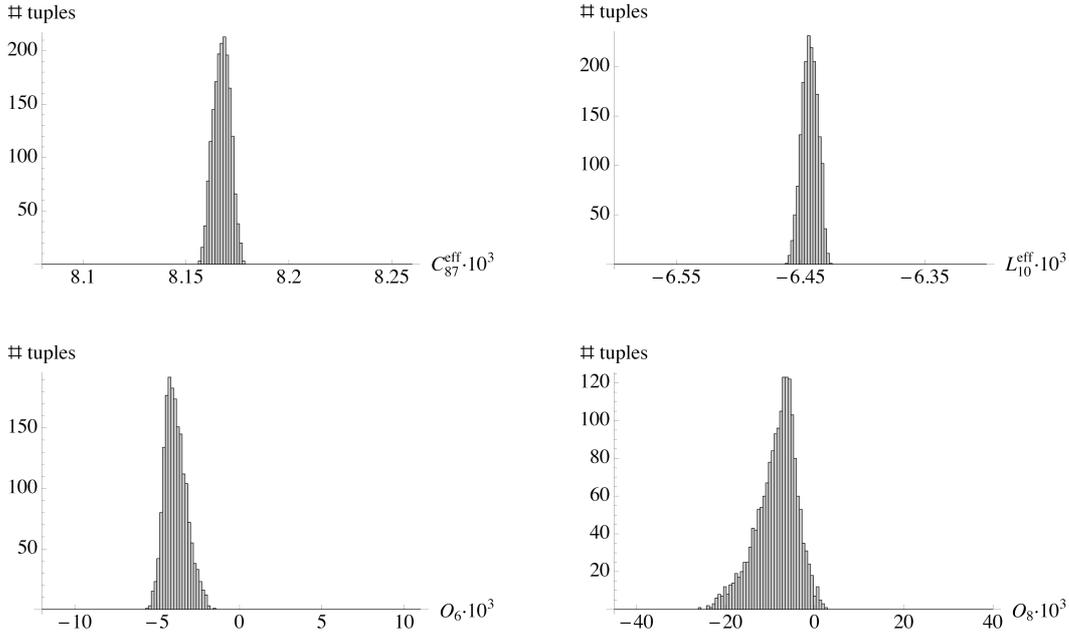
Figure 5.5: Statistical distribution of values of C_{87}^{eff} (upper-left), L_{10}^{eff} (upper-right), $\mathcal{O}_6$ (lower-left) and $\mathcal{O}_8$ (lower-right) for the accepted spectral functions, using the pinched-weight sum rules (5.29) - (5.32) with $s_{pw} = s_z \sim 2.1$ GeV^2. The parameters are expressed in GeV elevated to the corresponding power.

The results depend on the point where the weight is pinched, i.e. on the value of s_{pw}. In order to suppress the experimental error it is convenient to pinch the weight at the left of the matching point s_z, whereas in order to suppress the DV-error (dispersion of the histograms) it is convenient to pinch it at the right of s_z. We have scanned the region finding that the optimal choice of s_{pw}, that is, where the errors are minimized[7], is $s_{pw} \sim s_z \sim 2.1$ GeV^2. In the Fig. 5.5 we show the results obtained in this case. As we see the histograms are much more peaked around their central values and so we have better predictions (because as we said the data error is also minimized by the new weights[8]). The associated numerical results are

$$
\begin{aligned}
C_{87}^{eff} &= \left(8.168^{+0.003}_{-0.004} \pm 0.12\right) \cdot 10^{-3} \text{ GeV}^{-2} = (8.17 \pm 0.12) \cdot 10^{-3} \text{ GeV}^{-2}, & (5.33)\\
L_{10}^{eff} &= \left(-6.444^{+0.007}_{-0.004} \pm 0.05\right) \cdot 10^{-3} = (-6.44 \pm 0.05) \cdot 10^{-3}, & (5.34)\\
\mathcal{O}_6 &= \left(-4.33^{+0.68}_{-0.34} \pm 0.65\right) \cdot 10^{-3} \text{ GeV}^6 = \left(-4.3^{+0.9}_{-0.7}\right) \cdot 10^{-3} \text{ GeV}^6, & (5.35)\\
\mathcal{O}_8 &= \left(-7.2^{+3.1}_{-4.4} \pm 2.9\right) \cdot 10^{-3} \text{ GeV}^8 = \left(-7.2^{+4.2}_{-5.3}\right) \cdot 10^{-3} \text{ GeV}^8, & (5.36)
\end{aligned}
$$

where we have followed the same convention about the errors. The 95% probability

---

[7]Obviously the optimal point is different for every sum rule (5.29) - (5.32), but the differences are negligible within errors.

[8]Notice that in the case of $\mathcal{O}_8$ this is not true. This is because the pinched weight enhances the low-energy region errors sizably.

results are:

$$
\begin{aligned}
C_{87}^{eff} &= \left(8.168_{-0.008}^{+0.005} \pm 0.24\right) \cdot 10^{-3} \text{ GeV}^{-2} = (8.17 \pm 0.24) \cdot 10^{-3} \text{ GeV}^{-2}, & (5.37) \\
L_{10}^{eff} &= \left(-6.444_{-0.011}^{+0.011} \pm 0.1\right) \cdot 10^{-3} = (-6.4 \pm 0.1) \cdot 10^{-3} \,, & (5.38) \\
\mathcal{O}_6 &= \left(-4.33_{-0.68}^{+1.70} \pm 1.3\right) \cdot 10^{-3} \text{ GeV}^6 = \left(-4.3_{-1.5}^{+2.1}\right) \cdot 10^{-3} \text{ GeV}^6 \,, & (5.39) \\
\mathcal{O}_8 &= \left(-7.2_{-11.3}^{+6.3} \pm 5.8\right) \cdot 10^{-3} \text{ GeV}^8 = \left(-7.2_{-12.7}^{+8.6}\right) \cdot 10^{-3} \text{ GeV}^8 \,. & (5.40)
\end{aligned}
$$

As theoretically expected, the use of the pinched weights is less beneficial to the determination of the low-energy constants L_{10}^{eff} and C_{87}^{eff} than to the determination of the condensates. Our final results for the former are in excellent agreement with the most recent determination of them [78], that we explained in the previous chapter: $C_{87}^{\text{eff}} = (8.18 \pm 0.14) \cdot 10^{-3} \text{ GeV}^{-2}$ and $L_{10}^{\text{eff}} = -(6.48 \pm 0.06) \cdot 10^{-3}$. Notice that our estimation of the error, obtained through a completely different method, is based on more solid grounds than the error estimates of the previous chapter and represents a confirmation of them.

We have obtained quite precise measurements for the condensates $\mathcal{O}_6$ and $\mathcal{O}_8$ using the pinched-weights FESRs (5.31) and (5.32). In this way we have checked that the PW successes in minimizing the errors and we have that the most recent experimental information provided by ALEPH, together with the theoretical constraints (WSRs and πSR), fix with accuracy the value of $\mathcal{O}_6$ and almost determine[9] the sign of $\mathcal{O}_8$. Our results are compared in Fig. 5.6 with previous determinations of $\mathcal{O}_6$ and $\mathcal{O}_8$. One recognizes in the figure the existence of two groups of results that disagree between them. For $\mathcal{O}_6$ there is a small tension between a bigger or smaller value, whereas in the case of $\mathcal{O}_8$ the disagreement affects to the sign and is more sizable.

Our results agree with those of Refs. [30–33] since they also use pinched weights, but it is based on much more solid grounds, due to the completely different approach followed. We see in fact that the DV-error was slightly underestimated in Refs. [30, 31]. We also agree with the results of Ref. [41] based on the use of the second duality point, although that technique has a much larger error. It is remarkable the agreement with Ref. [104] that is the only one that follows a technique similar to ours, trying to analyze the possible behavior of the spectral function but through a neural network approach. Their result has a bigger uncertainty, maybe only due to the fact they used the old ALEPH data. There is a reasonable agreement also with the results of Refs. [109–111].

Our analysis indicates that the DV error associated to the use of the first duality point is very large and was grossly underestimated in Refs. [37,38], where also higher-dimensional condensates were neglected. In Refs. [68,112–114] the numerical values obtained at this first duality point are supported through theoretical analyses based on the so-called "minimal hadronic ansatz" (a large-N_C-inspired 3-pole model) or Padè approximants. Our results show however that the first duality point is very

---

[9]One can see in our final result (5.40) that at 2σ a positive value of $\mathcal{O}_8$ is already allowed, but it must not be forgotten that the distribution is highly non-gaussian and we can see in the corresponding histogram of Fig. 5.5 that the possibility of being positive is negligible.
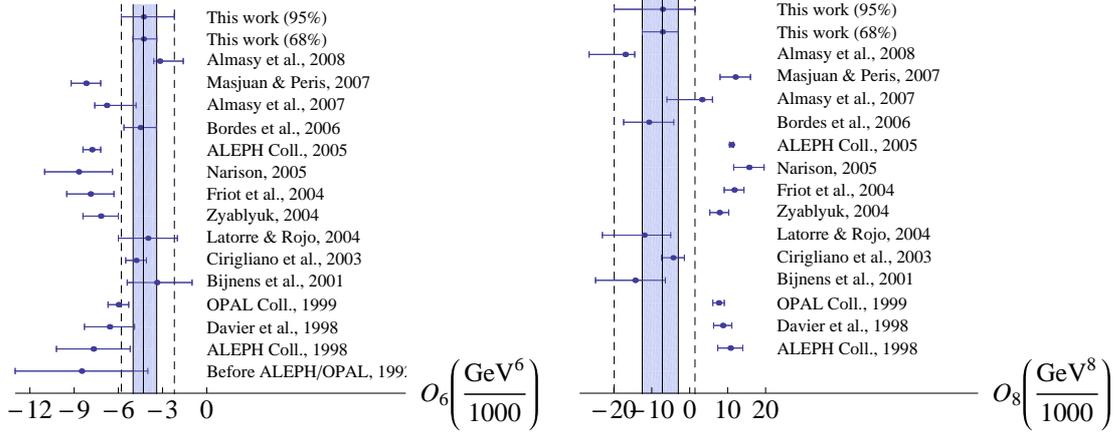
Figure 5.6: Comparison of our results for $\mathcal{O}_6$ (left) and $\mathcal{O}_8$ (right) with previous determinations [3, 30–33, 37, 38, 41, 42, 44, 53, 68, 104, 109, 111, 113] (we show for every method the most recent determination). The blue bands show our results at 65% C.L., while the 95% probability regions are indicated by the dotted lines.

unstable when we change from the WSRs to the $\mathcal{O}_{6,8}$ sum rules, indicating that the systematic error of these approaches is non-negligible. Essentially the same can be said about Refs. [42, 53] where the last available point $s_0 = m_\tau^2$ was used.

Summarizing, our results agree within two-sigmas with the other estimates of $\mathcal{O}_6$, but in the case of $\mathcal{O}_8$ show that its sign is negative, in disagreement with Refs. [37, 38, 42, 53, 68, 113].

5.5 Beyond the dimension eight condensate

We can play the same game with higher dimensional condensates, where using again pinched weights $w(s)$ that have a double zero in $s = s_{pw}$ we have

$$
\begin{aligned}
P_4(s_0) &\equiv \int_{s_{\text{th}}}^{s_0} \mathrm{d}s \; \rho(s) \; (s - s_{pw})^2 \left(s^2 + 2s_{pw}s + 3s_{pw}^2\right) \\
&= -8f_\pi^2 m_\pi^2 s_{pw}^3 + 6f_\pi^2 s_{pw}^4 + 2f_\pi^2 m_\pi^8 + \mathcal{O}_{10} - \mathrm{DV}[w_4, s_0] \,, \qquad (5.41)
\end{aligned}
$$

$$
\begin{aligned}
P_5(s_0) &\equiv \int_{s_{\text{th}}}^{s_0} \mathrm{d}s \; \rho(s) \; (s - s_{pw})^2 \left(s^3 + 2s_{pw}s^2 + 3s_{pw}^2 s + 4s_{pw}^3\right) \\
&= -10f_\pi^2 m_\pi^2 s_{pw}^4 + 8f_\pi^2 s_{pw}^5 + 2f_\pi^2 m_\pi^{10} - \mathcal{O}_{12} - \mathrm{DV}[w_5, s_0] \,, \qquad (5.42)
\end{aligned}
$$

$$
\begin{aligned}
P_6(s_0) &\equiv \int_{s_{\text{th}}}^{s_0} \mathrm{d}s \; \rho(s) \; (s - s_{pw})^2 \left(s^4 + 2s_{pw}s^3 + 3s_{pw}^2 s^2 + 4s_{pw}^3 s + 5s_{pw}^4\right) \\
&= -12f_\pi^2 m_\pi^2 s_{pw}^5 + 10f_\pi^2 s_{pw}^6 + 2f_\pi^2 m_\pi^{12} + \mathcal{O}_{14} - \mathrm{DV}[w_6, s_0] \,, \qquad (5.43)
\end{aligned}
$$

$$
\begin{aligned}
P_7(s_0) &\equiv \int_{s_{\text{th}}}^{s_0} \mathrm{d}s \; \rho(s) \; (s - s_{pw})^2 \left(s^5 + 2s_{pw}s^4 + 3s_{pw}^2 s^3 + 4s_{pw}^3 s^2 + 5s_{pw}^4 s + 6s_{pw}^5\right) \\
&= -14f_\pi^2 m_\pi^2 s_{pw}^6 + 12f_\pi^2 s_{pw}^7 + 2f_\pi^2 m_\pi^{14} - \mathcal{O}_{16} - \mathrm{DV}[w_7, s_0] \,. \qquad (5.44)
\end{aligned}
$$
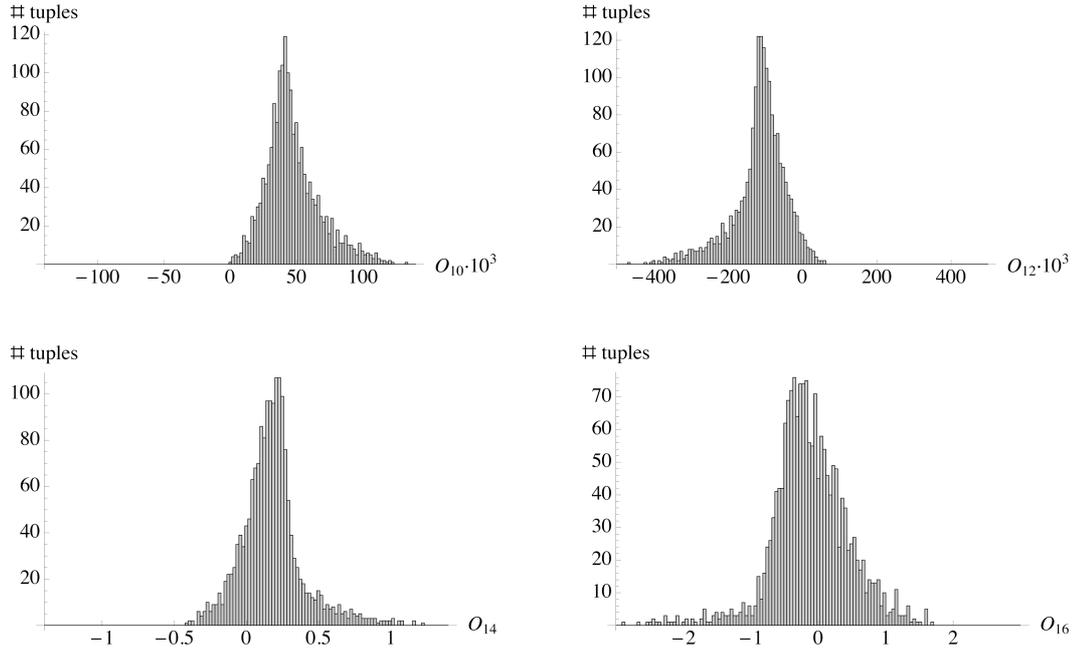
Figure 5.7: Statistical distribution of values of $\mathcal{O}_{10,12,14,16}$ for the accepted spectral functions, using the PW sum rules (5.41) - (5.44) with $s_{pw} = s_z \sim 2.1$ GeV^2. The parameters are expressed in GeV elevated to the corresponding power.

Working again with $s_{pw} \sim s_z \sim 2.1$ GeV^2 we find the results that are shown in the Fig. 5.7. The associated numerical results are

$$\mathcal{O}_{10} = \left(+4.1^{+1.8}_{-1.6}\right) \cdot 10^{-2} \text{ GeV}^{10} , \tag{5.45}$$

$$\mathcal{O}_{12} = \left(-0.12^{+0.07}_{-0.03}\right) \text{ GeV}^{12} , \tag{5.46}$$

$$\mathcal{O}_{14} = \left(+0.2^{+0.1}_{-0.2}\right) \text{ GeV}^{14} , \tag{5.47}$$

$$\mathcal{O}_{16} = \left(-0.2^{+0.5}_{-0.4}\right) \text{ GeV}^{16} , \tag{5.48}$$

where all the errors come from the dispersion of our histograms since the experimental error is very much smaller for these higher dimensional condensates. The 95% probability results are:

$$\mathcal{O}_{10} = \left(+4.1^{+5.6}_{-3.1}\right) \cdot 10^{-2} \text{ GeV}^{10} , \tag{5.49}$$

$$\mathcal{O}_{12} = \left(-0.12^{+0.13}_{-0.16}\right) \text{ GeV}^{12} , \tag{5.50}$$

$$\mathcal{O}_{14} = \left(+0.2 \pm 0.5\right) \text{ GeV}^{14} , \tag{5.51}$$

$$\mathcal{O}_{16} = \left(-0.2^{+1.8}_{-1.1}\right) \text{ GeV}^{16} . \tag{5.52}$$

It is really impressive that the sign of the condensates can be established for $\mathcal{O}_{10}$ and $\mathcal{O}_{12}$ since the importance of the high-energy region in their determination is huge. One could have expected that the differences between our possible spectral functions would generate a huge error in these higher dimensional condensates, but our conditions (WSRs+πSR+data) have turned out to be very restrictive about the possible spectral functions allowing quite precise extractions.

	$\mathcal{O}_{10} \times 10^3$	$\mathcal{O}_{12} \times 10^3$	$\mathcal{O}_{14} \times 10^3$	$\mathcal{O}_{16} \times 10^3$
This work	$+41^{+18}_{-16}$	-120^{+70}_{-30}	$+200^{+100}_{-200}$	-200^{+500}_{-400}
Masjuan & Peris [68]	-14 ± 12			
Narison [37]	-17.1 ± 4.4	$+14.7 \pm 3.7$	-9.6 ± 3.1	$+4.3 \pm 1.9$
Friot et al. [113]	-13.2 ± 3.6	$+13.3 \pm 3.9$	-12.8 ± 3.9	$+11.9 \pm 3.8$
Zyablyuk [38]	-4.5 ± 3.4			
Almasy et al. [111]	$+66^{+40}_{-14}$			
Bordes et al. [33]	$+72 \pm 28$	-240 ± 50		
Latorre & Rojo [104]	$+78 \pm 24$	-260 ± 80		
Cirigliano et al. [31]	$+48 \pm 10$	-160 ± 30	$+430 \pm 60$	-1030 ± 140

Table 5.1: Comparison of our determination of $\mathcal{O}_{10,12,14,16}$ with other works. The condensates are expressed in GeV to the corresponding power. The results shown for Ref. [31] are those obtained with the old ALEPH data (with the OPAL data the numbers are not very different), and the results shown for Ref. [113] are those obtained with the minimal hadronic ansatz, that is, without the addition of the ρ' resonance, that in any case modifies just slightly the results.

In Table 5.1 we show the different results available in the literature and we can again observe the existence of two groups of results. As in the case of $\mathcal{O}_{6,8}$, our results agree with Refs. [30–33, 41, 104] but not with Refs. [37, 38, 42, 53, 68, 113].

Looking at the results of Ref. [31], obtained working with pinched weights and the old ALEPH data, we can see what we have said several times through this work: even in the case when the pinched weights generate less DV than the standard weights s^n, the observed plateau is in part artificially created and hides the DV. That is why the errors of Ref. [31] are underestimated.

5.6   Summary

The phenomenological requirement for increasing precisions in the determinations of hadronic parameters makes necessary to assess the size of small effects which previously could be considered negligible. In particular, a substantial improvement of QCD Sum Rules results, needed to determine many hadronic observables both in the Standard Model and in models beyond it, could only be possible with a better control of DV.

Violations of quark-hadron duality are difficult to estimate because those effects are unknown by definition. They originate in the uncertainties associated with the use of the OPE to approximate the exact physical correlator. As defined in Eq. (5.4), DV effects correspond to an OPE approximation performed in the complex plane, outside the Minkowskian region, which deteriorates in the vicinity of the real axis. Using analyticity, the size of DV can be related with an integral of the hadronic spectral function from s_0 up to ∞, given in Eq. (5.12), which allows us to perform a phenomenological analysis.

We have studied the possible role of DV in the two-point correlation function $\Pi(s)$. This $V - A$ non-strange correlator is very well suited for this analysis because: i) it is a purely non-perturbative quantity in the chiral limit, ii) there are well-known theoretical constraints, and iii) there exist good available data from τ decays. Moreover, different moments of its spectral function provide hadronic parameters of high phenomenological relevance.

We have assumed a generic, but theoretically motivated, behaviour of the spectral function at high energies, where data are not available, with four free parameters. This allows us to study how much freedom in $\rho(s)$ could be tolerated, beyond the requirement that all known QCD constraints are satisfied. Performing a numerical scanning over the four-dimensional parameter space, we have generated a large number of "acceptable" spectral functions, satisfying all conditions, and have used them to extract the wanted hadronic parameters through a careful statistical analysis. The dispersion of the numerical results provides then a good quantitative assessment of the actual uncertainties.

This machinery has allowed us to address the question of the convenience of the pinched weights and how to estimate the size of the still present DV. We have found that it is worthwhile to use these weights and we have determined four hadronic parameters of special interest: C_{87}^{eff}, L_{10}^{eff}, $\mathcal{O}_6$ and $\mathcal{O}_8$

$$C_{87}^{eff} = (8.17 \pm 0.12) \cdot 10^{-3} \text{ GeV}^{-2}, \qquad (5.53)$$

$$L_{10}^{eff} = (-6.44 \pm 0.05) \cdot 10^{-3}, \qquad (5.54)$$

$$\mathcal{O}_6 = \left(-4.3_{-0.7}^{+0.9}\right) \cdot 10^{-3} \text{ GeV}^6, \qquad (5.55)$$

$$\mathcal{O}_8 = \left(-7.2_{-5.3}^{+4.2}\right) \cdot 10^{-3} \text{ GeV}^8. \qquad (5.56)$$

From the first two parameters one can extract the values of the χPT couplings $C_{87}^r(M_\rho)$ and $L_{10}^r(M_\rho)$. The vacuum condensate $\mathcal{O}_6$ is an important input for the calculation of the CP-violating kaon parameter ε'_K, it dominates the $\Delta I = 3/2$ contribution to ε'_K [30, 41, 54–57]. The determination of this contribution is an important goal of lattice QCD calculations and independent information is required to test the reliability of those results. We will study the consequences of our results for ε'_K in a forthcoming publication [115].

There is a small tension among the different determinations of $\mathcal{O}_6$ available in the literature, and the discrepancy is higher for the condensate $\mathcal{O}_8$. Our results agree with those of Refs. [30–33,41,104] and indicate that the other determinations [37,38, 42,53,68,113] (most of them associated to the first duality point) underestimated the DV contribution, what was generating the different results. Our values show that the analyses based on the use of pinched-weight FESRs have assigned a reasonable uncertainty for the lowest dimensional condensates $\mathcal{O}_{6,8}$ but have underestimated the error in the determination of higher dimensional condensates.

Our method indicates that the current experimental values for the $V - A$ spectral function in the region between $s \sim 2$ GeV^2 and $s \sim 3$ GeV^2 are somehow affected by a systematic error that shifts the points towards higher values. It is worth noting that this result is also suggested by the work of Ref. [104]. A significant improvement

in the experimental knowledge of the spectral functions in this intermediate region is expected with the future high-statistics τ-decay data samples. It will be very interesting to check the presence of this systematic error and validate our approach.

It is worth noting that in particular our method shows that $\mathcal{O}_6$ and $\mathcal{O}_8$ are both negative, whereas it suggests that the sign alternates for higher-dimensional condensates.

Chapter 6

Going beyond the SM

The show must go on.
Queen

The impressive precision achieved by the low-energy experiments in combination
with improved theoretical control of hadronic matrix elements and radiative correc-
tions make semileptonic decays of light quarks (kaons, pions, nuclear beta decays,
hadronic tau decays, etc.) and purely leptonic decays (muon and tau physics) a
deep probe of the nature of weak interactions. As we will see this low-energy ex-
periments are sensitive to energy scales Λ on the order of the TeV, which will be
directly probed at the LHC.

While the consequences of these low-energy tests of the Standard Model have
been considered in a number of explicit New Physics scenarios, a model-independent
analysis of leptonic and semileptonic processes beyond the SM is missing. The goal
of this investigation is to analyze in a model-independent effective theory setup new
physics contributions to low energy charged-current (CC) processes. The resulting
framework allows us to assess in a fairly general way the impact of (semi)leptonic
processes in constraining and discriminating SM extensions.

Assuming the existence of a mass gap between the SM and its extension, we
parametrize the effect of new degrees of freedom and interactions beyond the SM via
a series of higher dimensional operators constructed with the low-energy SM fields.
If the SM extension is weakly coupled, the resulting TeV-scale effective Lagrangian
linearly realizes the electro-weak (EW) symmetry $SU(2)_L \times U(1)_Y$ and contains a
SM-like Higgs doublet [116, 117]. This method is quite general and allows us to
study the implications of low-energy precision measurements on a large class of
models. For example, it will allow us to understand in a model-independent way
the significance of these low-energy tests compared to collider measurements.

The interplay of these kind of model-independent approaches and the studies
in particular scenarios stimulated by the model-builders efforts is very important
since the former can point to unexplored directions and trigger new ideas among
model-builders, whereas the later are completely necessary to reduce the enormous
number of parameters of any effective field theory based approach.

This chapter is organized as follows. In Section 6.1 we review the form of the most general weak scale effective Lagrangian including operators up to dimension six, contributing to precision electroweak measurements *and* (semi)leptonic decays. In Section 6.2 we derive the low-energy (~ 1 GeV) effective Lagrangian describing purely leptonic and semileptonic CC interaction. We discuss the flavor structure of the relevant effective couplings in Section 6.3 and section 6.4 contains our conclusions. In the next chapter we will apply this framework to the study of the CKM-unitarity tests and its significance constraining New Physics.

6.1   Weak scale effective Lagrangian

As discussed in the introduction, our aim is to analyze in a model-independent framework new physics contributions to both precision electroweak observables and muon and beta decays. Given the successes of the SM at energies up to the electroweak scale $v \sim 100$ GeV, we adopt here the point of view that the SM is the low-energy limit of a more fundamental theory. Specifically, we adopt the following assumptions:

- There is a gap between the weak scale v and the scale Λ where new degrees of freedom appear;

- The SM extension at the weak scale is weakly coupled, so the EW symmetry $SU(2)_L \times U(1)_Y$ is linearly realized and the low-energy theory contains a SM-like Higgs doublet [117]. Analyses of EW precision data in nonlinear realizations of EW symmetry can be found in the literature [101,102,118,119];

- The particle content of our Lagrangian will be then that of the Standard Model, including the SM-Higgs field and without considering the right-handed neutrinos as low-energy degrees of freedom;

- We will not consider operators that violate total lepton and baryon number (we assume they are suppressed by a scale much higher than $\Lambda \sim$ TeV [120]).

In the spirit of the effective field theory approach, we integrate out all the heavy fields and describe physics at the weak scale (and below) by means of an effective non-renormalizable Lagrangian of the form:

$$\mathcal{L}^{(\text{eff})} = \mathcal{L}_{\text{SM}} + \frac{1}{\Lambda}\mathcal{L}_5 + \frac{1}{\Lambda^2}\mathcal{L}_6 + \frac{1}{\Lambda^3}\mathcal{L}_7 + \ldots \tag{6.1}$$

$$\mathcal{L}_n = \sum_i \alpha_i^{(n)} O_i^{(n)}, \tag{6.2}$$

where Λ is the characteristic scale of the new physics and $\mathcal{O}_i^{(n)}$ are local gauge-invariant operators of dimension n built out of SM fields.

6.1.1 The fields and the SM Lagrangian

The building blocks to construct local operators are the gauge fields G_μ^A, W_μ^a, B_μ, corresponding to $SU(3) \times SU(2)_L \times U(1)_Y$, the five fermionic gauge multiplets,

$$\ell^i = \begin{pmatrix} \nu_L^i \\ e_L^i \end{pmatrix}, \qquad e^i = e_R^i, \qquad q^i = \begin{pmatrix} u_L^i \\ d_L^i \end{pmatrix}, \qquad u^i = u_R^i, \qquad d^i = d_R^i, \quad (6.3)$$

the Higgs doublet

$$\varphi = \begin{pmatrix} \varphi^+ \\ \varphi^0 \end{pmatrix}, \tag{6.4}$$

and the covariant derivative

$$D_\mu = I\, \partial_\mu \; - \; ig_s \frac{\lambda^A}{2} G_\mu^A \; - \; ig \frac{\sigma^a}{2} W_\mu^a \; - \; ig' Y B_\mu \; . \tag{6.5}$$

In the above expression λ^A are the $SU(3)$ Gell-Mann matrices, σ^a are the $SU(2)$ Pauli matrices, g_s, g, g' are the gauge couplings and Y is the hypercharge of a given multiplet ($Y(\ell) = -1/2, Y(e) = -1, Y(q) = 1/6, Y(u) = 2/3, Y(d) = -1/3, Y(\varphi) = 1/2$).

With this notation, the SM Lagrangian takes the form

$$\begin{aligned}
\mathcal{L}_{SM}(x) \;\; = \;\; & -\frac{1}{4} G_{\mu\nu}^A G^{A\mu\nu} - \frac{1}{4} W_{\mu\nu}^I G^{I\mu\nu} - \frac{1}{4} B_{\mu\nu} B^{\mu\nu} \\
& + (D_\mu \varphi)^\dagger (D^\mu \varphi) + m^2 \varphi^\dagger \varphi - \frac{1}{2} \lambda (\varphi^\dagger \varphi)^2 \\
& + \bar{\ell} \slashed{D} \ell + \bar{e} \slashed{D} e + \bar{q} \slashed{D} q + \bar{u} \slashed{D} u + \bar{d} \slashed{D} d \\
& + (\ell\, \Gamma_e\, e\, \varphi + \; q\, \Gamma_u\, u\, \tilde{\varphi} + \; q\, \Gamma_d\, d\, \varphi + \text{h.c.}) \; ,
\end{aligned} \tag{6.6}$$

where the $\Gamma_{e,u,d}$ are the Yukawa matrices (in flavor space).

6.1.2 The new physics corrections

Under the above-stated assumptions, it can be shown that the first corrections to the SM Lagrangian are of dimension six. The list of dimension-six operators was given by Leung et al. [116], Buchmüller and Wyler (BW) [117] and Burgess and Robinson [121]. Only the later list is complete and none of them is minimal. We will follow the BW-notation, with the following modifications in order to have a complete and minimal basis

- The four-fermion operator $O_{lq}^t = (\bar{\ell}_a \sigma^{\mu\nu} e)\epsilon^{ab}(\bar{q}_b \sigma_{\mu\nu} u)$ must be added to the list (the ϵ tensor is used to contract weak SU(2) indices)[1].

---

[1] This operator and its scalar version must be added to the list of Leung et al. [116] to make the list complete.

- The operators $O_{ll}^{(3)}, O_{qq}^{(8,1)}, O_{qq}^{(8,3)}, O_{uu}^{(8)}$ and $O_{dd}^{(8)}$ can be eliminated using the Fierz transformation and the completeness relation of the Pauli (Gell-Mann) matrices[2,3]: $\sum_I \tau_{ij}^I \tau_{kl}^I = -\delta_{ij}\delta_{kl} + 2\delta_{il}\delta_{kj}$;

- The dagger in the operator (3.55) of Ref. [117] should be replaced by a T (transpose symbol);

- The names O_{uG} and O_{dG} have been used twice in BW: operators (3.34, 3.36) and operators (3.61, 3.63) of Ref. [117].

As a result of these observations, the eighty operators of BW are reduced to seventy-six, and therefore truncating the expansion (6.1) at this order we have

$$\mathcal{L}_{BW}^{(\text{eff})} = \mathcal{L}_{\text{SM}} + \sum_{i=1}^{76} \frac{\alpha_i}{\Lambda^2}\, O_i \ . \tag{6.7}$$

For operators involving quarks and leptons, both the coefficients α_i and the operators O_i carry flavor indices. When needed, we will make the flavor indices explicit, using the notation $[\alpha_i]_{abcd}$ for four-fermion operators.

The above effective Lagrangian allows one to parameterize non-standard corrections to any observable involving SM particles. The contribution from the dimension six operators involve terms proportional to v^2/Λ^2 and E^2/Λ^2, where $v = \langle\varphi^0\rangle \simeq 174\,\text{GeV}$ is the vacuum expectation value (VEV) of the Higgs field and E is the characteristic energy scale of a given process. In order to be consistent with the truncation of (6.1) we will work at linear order in the above ratios[4].

We are interested in the minimal subset of the BW basis that contribute at tree level to CP-conserving electroweak precision observables *and* beta decays.

Once the CP-assumption is taken into account, we have seventy operators in our effective Lagrangian[5]. Moreover, we will not take into account the thirteen operators that involve only quark and gluon fields[6], because they will not appear in our observables (precision EW measurements and semileptonic decays) at the level we are working. Further operators that do not contribute to our observables are O_{qG}, O_{uG}, O_{dG}.

Since we are not considering processes involving the Higgs boson as an external particle, we can remove more operators from our list: $O_\varphi, O_{\partial\varphi}$ (they only involve

---

[2]I would like to thank Alberto Filipuzzi for calling my attention about this fact.

[3]It is worth noting that in the (as far as we know) first work [122] where a complete list of four-lepton operators was written the authors realized about this redundancy and their basis was minimal. Somehow this was forgotten in the subsequent publications [116, 117, 121, 123].

[4]When the SM amplitude vanishes the first contribution is quadratic in the ratios v^2/Λ^2 and E^2/Λ^2, but in this case one can consistently work at this order and neglect the eight-dimension operators, since their lowest contributions would be the interference with the dimension-six amplitude, that is, of third order in the above ratios.

[5]The six operators removed are O_X with $X = \tilde{G}, \tilde{W}, \varphi\tilde{G}, \varphi\tilde{W}, \varphi\tilde{B}, \tilde{W}B$.

[6]O_X with $X = G, qq^{(1)}, qq^{(8)}, uu^{(1)}, dd^{(1)}, qq^{(1,1)}, qq^{(1,3)}, ud^{(1)}, ud^{(8)}, qu^{(1)}, qu^{(8)}, qd^{(1)}, qd^{(8)}$.

scalar fields), and seven more operators[7] whose effect can be absorbed in a redefinition of the SM parameters g, g', g_s, v and the Yukawa couplings. In this way we end up with forty-five operators that can produce a linear correction to the SM-prediction of our observables. But a more detailed analysis of this list [124] shows that twenty-one of them either do not produce linear corrections (because the interference with the SM vanishes) or produce effects suppressed by an additional factor (for example, low energy four-quark operators of dimension seven).

So finally we end up with a basis involving twenty-four operators. In selecting the operators, flavor symmetries played no role (in fact at this level the coefficients α_i can carry any flavor structure). However, in order to organize the subsequent phenomenological analysis, it is useful to classify the operators according to their behavior under the $U(3)^5$ flavor symmetry of the SM gauge Lagrangian (the freedom to perform $U(3)$ transformations in family space for each of the five fermionic gauge multiplets, listed in Eq. 6.3).

6.1.3 $U(3)^5$ invariant operators

The operators that contain only vectors and scalars are

$$O_{WB} = (\varphi^\dagger \sigma^a \varphi) W^a_{\mu\nu} B^{\mu\nu}, \quad O_\varphi^{(3)} = |\varphi^\dagger D_\mu \varphi|^2 . \tag{6.8}$$

There are eleven four-fermion operators:

$$O_{ll}^{(1)} = \frac{1}{2}(\bar{l}\gamma^\mu l)(\bar{l}\gamma_\mu l), \quad O_{ll}^{(3)} = \frac{1}{2}(\bar{l}\gamma^\mu \sigma^a l)(\bar{l}\gamma_\mu \sigma^a l), \tag{6.9}$$

$$O_{lq}^{(1)} = (\bar{l}\gamma^\mu l)(\bar{q}\gamma_\mu q), \quad O_{lq}^{(3)} = (\bar{l}\gamma^\mu \sigma^a l)(\bar{q}\gamma_\mu \sigma^a q), \tag{6.10}$$

$$O_{le} = (\bar{l}\gamma^\mu l)(\bar{e}\gamma_\mu e), \quad O_{qe} = (\bar{q}\gamma^\mu q)(\bar{e}\gamma_\mu e), \tag{6.11}$$

$$O_{lu} = (\bar{l}\gamma^\mu l)(\bar{u}\gamma_\mu u), \quad O_{ld} = (\bar{l}\gamma^\mu l)(\bar{d}\gamma_\mu d), \tag{6.12}$$

$$O_{ee} = \frac{1}{2}(\bar{e}\gamma^\mu e)(\bar{e}\gamma_\mu e), \quad O_{eu} = (\bar{e}\gamma^\mu e)(\bar{u}\gamma_\mu u), \quad O_{ed} = (\bar{e}\gamma^\mu e)(\bar{d}\gamma_\mu d). \tag{6.13}$$

Some comments are in order. In principle, in order to avoid redundancy (see discussion above) one must discard either $O_{ll}^{(3)}$ or $O_{ll}^{(1)}$, but here we have followed the common practice to work with both operators[8]. Moreover, we use the structure $\bar{L}\gamma_\mu L \cdot \bar{R}\gamma^\mu R$ in operators (6.11), instead of their Fierz transformed $\bar{L}R \cdot \bar{R}L$, that BW use. They are related by a factor (-2).

There are seven operators containing two fermions that alter the couplings of fermions to the gauge bosons:

$$O_{\varphi l}^{(1)} = i(\varphi^\dagger D^\mu \varphi)(\bar{l}\gamma_\mu l) + \text{h.c.}, \quad O_{\varphi l}^{(3)} = i(\varphi^\dagger D^\mu \sigma^a \varphi)(\bar{l}\gamma_\mu \sigma^a l) + \text{h.c.}, \tag{6.14}$$

$$O_{\varphi q}^{(1)} = i(\varphi^\dagger D^\mu \varphi)(\bar{q}\gamma_\mu q) + \text{h.c.}, \quad O_{\varphi q}^{(3)} = i(\varphi^\dagger D^\mu \sigma^a \varphi)(\bar{q}\gamma_\mu \sigma^a q) + \text{h.c.}, \tag{6.15}$$

$$O_{\varphi u} = i(\varphi^\dagger D^\mu \varphi)(\bar{u}\gamma_\mu u) + \text{h.c.}, \quad O_{\varphi d} = i(\varphi^\dagger D^\mu \varphi)(\bar{d}\gamma_\mu d) + \text{h.c.}, \tag{6.16}$$

$$O_{\varphi e} = i(\varphi^\dagger D^\mu \varphi)(\bar{e}\gamma_\mu e) + \text{h.c.} . \tag{6.17}$$

---

[7] O_X with $X = \varphi W, \varphi B, \varphi^{(1)}, \varphi G, e\varphi, u\varphi, d\varphi$

[8] In the general case this redundancy is absurd, but in some particular frameworks, as MFV, it will allow us to consider only flavor structures factorized according to fermion bilinears.

Finally, there is one operator that modifies the triple gauge boson interactions

$$O_W = \epsilon^{abc} W_\mu^{a\nu} W_\nu^{b\lambda} W_\lambda^{c\mu}. \tag{6.18}$$

These twenty-one $U(3)^5$ invariant operators contribute to precision EW measurements (see Ref. [124]), whereas only five of them contribute to the semileptonic decays, as we will see.

6.1.4 Non $U(3)^5$ invariant operators

Three are three four-fermion operators

$$O_{qde} = (\bar{\ell}e)(\bar{d}q) + \text{h.c.}, \tag{6.19}$$

$$O_{lq} = (\bar{l}_a e)\epsilon^{ab}(\bar{q}_b u) + \text{h.c.}, \quad O_{lq}^t = (\bar{l}_a \sigma^{\mu\nu} e)\epsilon^{ab}(\bar{q}_b \sigma_{\mu\nu} u) + \text{h.c.}, \tag{6.20}$$

and one operator with two fermions

$$O_{\varphi\varphi} = i(\varphi^T \epsilon D_\mu \varphi)(\bar{u}\gamma^\mu d) + \text{h.c.} , \tag{6.21}$$

which gives rise to a right handed charged current coupling.

These four operators contribute both to precision EW measurements and to the semileptonic decays.

We conclude this section with some remarks on our convention for the coefficients of the "flavored" operators: (i) in those operators that include the h.c. in their definition, the flavor matrix α will appear in the h.c.-part with a dagger; (ii) for the operators $O_{ll}^{(1,3)}$ and O_{ee}, because of the symmetry between the two bilinears, we impose $[\alpha]_{ijkl} = [\alpha]_{klij}$; (iii) in order to ensure the hermiticity of the operators (6.9)-(6.13) we impose $[\alpha]_{ijkl} = [\alpha]_{jilk}^*$. None of these conditions entails any loss of generality.

6.2 Effective Lagrangian for μ and quark β decays

Our task is to identify new physics contributions to low-energy CC processes. In order to achieve this goal, we need to derive from the effective Lagrangian at the weak scale (in which heavy gauge bosons and heavy fermions are still active degrees of freedom) a low-energy effective Lagrangian describing muon and quark CC decays [125]. The analysis involves several steps which we discuss in some detail, since a complete derivation is missing in the literature, as far as we know.

6.2.1 Choice of weak basis for fermions

At the level of weak scale effective Lagrangian, we can use the $U(3)^5$ invariance to pick a particular basis for the fermionic fields. In general, a $U(3)^5$ transformation leaves the gauge part of the Lagrangian invariant while affecting both the Yukawa

couplings and the coefficients α_i of dimension six operators involving fermions. We perform a specific $U(3)^5$ transformation that diagonalizes the down-quark and charged lepton Yukawa matrices Y_D and Y_E and puts the up-type Yukawa matrix in the form $Y_U = V^\dagger Y_U^{\mathrm{diag}}$, where V is the CKM matrix. The flavored coefficients α_i correspond to this specific choice of weak basis for the fermion fields.

6.2.2 Electroweak symmetry breaking: transformation to propagating eigenstates

Once the Higgs acquires a VEV the quadratic part of the Lagrangian for gauge bosons and fermions becomes non-diagonal, receiving contributions from both SM interactions and dimension six operators. In particular, the NP contributions induce kinetic mixing of the weak gauge bosons, in addition to the usual mass mixing. Therefore the next step is to perform a change of basis so that the new fields have a canonically normalized kinetic term and definite masses.

Let us first discuss the gauge boson sector. We agree with the BW results on the definition of gauge field mass eigenstates and on the expressions for the physical masses[9]

$$W_\mu^3 = A_\mu \sin\theta_W^0 (1 - 2\sin\theta_W^0 \cos\theta_W^0 \ \hat{\alpha}_{WB}) + Z_\mu \cos\theta_W^0 (1 + 2\frac{\sin\theta_W^0{}^3}{\cos\theta_W^0}\hat{\alpha}_{WB}), \quad (6.22)$$

$$B_\mu = A_\mu \cos\theta_W^0 (1 - 2\sin\theta_W^0 \cos\theta_W^0 \ \hat{\alpha}_{WB}) - Z_\mu \sin\theta_W^0 (1 + 2\frac{c^3}{\sin\theta_W^0}\hat{\alpha}_{WB}), \quad (6.23)$$

$$m_W = m_W^0 = \frac{1}{2}g^2 v^2 \ , \quad (6.24)$$

$$m_Z = m_Z^0 (1 + 2\sin\theta_W^0 \cos\theta_W^0 \ \hat{\alpha}_{WB} + \ \hat{\alpha}_\varphi^{(3)})$$

$$= \frac{1}{2}(g^2 + g'^2)v^2 (1 + 2\sin\theta_W^0 \cos\theta_W^0 \ \hat{\alpha}_{WB} + \ \hat{\alpha}_\varphi^{(3)}) \ , \quad (6.25)$$

where θ_W^0 denotes the tree-level standard model weak angle

$$\cos\theta_W^0 = \frac{g}{\sqrt{g^2 + g'^2}} \ , \quad (6.26)$$

and where we have introduced the notation

$$\hat{\alpha}_X = \frac{v^2}{\Lambda^2} \alpha_X \ . \quad (6.27)$$

However, we find small differences from their results in the couplings of the W

---

[9]Notice that we have less operators than BW due to the reduced set of observables that we are interested in.

and Z to fermion pairs, which can be written as:

$$\mathcal{L}_J = \frac{g}{\sqrt{2}}\left(J_\mu^C W^{+\mu} + h.c.\right) + \frac{g}{\cos\theta_W^0}J_\mu^N Z^\mu \ , \tag{6.28}$$

$$J_\mu^C = \bar{\nu}_L\gamma_\mu\eta(\nu_L)e_L + \bar{u}_L\gamma_\mu\eta(u_L)d_L + \bar{u}_R\gamma_\mu\eta(u_R)d_R \ , \tag{6.29}$$

$$J_\mu^N = \bar{\nu}_L\gamma_\mu\epsilon(\nu_L)\nu_L + \bar{e}_L\gamma_\mu\epsilon(e_L)e_L + \bar{u}_L\gamma_\mu\epsilon(u_L)u_L + \bar{d}_L\gamma_\mu\epsilon(d_L)d_L$$
$$+ \bar{e}_R\gamma_\mu\epsilon(e_R)e_R + \bar{u}_R\gamma_\mu\epsilon(u_R)u_R + \bar{d}_R\gamma_\mu\epsilon(d_R)d_R \ . \tag{6.30}$$

Here the ϵ's and η's are 3×3 matrices in flavor space. In the case of the charged current we find (BW do not have the † in $\alpha_{\varphi l}^{(3)}$ and $\alpha_{\varphi q}^{(3)}$)

$$\eta(\nu_L) = \mathbb{I} + 2\,\hat{\alpha}_{\varphi l}^{(3)\dagger} \ , \tag{6.31}$$

$$\eta(u_L) = \mathbb{I} + 2\,\hat{\alpha}_{\varphi q}^{(3)\dagger} \ , \tag{6.32}$$

$$\eta(u_R) = -\hat{\alpha}_{\varphi\varphi} \ . \tag{6.33}$$

In the case of the neutral current (ϵ coefficients) we obtain the same results as BW except for the following replacement:

$$\hat{\alpha}_X \rightarrow \hat{\alpha}_X + \hat{\alpha}_X^\dagger \ , \tag{6.34}$$

for $\alpha_X = \alpha_{\varphi l}^{(3)}, \alpha_{\varphi l}^{(1)}, \alpha_{\varphi q}^{(3)}, \alpha_{\varphi q}^{(1)}, \alpha_{\varphi e}, \alpha_{\varphi u}, \alpha_{\varphi d}$.

Finally, we need to diagonalize the fermion mass matrices. With our choice of weak basis for the fermions, the only step that is left is the diagonalization of the up-quark mass matrix, proportional to the Yukawa matrix $Y_U = V^\dagger Y_U^{\mathrm{diag}}$, where V is the CKM matrix. This can be accomplished by a $U(3)$ transformation of the u_L fields:

$$u_L \rightarrow V^\dagger u_L \ . \tag{6.35}$$

As a consequence, the charged current and neutral current couplings involving up quarks change as follows:

$$\begin{aligned} \eta(u_L) &\rightarrow V\,\eta(u_L) \\ \epsilon(u_L) &\rightarrow V\,\epsilon(u_L)\,V^\dagger \ . \end{aligned} \tag{6.36}$$

Similarly, appropriate insertions of the CKM matrix will appear in every operator that contains the u_L field.

6.2.3   Effective Lagrangian for muon decay

The muon decay amplitude receives contributions from gauge boson exchange diagrams (with modified couplings) and from contact operators such as $O_{ll}^{(1)}$, $O_{ll}^{(3)}$, O_{le}. Since we work to first order in v^2/Λ^2, we do not need to consider diagrams contributing to $\mu \rightarrow e\bar{\nu}_\alpha\nu_\beta$ with the "wrong neutrino flavor", because they would

correct the muon decay rate to $O(v^4/\Lambda^4)$. After integrating out the W and Z, the muon decay effective Lagrangian reads:

$$\mathcal{L}_{\mu \to e\bar{\nu}_e \nu_\mu} = \frac{-g^2}{2m_W^2} \left[(1 + \tilde{v}_L) \cdot \bar{e}_L \gamma_\mu \nu_{eL} \; \bar{\nu}_{\mu L} \gamma^\mu \mu_L \; + \; \tilde{s}_R \cdot \bar{e}_R \nu_{eL} \; \bar{\nu}_{\mu L} \mu_R \right] \; + \; h.c. \; , \quad (6.37)$$

where $m_W^2 = (g^2 v^2)/2$ is the W mass and

$$\tilde{v}_L \;\; = \;\; 2 \, [\hat{\alpha}_{\varphi l}^{(3)}]_{11+22^*} - [\hat{\alpha}_{ll}^{(1)}]_{1221} - 2[\hat{\alpha}_{ll}^{(3)}]_{1122-\frac{1}{2}(1221)} \; , \quad (6.38)$$

$$\tilde{s}_R \;\; = \;\; +2[\hat{\alpha}_{le}]_{2112} \; , \quad (6.39)$$

represent the correction to the standard $(V-A) \otimes (V-A)$ structure and the coupling associated with the new $(S-P) \otimes (S+P)$ structure, respectively.

6.2.4 Effective Lagrangian for beta decays: $d_j \to u_i \, \ell^- \, \bar{\nu}_\ell$

The low-energy effective Lagrangian for semileptonic transitions receives contributions from both W exchange diagrams (with modified W-fermion couplings) and the four-fermion operators $O_{lq}^{(3)}$, O_{qde}, O_{lq}, O_{lq}^t. As in the muon case, we neglect lepton flavor violating contributions (wrong neutrino flavor). The resulting low-energy effective Lagrangian governing semileptonic transitions $d_j \to u_i \, \ell^- \, \bar{\nu}_\ell$ (for a given lepton flavor ℓ) reads:

$$
\begin{aligned}
\mathcal{L}_{d_j \to u_i \ell^- \bar{\nu}_\ell} \;\; = \;\; & \frac{-g^2}{2m_W^2} V_{ij} \left[\left(1 + [v_L]_{\ell\ell ij} \right) \bar{\ell}_L \gamma_\mu \nu_{\ell L} \; \bar{u}_L^i \gamma^\mu d_L^j \; + \; [v_R]_{\ell\ell ij} \; \bar{\ell}_L \gamma_\mu \nu_{\ell L} \; \bar{u}_R^i \gamma^\mu d_R^j \right. \\
& + \; [s_L]_{\ell\ell ij} \; \bar{\ell}_R \nu_{\ell L} \; \bar{u}_R^i d_L^j \; + \; [s_R]_{\ell\ell ij} \; \bar{\ell}_R \nu_{\ell L} \; \bar{u}_L^i d_R^j \\
& \left. + \; [t_L]_{\ell\ell ij} \; \bar{\ell}_R \sigma_{\mu\nu} \nu_{\ell L} \; \bar{u}_R^i \sigma^{\mu\nu} d_L^j \right] \; + \; h.c. \; ,
\end{aligned}
\quad (6.40)
$$

where

$$V_{ij} \cdot [v_L]_{\ell\ell ij} \;\; = \;\; 2 V_{ij} \left[\hat{\alpha}_{\varphi l}^{(3)} \right]_{\ell\ell} + 2 V_{im} \left[\hat{\alpha}_{\varphi q}^{(3)} \right]_{jm}^* - 2 V_{im} \left[\hat{\alpha}_{lq}^{(3)} \right]_{\ell\ell mj} \; , \quad (6.41)$$

$$V_{ij} \cdot [v_R]_{\ell\ell ij} \;\; = \;\; - [\hat{\alpha}_{\varphi\varphi}]_{ij} \; , \quad (6.42)$$

$$V_{ij} \cdot [s_L]_{\ell\ell ij} \;\; = \;\; - [\hat{\alpha}_{lq}]_{\ell\ell ji}^* \; , \quad (6.43)$$

$$V_{ij} \cdot [s_R]_{\ell\ell ij} \;\; = \;\; - V_{im} [\hat{\alpha}_{qde}]_{\ell\ell jm}^* \; , \quad (6.44)$$

$$V_{ij} \cdot [t_L]_{\ell\ell ij} \;\; = \;\; - [\hat{\alpha}_{lq}^t]_{\ell\ell ji}^* \; . \quad (6.45)$$

In Eqs. (6.41-6.45) the repeated indices i, j, ℓ are not summed over, while the index m is.

6.3 Flavor structure of the effective couplings

So far we have presented our results for the effective Lagrangian keeping generic flavor structures in the couplings $[\hat{\alpha}_X]_{abcd}$ (see Eqs. (6.38), (6.39), and (6.41) through (6.45)). However, some of the operators considered in the analysis contribute to flavor changing neutral current (FCNC) processes, so that their flavor structure cannot be generic if the effective scale is around $\Lambda \sim$ TeV: the off-diagonal coefficients are experimentally constrained to be very small. While it is certainly possible that some operators (weakly constrained by FCNC) have generic structures, we would like to understand the FCNC suppression needed for many operators in terms of a symmetry principle. Therefore, we organize the discussion in terms of perturbations around the $U(3)^5$ flavor symmetry limit.

If the underlying new physics respects the $U(3)^5$ flavor symmetry of the SM gauge Lagrangian, no problem arises from FCNC constraints. The largest contributions to the coefficients are flavor conserving and universal. Flavor breaking contributions arise through SM radiative corrections, due to insertions of Yukawa matrices that break the $U(3)^5$ symmetry. As a consequence, imposing exact $U(3)^5$ symmetry on the underlying model does not seem realistic. A weaker assumption, the Minimal Flavor Violation (MFV) hypothesis, requires that $U(3)^5$ is broken in the underlying model only by structures proportional to the SM Yukawa couplings [126], and by the structures generating neutrino masses [127]. We will therefore organize our discussion in several stages:

1. First, assume dominance of $U(3)^5$ invariant operators;

2. Consider the effect of $U(3)^5$ breaking induced within MFV;

3. Consider the effect of generic non-MFV flavor structures.

6.3.1 MFV allowed structures

In order to proceed with this program, we show in this section the flavor structures allowed within MFV for the relevant operators. We use Greek letters $\alpha, \beta, \rho, \sigma$ for the lepton flavor indices, while i, j for the quark flavor indices, and we neglect terms with more than two Yukawa insertions. Moreover, we denote by $\hat{\alpha}_X$, $\hat{\beta}_X$, and $\hat{\gamma}_X$ the numerical coefficients of $O(1) \times v^2/\Lambda^2$ that multiply the appropriate matrices in flavor space. For the operators that have a non-vanishing contribution in the $U(3)^5$ limit, we find:

$$[\hat{\alpha}_{\varphi l}^{(3)}]^{\alpha\beta} = \hat{\alpha}_{\varphi l}^{(3)} \, \delta^{\alpha\beta} + \hat{\beta}_{\varphi l}^{(3)} \, (\Delta_{LL}^{(\ell)})^{\alpha\beta} + \dots \,, \tag{6.46}$$

$$V^{im} [\hat{\alpha}_{\varphi q}^{(3)}]^{jm*} = \hat{\alpha}_{\varphi q}^{(3)} \, V^{ij} + \hat{\beta}_{\varphi q}^{(3)} \, (V \, \Delta_{LL}^{(q)})^{ij} + \dots \,, \tag{6.47}$$

$$\begin{aligned} V^{im} [\hat{\alpha}_{lq}^{(3)}]^{\alpha\beta mj} &= \hat{\alpha}_{lq}^{(3)} \, \delta^{\alpha\beta} \, V^{ij} + \hat{\beta}_{lq}^{(3)} \, (\Delta_{LL}^{(\ell)})^{\alpha\beta} \, V^{ij} \\ &+ \hat{\gamma}_{lq}^{(3)} \, \delta^{\alpha\beta} \, (V \, \Delta_{LL}^{(q)})^{ij} + \dots \,, \end{aligned} \tag{6.48}$$

$$\left[\hat{\alpha}_{ll}^{(n)}\right]^{\alpha\beta\rho\sigma} = \hat{\alpha}_{ll}^{(n)} \delta^{\alpha\beta} \delta^{\rho\sigma} + \hat{\beta}_{ll}^{(n)} \left[\delta^{\alpha\beta}(\Delta_{LL}^{(\ell)})^{\rho\sigma} + (\Delta_{LL}^{(\ell)})^{\alpha\beta}\delta^{\rho\sigma}\right] + \dots , \quad (6.49)$$

$$[\hat{\alpha}_{le}]^{\alpha\beta\rho\sigma} = \hat{\alpha}_{le} \, \delta^{\alpha\beta}\delta^{\rho\sigma} + \hat{\beta}_{le} \, (\Delta_{LL}^{(\ell)})^{\alpha\beta} \, \delta^{\rho\sigma} + \dots , \quad (6.50)$$

where $\Delta_{LL}^{(q/\ell)}$ are the leading "left-left" flavor structures in the quark and lepton sector, that read:

$$\Delta_{LL}^{(q)} = V^\dagger \, \bar{\lambda}_u^2 \, V , \quad (6.51)$$

$$\Delta_{LL}^{(\ell)} = \frac{\Lambda_{\rm LN}^2}{v^4} U \, \bar{m}_\nu^2 \, U^\dagger . \quad (6.52)$$

The notation here is as follows: we denote by $\bar{\lambda}_{u,d,e}$ the diagonal Yukawa matrices; $\bar{m}_\nu$ represents the diagonal light neutrino mass matrix; V denotes the CKM matrix, while U is the PMNS [128] neutrino mixing matrix; v is the Higgs VEV and Λ_{LN} is the scale of lepton number violation, that appears in the definition of MFV in the lepton sector (we follow here the "minimal" scenario of Ref. [127]).

For the operators that vanish in the limit of exact $U(3)^5$ symmetry, we find:

$$[\hat{\alpha}_{\varphi\varphi}]^{ij} = \hat{\alpha}_{\varphi\varphi} \left(\bar{\lambda}_u V \bar{\lambda}_d\right)^{ij} + \dots , \quad (6.53)$$

$$V^{im} [\hat{\alpha}_{qde}]^{\alpha\beta jm*} = \hat{\alpha}_{qde} \, \bar{\lambda}_e^{\alpha\beta} \, (V\bar{\lambda}_d)^{ij} + \hat{\beta}_{qde} \, (\bar{\lambda}_e \Delta_{LL}^{(\ell)})^{\alpha\beta} \, (V\bar{\lambda}_d)^{ij}$$
$$+ \hat{\gamma}_{qde} \, \bar{\lambda}_e^{\alpha\beta} \, (V\Delta_{LL}^{(q)}\bar{\lambda}_d)^{ij} + \dots , \quad (6.54)$$

$$[\hat{\alpha}_{lq}]^{\alpha\beta ji*} = \hat{\alpha}_{lq} \, \bar{\lambda}_e^{\alpha\beta} \, (\bar{\lambda}_u V)^{ij} + \hat{\beta}_{lq} \, (\bar{\lambda}_e \Delta_{LL}^{(\ell)})^{\alpha\beta} \, (\bar{\lambda}_u V)^{ij}$$
$$+ \hat{\gamma}_{lq} \, \bar{\lambda}_e^{\alpha\beta} \, (\bar{\lambda}_u V\Delta_{LL}^{(q)})^{ij} + \dots . \quad (6.55)$$

The coefficient of the tensor operator, $[\alpha_{lq}^{(t)}]$ has an expansion similar to the one of $[\alpha_{lq}]$.

Except for the top quark, the Yukawa insertions typically involve a large suppression factor, as $\bar{\lambda}_i = m_i/v$. In the case of SM extensions containing two Higgs doublets, this scaling can be modified if there is a hierarchy between the vacuum expectation values v_u, v_d of the Higgs fields giving mass to the up- or down-type quarks, respectively. In this case, for large $\tan\beta \equiv v_u/v_d$ the Yukawa insertions scale as:

$$\bar{\lambda}_u = \frac{m_u}{v \sin\beta} \rightarrow \frac{m_u}{v} , \quad (6.56)$$

$$\bar{\lambda}_d = \frac{m_d}{v \cos\beta} \rightarrow \frac{m_d}{v} \tan\beta , \quad (6.57)$$

$$\bar{\lambda}_\ell = \frac{m_\ell}{v \cos\beta} \rightarrow \frac{m_\ell}{v} \tan\beta . \quad (6.58)$$

6.4 Conclusions

From the most general effective Lagrangian with the SM particle content that respects the baryon and lepton number symmetries, we have identified a minimal set of

twenty-four weak scale effective operators describing corrections beyond the SM to precision electroweak measurements and leptonic and semileptonic decays. In terms of these new physics corrections at the TeV scale, we have derived the low-energy effective Lagrangians describing muon and beta decays, specifying both the most general flavor structure of the operators as well as the form allowed within Minimal Flavor Violation.

In the next chapter we will analyze the phenomenology of this Lagrangian in the simple flavor-blind case, that represents a good approximation to the MFV case. We will see that the expressions simplify substantially and one can make a clean phenomenological analysis of the NP constraints and their significance.

Chapter 7

NP constraints from CKM unitarity

> *Physics is like sex:*
> *sure, it may give some practical results,*
> *but that's not why we do it.*
> R. P. Feynman

In the introduction of the previous chapter we said that the precise lifetime and branching ratio measurements [129] combined with improvements also on the theoretical calculations make semileptonic decays of light quarks and purely leptonic decays a deep probe of the nature of weak interactions. We want to show it in this chapter explicitly, taking advantage of the theoretical framework developed previously.

In particular, the determination of the elements V_{ud} and V_{us} of the Cabibbo-Kobayashi-Maskawa (CKM) [130] quark mixing matrix is approaching the 0.025% and 0.5% level, respectively. Such precise knowledge of V_{ud} and V_{us} enables tests of Cabibbo universality, equivalent to the CKM unitarity condition[1] $|V_{ud}|^2 + |V_{us}|^2 + |V_{ub}|^2 = 1$, at the level of 0.001 or better. Assuming that new physics contributions scale as $\alpha/\pi(M_W^2/\Lambda^2)$, the unitarity test probes energy scales Λ on the order of the TeV, which will be directly probed at the LHC.

The implications of the Cabibbo universality tests have bee analyzed in some particular (mostly supersymmetric) scenarios [131, 132], but a model-independent analysis is missing and we will tackle it here [125].

The use of an effective Lagrangian allows us to understand in a model-independent way (i) the significance of Cabibbo universality constraints compared to other precision measurements (for example, could we expect sizable deviations from universality in light of no deviation from the SM in precision tests at the Z pole?); (ii) the correlations between possible deviations from universality and other precision observables, not always simple to identify in a specific model analysis.

---

[1] $V_{ub} \sim 10^{-3}$ contributes negligibly to this relation.

7.1   Phenomenology of V_{ud} and V_{us}: overview

Using the general effective Lagrangians of Eqs. (6.37) and (6.40) for charged current transitions, one can calculate the deviations from SM predictions in various semileptonic decays. In principle a rich phenomenology is possible. Helicity suppressed leptonic decays of mesons have recently been analyzed in Ref. [133]. Concerning semileptonic transitions, several reviews treat in some detail β decay differential distributions [134, 135]. Here we focus on the integrated decay rates, which give access to the CKM matrix elements V_{ud} and V_{us}: since both the SM prediction and the experimental measurements are reaching the sub-percent level, we expect these observables to provide strong constraints on NP operators.

V_{ud} and V_{us} can be determined with high precision in a number of channels. The degree of needed theoretical input varies, depending on which component of the weak current contributes to the hadronic matrix element. Roughly speaking, one can group the channels leading to $V_{ud,us}$ into three classes:

- Semileptonic decays in which the axial-vector component of the weak current does not contribute. These are theoretically favorable in the Standard Model because the matrix elements of the vector current at zero momentum transfer are known in the $SU(2)$ ($SU(3)$) limit of equal light quark masses: $m_u = m_d \,(= m_s)$. Moreover, corrections to the symmetry limit are quadratic in $m_{s,d} - m_u$ [136]. Super-allowed nuclear beta decays ($0^+ \to 0^+$), pion beta decay ($\pi^+ \to \pi^0 e^+ \nu_e$), and $K \to \pi \ell \nu$ decays belong to this class. The determination of $V_{ud,us}$ from these modes requires theoretical input on radiative corrections [137, 138] and hadronic matrix elements via analytic methods [65, 71, 139–141] or lattice QCD [142, 143].

- Semileptonic transitions in which both the vector and axial-vector components of the weak current contribute. Neutron decay ($n \to pe\bar\nu$) and hyperon decays ($\Lambda \to pe\bar\nu$, ...) belong to this class. In this case the matrix elements of the axial current have to be determined experimentally [144].

  Inclusive τ lepton decays $\tau \to h\nu_\tau$ belong to this class (both V and A current contribute), and in this case the relevant matrix elements can be calculated theoretically with the sum rule framework derived in Chapter 3 [5].

- Leptonic transitions in which the vector component of the weak current does not contribute. In this class one finds meson decays such as $\pi(K) \to \mu\nu$ but also exclusive τ decays such as $\tau \to \nu_\tau \pi(K)$. Experimentally one can determine the products $|V_{ud}F_\pi|$ and $|V_{us}F_K|$. With the advent of precision calculations of F_K/F_π in lattice QCD [145, 146], this class of decays provides a useful constraint on the ratio V_{us}/V_{ud} [147].

Currently, the determination of V_{ud} is dominated by $0^+ \to 0^+$ super-allowed nuclear beta decays [139], while the best determination of V_{us} arises from $K \to \pi\ell\nu$ decays [132]. Experimental improvements in neutron decay and τ decays, as well

as in lattice calculations of the decay constants will allow in the future competitive determinations from other channels. In light of this, we set out to perform a comprehensive analysis of possible new physics effects in the extraction of V_{ud} and V_{us}.

7.2 New physics effects on the V_{ij} extraction

As outlined in the previous chapter, we start our analysis by assuming dominance of the $U(3)^5$ invariant operators. These are not constrained by FCNC and can have a relatively low effective scale Λ. In the $U(3)^5$ limit the phenomenology of CC processes greatly simplifies: all V_{ij} receive the same universal shift (coming from the same short distance structure) and as a consequence, extractions of $V_{ud,us}$ from different channels (vector transitions, axial transitions, *etc.*) should agree within errors. Therefore, in this limit the new physics effects are entirely captured by the quantity

$$\Delta_{\text{CKM}} \equiv |V_{ud}^{(\text{pheno})}|^2 + |V_{us}^{(\text{pheno})}|^2 + |V_{ub}^{(\text{pheno})}|^2 - 1 , \qquad (7.1)$$

constructed from the $V_{ij}^{(\text{pheno})}$ elements extracted from semileptonic transitions using the standard procedure outlined below. We now make these points more explicit.

7.2.1 $U(3)^5$ limit

If we assume $U(3)^5$ invariance, only the SM structure survives in the muon decay Lagrangian of Eq. (6.37), with [2]

$$\tilde{v}_L = 4\,\hat{\alpha}_{\varphi l}^{(3)} - 2\,\hat{\alpha}_{ll}^{(3)} . \qquad (7.2)$$

Therefore, in this case the effect of new physics can be encoded into the following definition of the leptonic Fermi constant:

$$G_F^\mu = (G_F)^{(0)} \left(1 + \tilde{v}_L\right) , \qquad (7.3)$$

where $G_F^{(0)} = g^2/(4\sqrt{2}m_W^2)$. Similarly, in the $U(3)^5$ symmetry limit, only the SM operator survives in the effective langrangian for semileptonic quark decays of Eq. (6.40), with coupling:

$$[v_L]_{\ell\ell ij} \;\rightarrow\; v_L \equiv 2\left(\hat{\alpha}_{\varphi l}^{(3)} + \hat{\alpha}_{\varphi q}^{(3)} - \hat{\alpha}_{lq}^{(3)}\right) . \qquad (7.4)$$

As in the muon decay, the new physics can be encoded in a (different) shift to the effective semileptonic (SL) Fermi constant:

$$G_F^{\text{SL}} = (G_F)^{(0)} \left(1 + v_L\right) . \qquad (7.5)$$

---

[2]Notice that we disagree with the result of BW on the sign of $\hat{\alpha}_{ll}^{(3)}$. This error propagates for example to the work of Barbieri and Strumia [148] where the BW expression was used, although in this case the sign of the operator is irrelevant (one must only exchange the columns of Table 3 in that reference).

The value of V_{ij} extracted from semileptonic decays is affected by this redefinition of the semileptonic Fermi constant and by the shift in the muon Fermi constant G_F^μ, to which one usually normalizes semileptonic transitions. In fact one has

$$
\begin{aligned}
V_{ij}^{(\text{pheno})} &= V_{ij} \; \frac{G_F^{\text{SL}}}{G_F^\mu} = V_{ij} \; (1 + v_L - \tilde{v}_L) \\
&= V_{ij} \left[1 + 2 \left(\hat{\alpha}_{ll}^{(3)} - \hat{\alpha}_{lq}^{(3)} - \hat{\alpha}_{\varphi l}^{(3)} + \hat{\alpha}_{\varphi q}^{(3)} \right) \right] \; .
\end{aligned}
\tag{7.6}
$$

So in the $U(3)^5$ limit a common shift affects all the V_{ij} (from all channels). The only way to expose new physics contributions is to construct universality tests, in which the absolute normalization of V_{ij} matters. For light quark transitions this involves checking that the first row of the CKM matrix is a vector of unit length (see definition of Δ_{CKM} in Eq. (7.1)). The new physics contributions to Δ_{CKM} involve four operators of our basis and read:

$$
\Delta_{\text{CKM}} = 4 \left(\hat{\alpha}_{ll}^{(3)} - \hat{\alpha}_{lq}^{(3)} - \hat{\alpha}_{\varphi l}^{(3)} + \hat{\alpha}_{\varphi q}^{(3)} \right) \; .
\tag{7.7}
$$

In specific SM extensions, the $\hat{\alpha}_i$ are functions of the underlying parameters. Therefore, through the above relation one can work out the constraints of quark-lepton universality tests on any weakly coupled SM extension.

7.2.2 Beyond $U(3)^5$

Corrections to the $U(3)^5$ limit can be introduced both within MFV and via generic flavor structures. In MFV, as evident from the results of Section 6.3, the coefficients parameterizing deviations from $U(3)^5$ are highly suppressed. This is true even when one considers the flavor diagonal elements of the effective couplings, due to the smallness of the Yukawa eigenvalues and the hierarchy of the CKM matrix elements. As a consequence, in MFV we expect the conclusions of the previous subsections to hold. The various CKM elements V_{ij} receive a common dominant shift plus suppressed channel-dependent corrections, so that Eq. (7.7) remains valid to a good approximation. In other words, both in the exact $U(3)^5$ limit and in MFV, Δ_{CKM} probes the leading coefficients $\hat{\alpha}_X$ of the four operators $O_{\text{CKM}} = \{O_{ll}^{(3)}, O_{lq}^{(3)}, O_{\varphi l}^{(3)}, O_{\varphi q}^{(3)}\}$.

In a generic non-MFV framework, the channel-dependent shifts to V_{ij} could be appreciable, so that Δ_{CKM} would depend on the channels used to extract $V_{ud,us}$. Therefore, comparing the values of V_{us} and V_{ud} (or their ratios) extracted from different channels gives us a handle on $U(3)^5$ breaking structures beyond MFV. We will discuss this in the next chapter, where we will analyze the new physics contributions to the ratios $V_{ud}^{0^+ \to 0^+}/V_{ud}^{n \to pe\bar{\nu}}$, $V_{us}^{K \to \pi \ell \nu}/V_{ud}^{0^+ \to 0^+}$, $V_{us}^{K \to \mu\nu}/V_{ud}^{\pi \to \mu\nu}$, and $(V_{us}/V_{ud})^{\tau \to \nu h}$ from both inclusive and exclusive channels. In summary, we organize our analysis in two somewhat orthogonal parts, as follows:

- In the rest of this chapter we focus on the phenomenology of Δ_{CKM} and its relation to other precision measurements. This analysis applies to models of

TeV scale physics with approximate $U(3)^5$ invariance, in which flavor breaking is suppressed by a symmetry principle (as in MFV) or by the hierarchy $\Lambda_{\text{flavor}} \gg 1\,\text{TeV}$

- In the next chapter we will explore the constraints arising by comparing the values of V_{us} (V_{ud}) extracted from different channels. These constraints probe the $U(3)^5$ breaking structures, to which other precision measurements (especially at high energy) are essentially insensitive.

Classification	Standard Notation	Measurement	Ref.
Atomic parity violation (Q_W)	$Q_W(Cs)$	Weak charge in Cs	[149]
	$Q_W(Tl)$	Weak charge in Tl	[150]
DIS	g_L^2, g_R^2	ν_μ-nucleon scattering (NuTeV)	[151]
	R^ν	ν_μ-nucleon scattering (CDHS, CHARM)	[152]
	κ	ν_μ-nucleon scattering (CCFR)	[153]
	$g_V^{\nu e}, g_A^{\nu e}$	ν-e scattering (CHARM II)	[154]
Zline (lepton and light quark)	Γ_Z	Total Z width	[155]
	σ_0	e^+e^- hadronic cross section at Z pole	[155]
	$R^0_{(f=e,\mu,\tau)}$	Ratios of lepton decay rates	[155]
	$A^{0,(f=e,\mu,\tau)}_{FB}$	Forward-backward lepton asymmetries	[155]
pol	$A_{(f=e,\mu,\tau)}$	Polarized lepton asymmetries	[155]
bc (heavy quark)	$R^0_{(f=b,c)}$	Ratios of hadronic decay rates	[155]
	$A^{0,(f=b,c)}_{FB}$	Forward-backward hadronic asymmetries	[155]
	$A_{(f=b,c)}$	Polarized hadronic asymmetries	[155]
LEPII Fermion production	$\sigma_{(f=q,\mu,\tau)}$	Total cross sections for $e^+e^- \to f\overline{f}$	[155]
	$A^{(f=\mu,\tau)}_{FB}$	Forward-backward asymmetries for $e^+e^- \to f\overline{f}$	[155]
eOPAL	$\dfrac{d\sigma_e}{d\cos\theta}$	Differential cross section for $e^+e^- \to e^+e^-$	[156]
WL3	$\dfrac{d\sigma_W}{d\cos\theta}$	Differential cross section for $e^+e^- \to W^+W^-$	[157]
MW	M_W	W mass	[155, 158]
Q_{FB}	$\sin^2\theta^{lept}_{eff}$	Hadronic charge asymmetry	[155]

Table 7.1: Measurements included in this analysis. This summary table was taken directly from Table I of [124] and repeated here for convenience. We added some details in the classification column as well as additional experimental references.

7.3 Δ_{CKM} versus precision electroweak measurements

In the limit of approximate $U(3)^5$ invariance, we have shown in Eq. (7.7) that Δ_{CKM} constraints a specific combination of the coefficients $\hat{\alpha}_{ll}^{(3)}, \hat{\alpha}_{lq}^{(3)}, \hat{\alpha}_{\varphi l}^{(3)}, \hat{\alpha}_{\varphi q}^{(3)}$. Each of these coefficients also contributes to other low- and high-energy precision electroweak measurements [124], together with the remaining seventeen operators that make up the $U(3)^5$ invariant sector of our TeV scale effective Lagrangian (see Sect. 6.1.3). Therefore, we can now address concrete questions such as: what is the maximal deviation $|\Delta_{\text{CKM}}|$ allowed once all the precision electroweak constraints have been taken into account? Which observables provide the strongest constraints on the operators contributing to Δ_{CKM}? How does the inclusion of Δ_{CKM} affect the fit to precision electroweak measurements? Should a deviation $\Delta_{\text{CKM}} \neq 0$ be established, in what other precision observables should we expect a tension with the SM prediction? At what level?

Our task greatly benefits from the work of Han and Skiba (HS) [124], who studied the constraints on the same set of twenty-one $U(3)^5$ invariant operators via a global fit to precision electroweak data. We employ a modified version of their publicly available fitting code in what follows. The analysis utilizes the experimental data summarized in Table 7.1. The procedure involves constructing the χ^2 function for the observables listed in Table 7.1, which contains 237 generally correlated terms. Indicating with $X_{\text{th}}^i(\hat{\alpha}_k)$ the theoretical prediction for observable X^i (including SM plus radiative correction plus first order shift in $\hat{\alpha}_k = \alpha_k v^2/\Lambda^2$), and with X_{exp}^i the experimental value, the χ^2 reads

$$\chi^2(\hat{\alpha}_k) = \sum_{i,j} \left(X_{\text{th}}^i(\hat{\alpha}_k) - X_{\text{exp}}^i \right) \left(\sigma^2 \right)_{ij}^{-1} \left(X_{\text{th}}^j(\hat{\alpha}_k) - X_{\text{exp}}^j \right) , \qquad (7.8)$$

where $\sigma_{ij}^2 = \sigma_i \, \rho_{ij} \, \sigma_j$ is expressed in terms of the combined theoretical and experimental standard deviation σ_i and the correlation matrix ρ_{ij}. For more details, we refer to Ref. [124]. In our numerical analysis we essentially use the code of HS[3] and minimally extend it by including the Δ_{CKM} constraint in the χ^2 function. Given the phenomenological input $V_{ud} = 0.97425(22)$ [139], $V_{us} = 0.2252(9)$ [159], we obtain the constraint [159]

$$\Delta_{\text{CKM}} = (-1 \pm 6) \times 10^{-4} , \qquad (7.9)$$

that has essentially no correlation with the other precision measurements, due to the small fractional uncertainty in the Fermi constant.

We perform two different analyses, one in which all operators O_X are allowed to contribute, and one in which only a single operator at a time has non vanishing coefficient. These two regimes represent extreme model scenarios and possess different characteristics. In the global analysis, due to the large number of parameters, cancellations can dilute the impact of specific observables: the burden of satisfying

---

[3] We prefer to quote final results in terms of the dimensionless ratios $\hat{\alpha}_k = \alpha_k v^2/\Lambda^2$ ($v \simeq 174$ GeV) instead of $a_k = 1/\Lambda_k^2$ as in HS.

a tight constraint from a given observable can be "shared" by several operators. On the other hand, within the single-operator analysis one may easily find correlations between different sets of measurements. We think of the single operator analysis as a survey of a simplified class of models, in which only one dominant effective operator is generated.

7.3.1 Global analysis

In order to quantify the significance of the experimental CKM unitarity constraint, we first calculate the range of $\Delta_{\mathrm{CKM}}(\hat{\alpha}_k)$ allowed by existing bounds from all the precision electroweak measurements included in Table 7.1. In terms of the best fit values and the covariance matrix of the $\hat{\alpha}_i$ [124] obtained from the fit to electroweak precision data, we find

$$\Delta_{\mathrm{CKM}} = -(4.8 \pm 4.7) \cdot 10^{-3} \approx -(5 \pm 5) \cdot 10^{-3} \quad (90\% \text{ C.L.}) , \quad (7.10)$$

to be compared with the direct 90% C.L. bound $|\Delta_{\mathrm{CKM}}| \leq 1. \times 10^{-3}$ (see Eq. (7.9)). The first lesson from this exercise is that electroweak precision data leave ample room for a sizable non-zero Δ_{CKM}: the direct constraint is five times stronger than the indirect one! Therefore, one should include the Δ_{CKM} constraint in global fits to the effective theory parameters.

The next question we address is: what is the impact of adding the Δ_{CKM} constraint to the global electroweak fit? The chi-squared per degrees of freedom changes only marginally, from $\chi^2/d.o.f. = 180.12/215$ to $\chi^2/d.o.f. = 173.74/216$. We find that essentially the only impact is to modify the allowed regions for $\hat{\alpha}_{ll}^{(3)}, \hat{\alpha}_{lq}^{(3)}, \hat{\alpha}_{\varphi l}^{(3)}, \hat{\alpha}_{\varphi q}^{(3)}$. To illustrate this, in Figure 7.1, we display the projection of the twenty-one dimensional 90% confidence ellipsoid onto the relevant planes involving $\hat{\alpha}_{ll}^{(3)}, \hat{\alpha}_{lq}^{(3)}, \hat{\alpha}_{\varphi l}^{(3)}, \hat{\alpha}_{\varphi q}^{(3)}$. The black curves represent bounds before the inclusion of the Δ_{CKM} constraint. The dashed blue lines outline the allowed regions found by considering only the effect of current Δ_{CKM} bounds (Eq. 7.7): the regions are unbounded because large values of any of the $\hat{\alpha}_i$ may be canceled by a correspondingly large contribution of other operators. The situation changes when high-energy observables are taken into account, as can be seen from the combined fit solid blue curve. Despite the relatively weak indirect Δ_{CKM} constraints from high-energy data, the unbounded parameter directions are cut off at the edge of the allowed black contour. In the orthogonal direction, the combined ellipse is shrunk significantly by the strong Δ_{CKM} bound. Thus, the solid blue contour is rotated and contracted with respect to its parent black region. As evident from the figure, the main effect of including Δ_{CKM} is to strengthen the constraints on the four-fermion operator $O_{lq}^{(3)}$.

At this stage we may also ask how would this picture change if a significant deviation from Cabibbo universality were to be observed. To answer this question, we show in Fig. 7.1, the 90% C.L. allowed regions (red solid curve) obtained by assuming a $\sim 4\,\sigma$ deviation, namely $\Delta_{\mathrm{CKM}} = -0.0025 \pm 0.0006$[4]. One can see

---

[4]This value has been chosen for illustrative purposes and could be realized if the central value of
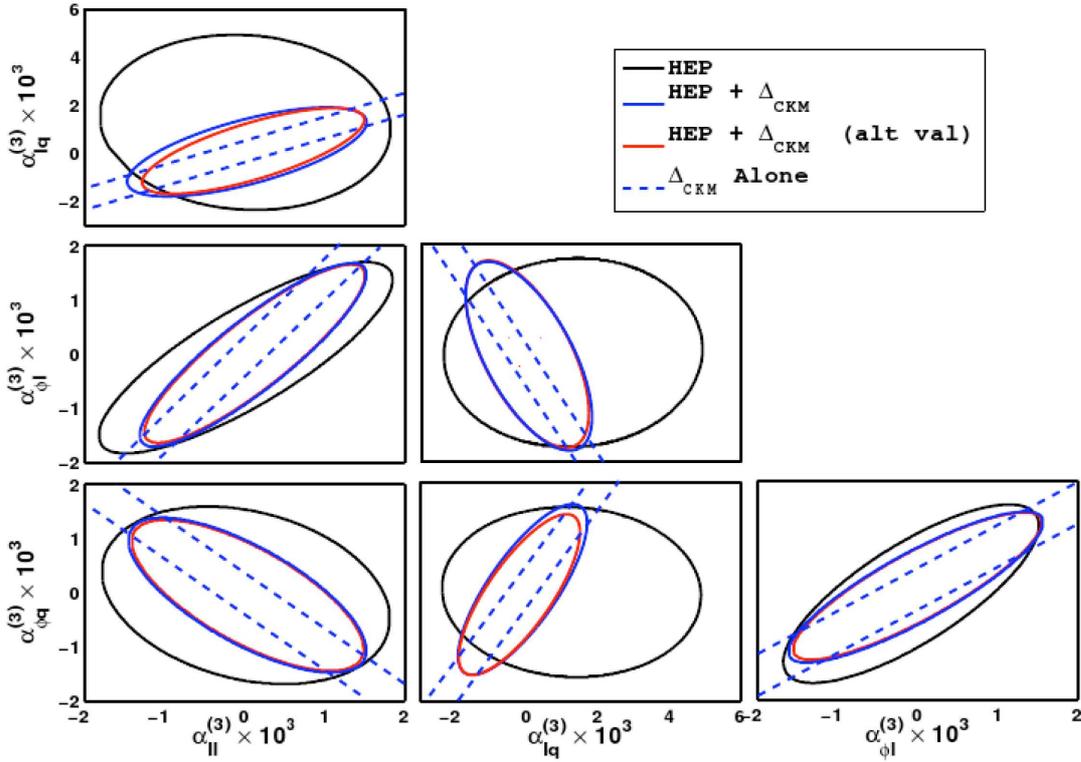
Figure 7.1: 90% allowed regions for the coefficients $\hat{\alpha}_{ll}^{(3)}, \hat{\alpha}_{lq}^{(3)}, \hat{\alpha}_{\varphi l}^{(3)}, \hat{\alpha}_{\varphi q}^{(3)}$. These are projections from the 21 dimensional ellipsoid, obtained from the fitting code. We include the results for high-energy observables alone (HEP, black unbroken curves), high-energy data plus the current Δ_{CKM} constraint (blue unbroken curve), high-energy data plus the alternative value of $\Delta_{\text{CKM}} = -0.0025 \pm 0.0006$ (red unbroken curve) and the bounds from the current Δ_{CKM} alone (blue dashed curve).

that changing the central value of Δ_{CKM} has only a minor effect on the allowed regions: the fit is driven by the comparatively small Δ_{CKM} uncertainty, rather than its central value. While the fitting procedure tends to minimize the χ^2 contribution from Δ_{CKM}, this does not generate much tension with the remaining observables, as other operators can compensate the effect of potentially non-vanishint $\hat{\alpha}_i \subset \hat{\alpha}_{\text{CKM}}$.

7.3.2   Single operator analysis

To gain a better understanding of the interplay between the Δ_{CKM} constraint and other precision measurements, we embark on a single operator analysis. We assume that a single operator at a time dominates the new physics contribution and set all others to zero. A similar analysis (not including the CKM constraints) has been performed in [148]. We will only consider the operator set $O_{\text{CKM}} =$

V_{us} from $K_{\ell 3}$ decays shifted down to $V_{us} = 0.2200$, which is preferred by current analytic estimates of the vector form factor (see Refs. [65, 71, 141]).

$\{O_{ll}^{(3)}, O_{lq}^{(3)}, O_{\varphi l}^{(3)}, O_{\varphi q}^{(3)}\}$ that contributes to Δ_{CKM}, because for the other operators the analysis would coincide with that of Ref. [148]. In this simplified context we can ask questions about

(i) The relative strength of Δ_{CKM} versus other precision electroweak measurements in constraining the non-zero $\hat{\alpha}_i$;

(ii) The size of correlations among SM deviations in various observables.

In order to address the first question above, for each coefficient $\hat{\alpha}_i \subset \hat{\alpha}_{\text{CKM}}$ we derive the 90 % C.L. allowed intervals implied by: (a) the global fit to all precision electroweak measurements except Δ_{CKM} (first column in Fig. 7.2, also denoted by horizontal gray bands); (b) the Δ_{CKM} constraint via Eq. (7.7) (second column in Fig. 7.2); (c) each subset of measurements listed in Table 7.1 (remaining columns in Fig. 7.2). Missing entries in Fig. (7.2) signify that the measurement sets are independent of the selected operator. The plot nicely illustrates that, for the
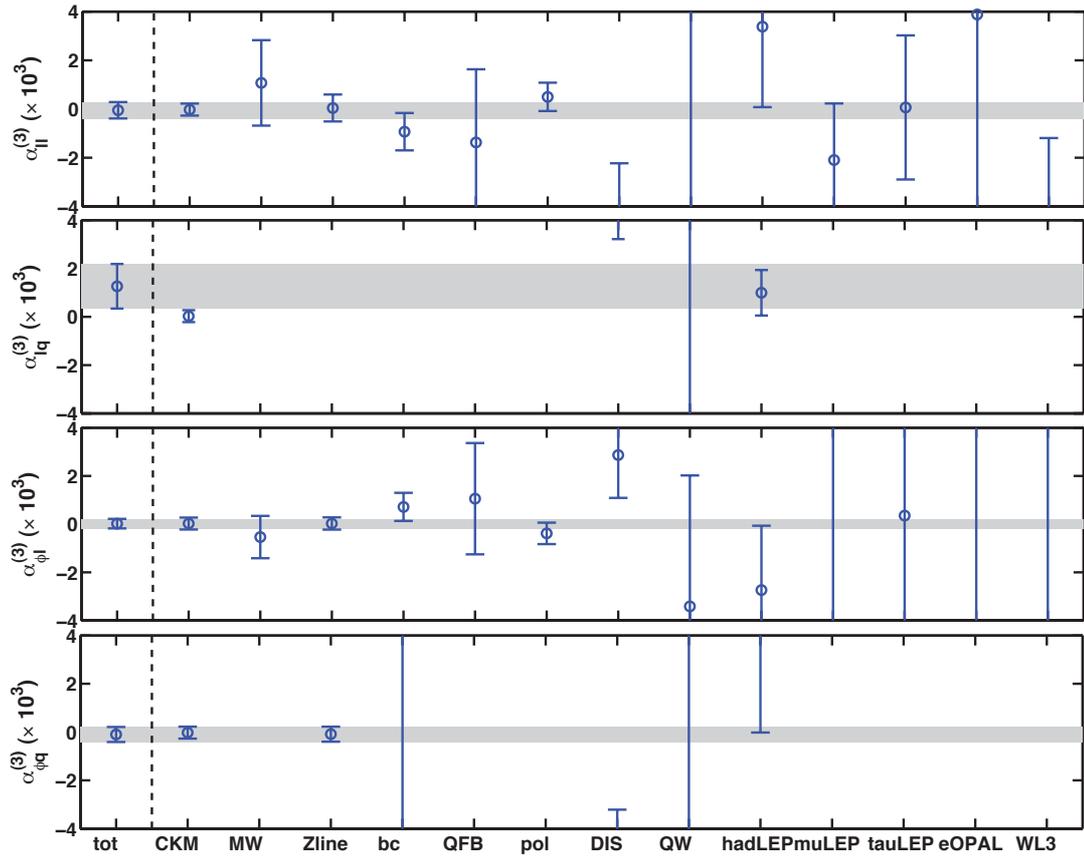

Figure 7.2: 90 % C.L. allowed regions for the coefficients $\hat{\alpha}_i$ within the single operator analysis. The first column displays the constraint from all precision observables except Δ_{CKM}, the second those constraint coming exclusively from Δ_{CKM}, and the rest the constraint derived from each subset of measurements listed in Table 7.1.

operators $O_i \subset O_{\mathrm{CKM}}$, the direct Δ_{CKM} measurement provides constraints at the same level (for $\hat{\alpha}_{\varphi l}^{(3)}$) or better then the Z pole observables. Looking at the size of the constraints, we can immediately conclude that the operators $O_{ll}^{(3)}$, $O_{\varphi l}^{(3)}$, $O_{\varphi q}^{(3)}$, are quite tightly constrained by Z lineshape observables (fourth column in Figure 7.2), so that very little room is left for CKM unitarity violations. On the other hand, the operator $O_{lq}^{(3)}$ is relatively poorly constrained by electroweak precision data (LEP2 $e^+e^- \to q\bar{q}$ cross section provides the best constraint) and could account for significant deviations of Δ_{CKM} from zero (first column of the second panel from top in Fig. 7.2). In this case, the direct constraint is by far the tightest.

Should a non-zero Δ_{CKM} be observed, in the single-operator framework it would be correlated to deviations from the SM expectation in other observables as well, since there is only one parameter in the problem (the coefficient $\hat{\alpha}_k$ of the dominant operator considered). We have studied quantitatively the expected correlation between Δ_{CKM} and the most sensitive electroweak measurements. In Figs. 7.3 and 7.4 we report the correlation between Δ_{CKM} and Z pole observables. In these figures, each black line (solid or broken) corresponds to a given single-operator model, in which only one $\hat{\alpha}_k \neq 0$. Each point on the black line correspond to a particular value of $\hat{\alpha}_k$. A flat black line indicate that no correlation exists between the two
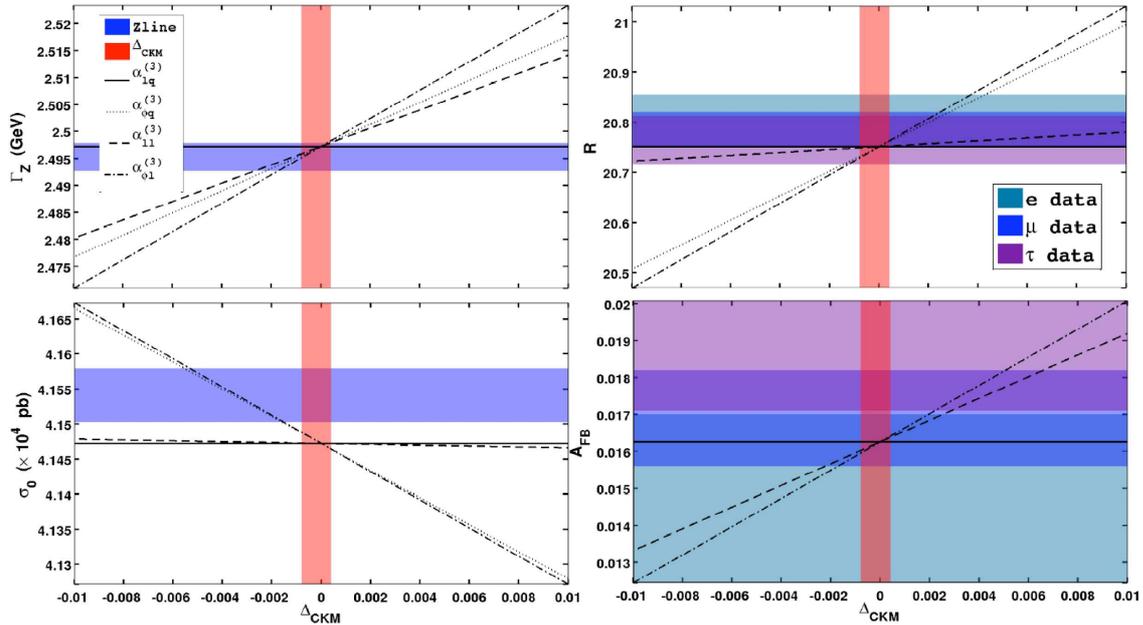

Figure 7.3: Correlation of various Z pole observables with Δ_{CKM}. Operator $O_{lq}^{(3)}$ is not constrained by these measurements. The $O_{lq}^{(3)}$ and $O_{\varphi q}^{(3)}$ lines are degenerate in the A_{FB} panel. The 1σ bands for Δ_{CKM} and Z pole measurements are shown in red and blue, respectively. The right panel bands are shaded differently to indicate e, μ and τ measurements separately. In the lower left panel $\sigma_0 = (12\pi\Gamma_{ee}\Gamma_{had})/(M_Z^2\Gamma_Z^2)$ parameterizes the maximum Z-pole cross-section for $e^+e^- \to$ had.

observables considered. The red shaded bands indicate the current 1-σ Δ_{CKM} direct constraint, while the blue bands correspond to the 1-σ Z-pole observables. We use different blue shading to indicate various measurements included in the analysis. For example, the forward backward asymmetries (A_{FB}) and decay branching ratios (R) are shown in different color for each charged lepton flavor.

Figs. 7.3 and 7.4 clearly illustrate how much we can move Δ_{CKM} from zero before getting into some tension with Z pole precision measurements. Moreover, should a given $\Delta_{\mathrm{CKM}} \neq 0$ be measured, we can immediately read off in which direction other precision measurement should move, and by how much, within this class of models.

The model in which $O_{lq}^{(3)}$ is the dominant operator is somewhat special, as Z-pole observables do not put any constraint. In this model, correlations arise among the following four observables: Δ_{CKM}, the LEP2 $e^+e^- \to q\bar{q}$ cross section, neutrino DIS (in particular the NuTeV measurements of the ratios of NC to CC in $\nu_\mu - N$ DIS), and Atomic Parity Violation, which has only a very weak dependence on $\hat{\alpha}_{lq}^{(3)}$. The two tightest constraints arise from Δ_{CKM} and LEP2. From the correlation plot in Fig. 7.5 (upper panel, solid line) one can see how LEP2 data in principle leave room for substantial quark-lepton universality violations, up to $|\Delta_{\mathrm{CKM}}| \sim 0.005$ at the 1-σ level. In the lower panel of Fig. 7.5. we report the correlation plot between Δ_{CKM} and the effective neutrino-nucleon coupling g_L^2 extracted from NuTeV data. The striking feature of this plot is that an explanation of the deviation between the
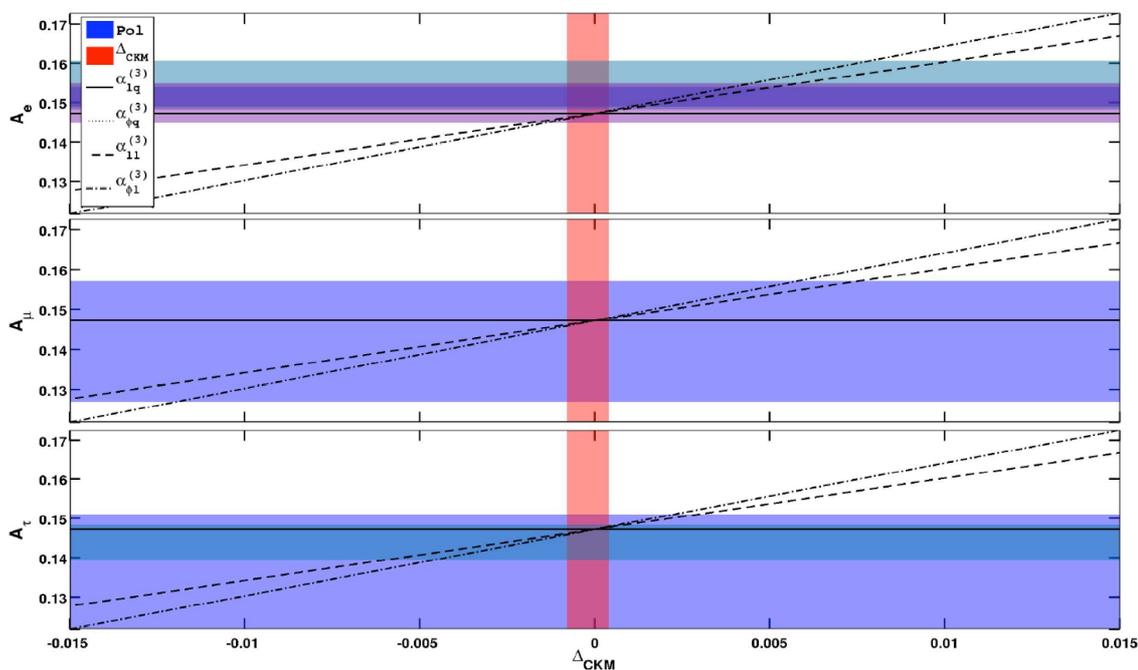

Figure 7.4: Correlation of Z-pole polarized lepton asymmetries with Δ_{CKM}. Operators $O_{lq}^{(3)}$ and $O_{\varphi q}^{(3)}$ are not constrained by these measurements. The 1σ bands for Δ_{CKM} and lepton asymmetries are shown in red and blue, respectively. Different blue shading correspond to different measurements.
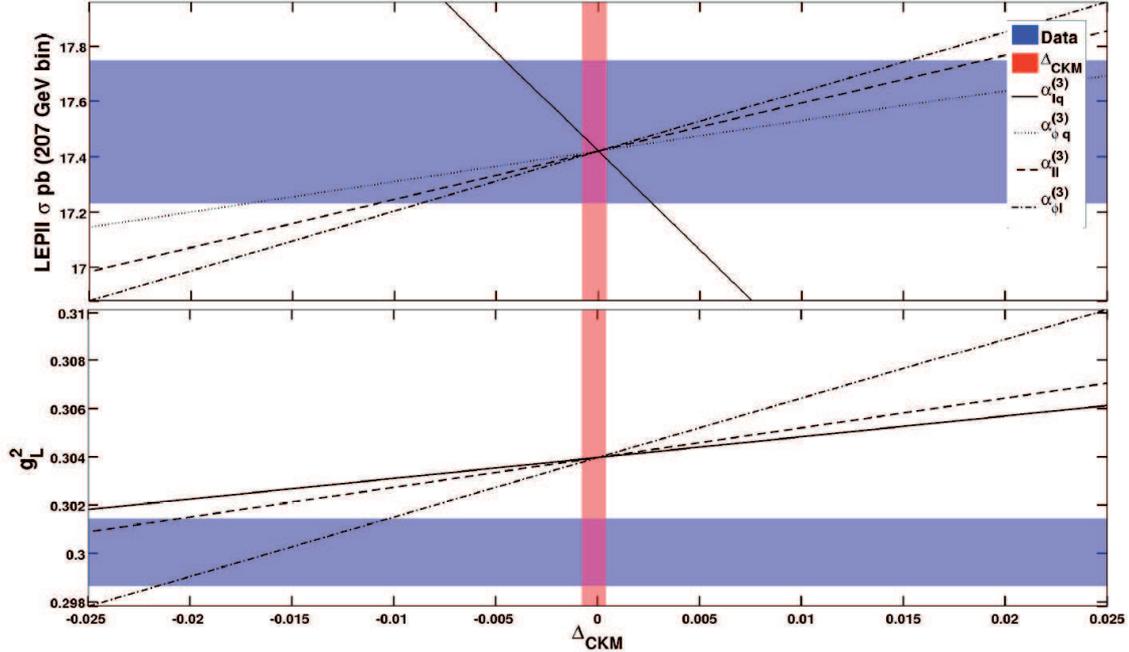
Figure 7.5: Upper panel: correlation between Δ_{CKM} and $\sigma(e^+e^- \rightarrow q\bar{q})(\sqrt{s} = 207$ GeV). Lower panel: correlation between Δ_{CKM} and the effective neutrino-nucleon couplings g_L^2 measured by NuTeV. The 1σ bands for Δ_{CKM} and the other observable are shown in red and blue, respectively.

SM prediction and the NuTeV measured range of g_L^2 in terms $O_{lq}^{(3)}$ (solid line) would require a Δ_{CKM} at least 16σ below its current value.

7.4   Conclusions

We have performed the phenomenological analysis assuming nearly flavor blind ($U(3)^5$ invariant) new physics interactions. In this framework flavor breaking is suppressed by a symmetry principle, such as the Minimal Flavor Violation hypothesis, or by the hierarchy $\Lambda_{\text{flavor}} \gg$ TeV. We have shown that in this limit, the extraction of V_{ud} and V_{us} from any channel should give the same result and the only significant probe of physics beyond the SM involves the quantity $\Delta_{\text{CKM}} \equiv |V_{ud}|^2 + |V_{us}|^2 + |V_{ub}|^2 - 1$. In the next chapter we will explore the constraints arising by comparing the values of V_{us} (V_{ud}) extracted from different channels. These constraints probe those $U(3)^5$-breaking structures to which FCNC and other precision measurements are quite insensitive.

We have shown that in the $U(3)^5$ limit Δ_{CKM} receives contributions from four short distance operators, namely $O_{\text{CKM}} = \{O_{ll}^{(3)}, O_{lq}^{(3)}, O_{\varphi l}^{(3)}, O_{\varphi q}^{(3)}\}$, which also shift SM predictions in other precision observables. Using the result of Eq. (7.7), one can work out the constraints imposed by Cabibbo universality on any weakly coupled extension of the SM. Here we have focused on the model-independent interplay of

Δ_{CKM} with other precision measurements. The main conclusions of our analysis are:

- The Δ_{CKM} constraint bounds the effective scale of all four operators $O_i \subset O_{\text{CKM}}$ to be $\Lambda > 11$ TeV (90 % C.L.). For the operators $O_{ll}^{(3)}, O_{\varphi l}^{(3)}, O_{\varphi q}^{(3)}$ this constraint is at the same level as the Z-pole measurements. For the four-fermion operator $O_{lq}^{(3)}$, Δ_{CKM} improves existing bounds from LEP2 by one order of magnitude.

- Another way to state this result is as follows: should the central values of V_{ud} and V_{us} move from the current values [132], precision electroweak data would leave room for sizable deviations from quark-lepton universality (roughly one order of magnitude above the current direct constraint). In a global analysis, the burden of driving a deviation from CKM unitarity could be shared by the four operators $O_i \subset O_{\text{CKM}}$. In a single operator analysis, essentially only the four-fermion operator $O_{lq}^{(3)}$ could be responsible for $\Delta_{\text{CKM}} \neq 0$, as the others are tightly bound from Z-pole observables.

Our conclusions imply that the study of semileptonic processes and Cabibbo universality tests provide constraints on new physics beyond the SM that currently cannot be obtained from other electroweak precision tests and collider measurements.

Chapter 8

Beyond MFV

*The important thing is
not to stop questioning.
A. Einstein*

As we said in the previous chapter, once we go beyond the flavor-blind case the new physics corrections received by the V_{ij} elements of the CKM matrix are channel dependent and consequently the phenomenology is very rich. In this chapter we will study which is exactly the form of these corrections in the main channels: $K_{\ell 3}$, $K_{\ell 2}/\pi_{\ell 2}$, nuclear beta decays and tau decays.

It is important to study these corrections because with the expectable improvements on the experimental and theoretical side these effects will appear sooner or later. In fact in the recent past there have been some tensions between the results obtained using different channels. It is important to know if these tensions, at the precision level that we are nowadays can be due to new physics effects, or if this possibility is ruled out by other precision measurements and the discrepancy comes probably from the underestimation of errors or just statistical fluctuations.

Moreover, once we are working with a general flavor structure in our operators, the new physics effects go beyond just the contamination of the V_{ij} extractions. One can for example study the corrections to the parameters that describe the angular decay of polarized muons and we will also take a look at this.

In this chapter we will derive the formal results for all these new physics corrections and the phenomenological analysis will be made in a future publication [160], where we will analyze the new physics bounds that can be extracted from these processes and the allowed discrepancies taking into account other precision measurements. This information is of an enormous practical interest since different experiments have been proposed to improve the determination of all these low-energy observables and therefore the analysis of their sensitivity to new physics effects is crucial.

The starting point of this Chapter is the low-energy effective Lagrangians gov-

erning the muon and beta decay, derived in Chapter 6 and that we remind here

$$\mathcal{L}_{\mu \to e \bar{\nu}_e \nu_\mu} = \frac{-g^2}{2m_W^2} \left[(1 + \tilde{v}_L) \cdot \bar{e}_L \gamma_\mu \nu_{eL} \ \bar{\nu}_{\mu L} \gamma^\mu \mu_L \ + \ \tilde{s}_R \cdot \bar{e}_R \nu_{eL} \ \bar{\nu}_{\mu L} \mu_R \right] + \text{h.c.,} \quad (8.1)$$

$$\mathcal{L}_{d_j \to u_i \ell^- \bar{\nu}_\ell} = \frac{-g^2}{2m_W^2} V_{ij} \left[\left(1 + [v_L]_{\ell\ell ij} \right) \bar{\ell}_L \gamma_\mu \nu_{\ell L} \ \bar{u}_L^i \gamma^\mu d_L^j \ + \ [v_R]_{\ell\ell ij} \ \bar{\ell}_L \gamma_\mu \nu_{\ell L} \ \bar{u}_R^i \gamma^\mu d_R^j \right.$$

$$+ \ [s_L]_{\ell\ell ij} \ \bar{\ell}_R \nu_{\ell L} \ \bar{u}_R^i d_L^j \ + \ [s_R]_{\ell\ell ij} \ \bar{\ell}_R \nu_{\ell L} \ \bar{u}_L^i d_R^j$$

$$+ \ [t_L]_{\ell\ell ij} \ \bar{\ell}_R \sigma_{\mu\nu} \nu_{\ell L} \ \bar{u}_R^i \sigma^{\mu\nu} d_L^j \Big] \ + \ h.c. \ , \qquad (8.2)$$

where the coefficients $\tilde{v}_L, \tilde{s}_R, v_L, \ldots$ were defined in Sections 6.2.3 and 6.2.4 in term of the coefficients of the short-distance operators of the BW Lagrangian. For simplicity, we will assume through this Chapter that our new physics coefficients are real, and therefore they will not generate CP violation.

8.1 Muon decay

8.1.1 Muon lifetime

In the previous chapter (Section 7.2.1) we saw that the correction to the muon lifetime in the $U(3)^5$-limit was given by the combination $\tilde{v}_L = 4\hat{\alpha}_{\varphi l}^{(3)} - 2\hat{\alpha}_{ll}^{(3)}$. Working with the most general flavor structure we have an additional correction but it is completely negligible compared with $\tilde{v}_L$; namely we find

$$\left(\tau_\mu^{(\text{exp})}\right)^{-1} \ = \ \sum_{\alpha\beta} \Gamma(\mu \to e\bar{\nu}_\alpha \nu_\beta) = \left(\tau_\mu^{SM}\right)^{-1} (1 + \delta_\mu) \ , \qquad (8.3)$$

where

$$\delta_\mu \ = \ 2 \ \tilde{v}_L + 2\frac{m_e}{m_\mu} \ \tilde{s}_R \approx 2 \ \tilde{v}_L \ , \qquad (8.4)$$

$$\left(\tau_\mu^{SM}\right)^{-1} \ = \ \frac{G_F^2 m_\mu^5}{192\pi^3} f\left(\frac{m_e^2}{m_\mu^2}\right) (1 + R.C.) \left(1 + \frac{3}{5} \frac{m_\mu^2}{m_W^2}\right) \ , \qquad (8.5)$$

and $f(x) = 1 - 8x + 8x^3 - x^4 - 12x^2 \ln x$. The expression for the $R.C.$ (radiative corrections[1]) can be found in [161] and the Fermi constant is defined in terms of $\text{SU}(2)_L \times \text{U}(1)_Y$ standard model parameters as $G_F = g_2^2/4\sqrt{2}m_W^2$ (at tree level, i.e., lowest order in perturbation theory), where g_2 is the $\text{SU}(2)_L$ gauge coupling and m_W is the $W^\pm$ gauge boson mass.

---

[1] The R.C. expression is somewhat arbitrary. Most quantum loop corrections to muon decay are absorbed into the renormalized parameter G_μ. For historical reasons and in the spirit of effective field theories, R.C. is defined to be the QED radiative corrections to muon decay in the local V-A four fermion description of muon decay. That separation is natural and practical, since those QED corrections are finite to all orders in perturbation theory.

Traditionally, the muon lifetime, τ_μ, has been used to define the Fermi constant because of its very precise experimental value and theoretical simplicity, but we see here that within our framework what we are really extracting is the value of the combination

$$(G_F^\mu)^{(pheno)} = (G_F^\mu)^{(0)} \left(1 + \frac{1}{2}\delta_\mu\right) = (G_F^\mu)^{(0)} \left(1 + \tilde{v}_L\right) . \tag{8.6}$$

The error in the muon lifetime measurement has been improved remarkably by the MuLan and FAST Collaborations [162] and both of them expect to reach the part-per-million precision in the future. We quote here the PDG value [129]

$$G_F^{(exp)} = 1.166367(5) \times 10^{-5} \text{GeV}^{-2} . \tag{8.7}$$

8.1.2 Decay parameters of polarized muons

The most general derivative-free four-lepton interaction hamiltonian for describing the process $\mu^- \to \nu_\mu e^- \bar{\nu}_e$, consistent with locality, Lorentz invariance and lepton-number conservation, can be written as [163]

$$\mathcal{H}_{\mu^- \to \nu_\mu e^- \bar{\nu}_e} = 4 \frac{G_{\mu e}}{\sqrt{2}} \sum_{\epsilon,\omega=R,L}^{n=S,V,T} g_{\epsilon\omega}^n \left[\overline{e_\epsilon}\Gamma^n(\nu_e)_\sigma\right] \left[\overline{(\nu_\mu)_\lambda}\Gamma_n\mu_\omega\right] , \tag{8.8}$$

where the label n refers to the type of interaction:

$$\Gamma^S = 1 , \qquad \Gamma^V = \gamma^\mu , \qquad \Gamma^T = \frac{1}{\sqrt{2}}\sigma^{\mu\nu} \equiv \frac{i}{2\sqrt{2}}\left(\gamma^\mu\gamma^\nu - \gamma^\nu\gamma^\mu\right) , \tag{8.9}$$

for the scalar, vector and tensor interactions, respectively. Once n and the charged-lepton chiralities, ϵ and ω, are chosen, the neutrino chiralities σ and λ are uniquely determined. Taking into account also that there are only two non-zero tensor terms and that one global phase may be taken away, we end up with 19 real constants.

In our case, without right-handed neutrinos, all the g's are zero except g_{LL}^V and g_{RR}^S, that correspond to the $\tilde{v}_L$ and $\tilde{s}_R$ coefficients of expression (8.1).

For an initial muon-polarization $\mathcal{P}_l$, the final electron distribution in the muon rest frame is usually parametrized in the form [164]

$$\frac{d^2\Gamma(\mathcal{P}_l, x, \cos\theta)}{dx\, d\cos\theta} = \frac{m_l\omega^4}{2\pi^3}(G_F^2 N)\sqrt{x^2 - x_0^2} \times$$

$$\times \left\{ x(1-x) + \frac{2}{9}\rho\left(4x^2 - 3x - x_0^2\right) + \eta\, x_0(1-x) \right.$$

$$\left. -\frac{1}{3}\mathcal{P}_l\,\xi\,\sqrt{x^2 - x_0^2}\cos\theta\left[1 - x + \frac{2}{3}\delta\left(4x - 4 + \sqrt{1 - x_0^2}\right)\right]\right\}, \tag{8.10}$$

where θ is the angle between the μ^- spin and the electron momentum, $\omega \equiv (m_l^2 + m_{l'}^2)/2m_l$ is the maximum e^- energy for massless neutrinos, $x \equiv E_{e^-}/\omega$ is the reduced energy and $x_0 \equiv m_e/\omega$.

For unpolarized $\mu's$, the distribution is characterized by the so-called Michel [165] parameter ρ and the low-energy parameter η. Two more parameters, ξ and δ can be determined when the muon polarization is known.

To determine the constraints on physics beyond the SM, it is convenient to express the Michel parameters in terms of their deviation from the SM values. One obtains (taking into account that most of the $g's$ vanish in our framework) for the four parameters and the overall normalization factor

$$
\begin{aligned}
\rho - \frac{3}{4} &= 0 \ , \\
\eta &= \frac{1}{2}\mathrm{Re}\left(g_{RR}^S g_{LL}^{V*}\right) \ , \\
\xi - 1 &= -\frac{1}{2}|g_{RR}^S|^2 \ , \\
(\xi\delta) - \frac{3}{4} &= -\frac{3}{8}|g_{RR}^S|^2 \ , \\
N &= \frac{1}{4}|g_{RR}^S|^2 + |g_{LL}^V|^2 \ .
\end{aligned}
\tag{8.11}
$$

Notice that even at this point, where we have not neglected the quadratic terms yet, we see some consequences of not considering the right-handed neutrinos like the fact that there is no NP correction in the ρ parameter and that the correction in ξ and $(\xi\delta)$ is the same (up to a factor 3/4). It is known that η is the only parameter that receives a linear correction from these new physics terms (see e.g. Ref. [166]) what makes it the most sensitive to NP of these four parameters[2].

$$
\begin{aligned}
\rho - \frac{3}{4} &= 0 \ , \\
\eta &= \frac{1}{2}\,\tilde{s}_R = [\hat{\alpha}_{le}]_{2112} \ , \\
\xi - 1 &= 0 \ , \\
(\xi\delta) - \frac{3}{4} &= 0 \ , \\
N &= 1 + 2\,\tilde{v}_L \ .
\end{aligned}
\tag{8.12}
$$

The TWIST Collaboration has published the most precise values for the parameters ρ, δ and $(\xi\delta)$ [167], and they expect to improve these measurements in the next years. For the moment, the results are compatible with the SM predictions, but if next measurements disagree in any of these parameters not only we would have a sign of physics beyond the SM but at the same time we would have extracted valuable information about the new physics structure. A discrepancy in ξ and/or $(\xi\delta)$ could be a quadratic effect of our $g's$, but a discrepancy in δ would be more interesting since it could be explained only with the introduction of right-handed neutrinos.

---

[2]It is worth mentioning that even in the most general framework with right-handed neutrinos, that is with all the $g's$ finite, if we write $g_{LL}^V = 1 + g_{LL}^{'V}$ and neglect the terms quadratic in the $g's$ we will find that all the differences with the SM vanish except $\eta = \frac{1}{2}g_{RR}^S$.

The situation is a bit different for the parameter η, that has been measured at the PSI [168], because as we have seen it is the only one where a difference with the SM can be generated linearly, what makes it the most sensitive to new physics. From its measurement and working within our framework one can extract the value of $[\hat{\alpha}_{le}]_{2112}$. Notice that is quite remarkable that this observable involves only one of our coefficients. The current result working in this linear approximation is compatible with zero [168], what can be translated into a bound on $[\hat{\alpha}_{le}]_{2112}$:

$$|\eta| < 0.015 \rightarrow (\Lambda^{(\text{eff.})})^2 \equiv \frac{\Lambda^2}{|[\alpha_{le}]_{2211}|} = \frac{v^2}{|\eta|} > (2 \text{ TeV})^2 \quad (95\% \text{ C.L.}). \qquad (8.13)$$

If the quadratic terms are kept then the extracted value for η is not so precise [129], $\eta = 0.001 \pm 0.024$, what generates $\Lambda^{(eff.)} > 1.1$ TeV.

8.2 Kaon and pion physics

The new results on the semi-leptonic decays K_{l3} and K_{l2} from BNL-E865, KTeV, NA48, KLOE, and ISTRA+ allow to perform very stringent SM tests [132], being some of them almost free from hadronic uncertainties, as the μ/e universality ratio in $K_{\ell2}$ decays. Moreover, this experimental improvement have stimulated a significant progress also on the theory side: most of the theory-dominated errors associated to hadronic form factors have recently been reduced below the 1% level.

We will first briefly review how the V_{us} and the ratio V_{us}/V_{ud} are extracted, assuming that the Standard Model holds, and then we will analyze the effects of the new terms in our low-energy effective Lagrangian on these extraction procedures.

8.2.1 $K_{\ell3}$ and $K_{\ell2}$ rates within the SM

The photon-inclusive $K_{\ell3}$ and $K_{\ell2}$ decay rates can be conveniently decomposed within the SM in the following way

$$\Gamma(K_{3(\gamma)}) = \frac{G_F^2 m_K^5}{192\pi^3} C_K S_{\text{ew}} |V_{us}|^2 f_+(0)^2 I_K^\ell(\lambda_{+,0}) \left(1 + \delta_{SU(2)}^K + \delta_{\text{em}}^{K\ell}\right)^2 \qquad (8.14)$$

$$\frac{\Gamma(K_{\ell2(\gamma)}^\pm)}{\Gamma(\pi_{\ell2(\gamma)}^\pm)} = \left|\frac{V_{us}}{V_{ud}}\right|^2 \frac{f_K^2 m_K}{f_\pi^2 m_\pi} \left(\frac{1 - m_\ell^2/m_K^2}{1 - m_\ell^2/m_\pi^2}\right)^2 \times (1 + \delta_{\text{em}}) \quad , \qquad (8.15)$$

where $C_K = 1$ (1/2) for the neutral (charged) kaon decays, S_{ew} is the universal short-distance electromagnetic correction and δ_{em} and $\delta_{\text{em}}^{K\ell}$ are the channel-dependent long-distance electromagnetic correction factors. $I_K^\ell(\lambda_{+,0})$ is the phase space integral that depends on the slopes of the form factors (generically denoted by $\lambda_{+,0}$)

$$I_K^\ell = \frac{1}{m_K^2 f_+(0)^2} \int dt \, \lambda^{3/2}(t) \left(1 + \frac{m_\ell^2}{2t}\right) \left(1 - \frac{m_\ell^2}{t}\right)^2$$
$$\times \left(f_+^2(t) + \frac{3m_\ell^2 (m_K^2 - m_\pi^2)^2}{(2t + m_\ell^2) m_K^4 \lambda(t)} |f_0(t)|^2\right), \qquad (8.16)$$

$$\lambda(t) \;\; = \;\; 1 - 2r_\pi + r_\pi^2 - 2t/m_K^2 - 2r_\pi t/m_K^2 + t^2/m_K^4 \; , \qquad (8.17)$$

where $r_{\pi,\ell} = m_{\pi,\ell}^2/M_K^2$. The hadronic $K \to \pi$ matrix element of the vector current is described by two form factors, $f_+(t)$ and $f_0(t)$, defined by

$$\langle \pi^-(k) | \bar{s}\gamma^\mu u | K^0(p) \rangle \;\; = \;\; (p+k)^\mu f_+(t) + (p-k)^\mu f_-(t) \qquad (8.18)$$
$$= \;\; (p+k)^\mu f_+(t) + (p-k)^\mu \frac{m_K^2 - m_\pi^2}{t} \left(f_0(t) - f_+(t) \right)$$

where $t = (p-k)^2$.

In order to compute the phase space integral (8.16) we need to know the form factors $f_{+,0}(t)$. In principle, Chiral Perturbation Theory and Lattice QCD are useful tools to set theoretical constraints, but in practice the t-dependence is better determined by measurements and by combining measurements and dispersion relations. With the recent experimental data the quantities $|V_{us}| \times f_+(0)$ and $|V_{us}|/|V_{ud}| \times f_K/f_\pi$ can be determined with very good accuracy [132]:

$$|V_{us}| \times f_+(0) \;\; = \;\; 0.2166(5), \qquad (8.19)$$
$$|V_{us}|/|V_{ud}| \times f_K/f_\pi \;\; = \;\; 0.2760(6) \; . \qquad (8.20)$$

The main obstacle in transforming these precise determinations into a determination of $|V_{us}|$ at the per-mil level are the theoretical uncertainties on the hadronic parameters $f_+(0)$ and f_K/f_π.

On one hand the parameter $f_+(0)$, although not calculable in perturbative QCD, it is very constrained by $SU(3)$ and chiral symmetry. In the $SU(3)$ limit ($m_u = m_d = m_s$) the conservation of the vector current implies $f_+(0)=1$. The chiral corrections are protected by the Ademollo–Gatto theorem that forbids corrections linear in the quark masses. The $\mathcal{O}(p^6)$ chiral corrections have been computed following different analytical approaches [65, 71, 169] and the different results, although in agreement with the original estimate by Leutwyler and Roos [140] $f_+(0) = 0.961(8)$, are systematically larger than it. In any case, the size of the error is still around or above 1%, which is not comparable to the 0.2% accuracy which has been reached for $|V_{us}| \times f_+(0)$. Recent progress in lattice QCD gives us more optimism in the reduction of the error on $f_+(0)$ below the 1% level [143,170]. We will follow the FlaviaNet group and adopt the lattice value from the UKQCD-RBC collaboration [171] is $f_+(0) = 0.964(5)$.

On the other hand the pseudoscalar decay constants are not protected by the Ademollo–Gatto theorem and as a result, in the determination of f_K/f_π lattice QCD has essentially no competition from purely analytical approaches. Again, following the FlaviaNet group we adopt the lattice result from the HPQCD/UKQCD Collaboration $f_K/f_\pi = 1.189(7)$ [146][3].

Using these numbers it is found:

$$|V_{us}| = 0.2246 \pm 0.0012 \; , \qquad |V_{us}|/|V_{ud}| = 0.2321 \pm 0.0015 \; . \qquad (8.21)$$

---

[3]It is worth noting that this result is in good agreement with the recent determinations performed by the MILC'09 [106] and BMW [172] Collaborations, using different lattice techniques.

It is interesting to notice that this value of $|V_{us}|$, based on the recent experimental data on kaon decays, is about two sigma higher than the previous one, $|V_{us}| = 0.2200(26)$ (PDG2004), that was based essentially on twenty years old measurements.

8.2.2 $K_{\ell 2}$ and $\pi_{\ell 2}$ beyond the SM

Working with our low-energy effective Lagrangian (8.2) we obtain

$$\Gamma(X^-_{\ell 2(\gamma)}) = \frac{(G_F^{(0)})^2 \, |V_{uj}|^2 \, F_X^2}{4\pi} m_\ell^2 M_X \left(1 - \frac{m_\ell^2}{M_X^2}\right)^2 (1 + \delta(X_{\ell 2})) \, , \quad (8.22)$$

$$\delta(X_{\ell 2}) = 2 \left(\delta A_{j\ell} - \frac{M_X^2}{(m_u + m_j)m_\ell}\delta P_{j\ell}\right) \, , \quad (8.23)$$

$$\delta A_{j\ell} = [v_L]_{j\ell} - [v_R]_{j\ell} \, , \quad (8.24)$$

$$\delta P_{j\ell} = [s_L]_{j\ell} - [s_R]_{j\ell} \, , \quad (8.25)$$

where $X = \pi(j=1), K(j=2)$ and $\ell = 1(e), 2(\mu)$.

Extraction of $|V_{us}|/|V_{ud}|$

From this result we can calculate the following ratio[4]

$$R_\ell \equiv \frac{\Gamma(K^-_{\ell 2(\gamma)})}{\Gamma(\pi^-_{\ell 2(\gamma)})} = \frac{|V_{us}|^2 \, f_K^2 m_K}{|V_{ud}|^2 \, f_\pi^2 m_\pi} \left(\frac{1 - \frac{m_\ell^2}{m_K^2}}{1 - \frac{m_\ell^2}{m_\pi^2}}\right)^2 (1 + \delta(R_\ell)) \, , \quad (8.27)$$

$$\begin{aligned}\delta(R_\ell) &= \delta(K_{\ell 2}) - \delta(\pi_{\ell 2}) \\ &= 2 \left((\delta A_{2\ell} - \delta A_{1\ell}) - \left(\frac{M_K^2}{(m_u+m_s)m_\ell}\delta P_{2\ell} - \frac{M_\pi^2}{(m_u+m_d)m_\ell}\delta P_{1\ell}\right)\right),\end{aligned} (8.28)$$

that is used to extract the value of the ratio $|V_{us}|/|V_{ud}|$. If we take into account the new terms what we are really measuring is the following quantity

$$\left(\frac{|V_{us}|}{|V_{ud}|}\right)^{(pheno)} = \frac{|V_{us}|}{|V_{ud}|} \times \left(1 + \frac{1}{2}\delta(R_\ell)\right) \, . \quad (8.29)$$

---

[4]The correction found for R_ℓ, Eq. (8.28), agrees with the result of Ref. [132]. In order to check it, it is necessary to take into account that, as we do not have right-handed neutrinos, $C_{LR}^V = C_{RR}^V = C_{LL}^S = C_{RL}^S = C_{LL}^T = 0$ in our approach. Notice also that they write the Lagrangian for $X^+_{\ell 2}$ and add the h.c. whereas we have written the Lagrangian for $X^-_{\ell 2}$ and add the h.c. This produces that C_{RR}^S is connected to s_L and not to s_R as one might have thought naively. In the end we have

$$\begin{aligned}\left[C_{LL}^V\right]_j &= [v_L]_{j\ell}^* / |V_{uj}| \, , & \left[C_{LR}^S\right]_j &= [s_R]_{j\ell}^* / |V_{uj}| \, , & \left[C_{RR}^T\right]_j &= [t_L]_{j\ell}^* / |V_{uj}| \, , \\ \left[C_{RL}^V\right]_j &= [v_R]_{j\ell}^* / |V_{uj}| \, , & \left[C_{RR}^S\right]_j &= [s_L]_{j\ell}^* / |V_{uj}| \, . & & (8.26)\end{aligned}$$

$\mu - e$ universality ratios

These $\mu - e$ ratios are very clean observables and can be used to put strong bounds to their NP-corrections. In our framework they take the form

$$R_\pi \equiv \frac{\Gamma(\pi^-_{e2(\gamma)})}{\Gamma(\pi^-_{\mu2(\gamma)})} = \frac{m_e^2}{m_\mu^2} \left(\frac{1 - \frac{m_e^2}{m_\pi^2}}{1 - \frac{m_\mu^2}{m_\pi^2}} \right)^2 (1 + \delta(R_\pi)) \ , \tag{8.30}$$

$$\begin{aligned} \delta(R_\pi) &= \delta(\pi_{e2}) - \delta(\pi_{\mu2}) \\ &= 2 \left((\delta A_{1e} - \delta A_{1\mu}) - \frac{M_\pi^2}{m_u + m_d} \left(\frac{1}{m_e} \delta P_{1e} - \frac{1}{m_\mu} \delta P_{1\mu} \right) \right) \ , \quad (8.31) \end{aligned}$$

$$R_K \equiv \frac{\Gamma(K^-_{e2(\gamma)})}{\Gamma(K^-_{\mu2(\gamma)})} = \frac{m_e^2}{m_\mu^2} \left(\frac{1 - \frac{m_e^2}{m_K^2}}{1 - \frac{m_\mu^2}{m_K^2}} \right)^2 (1 + \delta(R_K)) \ , \tag{8.32}$$

$$\begin{aligned} \delta(R_K) &= \delta(K_{e2}) - \delta(K_{\mu2}) \\ &= 2 \left((\delta A_{2e} - \delta A_{2\mu}) - \frac{M_K^2}{m_u + m_s} \left(\frac{1}{m_e} \delta P_{2e} - \frac{1}{m_\mu} \delta P_{2\mu} \right) \right) \ , \quad (8.33) \end{aligned}$$

8.2.3 $K_{\ell3}$ decay beyond the SM

In the general case we have, in addition to the vector-current matrix element, the tensor and scalar ones, and therefore we will need new form factors. Actually we only need to add the tensor one, since $f_0(t)$ allow us to parametrize also the scalar-current matrix element. More specifically, we have

$$\langle \pi^-(k) | (\bar{s}u) | K^0(p) \rangle = -\frac{m_K^2 - m_\pi^2}{(m_s - m_u)} f_0(t) \ , \tag{8.34}$$

$$\langle \pi^-(k) | (\bar{s}\sigma^{\mu\nu}u) | K^0(p) \rangle = i \frac{p^\mu k^\nu - p^\nu k^\mu}{m_K} B_T(t) \ . \tag{8.35}$$

Following the scheme of the FlaviaNet Kaon Working Group [132] it is found that the difference between the $K_{\ell3}$ rate obtained with our low-energy effective Lagrangian (8.2) to the SM one can be summarized as follows:

- Overall rescaling factor produced by the vector and axial-vector couplings

$$\Gamma(K_{\ell3(\gamma)}) \rightarrow \Gamma(K_{\ell3(\gamma)}) \times |C_V|^2 \ , \tag{8.36}$$

$$C_V \equiv 1 + [v_L + v_R]_{2\ell}^* \ . \tag{8.37}$$

- Scalar and pseudoscalar contributions can be encoded by substituting

$$f_0(t) \rightarrow f_0^H(t) = f_0(t) \left(1 + \frac{C_S}{m_s M_W} t \right) \ , \tag{8.38}$$

$$C_S \equiv \frac{M_W}{m_\ell} [s_R + s_L]_{2\ell}^* \ . \tag{8.39}$$

- The tensor coupling modify the phase space integral $I_K^\ell(\lambda_{+,0})$ of Eq. (8.14) by

$$I_K^\ell(\lambda_{+,0}) \rightarrow I_K^\ell(\lambda_{+,0}) - [t_L]_{2\ell}^* \, I_T^\ell(\lambda_{T,+,0}) \;, \tag{8.40}$$

where I_T^ℓ is defined below.

In conclusion, the integrated rate including electromagnetic corrections can be written as

$$
\begin{aligned}
\Gamma(K_{\ell 3(\gamma)}) \;=\;& \frac{G_F^2 m_K^5}{192\pi^3} C_K \, S_{\text{ew}} \, |V_{us}|^2 f_+(0)^2 \left(1 + \delta_{SU(2)}^K + \delta_{\text{em}}^{K\ell}\right)^2 \\
\times\;& |C_V|^2 \left(I_K^\ell - [t_L]_{2\ell}^* \, I_T^\ell\right) \;,
\end{aligned}
\tag{8.41}
$$

where

$$
\begin{aligned}
I_K^\ell = \frac{1}{m_K^2 f_+(0)^2} \int & dt \; \lambda^{3/2}(t) \left(1 + \frac{m_\ell^2}{2t}\right)\left(1 - \frac{m_\ell^2}{t}\right)^2 \\
& \times \left(f_+^2(t) + \frac{3 m_\ell^2 \left(m_K^2 - m_\pi^2\right)^2}{\left(2t + m_\ell^2\right) m_K^4 \lambda(t)} \, |f_0^H(t)|^2\right) \;,
\end{aligned}
$$

$$
I_T^\ell = \frac{1}{m_K^2 f_+(0)^2} \int dt \; \lambda^{3/2}(t) \frac{6 \, m_\ell}{m_K} \left(1 - \frac{m_\ell^2}{t}\right)^2 B_T(t) f_+(t)^* \;, \tag{8.42}
$$

where $\lambda(t)$ was defined in (8.17).

We see that we do not agree with the result of Ref. [132] for the I_T^ℓ integral. Comparing with the results of Ref. [173] we find that we agree in the fact that there is no interference between $B_T(t)$ and $f_0(t)$, and also in the interference between $B_T(t)$ and $f_0(t)$ but for a global sign[5].

V_{us} extraction

In most realistic new-physics scenarios the modification of the $K_{\ell 3}$ scalar form factor and the phase space integral is well below the present experimental and theoretical errors. In this way we would have

$$\Gamma(K_{\ell 3(\gamma)}) \;\approx\; \Gamma(K_{\ell 3(\gamma)})^{SM} \times |C_V|^2 = \Gamma(K_{\ell 3(\gamma)})^{SM} \left(1 + 2 \, [v_L + v_R]_{2\ell}\right), \tag{8.43}$$

and therefore

$$|V_{us}|_{K_{\ell 3}}^{pheno} = |V_{us}| \left(1 + [v_L + v_R]_{2\ell} - \tilde{v}_L\right) \;. \tag{8.44}$$

---

[5]We find a negative interference (notice the minus sign in the Eq. (8.40)). Altough there is also a minus sign in the interference found in Ref. [173] one must take into account the fact that there is an extra minus sign (and also some factors) that appears when we write their constant C_T^ℓ in terms of our constant t_L. And therefore we have the discrepancy in the sign of the interference.

8.3   Nuclear beta decay

The nuclear beta decay gives us the most precise measurement of V_{ud} through the study of the $0^+ \rightarrow 0^+$ transitions, and also gives one of the most precise alternative determinations through the study of the neutron decay. First we briefly review how these determinations are made (considering only the SM physics) and later we will analyze the new physics effects on these procedures.

8.3.1   Standard extraction of V_{ud} from nuclear beta decay

V_{ud} from $0^+ \rightarrow 0^+$ transitions

In order to find the appropriate formula needed for the extraction of V_{ud}, we start with the general expression for the differential rate for unpolarized nucleus:

$$\frac{d\Gamma}{dE_e d\Omega_e d\Omega_\nu} = \frac{F(-Z, E_e)}{(2\pi)^5} \frac{G_F^2}{2} |V_{ud}|^2 p_e E_e (E_0 - E_e)^2 \, \xi \left\{ 1 + a \frac{\mathbf{p_e} \cdot \mathbf{p_\nu}}{E_e E_\nu} + b \frac{m_e}{E_e} \right\}, (8.45)$$

where E_0 is the electron endpoint energy and $F(-Z, E_e)$ is the Fermi function that can be parametrized in the Primakoff-Rosen approximation [174] (good if the Q value[6] is not too small) as:

$$F(Z, E_e) = \frac{E_e}{p_e} \frac{2\pi\alpha Z}{1 - e^{-2\pi\alpha Z}} \; . \tag{8.46}$$

The correlation coefficients a and b vanish in the SM, whereas $\xi = 4g_V^2$ for the overall normalization[7]. Therefore we see that nuclear beta decays between 0^+ states are produced only via the vector component of the hadronic weak interaction. This is important because the CVC hypothesis protects the vector coupling constant G_V from renormalization by background strong interactions ($g_V = 1$ up to second order corrections in isospin breaking) and thus we have $G_V = G_F V_{ud}$. Consequently, using the G_F value extracted from muon decay and measuring G_V in nuclei we have the value of the CKM matrix element V_{ud}.

Performing the phase space integrations, the total decay rate reads:

$$\Gamma_{0^+ \rightarrow 0^+} = \frac{G_F^2 \, m_e^5}{2\pi^3} |V_{ud}|^2 f \; , \tag{8.51}$$

---

[6]The Q value is the difference in the atomic masses of neutral atoms in ground-state configurations and the quantity E_0 in Eq. (8.45) is related to Q by the equation $E_0 = Q - m_e$.

[7]The constants $g_i \equiv g_i(0)$ ($i = V, A, S, T$) are defined [134] as:

$$g_V(q^2) \, \bar{p}\gamma_\mu n = \langle p| \, \bar{u}\gamma_\mu d \, |n \rangle \; , \tag{8.47}$$

$$g_A(q^2) \, \bar{p}\gamma_\mu\gamma_5 n = \langle p| \, \bar{u}\gamma_\mu\gamma_5 d \, |n \rangle \; , \tag{8.48}$$

$$g_S(q^2) \, \bar{p}n = \langle p| \, \bar{u}d \, |n \rangle \; , \tag{8.49}$$

$$g_T(q^2) \, \bar{p}\sigma_{\mu\nu} n = \langle p| \, \bar{u}\sigma_{\mu\nu} d \, |n \rangle \; . \tag{8.50}$$

where f is the phase space integral.

To date, precise measurements of the beta decay between isospin analog states of spin, $J^\pi = 0^+$, and isospin, $T = 1$, provide the most precise value of V_{ud} [139]. A survey of the relevant experimental data has recently been completed by Hardy and Towner [139]. For each transition, three experimental quantities have to be determined: the decay energy Q (used to calculate the phase space integral f), the half-life of the decaying state $t_{1/2}$ and the branching ratio R for the particular transition under study. In Eq. (8.51) we see that, in the limit where isospin is an exact symmetry, the product ft (the partial half-life is defined as $t = t_{1/2}/R$) is

$$ft = \frac{K}{2\, G_F^2 V_{ud}^2}, \tag{8.52}$$

where $K = 2\pi^3 \ln 2/m_e^5 = 8.1202787(11) \times 10^{-13}$ GeV^{-5}. That is, according to CVC the ft value is a constant independent of the nucleus under study. In practice, however, isospin is a broken symmetry in nuclei, and so a 'corrected' ft value that takes into account the radiative corrections is defined by

$$\mathcal{F}t \equiv ft(1 + \delta_R')\,(1 - (\delta_C - \delta_{NS})) = \frac{K}{2\, G_F^2 V_{ud}^2\,(1 + \Delta_R^V)}; \tag{8.53}$$

so it is this corrected $\mathcal{F}t$ that is a constant. Here $\Delta_R^V = (2.631 \pm 0.038)\%$ [138] is a nucleus-independent part that includes the universal short-distance component S_{EW} affecting all semi-leptonic decays. The others corrections are transition dependent that require shell-model calculation.

In the upper panel of Fig. 8.1 are shown the experimental ft values from the survey of Hardy and Towner [139] for 13 transitions. This data represent an important test of the CVC statement that the $\mathcal{F}t$ values should be constant for all nuclear super-allowed transitions of this type. The disagreement between the different points is completely absent in the corrected $\mathcal{F}t$ values shown in the lower panel of Fig. 8.1, principally due to the nuclear-structure-dependent corrections, thus validating the theoretical calculations at the level of current experimental precision. The weighted average of the 13 data is

$$\overline{\mathcal{F}t} = 3071.83 \pm 0.85 \text{ s}. \tag{8.54}$$

The CKM matrix element V_{ud} is then obtained from

$$V_{ud}^2 = \frac{K}{2G_F^2(1 + \Delta_R^V)\overline{\mathcal{F}t}} \quad \rightarrow \quad |V_{ud}| = 0.97425 \pm 0.00022. \tag{8.55}$$

The error is completely dominated by theoretical uncertainties, principally by the nucleus-independent radiative correction Δ_R^V, that was recently reduced by a factor of two [138] and where further improvements will need some theoretical breakthroughs. Second in order of significance are the nuclear-structure-dependent corrections δ_C and δ_{NS}.
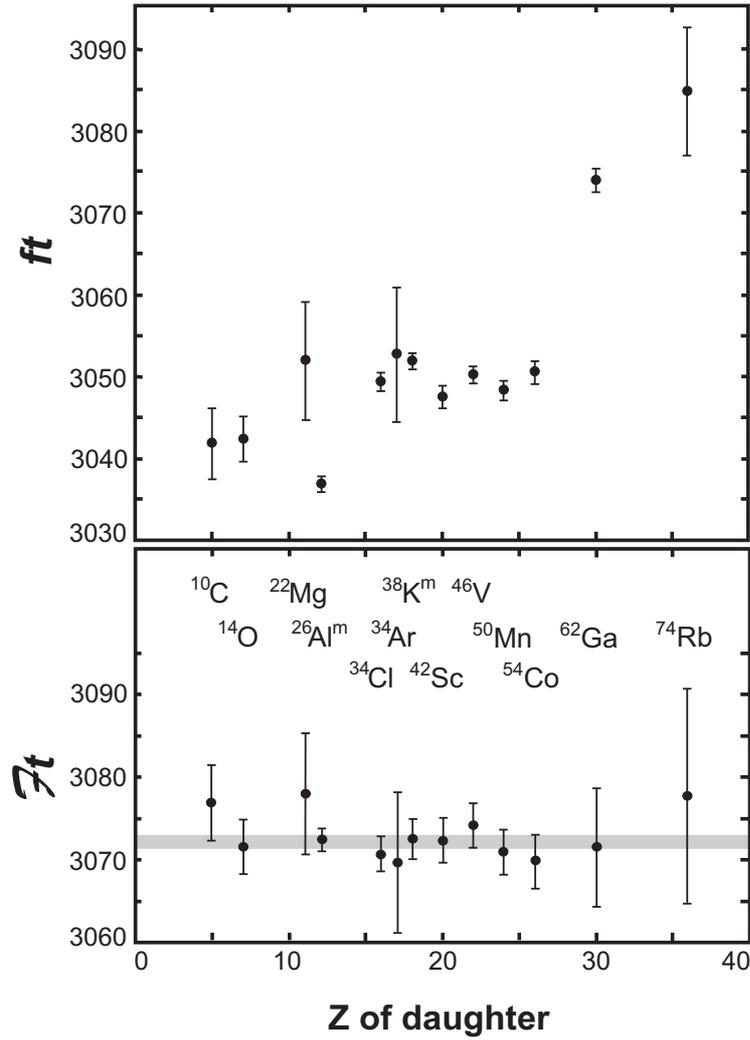
Figure 8.1: In the top panel are plotted the uncorrected experimental ft values as a function of the charge on the daughter nucleus. In the bottom panel, the corresponding $\mathcal{F}t$ values as defined in Eq. (8.53) are given. The horizontal grey band in the bottom panel gives one standard deviation around the average $\overline{\mathcal{F}t}$. (Figure taken from Ref. [139])

V_{ud} from neutron decay

The extraction of V_{ud} from neutron β-decay cannot compete yet with the extraction from $0^+ \to 0^+$ transitions, but it is interesting because the most complicated transition-dependent radiative corrections δ_C and δ_{NS} do not appear in the analysis. However, we still have δ'_R, and the nucleus-independent radiative correction Δ_R^V.

Neutron β-decay not only samples the weak vector interaction but also the axial-vector. Because of this, three parameters are required for a description of neutron β-decay: G_F, $\lambda \equiv g_A/g_V$ (the ratio of the weak axial-vector and vector coupling

constants) and V_{ud}. Thus, considering G_F as an input parameter coming from muon decay, measurements of at least two observables are required for a determination of V_{ud}.

A value for λ can be extracted from measurements of correlation coefficients in polarized neutron β-decay. The differential rate for polarized neutrons reads [175]:

$$\frac{d\Gamma}{dE_e d\Omega_e d\Omega_\nu} = \frac{1}{(2\pi)^5}\frac{(G_F^{(0)})^2}{2}|V_{ud}|^2 p_e E_e (E_0^{(n)} - E_e)^2 \times \tag{8.56}$$
$$\times \; \xi \left\{ 1 + a\frac{\mathbf{p_e}\cdot\mathbf{p_\nu}}{E_e E_\nu} + b\frac{m_e}{E_e} + \frac{\mathbf{J}}{J}\cdot\left[A\frac{\mathbf{p_e}}{E_e} + B\frac{\mathbf{p_\nu}}{E_\nu} + D\frac{\mathbf{p_e}\times\mathbf{p_\nu}}{E_e E_\nu}\right] \right\} \;,$$

where E_e (E_ν) and $\vec{p}_e$ ($\vec{p}_\nu$) denote, respectively, the electron (neutrino) energy and momentum; $E_0^{(n)} = \Delta - (\Delta^2 - m_e^2)/(2m_n)$ (with $\Delta = m_n - m_p$) is the electron end-point energy, m_e is electron mass and $\mathbf{J}$ is the neutron polarization.

Neglecting recoil-order corrections, the overall normalization ξ and the correlation coefficients can be expressed in terms of λ as [176]

$$a = \frac{1-\lambda^2}{1+3\lambda^2}, \qquad A = -2\frac{\lambda^2+\lambda}{1+3\lambda^2}, \qquad B = 2\frac{\lambda^2-\lambda}{1+3\lambda^2},$$
$$\xi = 2(1+3\lambda^2), \quad b = 0, \qquad\qquad D = 0. \tag{8.57}$$

At present, the neutron β-asymmetry A yields the most precise result for λ.

A second observable is the neutron lifetime, τ_n, which can be written in terms of the above parameters as [138, 177, 178]

$$\frac{1}{\tau_n} = \frac{G_F^2 m_e^5}{2\pi^3}|V_{ud}|^2(1+3\lambda^2)f(1+\text{RC}). \tag{8.58}$$

Here, $f = 1.6887 \pm 0.00015$ is a phase space factor, and $(1 + \text{RC}) = 1.03886 \pm 0.00039$ denotes the total effect of all electroweak radiative corrections [138, 177]. Summarizing we have that V_{ud} can be determined from τ_n and λ according to [138, 177]

$$|V_{ud}|^2 = \frac{4908.7 \pm 1.9 \text{ s}}{\tau_n(1+3\lambda^2)}. \tag{8.59}$$

The current status of a neutron-sector result for V_{ud} is summarized in Fig. 8.2. Using the PDG recommended value of $\tau_n = 885.7 \pm 0.8$ s yields the result [129]

$$|V_{ud}| = 0.9746 \pm 0.0004_{\tau_n} \pm 0.0018_\lambda \pm 0.0002_{\text{RC}}, \tag{8.60}$$

where the subscripts denote the error sources, showing that the uncertainty in the value of λ is by far the largest contribution to the error. This value is in good agreement with that from nuclear β-decay, although with an error bar that is a factor ~ 7–8 larger. The most recent result reported for τ_n of $878.5 \pm 0.7 \pm 0.3$ s [179] disagrees by 6σ with the PDG average, and would suggest a considerably larger value, $|V_{ud}| = 0.9786 \pm 0.0004_{\tau_n} \pm 0.0018_\lambda \pm 0.0002_{\text{RC}}$.

An ongoing series of precision measurements of neutron β-decay observables aims to reduce the error on λ and resolve the lifetime discrepancy.
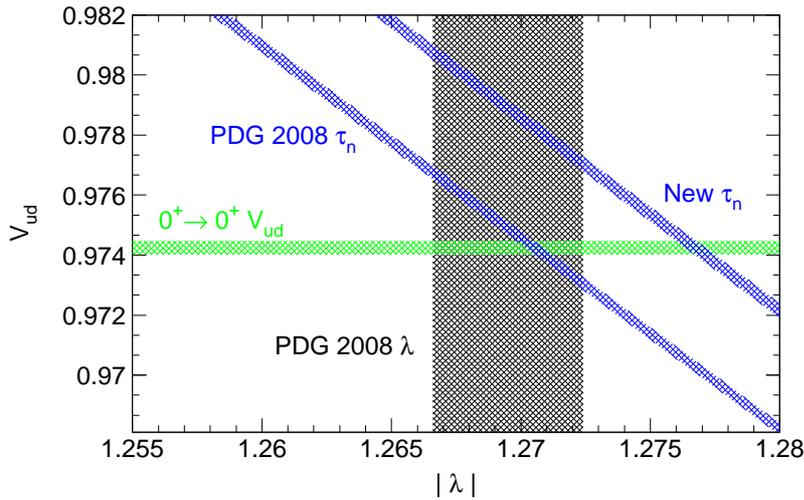
Figure 8.2: Current status of V_{ud} from neutron β-decay, showing the current PDG value of λ (vertical error band) and the constraints between V_{ud} and λ (angled error bands) coming from two values of the neutron lifetime: the PDG recommended value, and that from a recent 6σ-discrepant result [179]. The horizontal error band denotes the value of V_{ud} from 0^+ nuclear β-decays. (Figure taken from Ref. [159])

8.3.2   New physics effects on the standard extraction of V_{ud}

Once we go beyond the Standard Model and take into account the existence of new terms in the low-energy Lagrangian (8.2) we will have that the extracted value of V_{ud} using the standard procedure described above contained some new physics contamination that we want to estimate. The expression of the correlation coefficients of the beta decay in terms of the coefficients of the most general derivative-free, four-fermion interaction lagrangian describing the β decay process, consistent with locality and Lorentz invariance, are known [135, 175], and so we only have to apply these expressions to our particular Lagrangian[8]. We find:

$$C'_V = C_V \;\; = \;\; g_V \, \frac{g^2}{8M_W^2} V_{ud} \Big(1 + [v_L]_{ud} + [v_R]_{ud} \Big) \, , \tag{8.61}$$

$$C'_A = C_A \;\; = \;\; -g_A \, \frac{g^2}{8M_W^2} V_{ud} \Big(1 + [v_L]_{ud} - [v_R]_{ud} \Big) \, , \tag{8.62}$$

$$C'_S = C_S \;\; = \;\; g_S \, \frac{g^2}{8M_W^2} V_{ud} \Big([s_L]_{ud} + [s_R]_{ud} \Big) \, , \tag{8.63}$$

$$C'_T = C_T \;\; = \;\; g_T \, \frac{g^2}{8M_W^2} V_{ud} \, 4 \, [t_L]_{ud} \, . \tag{8.64}$$

C_P and C'_P can be neglected in calculations of experimental observables because, in a nonrelativistic treatment of nucleons, the pseudoscalar hadronic current $\bar{p}\gamma_5 n$

---

[8]In making this step it is important to realize that there is a minus sign of difference between our definition of γ_5 and that of Refs. [135, 175].

vanishes. To simplify the notation, we will use $[v_L]_{ud} \to v_L$, etc.

$0^+ \to 0^+$ transitions

The correlation coefficients ξ, a, b that parameterized the differential rate for unpolarized nucleus (8.45) take the following values within our framework

$$\xi = 4g_V^2(1 + 2v_L + 2v_R) , \tag{8.65}$$

$$a = 1 , \tag{8.66}$$

$$b = 2\gamma\, g_S(s_L + s_R) , \tag{8.67}$$

with $\gamma = \sqrt{1 - \alpha^2 Z}$. Taking into account the new physics effects in the extraction of G_F from the muon decay and performing the phase space integrations, the total decay rate reads:

$$
\begin{aligned}
\Gamma_{0^+ \to 0^+} &= \frac{G_\mu^2\, m_e^5}{2\pi^3}|V_{ud}|^2 \mathcal{F}\left(1 + \Delta_R^V\right)\left[1 + 2v_L - 2\tilde{v}_L + 2v_R + b\frac{I_1(x_0)}{I_0(x_0)}\right] \\
&= \left[\Gamma_{0^+ \to 0^+}\right]^{SM}\left[1 + 2v_L - 2\tilde{v}_L + 2v_R + b\frac{I_1(x_0)}{I_0(x_0)}\right] ,
\end{aligned}
\tag{8.68}
$$

where $\mathcal{F}$ and Δ_R^V were defined above (see Eq. (8.53)), and where $I_k(x_0)$ are the phase space integrals, defined by:

$$I_k(x_0) = \int_1^{x_0} dx\; x^{1-k}\,(x_0 - x)^2\,\sqrt{x^2 - 1} , \qquad x_0 = E_0/m_e . \tag{8.69}$$

Therefore we infer that the standard procedure to extract $|V_{ud}|^2$ determines the combination:

$$\left.|V_{ud}|^2\right|_{0^+ \to 0^+} = |V_{ud}|^2 \left[1 + 2v_L - 2\tilde{v}_L + 2v_R + b\frac{I_1(x_0)}{I_0(x_0)}\right] . \tag{8.70}$$

Neutron β decay

In this case the presence of the weak axial-vector coupling constant g_A (or equivalently λ) makes the expression of the correlation coefficients a bit more involved:

- Overall normalization:

$$\xi = 2\, g_V^2\left(1 + 3\lambda^2\right)\left[1 + 2v_L + 2v_R\frac{1 - 3\lambda^2}{1 + 3\lambda^2}\right] ; \tag{8.71}$$

- Beta-neutrino correlation coefficient:

$$a = \frac{1 - \lambda^2}{1 + 3\lambda^2}\left[1 + 2v_R\frac{8\lambda^2}{(1 - \lambda^2)(1 + 3\lambda^2)}\right] ; \tag{8.72}$$

- Fierz interference term:

$$b = \frac{2}{1+3\lambda^2}\left[g_S\left(s_L+s_R\right) - 12\lambda\, g_T\, t_L\right] ; \tag{8.73}$$

- Beta asymmetry parameter:

$$A = \frac{2\lambda(1-\lambda)}{1+3\lambda^2}\left[1 - 2v_R\frac{1-2\lambda-3\lambda^2}{(1-\lambda)(1+3\lambda^2)}\right] ; \tag{8.74}$$

- Neutrino asymmetry parameter:

$$\begin{aligned}
B &= \frac{2\lambda(1+\lambda)}{1+3\lambda^2}\left[1 - 2v_R\frac{1+2\lambda-3\lambda^2}{(1+\lambda)(1+3\lambda^2)}\right] \\
&+ 2\frac{m_e}{E_e}\left[g_S\left(s_L+s_R\right)\frac{\lambda}{1+3\lambda^2} - 4g_T t_L\frac{1+2\lambda}{1+3\lambda^2}\right] .
\end{aligned} \tag{8.75}$$

Expressing $G_F^{(0)}$ in terms of the Fermi constant determined in muon decay (G_μ) and performing the phase space integrations, the total decay rate reads:

$$\begin{aligned}
\frac{1}{\tau_n} &= \frac{G_\mu^2\, m_e^5}{2\pi^3}|V_{ud}|^2(1+3\lambda^2)f(1+\mathrm{RC}) \times \\
&\quad \times \left[1 + 2v_L - 2\tilde{v}_L + 2v_R\frac{1-3\lambda^2}{1+3\lambda^2} + b\frac{I_1(x_0^{(n)})}{I_0(x_0^{(n)})}\right] \\
&= \left[\frac{1}{\tau_n}\right]^{SM}\left[1 + 2v_L - 2\tilde{v}_L + 2v_R\frac{1-3\lambda^2}{1+3\lambda^2} + b\frac{I_1(x_0^{(n)})}{I_0(x_0^{(n)})}\right] ,
\end{aligned} \tag{8.76}$$

where $x_0^{(n)} = E_0/m_e$. Evaluating numerically the phase space integrals defined in (8.69) one has $I_1(x_0^{(n)})/I_0(x_0^{(n)}) = 0.652$.

So far we have considered λ as a theoretical quantity free from NP contributions (the matrix element of the axial current operator between a neutron and a proton at zero momentum transfer, calculable within Lattice QCD). But in practice, as we have explained, since current lattice QCD calculation are not accurate at the percent level, λ is usually extracted from the experimental measurement of the beta asymmetry A.

In presence of New Physics terms, the measurement of A determines λ as a function of the right-handed coupling v_R. Explicitly, we may write Eq. (8.74) as

$$A(\lambda,v_R) = A_0(\lambda)\left[1 + v_R\,\delta_A(\lambda)\right] , \qquad A_0(\lambda) = \frac{2\lambda(1-\lambda)}{1+3\lambda^2} . \tag{8.77}$$

Working to linear order in v_R, one then has:

$$\lambda = \lambda_0 - v_R A_{\exp} \frac{\delta_A(\lambda_0)}{A_0'(\lambda_0)} \ , \tag{8.78}$$

where λ_0 is determined by ignoring the NP contributions, as a solution of the equation $A_0(\lambda_0) = A_{\exp}$ (i.e. the standard procedure). This implies

$$1 + 3\lambda^2 \rightarrow (1 + 3\lambda_0^2) \left[1 - v_R \frac{6 A_{\exp} \lambda_0 \, \delta_A(\lambda_0)}{(1 + 3\lambda_0^2) \, A_0'(\lambda_0)} \right] \ . \tag{8.79}$$

Putting everything together, Eq. (8.76) tells us that the "standard" phenomenology of neutron decay does not determine $|V_{ud}|^2$ but rather the combination:

$$
\begin{aligned}
|V_{ud}|^2 \Big|_{\text{n} \rightarrow \text{pe}\bar{\nu}} = \ & |V_{ud}|^2 \left[1 + 2 v_L - 2 \tilde{v}_L \right. \\
& \left. + v_R \left(\frac{2(1 - 3\lambda_0^2)}{1 + 3\lambda_0^2} - \frac{6 A_{\exp} \lambda_0 \, \delta_A(\lambda_0)}{(1 + 3\lambda_0^2) \, A_0'(\lambda_0)} \right) + b \frac{I_1(x_0^{(n)})}{I_0(x_0^{(n)})} \right] .
\end{aligned} \tag{8.80}
$$

8.3.3 NP contributions to V_{ud} ratios

Using the previous results we find

$$\frac{|V_{ud}^{0^+ \rightarrow 0^+}|^2}{|V_{ud}^{n \rightarrow pe\bar{\nu}}|^2} = 1 + v_R \left(\frac{12\lambda_0^2}{1 + 3\lambda_0^2} + \frac{6 A_{\exp} \lambda_0 \, \delta_A(\lambda_0)}{(1 + 3\lambda_0^2) \, A_0'(\lambda_0)} \right) + b_{0^+} \frac{I_1(x_0)}{I_0(x_0)} - b_n \frac{I_1(x_0^{(n)})}{I_0(x_0^{(n)})} \ , \tag{8.81}$$

where λ_0 denotes the ratio g_A/g_V as extracted from the beta asymmetry measurement (A) ignoring possible NP terms.

8.4 Inclusive τ decay

Thanks to the very precise measurement of the hadronic spectral functions of the τ-decay (see Chapter 2) and making use of the theoretical framework explained in Chapter 3, the τ-decay has been a very rich field to test the SM and determine different parameters. In particular, the difference between the strange and non-strange spectral functions have been used to determine V_{us} with good accuracy [5]. Another very important application of these decays is the most precise determination of the strong coupling constant α_S.

So we see that it is very interesting to analyze the new physics effects on the hadronic tau decays and the possible contamination produced in the extraction of the different parameters. In this section we will explain how to address the problem and we will see the main features of the results, whereas a more complete analysis including a phenomenological study will be made in a future publication [160].

8.4.1 V_{us} determination from tau decays

As we carefully explained in Chapter 3 the inclusive character of the total τ hadronic width makes possible an accurate calculation of the ratio

$$R_\tau \equiv \frac{\Gamma[\tau^- \to \nu_\tau \text{ hadrons}\,(\gamma)]}{\Gamma[\tau^- \to \nu_\tau e^- \bar{\nu}_e(\gamma)]} = R_{\tau,nS} + R_{\tau,S}\,, \tag{8.82}$$

where $R_{\tau,nS}$ and $R_{\tau,S}$ are the Cabibbo-allowed and Cabibbo-suppressed contributions, respectively. In principle if we neglect the small SU(3)-breaking corrections from the $m_s - m_d$ quark-mass difference, we can obtain the value of $|V_{us}|$ directly from experimental measurements, without any theoretical input:

$$|V_{us}|^{\text{SU(3)}} = |V_{ud}|\,\left(\frac{R_{\tau,S}}{R_{\tau,nS}}\right)^{1/2} = 0.210 \pm 0.003\,, \tag{8.83}$$

where we have used $|V_{ud}| = 0.97425 \pm 0.00022$, from Eq. (8.55), $R_\tau = 3.640 \pm 0.010$ and the value $R_{\tau,S} = 0.1617 \pm 0.0040$ [51], which comes from the recent BaBar and Belle measurements [46]. It is worth noting that the previous value for the strange contribution to the tau width was larger ($R_{\tau,S} = 0.1686 \pm 0.0047$ [48]), what translated into a smaller value of the $|V_{us}|$ element ($|V_{us}|^{\text{SU(3)}} = 0.215 \pm 0.003$).

The shift in this determination of $|V_{us}|$ due to the small SU(3)-breaking contributions induced by the strange quark mass can be calculated through an OPE analysis of the difference [5, 6, 35, 51]

$$\delta R_\tau \equiv \frac{R_{\tau,nS}}{|V_{ud}|^2} - \frac{R_{\tau,S}}{|V_{us}|^2}\,, \tag{8.84}$$

The only non-zero contributions are proportional to the mass-squared difference $m_s^2 - m_d^2$ or to vacuum expectation values of SU(3)-breaking operators such as $\langle 0|m_s\bar{s}s - m_d\bar{d}d|0\rangle$. The dimensions of these operators are compensated by the appropriate powers of m_τ^2, what suppresses these contributions.

The value of the strange quark mass is obviously crucial for this analysis. Working with the range

$$m_s(m_\tau) = (100 \pm 10)\,\text{MeV} \quad [m_s(2\,\text{GeV}) = (96 \pm 10)\,\text{MeV}]\,, \tag{8.85}$$

which includes the most recent m_s-determinations from QCD Sum Rules and lattice [180], one gets $\delta R_{\tau,th} = 0.216 \pm 0.016$, which implies [51]

$$|V_{us}| = \left(\frac{R_{\tau,S}}{\frac{R_{\tau,nS}}{|V_{ud}|^2} - \delta R_{\tau,\text{th}}}\right)^{1/2} = 0.2165 \pm 0.0030_{\text{exp}} \pm 0.0005_{\text{th}}\,, \tag{8.86}$$

that is at 2.5σ's from the value extracted from kaon decays (8.21) (and hence from unitarity). Notice that if we use the old world average for $R_{\tau,S}$ this tension disappears $|V_{us}| = 0.2212 \pm 0.0031$. In any case we see in (8.86) that experimental errors

dominate over the theoretical ones, in contrast to the situation encountered in $K_{\ell 3}$ decays, what makes this channel very interesting.

In the near future, the full analysis of the large BaBar and Belle data samples could produce significant changes on the experimental determination of $R_{\tau,S}$, and hence on the result (8.86), although in any case the final error of the V_{us} determination from τ decay will probably remain dominated by the experimental uncertainties. A 1% precision measurement of $R_{\tau,S}$ would make the τ decay a competitive source of information about V_{us}.

In principle it is possible to perform a simultaneous determination of V_{us} and the strange quark mass through a correlated analysis of several SU(3)-breaking observables constructed with weighted moments of the hadronic distribution [5, 6]. However, the extraction of m_s suffers from theoretical uncertainties related to the convergence of the associated perturbative QCD series, what limits the present determination of m_s [5, 6].

8.4.2 The effective lagrangian

The starting point for the study of the New Physics effects in the τ-decay is our effective Lagrangian (8.2) (notice that in this case we need the h.c. part). For notational convenience we define the following leptonic and quark currents

$$
\begin{aligned}
& L_\mu \equiv \bar{\nu}_L^\ell \gamma_\mu \ell_L , && R \equiv \bar{\nu}_L^\ell \ell_R , && R_{\mu\nu} \equiv \bar{\nu}_L^\ell \sigma_{\mu\nu} \ell_R \\
& V_{ij}^\mu \equiv \bar{d}^j \gamma^\mu u^i , && A_{ij}^\mu \equiv \bar{d}^j \gamma^\mu \gamma_5 u^i , \\
& S_{ij} \equiv \bar{d}^j u^i , && P_{ij} \equiv \bar{d}^j \gamma_5 u^i , && T_{ij}^{\mu\nu} \equiv \bar{d}^j \sigma^{\mu\nu}(1 - \gamma_5) u^i .
\end{aligned}
\tag{8.87}
$$

and also the following combinations of effective couplings:

$$
\begin{aligned}
\kappa_V &= 1 + [v_L^*]_{ij} + [v_R^*]_{ij} , & (8.88) \\
\kappa_A &= 1 + [v_L^*]_{ij} - v_R^*]_{ij} , & (8.89) \\
\kappa_S &= [s_L^*]_{ij} + [s_R^*]_{ij} , & (8.90) \\
\kappa_P &= [s_L^*]_{ij} - [s_R^*]_{ij} , & (8.91) \\
\kappa_T &= [t_L^*]_{\ell\ell ij} . & (8.92)
\end{aligned}
$$

8.4.3 The inclusive decay rate

The total rate for the $\tau \to \nu_\tau e \bar{\nu}_e$ decay reads:

$$
\Gamma_{(\tau \to \nu_\tau e \bar{\nu}_e)} = \frac{G_F^2}{192\pi^3} m_\tau^5 \left[1 + \mathcal{O}\left(\frac{m_e^2}{m_\tau^2}\right)\right] .
\tag{8.93}
$$

The inclusive τ decay rate reads:

$$
\begin{aligned}
\sum_n \Gamma_{(\tau \to \nu_\tau n)} &= \frac{1}{2m_\tau} \int \frac{dp_\nu^3}{(2\pi)^3 2E_\nu} \frac{1}{2} \sum_{s,s'} \sum_n \int d\phi_n \\
&\quad \times \Big| \langle \nu_\tau n | \, \mathcal{H}_{(\ell \to \nu_\ell u_i \bar{d}_j)} \, | \tau \rangle \, \Big|^2 (2\pi)^4 \delta^4(q - p_n) \\
&= \sum_{j=d,s} \frac{G_F^2 |V_{uj}|^2}{16\pi m_\tau} \int ds \left(1 - \frac{s}{m_\tau^2} \right) \\
&\quad \times \Bigg\{ Tr\big[L_\mu L_\nu^\dagger\big] \left[|\kappa_V|^2 \, \rho_{VV}^{\mu\nu}(q) + |\kappa_A|^2 \, \rho_{AA}^{\mu\nu}(q) \right] \\
&\quad\quad + Tr\big[L_\mu R^\dagger\big] \left[2\,\mathrm{Re}(\kappa_V \kappa_S^*)\, \rho_{VS}^\mu(q) + 2\,\mathrm{Re}(\kappa_A \kappa_P^*)\, \rho_{AP}^\mu(q) \right] \\
&\quad\quad + Tr\big[L_\mu R_{\nu\rho}^\dagger\big]\, 2\mathrm{Re}(\kappa_V \kappa_T^*)\, \rho_{VT}^{\mu\nu\rho}(q) \Bigg\} \,,
\end{aligned}
\tag{8.94}
$$

where $q = p_\tau - p_\nu$ and p_n is the total momentum of the hadronic final state. The spectral functions $\rho_{AB}(q)$ were defined in Eq. (2.9). We write as an example the VV case, with its Lorentz expansion:

$$
\begin{aligned}
\rho_{ij,VV}^{\mu\nu}(q) &\equiv \int d\phi_n (2\pi)^3 \delta^4(q - p_n) \sum_n \langle 0| \, V_{ij}^\mu \, |n\rangle \, \langle n| \, V_{ij}^{\nu\dagger} \, |0\rangle \qquad (8.95) \\
&\equiv (q^\mu q^\nu - g^{\mu\nu} q^2)\rho_{ij,VV}^{(1)}(q^2) + q^\mu q^\nu \rho_{ij,VV}^{(0)}(q^2) \,.
\end{aligned}
$$

For the rest of the spectral functions the Lorentz-decomposition is the following (we omit for simplicity the flavour indices i, j)

$$
\begin{aligned}
\rho_{AA}^{\mu\nu}(q) &= \left[q^\mu q^\nu - g^{\mu\nu} q^2\right]\rho_{AA}^{(1)}(q^2) + q^\mu q^\nu \rho_{AA}^{(0)}(q^2) \,, & (8.96) \\
\rho_{VS}^\mu(q) &= q^\mu \rho_{VS}(q^2) \,, & (8.97) \\
\rho_{AP}^\mu(q) &= q^\mu \rho_{AP}(q^2) \,, & (8.98) \\
\rho_{VT}^{\mu\nu\rho}(q) &= i\left[q^\nu g^{\mu\rho} - q^\rho g^{\mu\nu}\right]\rho_{VT}(q^2) \,, & (8.99)
\end{aligned}
$$

where the factor i in the last line was extracted in order to have a real spectral function $\rho_{VT}(q^2)$, as can be seen explicitly in the work of Ref. [13].

Making use of these expressions and normalizing to the τ decay rate we get[9]:

$$
R_\tau = \frac{\sum_n \Gamma_{(\tau \to \nu_\tau n)}}{\Gamma_{(\tau \to \nu_\tau e \bar{\nu}_e)}} \;\; = \;\; 12\pi^2 |V_{ud}|^2 \int \frac{ds}{m_\tau^2} \left(1 - \frac{s}{m_\tau^2}\right)^2 \times
$$

$$
\times \left\{ |\kappa_V|^2 \left[\left(1 + \frac{2s}{m_\tau^2}\right) \rho_{VV}^{(1)}(s) + \rho_{VV}^{(0)}(s) \right] \right.
$$

$$
+ |\kappa_A|^2 \left[\left(1 + \frac{2s}{m_\tau^2}\right) \rho_{AA}^{(1)}(s) + \rho_{AA}^{(0)}(s) \right]
$$

$$
+ 2\,\mathrm{Re}(\kappa_V \kappa_S^*)\, \frac{\rho_{VS}(s)}{m_\tau} \;+\; 2\,\mathrm{Re}(\kappa_A \kappa_P^*)\, \frac{\rho_{AP}(s)}{m_\tau}
$$

$$
\left. + 6 \times 2\,\mathrm{Re}(\kappa_V \kappa_T^*)\, \frac{\rho_{VT}(s)}{m_\tau} \right\} \times \left[1 - 2\tilde{v}_L\right] . \quad (8.100)
$$

As we know these spectral functions are equal to the imaginary part of the associated correlators, applying to them the same Lorentz-decomposition. For example, in the VV-case we have

$$
\Pi_{ij,VV}^{\mu\nu}(q) \;\; \equiv \;\; i \int d^4x\, e^{iqx} \langle 0 | T \left\{ V_{ij}^\mu(x) V_{ij}^{\nu\dagger}(0) \right\} | 0 \rangle
$$

$$
= \;\; \left[(q^\mu q^\nu - g^{\mu\nu} q^2) \Pi_{ij,VV}^{(1)}(q^2) + q^\mu q^\nu \Pi_{ij,VV}^{(0)}(q^2) \right] . \quad (8.101)
$$

As we have explained in previous chapters, this formal result for R_τ is not very useful in this form, since we do not know how to calculate from pure QCD the spectral functions for small value of q^2 (we need them here in the range $0 - 3.15 \text{ GeV}^2$), where perturbative techniques are not valid. But making use of the QCD Sum Rules framework, we can apply Cauchy's theorem and rewrite the expression in terms of contour integrals of the associated correlators:

$$
R_\tau \;\; = \;\; 6\pi i |V_{ud}|^2 \oint_{|s|=m_\tau^2} \frac{ds}{m_\tau^2} \left(1 - \frac{s}{m_\tau^2}\right)^2 \times
$$

$$
\times \left\{ |\kappa_V|^2 \left[\left(1 + \frac{2s}{m_\tau^2}\right) \Pi_{VV}^{(1)}(s) + \Pi_{VV}^{(0)}(s) \right] \right.
$$

$$
+ |\kappa_A|^2 \left[\left(1 + \frac{2s}{m_\tau^2}\right) \Pi_{AA}^{(1)}(s) + \Pi_{AA}^{(0)}(s) \right]
$$

$$
+ 2\,\mathrm{Re}(\kappa_V \kappa_S^*)\, \frac{\Pi_{VS}(s)}{m_\tau} \;+\; 2\,\mathrm{Re}(\kappa_A \kappa_P^*)\, \frac{\Pi_{AP}(s)}{m_\tau}
$$

$$
\left. + 6 \times 2\,\mathrm{Re}(\kappa_V \kappa_T^*)\, \frac{\Pi_{VT}(s)}{m_\tau} \right\} \times \left[1 - 2\tilde{v}_L\right] , \quad (8.102)
$$

---

[9]In order to save space with indices, we quote only the non-strange result, proportional to $|V_{ud}|^2$.

where the DV has been neglected. The value of the different correlators can be calculated for $|s| = m_\tau^2$ using the Operator Product Expansion. The results for the (0) and (1) components of the vector and axial-vector correlators are very well known and can be found in Ref. [4]. The VS and AP correlators can be calculated from the (0)-component of the VV and AA correlators using the Ward-identities following from chiral symmetry and the QCD equations of motion

$$
\begin{aligned}
q^2 \Pi_{Vij}^{(0)}(q^2) &= (m_i - m_j) \, \Pi_{VSij}(q^2) \, , \\
q^2 \Pi_{Aij}^{(0)}(q^2) &= (m_i + m_j) \, \Pi_{APij}(q^2) \, .
\end{aligned}
\tag{8.103}
$$

whereas at last the VT correlator to leading non-trivial order in the $SU(3)$ breaking (quark masses) can be found in Ref. [181].

Chapter 9

Conclusions

If I was young, I'd flee this town,
I'd bury my dreams underground;
as did I, we drink to die, we drink tonight...
Beirut

In this work we have addressed two different aspects of the theoretical challenge of discovering the new theory that rules the physics at high energies. First, we have dealt with the non-perturbative character of the strong interactions, analyzing critically and applying the QCD Sum Rules, a useful tool in the search of precise predictions for the different observables in the Standard Model. Secondly, we have studied the impact of the New Physics on (semi)leptonic low-energy processes, where the experimental and theoretical accuracy is so high that very strong bounds can be obtained. We develop now our conclusions associated with these two aspects.

9.1   QCD Sum Rules

In Chapter 2 we have introduced the spectral functions and we have explained how they can be measured in the hadronic τ decays. These observables represent the experimental input of the subsequent analyses, and they encode very valuable perturbative and non-perturbative information, as we have shown later.

In Chapter 3, we have performed a careful derivation from very general principles like analyticity and unitarity of the expression of a generic QCD Sum Rule, a very useful method that connects hadrons and quarks. Its different elements have been introduced and thoroughly explained: (i) the Wilson operator-product expansion that allows a QCD calculation of the correlator in the deep euclidean region, (ii) Chiral Perturbation Theory that gives us the value of the correlator near the origin, (iii) the spectral functions that are directly related with the experiment, and (iv) the often disregarded duality violation.

In the subsequent phenomenological analysis, we have focused on the Finite Energy Sum Rules and the non-strange left-right two-point correlation function $\Pi_{LR}(s)$.

This correlator is particularly well suited for the study of non-perturbative QCD for different reasons:

- The perturbative contribution to $\Pi_{LR}(s)$ vanishes in the chiral limit;

- There is valuable theoretical information, like the Weinberg Sum Rules;

- There is precise available data for its associated spectral function $\rho_{LR}(s)$ coming from the hadronic τ decays [3];

- And last but not least, the different moments of $\rho_{LR}(s)$ provide hadronic parameters of high phenomenological relevance.

First, in Chapter 4, we have applied this theoretical framework to determine very accurately, from the most recent hadronic τ-decay data, the chiral low-energy constants $L_{10}^r(M_\rho)$, $\bar{l}_5$, $C_{87}^r(M_\rho)$ and $c_{50}^r(M_\rho)$, working both at $\mathcal{O}(p^4)$ and $\mathcal{O}(p^6)$ in the chiral expansion. Taking into account the results of Refs. [72, 73] we have also extracted the values of $L_9^r(M_\rho)$ and $\bar{l}_6$. The results are summarized in Tables 9.1 and 9.2 and they include a careful analysis of the theoretical and experimental uncertainties. Our present ignorance on some LECs dominates the final uncertainty of the $L_{10}^r(M_\rho)$ determination at $\mathcal{O}(p^6)$, whereas in the $C_{87}^r(M_\rho)$ case the error is equally shared by the experimental and LECs errors. The different analytical approaches and the various lattice calculations agree very well with our precise phenomenological values, showing that the theoretical methods used in QCD are in good shape.

χPT$_2$	χPT$_3$
$\bar{l}_5 = 13.30 \pm 0.11$	$L_{10}^r(M_\rho) = -(5.22 \pm 0.06) \cdot 10^{-3}$
$\bar{l}_6 = 15.80 \pm 0.29$	$L_9^r(M_\rho) = (6.54 \pm 0.15) \cdot 10^{-3}$

Table 9.1: Results for the χPT LECs obtained at $\mathcal{O}(p^4)$.

χPT$_2$	χPT$_3$
$\bar{l}_5 = 12.24 \pm 0.21$	$L_{10}^r(M_\rho) = -(4.06 \pm 0.39) \cdot 10^{-3}$
$\bar{l}_6 = 15.22 \pm 0.39$	$L_9^r(M_\rho) = (5.50 \pm 0.40) \cdot 10^{-3}$
$c_{50}^r = (4.95 \pm 0.18) \cdot 10^{-3} \text{ GeV}^{-2}$	$C_{87}^r(M_\rho) = (4.89 \pm 0.18) \cdot 10^{-3} \text{ GeV}^{-2}$

Table 9.2: Results for the χPT LECs obtained at $\mathcal{O}(p^6)$.

In Chapter 5 we have performed a very careful study of the usually disregarded quark-hadron duality violation, focusing on the FESRs generated by the weights $w(s) = 1/s^2, 1/s, s^2$ and s^3. The need of a determination of the DV effects is the result of the advent of precise data and refined perturbative calculations, that make relevant the contributions that before could be neglected.

Violations of quark-hadron duality are difficult to estimate and are originated in the uncertainties associated with the use of the OPE to approximate the exact physical correlator. Using analyticity, the size of DV can be related with the following

integral of the hadronic spectral function

$$\mathrm{DV}[w(s), s_0] \;=\; \int_{s_0}^{\infty} \mathrm{d}s \, w(s) \, \rho(s) \;, \tag{9.1}$$

that has been the starting point of our analysis.

We have assumed a generic, but theoretically motivated, behavior of the spectral function at high energies, where data are not available, with four free parameters. This parameterization allows us to study how much freedom in $\rho(s)$ could be tolerated, beyond the requirement that all known QCD constraints are satisfied. We have performed a numerical scanning over the four-dimensional parameter space, generating a large number of "acceptable" spectral functions that satisfy all conditions, and we have used them to extract the wanted hadronic parameters through a careful statistical analysis. The dispersion of the numerical results provides then a good quantitative assessment of the actual DV uncertainties.

This machinery allows to address certain questions about the DV so far inaccessible, like the convenience of the pinched weights and how to estimate the size of the still present DV. We have found that it is worthwhile to use these weights and we have determined four hadronic parameters of special interest: C_{87}^{eff}, L_{10}^{eff}, $\mathcal{O}_6$ and $\mathcal{O}_8$

$$C_{87}^{eff} \;=\; (8.17 \pm 0.12) \cdot 10^{-3} \; \mathrm{GeV}^{-2}, \tag{9.2}$$
$$L_{10}^{eff} \;=\; (-6.44 \pm 0.05) \cdot 10^{-3} \;, \tag{9.3}$$
$$\mathcal{O}_6 \;=\; \left(-4.3^{+0.9}_{-0.7}\right) \cdot 10^{-3} \; \mathrm{GeV}^6 \;, \tag{9.4}$$
$$\mathcal{O}_8 \;=\; \left(-7.2^{+4.2}_{-5.3}\right) \cdot 10^{-3} \; \mathrm{GeV}^8 \;. \tag{9.5}$$

From the first two parameters one can extract the values of the χPT couplings $C_{87}^{r}(M_\rho)$ and $L_{10}^{r}(M_\rho)$, and the results obtained with this method are in perfect agreement with those presented in Chapter 4. The vacuum condensate $\mathcal{O}_6$ is an important input for the calculation of the CP-violating kaon parameter ε'_K.

There is a small tension among the different determinations of $\mathcal{O}_6$ available in the literature, and the discrepancy is higher for the condensate $\mathcal{O}_8$. We conclude that some of the previous determinations of $\mathcal{O}_{6,8}$ underestimated the DV contribution, what was generating the different results. Our values show that the analyses based on the use of pinched-weight FESRs have assigned a reasonable uncertainty for the lowest dimensional condensates $\mathcal{O}_{6,8}$ but have underestimated the error in the determination of higher dimensional condensates.

Our method indicates that the current experimental values for the $V - A$ spectral function in the region between $s \sim 2 \; \mathrm{GeV}^2$ and $s \sim 3 \; \mathrm{GeV}^2$ are somehow affected by a systematic error that shifts the points towards higher values. It is worth noting that this result is also suggested by the work of Ref. [104]. A significant improvement in the experimental knowledge of the spectral functions in this intermediate region is expected with the future high-statistics τ-decay data samples. It will be very interesting to check the presence of this systematic error and validate our approach.

9.2 (Semi)leptonic decays beyond the SM

From the most general effective Lagrangian with the SM particle content that respects the baryon and lepton number symmetries [116, 117], we have identified a minimal set of twenty-four weak scale effective operators describing corrections beyond the SM to precision electroweak measurements and leptonic and semileptonic decays. In terms of these new physics corrections at the TeV scale, we have derived the low-energy effective Lagrangians describing muon and beta decays, specifying both the most general flavor structure of the operators as well as the form allowed within Minimal Flavor Violation.

We have performed the phenomenological analysis assuming nearly flavor blind ($U(3)^5$ invariant) new physics interactions. In this framework flavor breaking is suppressed by a symmetry principle, such as the Minimal Flavor Violation hypothesis, or by the hierarchy $\Lambda_{\text{flavor}} \gg$ TeV. We have shown that in this limit, the extraction of V_{ud} and V_{us} from any channel should give the same result and the only significant probe of physics beyond the SM involves the quantity $\Delta_{\text{CKM}} \equiv |V_{ud}|^2 + |V_{us}|^2 + |V_{ub}|^2 - 1$, that parameterizes the deviation from CKM-unitarity or equivalently from quark-lepton universality. We have shown that in the $U(3)^5$ limit Δ_{CKM} receives contributions from four short distance operators, namely

$$O_{ll}^{(3)} = \frac{1}{2}(\bar{l}\gamma^\mu \sigma^a l)(\bar{l}\gamma_\mu \sigma^a l) \ , \tag{9.6}$$

$$O_{lq}^{(3)} = (\bar{l}\gamma^\mu \sigma^a l)(\bar{q}\gamma_\mu \sigma^a q) \ , \tag{9.7}$$

$$O_{\varphi l}^{(3)} = i(h^\dagger D^\mu \sigma^a \varphi)(\bar{l}\gamma_\mu \sigma^a l) + \text{h.c.} \ , \tag{9.8}$$

$$O_{\varphi q}^{(3)} = i(\varphi^\dagger D^\mu \sigma^a \varphi)(\bar{q}\gamma_\mu \sigma^a q) + \text{h.c.} \ , \tag{9.9}$$

which also shift SM predictions in other precision observables. More specifically we have found

$$\Delta_{\text{CKM}} = 4 \left(\hat{\alpha}_{ll}^{(3)} - \hat{\alpha}_{lq}^{(3)} - \hat{\alpha}_{\varphi l}^{(3)} + \hat{\alpha}_{\varphi q}^{(3)} \right) \ , \tag{9.10}$$

that can be used to work out the constraints imposed by Cabibbo universality on any weakly coupled extension of the SM. We have focused on the model-independent interplay of Δ_{CKM} with other precision measurements. The main conclusion of our analysis is that the direct constraint [159]

$$\Delta_{\text{CKM}} = (-1 \pm 6) \times 10^{-4} \ , \tag{9.11}$$

bounds the effective scale of all four operators to be $\Lambda > 11$ TeV (90 % C.L.). For the operators $O_{ll}^{(3)}, O_{\varphi l}^{(3)}, O_{\varphi q}^{(3)}$, this is at the same level as the constraints coming from Z-pole measurements , whereas for the four-fermion operator $O_{lq}^{(3)}$ it improves existing bounds from LEP2 by almost an order of magnitude.

This result can be restated as follows: should the central values of V_{ud} and V_{us} move from the current values [132], precision electroweak data would leave room for sizable deviations from quark-lepton universality (roughly one order of magnitude

above the current direct constraint). In a global analysis, the burden of driving a deviation from CKM unitarity could be shared by the four operators, but in a single operator analysis, essentially only the four-fermion operator $O_{lq}^{(3)}$ could be responsible for $\Delta_{\mathrm{CKM}} \neq 0$, as the others are tightly bound from Z-pole observables.

In this way our conclusions imply that the study of semileptonic processes and Cabibbo universality tests provide constraints on new physics that currently cannot be obtained from other electroweak precision tests and collider measurements.

We have also explored the scenario where the flavor structure is not flavor blind. In this case the new physics corrections received by the V_{ij} elements of the CKM matrix are channel dependent and the phenomenology is very rich. We have studied how the SM results are modified in semileptonic kaon and pion decays, muon and tau physics and nuclear processes, and which bounds can be obtained by comparing the values of V_{ud} (V_{us}) extracted from different channels. These constraints probe those $U(3)^5$-breaking structures to which FCNC and other precision measurements are quite insensitive.

It is worth stressing that there have already been some contradictory results in the recent past between values obtained from different channels. It is important to know if these tensions, at the precision level that we are nowadays, can be due to New Physics effects, or if on the contrary this possibility is ruled out by other precision measurements and the discrepancy comes probably from the underestimation of errors or just statistical fluctuations.

The study of these analyses of low-energy processes and their relevance in the search of New Physics is very opportune, since in the next years several experiments will achieve unprecedented precision and the theoretical predictions are also expected to improve. So we expect New Physics effects to appear in the near future in these low-energy observables, what makes necessary the theoretical analyses of the possible discrepancies with the SM.

Conclusiones

En este trabajo hemos abordado dos aspectos diferentes del reto teórico que supone descubrir la nueva teoría que gobierna la Naturaleza a energías altas. Primero, hemos estudiado el carácter no-perturbativo de las interacciones fuertes, utilizando y analizando con mirada crítica las Reglas de Suma de QCD, una herramienta muy útil en la búsqueda de predicciones precisas para los distintos observables en el Modelo Estándar. En segundo lugar hemos estudiado el impacto de Nueva Física en los procesos leptónicos y semileptónicos de energías bajas, donde la precisión experimental y teórica es tan alta que pueden obtenerse cotas muy fuertes. A continuación desarrollamos nuestras conclusiones en relación con estos dos puntos.

Reglas de Suma de QCD

En el Capítulo 2 hemos introducido las funciones espectrales, explicando cómo pueden medirse en las desintegraciones hadrónicas del leptón τ. Estos observables representan el input experimental de los subsiguientes análisis, y contienen información de gran valor, tanto perturbativa como no-perturbativa, como hemos demostrado posteriormente.

En el Capítulo 3, hemos realizado una cuidadosa derivación desde principios muy generales, como analiticidad y unitariedad, de una Regla de Suma genérica, un método muy útil que conecta hadrones y quarks. Sus diferentes elementos han sido introducidos y minuciosamente explicados: (i) la expansión de Wilson de un producto de operadores que permite calcular desde QCD el correlador en la región lejana euclídea, (ii) la Teoría de Perturbaciones Quirales que nos da el valor del correlador en las cercanías del origen, (iii) las funciones espectrales que están directamente relacionadas con el experimento, y (iv) la frecuentemente ignorada violación de la dualidad quark-hadrón.

En el análisis fenomenológico posterior, nos hemos centrado en las Reglas de Suma de Energía Finita y la función de correlación de dos puntos V-A sin extrañeza $\Pi_{LR}(s)$. Este correlador es particularmente apropiado para el análisis de los efectos no-perturbativos de QCD por diversas razones:

- La contribución perturbativa a $\Pi_{LR}(s)$ es nula en el límite quiral;

- Disponemos de valiosa información teórica, como las reglas de suma de Weinberg;

- Existen medidas experimentales de gran precisión de la correspondiente función espectral $\rho_{LR}(s)$, obtenidas de las desintegraciones hadrónicas del leptón τ [3];

- Y por último, aunque no por ello menos importante, se da la circunstancia de que los diferentes momentos de $\rho_{LR}(s)$ proporcionan parámetros hadrónicos de gran relevancia fenomenológica.

En primer lugar, en el Capítulo 4, hemos hecho uso de este marco teórico para determinar con precisión, a partir de los datos más recientes de las desintegraciones del τ, las constantes quirales de energías bajas $L_{10}^r(M_\rho)$, $\bar{l}_5$, $C_{87}^r(M_\rho)$ y $c_{50}^r(M_\rho)$, trabajando tanto a orden $\mathcal{O}(p^4)$ como $\mathcal{O}(p^6)$ en la expansión quiral. Teniendo en cuenta los resultados de las referencias [72, 73] hemos extraído también los valores de $L_9^r(M_\rho)$ y $\bar{l}_6$. Los resultados, que aparecen resumidos en las Tablas 9.3 y 9.4, incluyen un cuidadoso análisis de las incertidumbres teóricas y experimentales. Nuestra ignorancia actual en algunas LECs domina el error final en la determinación de $L_{10}^r(M_\rho)$ a orden p^6, mientras que en el caso de $C_{87}^r(M_\rho)$ el error está compartido equitativamente por la contribución experimental y la de las LECs. Los diferentes métodos analíticos y los distintos cálculos en el retículo están en buen acuerdo con nuestros precisos valores fenomenológicos, certificando que los métodos teóricos usados en QCD están en buena forma.

χPT_2	χPT_3
$\bar{l}_5 = 13.30 \pm 0.11$	$L_{10}^r(M_\rho) = -(5.22 \pm 0.06) \cdot 10^{-3}$
$\bar{l}_6 = 15.80 \pm 0.29$	$L_9^r(M_\rho) = (6.54 \pm 0.15) \cdot 10^{-3}$

Table 9.3: Resultados para las constantes de energías bajas de χPT obtenidas a orden p^4.

χPT_2	χPT_3
$\bar{l}_5 = 12.24 \pm 0.21$	$L_{10}^r(M_\rho) = -(4.06 \pm 0.39) \cdot 10^{-3}$
$\bar{l}_6 = 15.22 \pm 0.39$	$L_9^r(M_\rho) = (5.50 \pm 0.40) \cdot 10^{-3}$
$c_{50}^r = (4.95 \pm 0.18) \cdot 10^{-3} \text{ GeV}^{-2}$	$C_{87}^r(M_\rho) = (4.89 \pm 0.18) \cdot 10^{-3} \text{ GeV}^{-2}$

Table 9.4: Resultados para las constantes de energías bajas de χPT obtenidas a orden p^6.

En el Capítulo 5 hemos llevado a cabo un estudio muy cuidadoso de la violación de la dualidad quark-hadrón, tantas veces ignorada, centrándonos en las Reglas de Suma de Energía Finita generadas por los pesos $w(s) = 1/s^2, 1/s, s^2$ y s^3. La necesidad de una determinación de los efectos de DV surge como resultado de la llegada de datos de precisión y de refinados cálculos perturbativos, que convierten en relevantes las contribuciones que antes podían ser ignoradas.

Las violaciones de la dualidad quark-hadrón son difíciles de estimar y están originadas en las incertidumbres asociadas con el uso de la OPE para aproximar

el valor del correlador. Haciendo uso de las propiedades analíticas de la función de correlación, la DV puede relacionarse con la siguiente integral de la función espectral hadrónica

$$\mathrm{DV}[w(s), s_0] \;=\; \int_{s_0}^{\infty} \mathrm{d}s \; w(s) \, \rho(s) \;, \tag{9.12}$$

que ha sido el punto de partida de nuestro análisis.

Hemos trabajado con un determinado modelo, motivado teóricamente y con cuatro parámetros libres, para el comportamiento de la función espectral a energías intermedias, donde no tenemos datos disponibles ni predicciones teóricas. Esta parametrización nos permite estudiar cuál es la libertad en el comportamiento de $\rho(s)$, más allá del requisito de que todas las restricciones conocidas de QCD sean satisfechas. Hemos escaneado numéricamente el espacio de parámetros 4-dimensional, generando un gran número de funciones espectrales aceptables que satisfacen todas las condiciones, y las hemos usado para extraer los parámetros hadrónicos deseados por medio de un cuidadoso análisis estadístico. La dispersión de los resultados numéricos representa un método conveniente para la evaluación cuantitativa de las incertidumbres asociadas a la DV.

Esta maquinaria nos permite abordar ciertas cuestiones sobre la DV que hasta ahora eran inaccesibles, como la conveniencia de los pesos conocidos como *pinched weights* o cómo estimar el valor de la DV en ese caso. Hemos concluido que el uso de estos pesos es efectivamente beneficioso y hemos determinado cuatro parámetros hadrónicos de especial interés:

$$C_{87}^{eff} \;=\; (8.17 \pm 0.12) \cdot 10^{-3} \; \mathrm{GeV}^{-2}, \tag{9.13}$$
$$L_{10}^{eff} \;=\; (-6.44 \pm 0.05) \cdot 10^{-3} \;, \tag{9.14}$$
$$\mathcal{O}_6 \;=\; \left(-4.3_{-0.7}^{+0.9}\right) \cdot 10^{-3} \; \mathrm{GeV}^6 \;, \tag{9.15}$$
$$\mathcal{O}_8 \;=\; \left(-7.2_{-5.3}^{+4.2}\right) \cdot 10^{-3} \; \mathrm{GeV}^8 \;. \tag{9.16}$$

De los dos primeros parámetros es posible extraer los valores de los acoplamientos quirales $C_{87}^{r}(M_\rho)$ y $L_{10}^{r}(M_\rho)$, y los resultados obtenidos con este método están en perfecto acuerdo con los presentados en el Capítulo 4. El condensado en el vacío $\mathcal{O}_6$ es un importante input para el cálculo del parámetro ε'_K, que mide la violación directa de la simetría CP en kaones.

Existe una cierta tensión entre las diferentes determinaciones de $\mathcal{O}_6$ disponibles en la literatura, y la discrepancia es aún mayor para el condensado $\mathcal{O}_8$. De nuestro trabajo se concluye que muchas de las determinaciones previas de $\mathcal{O}_{6,8}$ subestiman la contribución de DV, lo que explica los diferentes valores obtenidos. Nuestros resultados muestran que los análisis previos basados en el uso de Reglas de Suma de Energía Finita con *pinched weights* han asignado una incertidumbre razonable para los condensados de dimensiones más bajas $\mathcal{O}_{6,8}$ pero que han subestimado el error en la determinación de los condensados de dimensión más alta.

Nuestro método indica que las medidas experimentales actuales para la función espectral $V - A$ en la región entre $s \sim 2 \; \mathrm{GeV}^2$ y $s \sim 3 \; \mathrm{GeV}^2$ (dominadas por la determinación de ALEPH [3]) están de alguna forma afectadas por un error sistemático

que mueve los puntos hacia valores mayores. Es interesante destacar que el trabajo de la Ref. [104] sugiere también la presencia de este efecto. Podemos esperar una mejora significativa en el conocimiento experimental de estas funciones espectrales en esta región intermedia gracias a la llegada en el futuro cercano de nuevos datos sobre las desintegraciones del leptón τ con una estadística mejorada. Será muy interesante poder comprobar la presencia de este error sistemático y validar nuestro método.

Desintegraciones (semi)leptónicas más allá del SM

Partiendo del Lagrangiano efectivo más general con el contenido de partículas del Modelo Estándar y compatible con la conservación del número leptónico y bariónico [116,117], hemos identificado un conjunto mínimo de veinticuatro operadores efectivos a la escala electrodébil que describen las correcciones debidas a la Nueva Física sobre las medidas de precisión electrodébiles y las desintegraciones leptónicas y semileptónicas. En términos de estas correcciones asociadas a la física del tera-electronvoltio (TeV), hemos derivado el Lagrangiano efectivo de energías bajas que gobierna la desintegración del muón y de los quarks ligeros, especificando tanto la estructura de sabor más general de los operadores como la forma permitida en el contexto de Violación Mínima de Sabor.

Hemos llevado a cabo un análisis fenomenológico, suponiendo unas interacciones de Nueva Física prácticamente independientes de sabor (invariantes bajo la simetría $U(3)^5$). En este caso, la rotura de esta simetría de sabor está suprimida por un principio de simetría, como la Violación Mínima de Sabor, o por la jerarquía $\Lambda_{\text{flavor}} \gg$ TeV. Hemos demostrado que en este límite la extracción de V_{ud} y V_{us} desde cualquier canal da el mismo resultado y que el único observable sensible a la física más allá del Modelo Estándar viene dado por

$$\Delta_{\text{CKM}} \equiv |V_{ud}|^2 + |V_{us}|^2 + |V_{ub}|^2 - 1 \ , \tag{9.17}$$

que parametriza la desviación de la unitariedad en la matriz CKM, o equivalentemente de la universalidad entre quarks y leptones. Hemos mostrado cómo en el límite en el que el Lagrangiano respeta la simetría de sabor $U(3)^5$, esta cantidad Δ_{CKM} recibe contribuciones de los siguientes cuatro operadores de corta distancia

$$O_{ll}^{(3)} = \frac{1}{2}(\bar{l}\gamma^\mu\sigma^a l)(\bar{l}\gamma_\mu\sigma^a l) \ , \tag{9.18}$$

$$O_{lq}^{(3)} = (\bar{l}\gamma^\mu\sigma^a l)(\bar{q}\gamma_\mu\sigma^a q) \ , \tag{9.19}$$

$$O_{\varphi l}^{(3)} = i(h^\dagger D^\mu\sigma^a\varphi)(\bar{l}\gamma_\mu\sigma^a l) + \text{h.c.} \ , \tag{9.20}$$

$$O_{\varphi q}^{(3)} = i(\varphi^\dagger D^\mu\sigma^a\varphi)(\bar{q}\gamma_\mu\sigma^a q) + \text{h.c.} \ , \tag{9.21}$$

que también modifican las predicciones del Modelo Estándar en otros observables de precisión. Más concretamente hemos encontrado el siguiente resultado

$$\Delta_{\text{CKM}} = 4\left(\hat{\alpha}_{ll}^{(3)} - \hat{\alpha}_{lq}^{(3)} - \hat{\alpha}_{\varphi l}^{(3)} + \hat{\alpha}_{\varphi q}^{(3)}\right) \ , \tag{9.22}$$

que puede usarse para extraer las cotas impuestas por la universalidad de Cabibbo sobre cualquier extensión débilmente acoplada del Modelo Estándar. Sin embargo, en este trabajo hemos optado por un análisis independiente del modelo y nos hemos centrado en estudio de la sinergia de Δ_{CKM} con otros observables de precisión. La principal conclusión de nuestro análisis es que la medida directa [159]

$$\Delta_{\text{CKM}} = (-1 \pm 6) \times 10^{-4} \, , \tag{9.23}$$

pone un límite inferior la escala efectiva Λ_i de los cuatro operadores igual a 11 TeV (con un intervalo de confianza del 90%). Para los operadores $O_{ll}^{(3)}, O_{\varphi l}^{(3)}, O_{\varphi q}^{(3)}$, esta cota está al mismo nivel que las que se derivan de las medidas en el polo del Z (LEP1), mientras que para el operador de dos quarks y dos leptones $O_{lq}^{(3)}$ esta cota mejora casi en un orden de magnitud el límite existente, que se obtenía básicamente de LEP2.

Este resultado puede reformularse de la siguiente manera: en el caso en que los valores centrales de los elementos V_{ud} y V_{us} se movieran de sus valores actuales [132] (como ha sido sugerido en el pasado reciente por algunas determinaciones), no se tendría ninguna contradicción con las medidas de precisión electrodébiles, ya que éstas dejan lugar para una considerable desviación de universalidad quark-leptón (aproximadamente un orden de magnitud sobre el actual límite directo). En un análisis global, el peso de esta desviación de unitariedad podría ser distribuido entre los cuatro operadores, mientras que en el caso en el que sólo un operador está presente sólo el operador de cuatro fermiones $O_{lq}^{(3)}$ podría ser responsable de $\Delta_{\text{CKM}} \neq 0$, ya que los otros tres están fuertemente acotados por las medidas en el polo del Z.

De esta forma, nuestras conclusiones implican que el estudio de procesos semileptónicos y de los test de la universalidad de Cabibbo generan límites sobre la Nueva Física que no pueden ser obtenidos actualmente por otros test de precisión electrodébiles ni por medidas realizadas en potentes aceleradores, como LEP o Tevatrón.

También hemos explorado el escenario donde la estructura de los operadores no es independiente del sabor. En este caso las correcciones debidas a la Nueva Física que reciben los elementos V_{ij} de la matriz CKM dependen fuertemente del canal y la fenomenología es muy rica. Hemos estudiado la forma en que los resultados del Modelo Estándar se ven modificados en las desintegraciones semileptónicas de kaones y piones, en la física del muón y el tau y en los procesos nucleares, y qué cotas pueden obtenerse comparando los valores de V_{ud} (V_{us}) extraídos de diferentes canales. Estos límites exploran las estructuras que rompen la simetría $U(3)^5$, a las que las medidas de FCNC y otras medidas de precisión son esencialmente insensibles.

Cabe destacar que en los últimos años ha habido algunos resultados contradictorios entre los valores obtenidos usando distintos canales. Es importante saber si estas tensiones, al nivel de precisión que nos encontramos hoy en día, pueden ser debidas a efectos de Nueva Física o si por el contrario esta posibilidad está descartada por otras medidas electrodébiles o de colisionadores y por tanto la discrepancia viene probablemente de la subestimación de errores o de simples fluctuaciones estadísticas.

Estos análisis de procesos de energías bajas y su relevancia en la búsqueda de Nueva Física es muy pertinente, ya que en los próximos años diversos experimentos

alcanzarán precisiones sin precedentes, a lo que se sumará una considerable mejora en las predicciones teóricas gracias a los avances en *lattice QCD* y en los enfoques analíticos. Es por lo tanto de esperar que los efectos de Nueva Física sean detectables en el futuro cercano en estos experimentos de energías bajas, lo que hace necesario este análisis teórico de las posibles discrepancias con el Modelo Estándar.

Appendix A

Demonstration of dispersion relations

It is interesting to notice that in the Standard Model, given its $(V\text{-}A) \otimes (V\text{-}A)$ structure, we will find only the VV and AA correlators in the calculation of observables. Due to this, the usual derivation of the dispersion relations [8, 11] assumes that the two currents of the correlator coincide, i.e. $A(x) = B(x)$. But once we go beyond the SM, correlators with two different currents appear in the calculation of observables, and therefore we will make the demonstration for the general case when the two currents $A(x)$ and $B(x)$ are different and not necessary hermitian. We will follow the scheme of the proof given in Ref. [8], but extending it to this more general case.

From the definition of the two-point correlation function of two scalar operators $A(x)$ and $B(x)$ (the generalization to vector and tensor cases is straightforward) and inserting a complete set of states $\sum_\Gamma |\Gamma\rangle\langle\Gamma|$ we have

$$
\begin{aligned}
\Pi_{AB}(q) \;\equiv\;\; & i \int d^4x \, e^{iq\cdot x} \, \langle 0|T[A(x)B(0)^\dagger]|0\rangle && \text{(A.1)} \\[2mm]
\equiv\;\; & i \int d^4x \, e^{iq\cdot x} \, \langle 0|\theta(x^0)A(x)B(0)^\dagger + \theta(-x^0)B(0)^\dagger A(x)|0\rangle && \text{(A.2)} \\[2mm]
=\;\; & i \int d^4x \, e^{iq\cdot x} \sum_\Gamma \big(\langle 0|\theta(x^0)A(x)|\Gamma\rangle\langle\Gamma|B(0)^\dagger|0\rangle \\
& \hspace{3.5cm} + \langle 0|\theta(-x^0)B(0)^\dagger|\Gamma\rangle\langle\Gamma|A(x)|0\rangle \big) && \text{(A.3)} \\[2mm]
=\;\; & i \int d^4x \, e^{iq\cdot x} \sum_\Gamma \big(e^{-ip_\Gamma\cdot x}\langle 0|\theta(x^0)A(0)|\Gamma\rangle\langle\Gamma|B(0)^\dagger|0\rangle \\
& \hspace{3.5cm} + e^{ip_\Gamma\cdot x}\,\langle 0|\theta(-x^0)B(0)^\dagger|\Gamma\rangle\langle\Gamma|A(0)|0\rangle \big) \ , && \text{(A.4)}
\end{aligned}
$$

where in the last step we have made use of translation invariance, that tells us that

$$
\langle 0|J(x)|\Gamma\rangle = e^{-ip_\Gamma\cdot x}\,\langle 0|J(0)|\Gamma\rangle \ , \tag{A.5}
$$

where p_Γ denotes the sum of the energy–momenta of all the particles which define the state $|\Gamma\rangle$. All the particles in the state $|\Gamma\rangle$ are on–shell. This constrains the total energy–momentum p_Γ to be a time–like vector: $p_\Gamma^2 = t$ with $t \geq 0$. With these

constrains on p_Γ we can insert the identity

$$\int_0^\infty dt \int d^4p\, \theta(p^0)\, \delta(p^2 - t)\, \delta^{(4)}(p - p_\Gamma) = 1 \tag{A.6}$$

inside the sum $\sum_\Gamma$ over the complete set of states

$$
\begin{aligned}
\Pi_{AB}(q) &= i \int d^4x\, e^{iq\cdot x} \sum_\Gamma \int_0^\infty dt \int d^4p\, \theta(p^0)\, \delta(p^2 - t)\, \delta^{(4)}(p - p_\Gamma) \\
&\quad \big(e^{-ip_\Gamma \cdot x} \langle 0|\theta(x^0) A(0)|\Gamma\rangle\langle\Gamma|B(0)^\dagger|0\rangle \\
&\quad + e^{ip_\Gamma \cdot x}\, \langle 0|\theta(-x^0) B(0)^\dagger|\Gamma\rangle\langle\Gamma|A(0)|0\rangle\big) \\[4pt]
&= i \int d^4x\, e^{iq\cdot x} \int_0^\infty dt \int d^4p\, \theta(p^0)\, \delta(p^2 - t) \\
&\quad \Bigg(e^{-ip\cdot x}\theta(x^0) \sum_\Gamma \delta^{(4)}(p - p_\Gamma)\langle 0|A(0)|\Gamma\rangle\langle\Gamma|B(0)^\dagger|0\rangle \\
&\quad + e^{ip\cdot x}\theta(-x^0) \sum_\Gamma \delta^{(4)}(p - p_\Gamma)\, \langle 0|B(0)^\dagger|\Gamma\rangle\langle\Gamma|A(0)|0\rangle \Bigg) \\[4pt]
&= i \int d^4x\, e^{iq\cdot x} \int_0^\infty dt \int \frac{d^4p}{(2\pi)^3}\, \theta(p^0)\, \delta(p^2 - t) \\
&\quad \big(e^{-ip\cdot x}\theta(x^0)\rho_{AB}(p^2) + e^{ip\cdot x}\theta(-x^0)\rho_{B^\dagger A^\dagger}(p^2)\big) \ ,
\end{aligned}
$$

with equation numbers (A.7), (A.8), (A.9) respectively.

where we have exchanged the order of the sum over Γ and the integration over t and p, finding the AB spectral function defined by (3.17), that is a scalar function of the Lorentz invariant p^2 and the masses of the particles in the states $|\Gamma\rangle$ only.

In general, unless $A = B$ or $A^\dagger = A$ and $B^\dagger = B$, it is not trivial to prove that $\rho_{AB}(s) = \rho_{B^\dagger A^\dagger}(s)$, which we need in order to derive the spectral representation. The proof can be achieved invoking micro-causality, which in turn implies that for space-like distances the commutator of any two operators must vanish:

$$\Big[A(x), B(0)\Big]\Big|_{x^2<0} = 0 \qquad \longrightarrow \qquad \langle 0|\Big[A(x), B(0)\Big]|0\rangle\Big|_{x^2<0} = 0 \ . \tag{A.10}$$

The equality $\rho_{AB}(s) = \rho_{B^\dagger A^\dagger}(s)$ follows from

$$\langle 0|\Big[A(x), B(0)\Big]|0\rangle\Big|_{x^2<0} = \int_0^\infty dt \left[\Delta_+(x;t)\rho_{AB}(t) - \Delta_+(-x;t)\rho_{B^\dagger A^\dagger}(t)\right] \tag{A.11}$$

$$= \int_0^\infty dt\, \Delta_+(x,t)\left[\rho_{AB}(t) - \rho_{B^\dagger A^\dagger}(t)\right] , \tag{A.12}$$

in which we have used that

$$\Delta_\pm(x;t) = \frac{1}{(2\pi)^3} \int d^4p\, e^{\mp ix\cdot p}\, \theta(p^0)\, \delta(p^2 - t) \tag{A.13}$$

is an even function of x for $x^2 < 0$ (one can choose $x = (0, \vec{x})$ to evaluate the above integral). So we have

$$
\begin{aligned}
\Pi_{AB}(q) &= i \int d^4x\, e^{iq \cdot x} \int_0^\infty dt\, \rho_{AB}(t) \int \frac{d^4p}{(2\pi)^3}\, \theta(p^0)\, \delta(p^2 - t) \\
&\quad \left(e^{-ip \cdot x}\theta(x^0) + e^{ip \cdot x}\theta(-x^0) \right) \tag{A.14} \\
&= i \int d^4x\, e^{iq \cdot x} \int_0^\infty dt\, \rho_{AB}(t) \left(\theta(x^0)\Delta^+(x; t) + \theta(-x^0)\Delta^-(x; t) \right) . \tag{A.15}
\end{aligned}
$$

The combination that appears is nothing but the Feynman propagator function

$$
\Delta_{\mathrm{F}}(x; t) = i\theta(x^0)\Delta^+(x; t) + i\theta(-x^0)\Delta^-(x; t) = \int \frac{d^4p}{(2\pi)^4} \frac{e^{-ip \cdot x}}{t - p^2 - i\epsilon} . \tag{A.16}
$$

The two–point function $\Pi_{AB}(q^2)$ appears then to be the Fourier transform of a scalar free field propagating with an arbitrary mass squared t weighted by the spectral function density $\rho_{AB}(t)$ and integrated over all possible values of t,

$$
\Pi_{AB}(q^2) = \int d^4x\, e^{iq \cdot x} \int_0^\infty dt\, \rho_{AB}(t)\, \Delta_{\mathrm{F}}(x; t). \tag{A.17}
$$

Integrating over x and p results finally the wanted representation

$$
\Pi_{AB}(q^2) = \int_0^\infty dt\, \rho_{AB}(t) \frac{1}{t - q^2 - i\epsilon}. \tag{A.18}
$$

We would like to make some comments:

- The spectral function of two different currents is not positive definite in general (we can see in Fig. 3.3 for the LR case);

- The spectral function is not real in general, but if the associated correlator satisfies the Schwarz reflection property $\Pi_{AB}((q^2)^*) = [\Pi_{AB}(q^2)]^*$ (see Section 3.1.2), and using the identity (3.18), then we have

$$
\rho_{AB}(q^2) = \frac{1}{\pi} \operatorname{Im} \Pi_{AB}(q^2 + i\epsilon) , \tag{A.19}
$$

and $\rho_{AB}(q^2)$ is obviously real.

- There is a subtlety that we have ignored when going from (A.7) to (A.8). The exchange of sum over Γ and integrations implicitly assumes good convergence properties for the integrand. But in general the product of the distributions $\theta(x^0)$ and $\int_0^\infty dt\, \rho_{AB}(t)\, \Delta^+(x; t)$ may not be a well–defined distribution. The ambiguity manifests by the presence of an arbitrary polynomial in q^2 in the r.h.s. of the PP–integral

$$
\operatorname{Re}\Pi(q^2) = \mathrm{PP} \int_0^\infty dt\, \frac{1}{t - q^2} \frac{1}{\pi} \operatorname{Im}\Pi(t) + \mathrm{a} + \mathrm{b}q^2 + \dots . \tag{A.20}
$$

Notice that the ambiguity of the short–distance behavior reflects only in the evaluation of the real part of the correlator, not in the imaginary part. The physical meaning of these coefficients depends of course on the choice of $A(x)$ and $B(x)$. In general it is always possible to get rid of the polynomial terms by taking an appropriate number of derivatives with respect to q^2.

Appendix B

Convenience (or not) of the use of the pinched-weights FESR

B.1 Definition and motivation

As we have explained in the main text (Section 3.5.3), the traditional definition of DV is

$$\text{DV}[w(z), s_0] = \oint_{|z|=s_0} \frac{dz}{2\pi i} \left(\Pi(z) - \Pi^{\text{OPE}}(z) \right) w(z) dz \ , \tag{B.1}$$

where the main contribution to this integral comes from the region near the positive real axis. Because of this, different authors have used polynomial weights that vanish at $s = s_0$ (pinched weights). Although it seems clear from (B.1) that these weights will decrease the size of the DV, the alternative expression for the DV shows that this is not that obvious[1]

$$\text{DV}[w(z), s_0] = \int_{s_0}^{\infty} ds \ w(s)\rho(s) \ , \tag{B.2}$$

where we see that one does not have to care only about the point $s = s_0$ but also about not enhancing the rest of the high-energy region[2].

We will say that the "duality region" has arrived when the DV is zero compared with the experimental error. If we represent

$$I(s_0) = \int_0^{s_0} ds \ w(s)\rho(s) \ , \tag{B.3}$$

we will see the arrival of this region with the appearance of a plateau. Due to the oscillatory behavior of the spectral function, there will be a set of points (before the arrival of the plateau) where the duality violation will vanish (duality points). Notice that these points will change in general from a sum rule to another.

---

[1]Hereafter in this appendix we will work with the V-A case, although the ideas explained here about the usefulness of the weight functions are obviously true beyond this particular case.

[2]In light of this expression, modifications of the pinched weights shifting the zeros to slightly higher values have been also suggested [22].

B.2   Example: extraction of L_{10}^{eff}

Let us assume that we are interested in the determination of L_{10}^{eff}. The basic sum rule is then (see Chapter 4)

$$- 8L_{10}^{\text{eff}} = \int_{s_{th}}^{\infty} ds \, \frac{\rho(s)}{s} \; . \tag{B.4}$$

Taking advantage of the WSRs[3], we can write new sum rules that do not involve new unknown parameters

$$- 8L_{10}^{\text{eff}} + 2\alpha \frac{F_{\pi}^2}{s_0} = \int_{s_{th}}^{\infty} ds \left(\frac{1}{s} + \alpha \frac{1}{s_0} + \beta \frac{s}{s_0^2} \right) \rho(s) = I_{-1}^{\alpha\beta}(s_0) + DV_{-1}^{\alpha\beta}(s_0) \tag{B.5}$$

where every sum rule will have a different set of duality points and a different value of the plateau arrival.

B.2.1   Example with a toy function

For illustration let us assume we know the spectral function $\rho(s)$ for any value of s (see Fig. B.1).
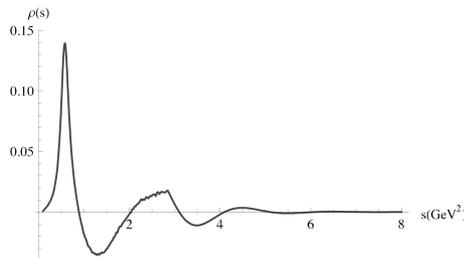

Figure B.1: Hypothetical shape of the spectral function.

Although the choice of weight function used in order to extract the parameter L_{10}^{eff} is irrelevant if we integrate our toy spectral function up to infinite, it becomes very important given that we have access only to the value of the spectral function between 0 and 3.15 GeV^2. In other words, in order to estimate L_{10}^{eff} there are some weights $w_{\alpha\beta}(s)$ more convenient than others. A weight that enhance the region that is beyond s_0 will produce large duality violations. Here we have an example of a "bad" weight and a "good" one (see Fig. B.2)

$$w_A(s, s_0) \equiv \frac{1}{s} + 5\frac{s}{s_0^2} \tag{B.6}$$

$$w_B(s, s_0) \equiv \frac{1}{s} - \frac{1}{s_0} \; , \tag{B.7}$$

respectively.

---

[3]It is worth emphasizing that without the existence of the WSRs all the weight functions would be equivalent in the extraction of L_{10}^{eff} or any other individual parameter. The PW would allow us in that case to extract with more precision certain combination of parameters.
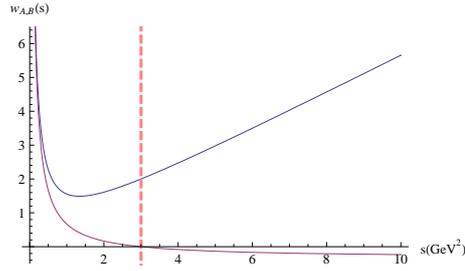
Figure B.2: Weight functions $w_A(s, s_0 = 3 \text{ GeV}^2)$ (upper curve) and $w_B(s, s_0 = 3 \text{ GeV}^2)$ (lower curve). The dashed line at $s_0 = 3 \text{ GeV}^2$ separates the DV-region from the experimentally accesible region.

In the Fig. B.3 we can see the figure obtained for $\mathrm{L}_{10}^{\mathrm{eff}}$ using these two weight functions. The difference is clear. The oscillations are almost negligible for the "good" weight and very big for the "bad" one.
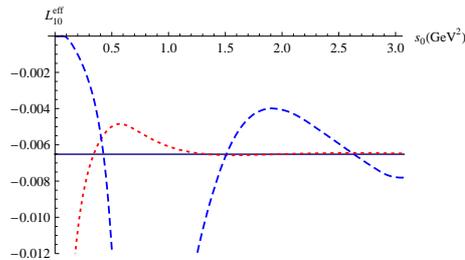

Figure B.3: Curves obtained for $\mathrm{L}_{10}^{\mathrm{eff}}(s_0)$ using the expression (B.5) with the weights (B.6) (blue dashed line) and (B.7) (red dotted line). The horizontal line represents the true value of $\mathrm{L}_{10}^{\mathrm{eff}}$ for our toy function.

Once we leave the toy function and go to the real case, we cannot answer the question of which is the best weight because we do not know the spectral function beyond $s_0 \sim 3 \text{ GeV}^2$. All we know is that it goes to zero in an oscillatory way, but we do not know how fast it does. And that information, as we will see is very relevant.

B.2.2 What about the pinched weights?

Here we want to show that the pinched weights may be more appropriate than the ordinary weight $1/s$ or maybe not. It depends on how fast the spectral function goes to zero[4].

---

[4]Notice that even if we knew that the PW sum rules have smaller DV errors than the ordinary FESRs, it would not mean that the arrival of the duality region is going to be before the end of the data.

We want to compare the following spectral functions:

$$w_0(s, s_0) \equiv \frac{1}{s} , \tag{B.8}$$

$$w_1(s, s_0) \equiv \frac{1}{s} - \frac{1}{s_0} , \tag{B.9}$$

$$w_2(s, s_0) \equiv \frac{1}{s} - \frac{2}{s_0} + \frac{s}{s_0^2} , \tag{B.10}$$

that are plotted in Fig. B.4. There we can see that the PW suppress more the region between 3 and 4 GeV^2, but the $1/s$ weight suppress more the region beyond 4 GeV^2.
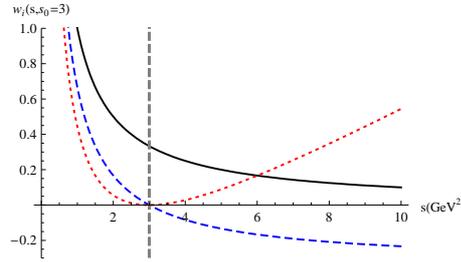

Figure B.4: Curves corresponding to the weights (B.8) (solid black line), (B.9) (blue dashed line) and (B.10) (red dotted line), setting $s_0 = 3$ GeV^2. The gray dashed line at $s_0 = 3$ GeV^2 separates the DV-region from the experimentally accesible region.

We can see that depending on how fast the spectral function goes to zero we should take one weight or another:

- If $\rho(s)$ decreases as e^{-s} we can try to estimate the DV error associated to each weight (see Fig. B.5)

$$DV_0(s_0) \equiv \int_{s_0}^{\infty} ds \; w_0(s, s_0)\rho(s) \sim \int_{s_0}^{\infty} ds \frac{1}{s} e^{-s} \sim 0.0130 ,$$

$$DV_1(s_0) \equiv \int_{s_0}^{\infty} ds \; w_1(s, s_0)\rho(s) \sim \int_{s_0}^{\infty} ds \left(\frac{1}{s} - \frac{1}{s_0} \right) e^{-s} \sim -0.0035 ,$$

$$DV_2(s_0) \equiv \int_{s_0}^{\infty} ds \; w_2(s, s_0)\rho(s) \sim \int_{s_0}^{\infty} ds \left(\frac{1}{s} - \frac{2}{s_0} + \frac{s}{s_0^2} \right) e^{-s} \sim 0.0020 ,$$

where we have taken $s_0 = 3$ GeV^2 for the numerical evaluation. So we can see that $w_2(s, s_0)$ is the best option and $w_0(s, s_0)$ the worst.

- If $\rho(s)$ decreases as $e^{-0.1s}$ we have (see Fig. B.5)

$$DV_0(s_0) \equiv \int_{s_0}^{\infty} ds w_0(s, s_0)\rho(s) \sim \int_{s_0}^{\infty} ds \frac{1}{s} e^{-0.1s} \sim 0.9 ,$$

$$DV_1(s_0) \equiv \int_{s_0}^{\infty} ds w_1(s, s_0)\rho(s) \sim \int_{s_0}^{\infty} ds \left(\frac{1}{s} - \frac{1}{s_0} \right) e^{-0.1s} \sim -1.6 ,$$

$$DV_2(s_0) \equiv \int_{s_0}^{\infty} ds w_2(s, s_0)\rho(s) \sim \int_{s_0}^{\infty} ds \left(\frac{1}{s} - 2\frac{1}{s_0} + \frac{s}{s_0^2} \right) e^{-0.1s} \sim 6.7 ,$$
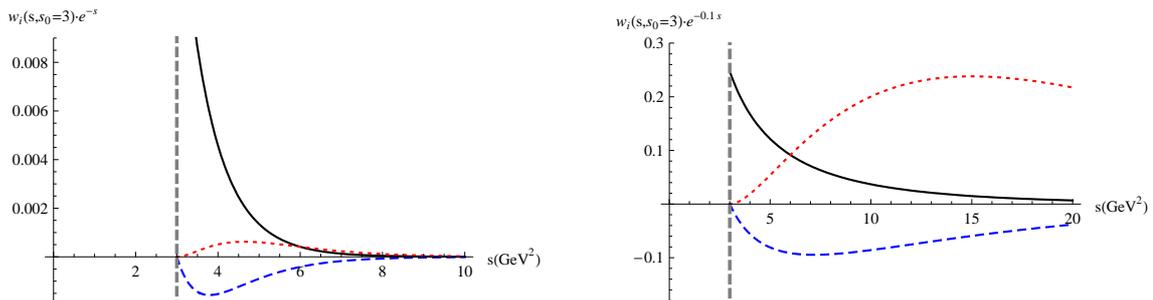
Figure B.5: Part of the integration that we "forget" and represents the DV, assuming that $\rho(s)$ decreases as e^{-s} (left) and $e^{-0.1s}$ (right).

where we have again taken $s_0 = 3$ GeV^2 for the numerical evaluation. So we see that now the order is the opposite and the best choice to minimize the DV is $w_0(s, s_0)$.

B.2.3   What can we do?

The question then is what should we do taking into account that we do not know how fast goes to zero the spectral function, and if we must use the PW or not.

As was explained in Section 3.5.3, the observation of a plateau in the final part of the data is a necessary but not sufficient condition, because the plateau could be temporary. Given that the high correlations generated by the PWs do not make possible a normal fit [30,31,36], one can only perform indirect checks. A possibility is to extend the available window beyond $s_0 \sim 3.15$ GeV^2 and demand the continuance of the plateau[5], until $s_0 \sim 3.4 - 3.5$ GeV^2. Any separation of the curve from a horizontal line can be used as an estimation of the DV error. Another check that can be done is to use the modified PW [22] that are expected to produce smaller DV.

We can see in Figs. B.6 that the plateau is very stable until that point for $\mathrm{L}_{10}^{\mathrm{eff}}$, and the very small oscillations can be included in the error. So we do not expect the curve to leave that region if one includes new data beyond $s_0 \sim 3.15$ GeV^2.

In Chapter 5 we follow a more sophisticated analysis, where we study the possible behavior of the spectral function beyond the end of the data, according to a physically motivated parameterization and the QCD-known sum rules. This represents a qualitatively different approach and allows us to answer the question of the convenience of the pinched weights. As can be seen in the results of that chapter, we conclude that in the extraction of the parameters $\mathrm{L}_{10}^{\mathrm{eff}}, \mathrm{C}_{87}^{\mathrm{eff}}, \mathcal{O}_6, \mathcal{O}_8$ the use of the PWs minimizes the error with respect to the simple weights $w(s) = s^n$. There we take into account the presence of the experimental error, that can also be minimized using the pinched weights.

---

[5]As was explained in [22] it does not matter if we do not know the value of the spectral function between $s_0 \sim 3.15$ GeV^2 and $s_0 \sim 3.5$ GeV^2, because the weight suppresses that part.
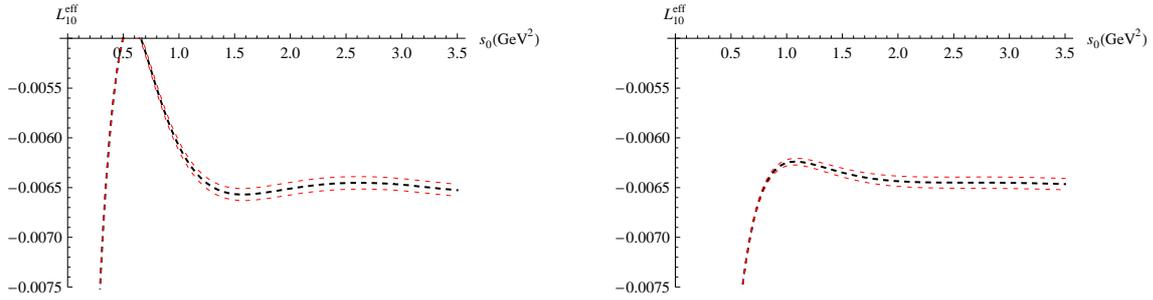
Figure B.6: Curve obtained from the ALEPH data [3] for L_{10}^{eff} using the PW $w_1(s, s_0)$ (left) and $w_2(s, s_0)$ (right).

The same analysis can be done for C_{87}^{eff} with the same conclusions. The only difference is that the the weight $1/s^2$ suppresses more the high-energy region than $1/s$ and therefore, one needs a more decreasing spectral function for the PWSR to be better than the simple FESR. In other words, the benefit of using PW will be always smaller (and could even be negative) for C_{87}^{eff} than for L_{10}^{eff}. Our data confirm perfectly this conclusion.

B.3 Condensates

In the case of the V-A condensates $\mathcal{O}_{6,8}$ (see Chapter 5) the discussion is specially important since the DV effects are larger. If we restrict ourselves to pinched weights that have a double zero at $s = s_0$ then it can be shown that the weights take the form

$$
\begin{aligned}
w_n(s, s_0) &= \pm(s - s_0)^2 \left(s^{n-2} + 2s_0 s^{n-3} + \ldots + (n-2)s_0^{n-3}s + (n-1)s_0^{n-2}\right) \\
&= \pm\left(s^n - n\, s\, s_0^{n-1} + (n-1)s_0^n\right) ,
\end{aligned} \tag{B.11}
$$

where the global sign is plus if $n = 6, 10, 14, \ldots$ and minus otherwise. It can be easily shown that these particular pinched weights are such that

$$
|w_n(s, s_0)| < s^n , \qquad (s > s_0) , \tag{B.12}
$$

or in other words these PW enhance less the high-energy region than the standard weights s^n, and therefore produce less quark-hadron duality violation[6].

Therefore the first question is answered in this case: the pinched weights entails a smaller DV than the standard weights. But we still have to address the question about how to estimate the remaining DV error of the PW sum rule.

Let us look to the particular case of the condensates of dimension six and eight, where we have

$$
\begin{aligned}
w_6(s, s_0) &= (s - s_0)^2 \tag{B.13} \\
w_8(s, s_0) &= -(s - s_0)^2(s + 2s_0) . \tag{B.14}
\end{aligned}
$$

---

[6]Notice that this argument could be spoiled by accidental numerical cancellations due to the oscillatory behavior of the spectral function.

If we represent $\mathcal{O}_{6,8}(s_0)$ we find an acceptable plateau in the final part (between approximately 2.3 GeV^2 and 3 GeV^2), and the usual conclusion is that the DV is much smaller than the experimental error and can be neglected, but as we have explained in the main text (see Section 3.5.3) this is not necessarily true because the plateau could be temporary. A possible solution is to extend the working window up to 3.5 GeV^2. The results are shown in Figs. B.7. Apparently the nice plateau disappears, but the experimental error grows up in such a way that we cannot be conclusive.
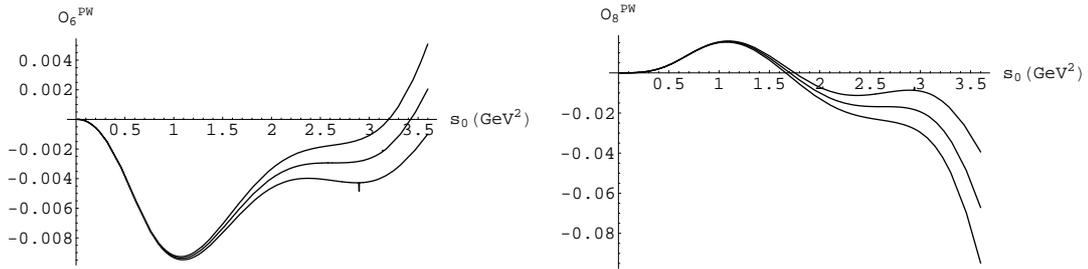

Figure B.7: Curve obtained from the ALEPH 2005 data [3] for $\mathcal{O}_{6,8}$ using the PW $w_6(s, s_0) = (s - s_0)^2$ and $w_8(s, s_0) = -(s - s_0)^2(s + 2s_0)$.

If we work with modified PW the graphics are very similar. So the problem here is the following: the experimental errors are quite big and they prevent us from knowing if the plateau is temporary or not.

Our investigations (see Chapter 5) with possible (realistic) spectral functions indicate that the plateau does not disappear[7].

---

[7]When we say that the plateau is temporary or not we mean *within the experimental error.* Therefore if the plateau is temporary one should add the DV error (very difficult to estimate) to the final error.

Appendix C

$\mathcal{O}(p^6)$ χPT expression of the V-A correlator $\Pi(s)$

C.1 $\mathcal{O}(p^6)$ χPT expression of the V-A correlator $\Pi(s)$

From the results of Ref. [89] we have[1]

$$
\begin{aligned}
\overline{\overline{\Pi}}(s) \;=\; & -\, 8\, \mathrm{L}_{10}^r - 8 B_V^{\pi\pi}(s) - 4 B_V^{KK}(s) \\
& + 16\, \mathrm{C}_{87}^r\; s \\
& - 32\, \mathrm{m}_\pi^2\, (C_{61}^r - C_{12}^r - C_{80}^r) - \; 32\, (\mathrm{m}_\pi^2 + 2\mathrm{m}_K^2)\, (C_{62}^r - C_{13}^r - C_{81}^r) \\
& + 16\left((2\mu_\pi + \mu_K)(L_9^r + 2\mathrm{L}_{10}^r) - (2 B_V^{\pi\pi}(s) + B_V^{KK}(s))\, L_9^r\, \frac{s}{f_\pi^2} \right) \\
& - 8\, G_{2L}(s) \;,
\end{aligned}
\tag{C.1}
$$

where

$$
\begin{aligned}
B_V^{ii}(s) \;&\equiv\; -\left(\frac{1}{192\pi^2}\, \sigma_i^2(\sigma_i \log \frac{\sigma_i - 1}{\sigma_i + 1} + 2) - \frac{1}{6}\frac{1}{32\pi^2}(\log \frac{m_i^2}{\mu^2} + 1) + \frac{1}{288\pi^2} \right) \;, \\
\sigma_i \;&\equiv\; \sqrt{1 - \frac{4m_i^2}{s}} \;, \\
\mu_i \;&\equiv\; \frac{m_i^2}{32\pi^2 f_\pi^2} \log \frac{m_i^2}{\mu^2} \;,
\end{aligned}
\tag{C.2}
$$

and where $G_{2L}(s)$ refers to the two-loop contribution, that we can divide in four parts just to organize the calculation:

$$
G_{2L}(s) = \frac{-1}{8 f_\pi^2}\left(G_{2L}^V(s) - G_{2L}^A(s) \right) = \frac{-1}{8 f_\pi^2}\left(G_{2L}^V(s) - F_1(s) - \frac{F_2(s)}{s} - \frac{F_3(s)}{s} \right), \tag{C.3}
$$

---

[1] In order to obtain this result it must be taken into account that there is a typo in the expression (19) of [89]. In particular, the term with $(L_9^r + \mathrm{L}_{10}^r)$ does not have the right dimensions. The factor q^2 must be removed.

where

$$G_{2L}^V(q^2) \;=\; 4q^2 \Big(2B_V^{\pi\pi}(q^2) + B_V^{KK}(q^2) \Big)^2 , \tag{C.4}$$

$$
\begin{aligned}
F_1(q^2) \;=\;& \frac{1}{(16\pi^2)^2}\left(\frac{1}{6}\,m_\pi^2\,\pi^2 + \frac{1}{3}\,m_\pi^2 + \frac{1}{12}\,m_K^2\,\pi^2 - \frac{5}{24}\,m_K^2 + \frac{3}{32}\,q^2 \right) \\
& + \frac{f_\pi^2}{16\pi^2}\,(2\mu_\pi + \mu_K) + 4\,f_\pi^4\frac{\mu_\pi^2}{m_\pi^2} + 2\,f_\pi^4\frac{\mu_K^2}{m_K^2} , \tag{C.5}
\end{aligned}
$$

$$
\begin{aligned}
F_2(q^2) \;=\;& +5/3\,m_\pi^4\,H^{F\prime}(m_\pi^2,m_\pi^2,m_\pi^2;m_\pi^2) - 2\,m_\pi^2\,H^F(m_\pi^2,m_\pi^2,m_\pi^2;m_\pi^2) \\
& +2\,m_\pi^2\,H^F(m_\pi^2,m_\pi^2,m_\pi^2;q^2) - 5/4\,m_\pi^4\,H^{F\prime}(m_\pi^2,m_K^2,m_K^2;m_\pi^2) \\
& +1/4\,m_\pi^2\,H^F(m_\pi^2,m_K^2,m_K^2;m_\pi^2) - 1/4\,m_\pi^2\,H^F(m_\pi^2,m_K^2,m_K^2;q^2) \\
& +1/9\,m_\pi^4\,H^{F\prime}(m_\pi^2,m_\eta^2,m_\eta^2;m_\pi^2) + 2\,m_\pi^2\,m_K^2\,H^{F\prime}(m_K^2,m_\pi^2,m_K^2;m_\pi^2) \\
& -2\,m_K^2\,H^F(m_K^2,m_\pi^2,m_K^2;m_\pi^2) + 2\,m_K^2\,H^F(m_K^2,m_\pi^2,m_K^2;q^2) \\
& -5/3\,m_\pi^4\,H^{F\prime}(m_K^2,m_K^2,m_\eta^2;m_\pi^2) + \Big(m_\pi^2\,H^{F\prime}(m_\eta^2,m_K^2,m_K^2;m_\pi^2) \\
& -H^F(m_\eta^2,m_K^2,m_K^2;m_\pi^2) + H^F(m_\eta^2,m_K^2,m_K^2;q^2) \Big)\,(-1/4\,m_\pi^2 + m_K^2) \\
& +2\,m_\pi^4\,H_1^{F\prime}(m_\pi^2,m_K^2,m_K^2;m_\pi^2) + 4\,m_\pi^4\,H_1^{F\prime}(m_K^2,m_K^2,m_\eta^2;m_\pi^2) \\
& +2\,H^T(m_\pi^2,m_\pi^2,m_\pi^2;q^2;m_\pi^2) - 1/4\,H^T(m_\pi^2,m_K^2,m_K^2;q^2;m_\pi^2) \\
& +2\,H^T(m_K^2,m_\pi^2,m_K^2;q^2;m_\pi^2) + 3/4\,H^T(m_\eta^2,m_K^2,m_K^2;q^2;m_\pi^2) , \tag{C.6}
\end{aligned}
$$

$$
\begin{aligned}
F_3(q^2) \;=\;& +1/3\,H^L(m_\pi^2,m_\pi^2,m_\pi^2;q^2;m_\pi^2)\,m_\pi^4 - 2\,H^M(m_\pi^2,m_\pi^2,m_\pi^2;q^2;m_\pi^2)\,m_\pi^6 \\
& +H^L(m_\pi^2,m_K^2,m_K^2;q^2;m_\pi^2)\,m_\pi^4 + 1/4\,H^M(m_\pi^2,m_K^2,m_K^2;q^2;m_\pi^2)\,m_\pi^6 \\
& -1/9\,H^L(m_\pi^2,m_\eta^2,m_\eta^2;q^2;m_\pi^2)\,m_\pi^4 - 2\,H^M(m_K^2,m_\pi^2,m_K^2;q^2;m_\pi^2)\,m_\pi^4\,m_K^2 \\
& +\frac{5}{3}\,H^L(m_K^2,m_K^2,m_\eta^2;q^2;m_\pi^2)\,m_\pi^4 - \frac{3}{4}\,H^M(m_\eta^2,m_K^2,m_K^2;q^2;m_\pi^2)\,m_\pi^4 m_\eta^2 \\
& -2\,H_1^L(m_\pi^2,m_K^2,m_K^2;q^2;m_\pi^2)\,m_\pi^4 - 4\,H_1^L(m_K^2,m_K^2,m_\eta^2;q^2;m_\pi^2)\,m_\pi^4 \\
& -6\,H_{21}^L(m_\pi^2,m_\pi^2,m_\pi^2;q^2;m_\pi^2)\,m_\pi^4 + 3/4\,H_{21}^L(m_\pi^2,m_K^2,m_K^2;q^2;m_\pi^2)\,m_\pi^4 \\
& -6\,H_{21}^L(m_K^2,m_\pi^2,m_K^2;q^2;m_\pi^2)m_\pi^4 - \frac{9}{4}H_{21}^L(m_\eta^2,m_K^2,m_K^2;q^2;m_\pi^2)m_\pi^4 . \tag{C.7}
\end{aligned}
$$

The different H functions are defined as follows

$$H^T(m_1^2,m_2^2,m_3^2;q^2;m_4^2) \;=\; 3m_4^4 H_{21}^{F\prime}(m_1^2,m_2^2,m_3^2;m_4^2) - q^2 H_{21}^F(m_1^2,m_2^2,m_3^2;q^2), \tag{C.8}$$

$$H^M(m_1^2, m_2^2, m_3^2; q^2; m_4^2) = \frac{1}{(q^2 - m_4^2)^2}\left(H^F(m_1^2, m_2^2, m_3^2; q^2) \right.$$
$$\left. -H^F(m_1^2, m_2^2, m_3^2; m_4^2) - (q^2 - m_4^2)H^{F\prime}(m_1^2, m_2^2, m_3^2; m_4^2) \right), \qquad \text{(C.9)}$$

$$H_i^L(m_1^2, m_2^2, m_3^2; q^2; m_4^2) = \frac{1}{(q^2 - m_4^2)^2}\left(q^2 H_i^F(m_1^2, m_2^2, m_3^2; q^2) \right.$$
$$\left. -q^2 H_i^F(m_1^2, m_2^2, m_3^2; m_4^2) - m_4^2(q^2 - m_4^2)H_i^{F\prime}m_1^2, m_2^2, m_3^2; m_4^2) \right), \text{ (C.10)}$$

in terms of the functions $H_i^F = \{H^F, H_1^F, H_{21}^F\}$, which are given by[2]

$$H_i^F(m_1^2, m_2^2, m_3^2; p^2) = H_i^F(m_1^2, m_2^2, m_3^2; 0) + p^2 \frac{\partial}{\partial p^2} H_i^F(m_1^2, m_2^2, m_3^2; 0)$$
$$+\overline{H}_i(m_1^2, m_2^2, m_3^2; p^2). \qquad \text{(C.11)}$$

Next we give the value of $H_i^F(m_1^2, m_2^2, m_3^2; 0)$ and $\frac{\partial}{\partial p^2} H_i^F(m_1^2, m_2^2, m_3^2; 0)$

$$(16\pi^2)^2 H(m_1^2, m_2^2, m_3^2; 0) = -\frac{1}{2}\Psi(m_1^2, m_2^2, m_3^2)$$
$$+m_1^2\left(\frac{\pi^2}{12} + \frac{3}{2} - \ln_1 + \frac{1}{2}\left(-\ln_2 \ln_3 + \ln_1 \ln_4 \right) \right)$$
$$+m_2^2\left(\frac{\pi^2}{12} + \frac{3}{2} - \ln_2 + \frac{1}{2}\left(-\ln_1 \ln_3 + \ln_2 \ln_4 \right) \right)$$
$$+m_3^2\left(\frac{\pi^2}{12} + \frac{3}{2} - \ln_3 + \frac{1}{2}\left(-\ln_1 \ln_2 + \ln_3 \ln_4 \right) \right), \qquad \text{(C.12)}$$

$$(16\pi^2)^2 \frac{\partial}{\partial p^2} H(m_1^2, m_2^2, m_3^2; 0) = + \frac{m_1^2 m_2^2 m_3^3}{\lambda_m^2}\Psi(m_1^2, m_2^2, m_3^2) + \frac{1}{8}$$
$$+ \frac{m_1^2 \delta_m}{2\lambda_m}\ln_1$$
$$+ \frac{m_2^2}{2\lambda_m}(m_2^2 - m_1^2 - m_3^2)\ln_2$$
$$+ \frac{m_3^2}{2\lambda_m}(m_3^2 - m_1^2 - m_2^2)\ln_3, \qquad \text{(C.13)}$$

---

[2] $H_i^{F\prime}(m_1^2, m_2^2, m_3^2; q^2)$ are just the derivatives with respect to q^2, of the functions $H_i^F(m_1^2, m_2^2, m_3^2; q^2)$.

$$(16\pi^2)^2 H_1(m_1^2, m_2^2, m_3^2; 0) = +\frac{1}{4}\left(-1 + \frac{m_1^2\delta_m}{\lambda_m}\right)\Psi(m_1^2, m_2^2, m_3^2)$$

$$+ \ m_1^2\left(\frac{3}{8} - \frac{1}{2}\ln_1\right)$$

$$+ \ m_2^2\left(\frac{\pi^2}{24} + \frac{9}{16} - \frac{1}{4}\ln_2 + \frac{1}{4}(\ln_2\ln_4 - \ln_1\ln_3)\right)$$

$$+ \ m_3^2\left(\frac{\pi^2}{24} + \frac{9}{16} - \frac{1}{4}\ln_3 + \frac{1}{4}(\ln_3\ln_4 - \ln_1\ln_2)\right), \qquad \text{(C.14)}$$

$$(16\pi^2)^2\frac{\partial}{\partial p^2}H_1(m_1^2, m_2^2, m_3^2; 0) = +\frac{m_1^4 m_2^2 m_3^2 \delta_m}{\lambda_m^3}\Psi(m_1^2, m_2^2, m_3^2) - \frac{m_1^2\delta_m}{6\lambda_m}$$

$$+\frac{m_1^4\ln_1}{6\lambda_m}\left(1 + 12\frac{m_2^2 m_3^2}{\lambda_m}\right)$$

$$+\frac{m_2^2\ln_2}{6\lambda_m}\left(m_2^2 - m_3^2 - 2m_1^2 - \frac{6m_1^2 m_3^2}{\lambda_m}(\delta_m + 2m_2^2)\right)$$

$$+\frac{m_3^2\ln_3}{6\lambda_m}\left(m_3^2 - m_2^2 - 2m_1^2 - \frac{6m_1^2 m_2^2}{\lambda_m}(\delta_m + 2m_3^2)\right) + \frac{7}{72}, \qquad \text{(C.15)}$$

$$(16\pi^2)^2 H_{21}(m_1^2, m_2^2, m_3^2; 0) =$$

$$+\frac{1}{6\lambda_m^2}\left(-\lambda_m^2 + \lambda_m m_1^2\delta_m + 2m_1^4 m_2^2 m_3^2\right)\Psi(m_1^2, m_2^2, m_3^2)$$

$$+m_1^2\left(\frac{17}{72} - \frac{1}{3}\ln_1 + \frac{m_1^2\ln_1\delta_m}{6\lambda_m}\right)$$

$$+m_2^2\left(\frac{\pi^2}{36} + \frac{19}{54} - \frac{1}{9}\ln_2 - \frac{m_1^2}{6\lambda_m}(\delta_m + 2m_3^2)\ln_2 + \frac{1}{6}(\ln_2\ln_4 - \ln_1\ln_3)\right)$$

$$+m_3^2\left(\frac{\pi^2}{36} + \frac{19}{54} - \frac{1}{9}\ln_3 - \frac{m_1^2}{6\lambda_m}(\delta_m + 2m_2^2)\ln_3 + \frac{1}{6}(\ln_3\ln_4 - \ln_1\ln_2)\right), \text{(C.16)}$$

$$(16\pi^2)^2 \frac{\partial}{\partial p^2} H_{21}(m_1^2, m_2^2, m_3^2; 0) = +\frac{17}{288} - \frac{m_1^2}{24\lambda_m}(\delta_m + 2m_1^2) - \frac{5m_1^4 m_2^2 m_3^2}{6\lambda_m^2}$$
$$+ \frac{m_1^6 m_2^2 m_3^2}{\lambda_m^3}\left(1 + \frac{5m_2^2 m_3^2}{\lambda_m}\right)\Psi(m_1^2, m_2^2, m_3^2) + \frac{m_1^6 \delta_m}{12\lambda_m^2}\ln_1\left(1 + 30\frac{m_2^2 m_3^2}{\lambda_m}\right)$$
$$+ \frac{m_1^4 m_2^2 m_3^4}{\lambda_m^3}\ln_3\frac{5}{2}(m_3^2 - m_1^2 - m_2^2) + \frac{m_3^2}{12\lambda_m}(m_3^2 - m_2^2)\ln_3$$
$$+ \frac{m_1^2 m_3^2}{12\lambda_m^2}\ln_3\left(-3m_1^4 - 12m_1^2 m_2^2 + 5m_1^2 m_3^2 + 3m_2^4 - m_2^2 m_3^2 - 2m_3^4\right)$$
$$+ \frac{m_1^4 m_3^2 m_2^4}{\lambda_m^3}\ln_2\frac{5}{2}(m_2^2 - m_1^2 - m_3^2) + \frac{m_2^2}{12\lambda_m}(m_2^2 - m_3^2)\ln_2$$
$$+ \frac{m_1^2 m_2^2}{12\lambda_m^2}\ln_2\left(-3m_1^4 - 12m_1^2 m_3^2 + 5m_1^2 m_2^2 + 3m_3^4 - m_2^2 m_3^2 - 2m_2^4\right). \quad \text{(C.17)}$$

Here we used

$$\begin{aligned}
\ln_i &\equiv \ln m_i^2, \\
\lambda_m &\equiv (m_1^2 - m_2^2 - m_3^2)^2 - 4\, m_2^2\, m_3^2, \\
\ln_4 &\equiv \ln_1 + \ln_2 + \ln_3, \\
\delta_m &\equiv m_1^2 - m_2^2 - m_3^2.
\end{aligned} \quad \text{(C.18)}$$

The expression for Ψ depends on the relation between the various masses. For the case $\lambda_m \leq 0$

$$\Psi(m_1^2, m_2^2, m_3^2) = 2\sqrt{-\lambda_m}\left\{\text{Cl}_2(2\arccos z_1) + \text{Cl}_2(2\arccos z_2) + \text{Cl}_2(2\arccos z_3)\right\}, \quad \text{(C.19)}$$

with

$$z_1 = \frac{-m_1^2 + m_2^2 + m_3^2}{2m_2 m_3}, \quad z_2 = \frac{-m_2^2 + m_3^2 + m_1^2}{2m_3 m_1}, \quad z_3 = \frac{-m_3^2 + m_1^2 + m_2^2}{2m_1 m_2}. \quad \text{(C.20)}$$

The case $m_1 + m_2 \leq m_3$, with $\lambda_m \geq 0$, is

$$\begin{aligned}
\Psi(m_1^2, m_2^2, m_3^2) = -\sqrt{\lambda_m}\Bigg\{&2\ln x_1 \ln x_2 - \ln\frac{m_1^2}{m_3^2}\ln\frac{m_2^2}{m_3^2} \\
&+ \frac{\pi^2}{3} - 2\text{Li}_2(x_1) - 2\text{Li}_2(x_2)\Bigg\},
\end{aligned} \quad \text{(C.21)}$$

with

$$x_1 = \frac{m_3^2 + m_1^2 - m_2^2 - \sqrt{\lambda_m}}{2m_3^2}, \quad x_2 = \frac{m_3^2 + m_2^2 - m_1^2 - \sqrt{\lambda_m}}{2m_3^2}. \quad \text{(C.22)}$$

The cases $m_1 + m_3 \leq m_2$ and $m_2 + m_3 \leq m_1$ can be obtained from the last one by relabelling masses. $\mathrm{Li}_2(x)$ is the dilogarithm defined by

$$\mathrm{Li}_2(x) = -\int_0^1 \frac{dt}{t} \ln(1 - xt), \tag{C.23}$$

and $\mathrm{Cl}_2(x)$ is Clausen's function defined by

$$\mathrm{Cl}_2(x) = -\int_0^x dt \ln \left| 2 \sin \frac{t}{2} \right| = -i \left(\mathrm{Li}_2(e^{ix}) - \mathrm{Li}_2(1) \right) - i \frac{\pi x}{2} + i \frac{x^2}{4}. \tag{C.24}$$

Now we define $\overline{H}_i(m_1^2, m_2^2, m_3^2; p^2)$

$$\{\overline{H}, \overline{H}_1, \overline{H}_{21}\}(m_1^2, m_2^2, m_3^2; p^2) = \int_{(m_2+m_3)^2}^\infty d\sigma \lambda^{1/2} \left(1, \frac{m_2^2}{\sigma}, \frac{m_3^2}{\sigma} \right)$$
$$\times \int_0^1 dx \, \mathcal{K}_2(x, \sigma, p^2) \{1, x, x^2\}, \tag{C.25}$$

with

$$\mathcal{K}_2(x, \sigma, p^2) = \frac{1}{(16\pi^2)^2} \left(\ln \frac{m_1^2(1-x) + \sigma x - x(1-x)p^2}{m_1^2(1-x) + \sigma x} + \frac{p^2 x(1-x)}{m_1^2(1-x) + \sigma x} \right),$$
$$\lambda(x, y, z) = (x - y - z)^2 - 4yz. \tag{C.26}$$

C.2   Calculation of $F_2(0) + F_3(0)$

We expect the quantity $F_2(0) + F_3(0)$ to be zero because the correlator has to be non-singular at the origin. Now we are going to check it.

If we use the definition of H^T, H^M, H_i^L and $H_i^F(m_1, m_2, m_3; s)$ given in the preceding section, we can write $F_2(s) + F_3(s)$ in terms of the masses m_π, m_K, m_η, s and the functions ψ, $\overline{H}$ and $\overline{H}'$ evaluated at different combinations of masses and s. This expression is almost endless and therefore we will not show it here, but if we evaluate it in $s = 0$ it takes the very simple form

$$F_2(0) + F_3(0) = \frac{1}{4} \left(4m_K^2 - 3m_\eta^2 - m_\pi^2 \right) \left(\overline{H}' \left(m_\eta, m_K, m_K, m_\pi^2 \right) m_\pi^2 \right.$$
$$\left. + \overline{H}(m_\eta, m_K, m_K, 0) - \overline{H} \left(m_\eta, m_K, m_K, m_\pi^2 \right) \right). \tag{C.27}$$

Using the Gell-Mann-Okubo relation[3]

$$3m_\eta^2 = 4m_K^2 - m_\pi^2, \tag{C.28}$$

we have that $F_2(0) + F_3(0) = 0$.

---

[3] This relation holds for the η_8, but the difference between m_η and m_{η_8} is of order p^2 in χPT, and therefore is of order p^8 in (C.27) and hence we can omit it.

C.3   Two-loop correction to L$_{10}^r$: $F_2'(0) + F_3'(0)$

As we have seen the structure of this correction is

$$
\begin{aligned}
G_{2L}(0) &= \frac{-1}{8f_\pi^2}\left(G_{2L}^V(0) - F_1(0) - \lim_{s\to 0}\left(\frac{F_2(s) + F_3(s)}{s}\right)\right) , \\
&= \frac{-1}{8f_\pi^2}\left(G_{2L}^V(0) - F_1(0) - (F_2'(0) + F_3'(0))\right) ,
\end{aligned}
\tag{C.29}
$$

where we have used $F_2(0) + F_3(0) = 0$ in the last step. For the first two terms we have

$$
G_{2L}^V(0) = \lim_{s\to 0} 4s\left(2B_V^{\pi\pi}(s) + B_V^{KK}(s)\right)^2 = 0 ,
\tag{C.30}
$$

$$
\begin{aligned}
F_1(0) &= \frac{1}{(16\pi^2)^2}\left(\frac{1}{6}m_\pi^2\,\pi^2 + \frac{1}{3}m_\pi^2 + \frac{1}{12}m_K^2\,\pi^2 - \frac{5}{24}m_K^2\right) \\
&\quad + \frac{f_\pi^2}{16\pi^2}(2\mu_\pi + \mu_K) + 4\,f_\pi^4\frac{\mu_\pi^2}{m_\pi^2} + 2\,f_\pi^4\frac{\mu_K^2}{m_K^2} \\
&= 0.712 \cdot 10^{-3}m_\pi^2 = 0.01356 \cdot 10^{-3} \text{ GeV}^2 .
\end{aligned}
\tag{C.31}
$$

If we calculate the derivative of $F_2(s) + F_3(s)$ we obtain another endless expression that in this case does not simplify too much when we do $s = 0$. In order to simplify it a bit, we use then that the $\overline{H}^F$ (and their first derivatives) are zero at $s = 0$ for any combination of masses. After that we write

$$
m_K = 3.586\,m_\pi , \quad m_\eta = 3.966\,m_\pi , \quad \mu = m_\rho = 5.618\,m_\pi ,
\tag{C.32}
$$

in order to have only one dimensional parameter: the pion mass. After this, we found a not so long expression

$$
\begin{aligned}
F_2'(0) &+ F_3'(0) = \\
&= -4.290 \cdot 10^{-3}m_\pi^2 \\
&\quad + 54.651 \cdot 10^{-6}\,\Psi(m_K, m_\pi, m_K) + 6.479 \cdot 10^{-6}\,\Psi(m_\eta, m_K, m_K) \\
&\quad - 1.286 \cdot 10^{-6}\,\Psi(m_\pi, m_K, m_K) + 14.852 \cdot 10^{-6}\,\Psi(m_\pi, m_\pi, m_\pi) \\
&\quad - \frac{5}{3}\,\overline{H}\left(m_K, m_K, m_\eta, m_\pi^2\right) + 51.435\,\overline{H}\left(m_K, m_\pi, m_K, m_\pi^2\right)
\end{aligned}
$$

$$+23.597\ \overline{H}\left(m_\eta, m_K, m_K, m_\pi^2\right) - 1.5\ \overline{H}\left(m_\pi, m_K, m_K, m_\pi^2\right)$$

$$+\frac{1}{9}\ \overline{H}\left(m_\pi, m_\eta, m_\eta, m_\pi^2\right) + \frac{11}{3}\ \overline{H}\left(m_\pi, m_\pi, m_\pi, m_\pi^2\right)$$

$$+4\ \overline{H}_1\left(m_K, m_K, m_\eta, m_\pi^2\right) + 2\ \overline{H}_1\left(m_\pi, m_K, m_K, m_\pi^2\right)$$

$$+6\ \overline{H}_{21}\left(m_K, m_\pi, m_K, m_\pi^2\right) + 2.25\ \overline{H}_{21}\left(m_\eta, m_K, m_K, m_\pi^2\right)$$

$$-0.75\ \overline{H}_{21}\left(m_\pi, m_K, m_K, m_\pi^2\right) + 6\ \overline{H}_{21}\left(m_\pi, m_\pi, m_\pi, m_\pi^2\right)$$

$$+m_\pi^2\Bigg(-4\ \overline{H}_1'\left(m_K, m_K, m_\eta, m_\pi^2\right) - 2\ \overline{H}_1'\left(m_\pi, m_K, m_K, m_\pi^2\right)$$

$$-6\ \overline{H}_{21}'\left(m_K, m_\pi, m_K, m_\pi^2\right) - 2.25\ \overline{H}_{21}'\left(m_\eta, m_K, m_K, m_\pi^2\right)$$

$$+0.75\ \overline{H}_{21}'\left(m_\pi, m_K, m_K, m_\pi^2\right) - 6\ \overline{H}_{21}'\left(m_\pi, m_\pi, m_\pi, m_\pi^2\right)$$

$$+\frac{5}{3}\ \overline{H}'\left(m_K, m_K, m_\eta, m_\pi^2\right) - 25.718\ \overline{H}'\left(m_K, m_\pi, m_K, m_\pi^2\right)$$

$$-11.798\ \overline{H}'\left(m_\eta, m_K, m_K, m_\pi^2\right) + 1.25\ \overline{H}'\left(m_\pi, m_K, m_K, m_\pi^2\right)$$

$$-\frac{1}{9}\ \overline{H}'\left(m_\pi, m_\eta, m_\eta, m_\pi^2\right) - \frac{5}{3}\ \overline{H}'\left(m_\pi, m_\pi, m_\pi, m_\pi^2\right)\Bigg)$$

$$= -4.290 \cdot 10^{-3}m_\pi^2 + C_\psi + C_H + C_{prime}\ , \tag{C.33}$$

where we have split the result in four terms: the one that does not depend on any not-defined (so far) function, the term that contains the ψ functions, the term that contains the $\overline{H}$ functions and the term that contain the $\overline{H}'$ functions. We find[4]

$$C_\psi \quad = \quad +1.69 \cdot 10^{-3}m_\pi^2 = 0.032328 \cdot 10^{-3}\ \text{GeV}^2\ , \tag{C.34}$$

$$C_H \quad = \quad -4.79 \cdot 10^{-6}m_\pi^2 = -9.13 \cdot 10^{-8}\ \text{GeV}^2\ , \tag{C.35}$$

$$C_{prime} \quad = \quad 5.20 \cdot 10^{-6}m_\pi^2 = 9.92 \cdot 10^{-8}\ \text{GeV}^2\ . \tag{C.36}$$

Therefore, we have

$$F_2'(0) + F_3'(0) \quad = \quad -2.60 \cdot 10^{-3}\ m_\pi^2 = -4.94 \cdot 10^{-5}\ \text{GeV}^2\ . \tag{C.37}$$

And hence

$$G_{2L}^V(0) - F_1(0) - F_2'(0) - F_3'(0) = 0 - 0.712 \cdot 10^{-3}m_\pi^2 - (-2.60 \cdot 10^{-3}\ m_\pi^2)$$

$$= \quad +1.888 \cdot 10^{-3}m_\pi^2 = 3.600 \cdot 10^{-5}\ \text{GeV}^2\ , \tag{C.38}$$

$$G_{2L}(0) = -0.236 \cdot 10^{-3}\frac{m_\pi^2}{f_\pi^2} = -27.642 \cdot 10^{-3}\ \text{GeV}^{-2}m_\pi^2 = -0.527 \cdot 10^{-3}\ . \tag{C.39}$$

---

[4]The big cancelation between C_H and C_{prime} is not very surprising since we can see in our expression for $F_2'(0) + F_3'(0)$ that the coefficients of the $\overline{H}$ and $\overline{H}'$ are always of opposite sign.

C.4 Two-loop correction to C$_{87}^r$: $F_2''(0) + F_3''(0)$

Again we have the following structure

$$G_{2L}'(0) = \frac{-1}{8f_\pi^2} \left(G_{2L}^{V\prime}(0) - F_1'(0) - \lim_{s\to 0} \frac{d}{ds} \frac{F_2(s) + F_3(s)}{s} \right) , \tag{C.40}$$

and we have for each term that

$$G_{2L}^{V\prime}(0) = \lim_{s\to 0} \frac{d}{ds} \left(4s \left(2B_V^{\pi\pi}(s) + B_V^{KK}(s) \right)^2 \right)$$

$$= \frac{\left(\log\left(\frac{m_K^2}{\mu^2}\right) + 2\log\left(\frac{m_\pi^2}{\mu^2}\right) + 3 \right)^2}{9216\pi^4} = 25.684 \cdot 10^{-6} , \tag{C.41}$$

$$F_1'(0) = \frac{1}{(16\pi^2)^2} \frac{3}{32} = 3.76 \cdot 10^{-6} , \tag{C.42}$$

$$\lim_{s\to 0} \frac{d}{ds} \frac{F_2(s) + F_3(s)}{s} = \frac{1}{2} \left(F_2''(0) + F_3''(0) \right) , \tag{C.43}$$

where we have used $F_2(0) + F_3(0) = 0$ in the last step. If we calculate the second derivative of $F_2(s) + F_3(s)$ we obtain another endless expression that again does not simplify too much when we do $s = 0$. In order to simplify it a bit, we use again that the $\overline{H}^F$ (and their first derivatives) are zero at $s = 0$ for any combination of masses. This is not true for one second derivative of $\overline{H}^F$ that appear in our expression, but if we pay attention the exact form of that term is

$$\left(m_K^2 - \frac{m_\pi^2}{4} - \frac{3}{4} m_\eta^2 \right) \overline{H}^{F\prime\prime}(m_\eta, m_K, m_K, 0) , \tag{C.44}$$

that again is zero if we use the Gell-Mann-Okubo relation. Now we use again (C.32) in order to have only one dimensional parameter: the pion mass. After this, we found a not so long expression

$$F_2''(0) + F_3''(0) =$$
$$+214.278 \cdot 10^{-6}$$
$$+ \frac{1}{m_\pi^2} \left(-9.393 \cdot 10^{-6} \Psi(m_K, m_\pi, m_K) - 1.03 \cdot 10^{-7} \Psi(m_\eta, m_K, m_K) \right.$$
$$+3.98 \cdot 10^{-7} \Psi(m_\pi, m_K, m_K) - 3.961 \cdot 10^{-6} \Psi(m_\pi, m_\pi, m_\pi)$$
$$+16\overline{H}_1\left(m_K, m_K, m_\eta, m_\pi^2\right) + 8\overline{H}_1\left(m_\pi, m_K, m_K, m_\pi^2\right)$$
$$+24\overline{H}_{21}\left(m_K, m_\pi, m_K, m_\pi^2\right) + 9\overline{H}_{21}\left(m_\eta, m_K, m_K, m_\pi^2\right)$$

$$-3\overline{H}_{21}\left(m_\pi, m_K, m_K, m_\pi^2\right) + 24\overline{H}_{21}\left(m_\pi, m_\pi, m_\pi, m_\pi^2\right)$$

$$-\frac{20}{3}\overline{H}\left(m_K, m_K, m_\eta, m_\pi^2\right) + 154.306\overline{H}\left(m_K, m_\pi, m_K, m_\pi^2\right)$$

$$+70.79\overline{H}\left(m_\eta, m_K, m_K, m_\pi^2\right) - 5.5\overline{H}\left(m_\pi, m_K, m_K, m_\pi^2\right)$$

$$+\frac{4}{9}\overline{H}\left(m_\pi, m_\eta, m_\eta, m_\pi^2\right) + \frac{32}{3}\overline{H}\left(m_\pi, m_\pi, m_\pi, m_\pi^2\right))$$

$$-8\overline{H}'_1\left(m_K, m_K, m_\eta, m_\pi^2\right) - 4\overline{H}'_1\left(m_\pi, m_K, m_K, m_\pi^2\right)$$

$$-12\overline{H}'_{21}\left(m_K, m_\pi, m_K, m_\pi^2\right) - 4.5\overline{H}'_{21}\left(m_\eta, m_K, m_K, m_\pi^2\right)$$

$$+1.5\overline{H}'_{21}\left(m_\pi, m_K, m_K, m_\pi^2\right) - 12\overline{H}'_{21}\left(m_\pi, m_\pi, m_\pi, m_\pi^2\right)$$

$$+\frac{10}{3}\overline{H}'\left(m_K, m_K, m_\eta, m_\pi^2\right) - 51.435\overline{H}'\left(m_K, m_\pi, m_K, m_\pi^2\right)$$

$$-23.597\overline{H}'\left(m_\eta, m_K, m_K, m_\pi^2\right) + 2.5\overline{H}'\left(m_\pi, m_K, m_K, m_\pi^2\right)$$

$$-\frac{2}{9}\overline{H}'\left(m_\pi, m_\eta, m_\eta, m_\pi^2\right) - \frac{10}{3}\overline{H}'\left(m_\pi, m_\pi, m_\pi, m_\pi^2\right)$$

$$= +214.278 \cdot 10^{-6} + D_\psi + D_H + D_{prime} , \qquad (C.45)$$

where we have again split the result in four terms. We obtain for them

$$\begin{aligned}
D_\psi &= -200.346 \cdot 10^{-6} , & (C.46) \\
D_H &= -14.743 \cdot 10^{-6} , & (C.47) \\
D_{prime} &= +10.410 \cdot 10^{-6} . & (C.48)
\end{aligned}$$

We can see that there is a big cancelation between the first and second terms, that finally gives

$$F_2''(0) + F_3''(0) = +9.6 \cdot 10^{-6} . \qquad (C.49)$$

Then

$$\begin{aligned}
-8f_\pi^2\, G'_{2L}(0) &= G_{2L}^{V\prime}(0) - F_1'(0) - \frac{1}{2}\left(F_2''(0) + F_3''(0)\right) = 17.1 \cdot 10^{-6} , & (C.50) \\
\frac{-1}{2}G'_{2L}(0) &= 1.07 \cdot 10^{-6}\frac{1}{f_\pi^2} = 0.13 \cdot 10^{-3}\ \text{GeV}^{-2} . & (C.51)
\end{aligned}$$

Bibliography

[1] R. D. Peccei and J. Sola, "A phenomenological analysis of the Weinberg Sum Rules and of the π^+-π^0 mass difference," *Nucl. Phys.* **B281** (1987) 1.

[2] W. J. Marciano and A. Sirlin, "Electroweak Radiative Corrections to tau Decay," *Phys. Rev. Lett.* **61** (1988) 1815–1818.

[3] **ALEPH** Collaboration, S. Schael *et al.*, "Branching ratios and spectral functions of tau decays: Final ALEPH measurements and physics implications," *Phys. Rept.* **421** (2005) 191–284, `arXiv:hep-ex/0506072`.

[4] E. Braaten, S. Narison, and A. Pich, "QCD analysis of the tau hadronic width," *Nucl. Phys.* **B373** (1992) 581–612.

[5] A. Pich and J. Prades, "Perturbative quark mass corrections to the tau hadronic width," *JHEP* **06** (1998) 013, `arXiv:hep-ph/9804462`.

E. Gámiz *et al.*, "Determination of m_s and $|V_{us}|$ from hadronic tau decays," *JHEP* **01** (2003) 060, `arXiv:hep-ph/0212230`.

E. Gámiz *et al.*, "V_{us} and m_s from hadronic tau decays," *Phys. Rev. Lett.* **94** (2005) 011803, `arXiv:hep-ph/0408044`.

[6] A. Pich and J. Prades, "Strange quark mass determination from Cabibbo-suppressed tau decays," *JHEP* **10** (1999) 004, `arXiv:hep-ph/9909244`.

[7] M. A. Shifman, A. I. Vainshtein, and V. I. Zakharov, "QCD and Resonance Physics. Sum Rules," *Nucl. Phys.* **B147** (1979) 385–447.

M. A. Shifman, A. I. Vainshtein, and V. I. Zakharov, "QCD and Resonance Physics: Applications," *Nucl. Phys.* **B147** (1979) 448–518.

[8] E. de Rafael, "An introduction to sum rules in QCD," `arXiv:hep-ph/9802448`.

[9] P. Colangelo and A. Khodjamirian, "QCD sum rules, a modern perspective," `arXiv:hep-ph/0010175`.

[10] K. G. Wilson, "Nonlagrangian models of current algebra," *Phys. Rev.* **179** (1969) 1499–1512.

[11] G. Kallen, "On the Properties of propagation functions and renormalization contants of quantized fields," *Nuovo Cim.* **11** (1954) 342–357.

H. Lehmann, "On the Properties of propagation functions and renormalization contants of quantized fields," *Nuovo Cim.* **11** (1954) 342–357.

[12] M. Gell-Mann, M. L. Goldberger, and W. E. Thirring, "Use of causality conditions in quantum theory," *Phys. Rev.* **95** (1954) 1612–1627.

R. Eden, P. Landshoff, D. Olive, and J. Polkinghorne, *The Analytic S-Matrix.* Cambridge University Press, 1966.

[13] O. Catà and V. Mateu, "Chiral Perturbation Theory with tensor sources," *JHEP* **09** (2007) 078, `arXiv:0705.2948 [hep-ph]`.

[14] W. Zimmermann, "Lectures on elementary particles and qft," in *1970 Brandeis Summer Institute in Theor. Phys.* MIT Press, 1971. p.396 (Secs. 1.1, 4.1, 4.2).

W. Zimmermann, "Normal products and the short distance expansion in the perturbation theory of renormalizable interactions," *Ann. Phys.* **77** (1973) 570–601.

[15] S. L. Adler, "Some simple vacuum polarization phenomenology: $e^+e^- \rightarrow$ hadrons: The μ-mesic atom x-ray discrepancy and (g-2) of the muon," *Phys. Rev.* **D10** (1974) 3714.

A. De Rujula and H. Georgi, "Counting Quarks in e+ e- Annihilation," *Phys. Rev.* **D13** (1976) 1296–1301.

R. Shankar, "Determination of the Quark-Gluon Coupling Constant," *Phys. Rev.* **D15** (1977) 755–758.

R. M. Barnett, M. Dine, and L. D. McLerran, "The problem of R in e^+e^- annihilation," *Phys. Rev.* **D22** (1980) 594.

[16] E. C. Poggio, H. R. Quinn, and S. Weinberg, "Smearing the Quark Model," *Phys. Rev.* **D13** (1976) 1958.

[17] M. A. Shifman, "Snapshots of hadrons," *Prog. Theor. Phys. Suppl.* **131** (1998) 1, `arXiv:hep-ph/9802214`.

M. A. Shifman, "Quark-hadron duality," `arXiv:hep-ph/0009131`.

[18] S. Ciulli, C. Pomponiu, and I. Sabba-Stefanescu, "Analytic extrapolation techniques and stability problems in dispersion relation theory," *Phys. Rept.* **17** (1975) no. 4, 133 – 224.

G. Auberson, M. B. Causse, and G. Mennessier, "A new method for QCD sum rules: the L (infinity) norm approach,". PM-89-18.

P. Kolar, "On the local duality in QCD,". BUTP-91-39-BERN.

[19] B. Chibisov, R. D. Dikeman, M. A. Shifman, and N. Uraltsev, "Operator product expansion, heavy quarks, QCD duality and its violations," *Int. J. Mod. Phys.* **A12** (1997) 2075–2133, `arXiv:hep-ph/9605465`.

[20] B. Blok, M. A. Shifman, and D.-X. Zhang, "An illustrative example of how quark-hadron duality might work," *Phys. Rev.* **D57** (1998) 2691–2700, `arXiv:hep-ph/9709333`.

[21] O. Catà, M. Golterman, and S. Peris, "Duality violations and spectral sum rules," *JHEP* **08** (2005) 076, `arXiv:hep-ph/0506004`.

[22] M. González-Alonso, "Estimación de los condensados de QCD del correlador V-A de quarks ligeros," *València Univ. Master Thesis (2007)* .

[23] O. Catà, M. Golterman, and S. Peris, "Possible duality violations in tau decay and their impact on the determination of α_s," *Phys. Rev.* **D79** (2009) 053002, `arXiv:0812.2285 [hep-ph]`.

O. Catà, M. Golterman, and S. Peris, "Unraveling duality violation in hadronic τ decays," *Phys. Rev.* **D77** (2008) 093006, `arXiv:0803.0246 [hep-ph]`.

[24] O. Catà, M. Golterman, and S. Peris, "Contribution from Duality Violations to the theoretical error on α_s," `arXiv:0904.4443 [hep-ph]`.

[25] M. González-Alonso, A. Pich, and J. Prades, "Violation of Quark-Hadron Duality and Spectral Chiral Moments in QCD," *Phys. Rev.* **D81** (2010) 074007, `arXiv:1001.2269 [hep-ph]`.

[26] M. Gonzalez-Alonso, A. Pich, and J. Prades, "Pinched weights and Duality Violation in QCD Sum Rules: a critical analysis," `arXiv:1004.4987 [hep-ph]`.

[27] S. Weinberg, "Precise relations between the spectra of vector and axial vector mesons," *Phys. Rev. Lett.* **18** (1967) 507–509.

[28] E. G. Floratos, S. Narison, and E. de Rafael, "Spectral Function Sum Rules in QCD. 1. Charged Currents Sector," *Nucl. Phys.* **B155** (1979) 115.

[29] F. Le Diberder and A. Pich, "The perturbative QCD prediction to R(tau) revisited," *Phys. Lett.* **B286** (1992) 147–152.

F. Le Diberder and A. Pich, "Testing QCD with tau decays," *Phys. Lett.* **B289** (1992) 165–175.

[30] V. Cirigliano, J. F. Donoghue, E. Golowich, and K. Maltman, "Improved determination of the electroweak penguin contribution to ϵ'/ϵ in the chiral limit," *Phys. Lett.* **B555** (2003) 71–82, `arXiv:hep-ph/0211420`.

[31] V. Cirigliano, E. Golowich, and K. Maltman, "QCD condensates for the light quark V-A correlator," *Phys. Rev.* **D68** (2003) 054013, `arXiv:hep-ph/0305118`.

[32] C. A. Domínguez and K. Schilcher, "Finite energy chiral sum rules in QCD," *Phys. Lett.* **B581** (2004) 193–198, `arXiv:hep-ph/0309285`.

C. A. Domínguez and K. Schilcher, "Chiral sum rules and duality in QCD," *Phys. Lett.* **B448** (1999) 93–98, `arXiv:hep-ph/9811261`.

[33] J. Bordes, C. A. Domínguez, J. Peñarrocha, and K. Schilcher, "Chiral condensates from tau decay: A critical reappraisal," *JHEP* **02** (2006) 037, `arXiv:hep-ph/0511293`.

[34] K. Maltman and T. Yavin, "$\alpha_s(M_Z)$ from hadronic tau decays," *Phys. Rev.* **D78** (2008) 094020, `arXiv:0807.0650 [hep-ph]`.

[35] K. Maltman *et al.*, "Status of the Hadronic Tau Determination of V_{us}," *Int. J. Mod. Phys.* **A23** (2008) 3191–3195, `arXiv:0807.3195 [hep-ph]`.

[36] G. D'Agostini, "On the use of the covariance matrix to fit correlated data," *Nucl. Instrum. Meth.* **A346** (1994) 306–311.

[37] S. Narison, "V-A hadronic tau decays: A laboratory for the QCD vacuum," *Phys. Lett.* **B624** (2005) 223–232, `arXiv:hep-ph/0412152`.

[38] B. L. Ioffe and K. N. Zyablyuk, "The V-A sum rules and the operator product expansion in complex q^2-plane from tau decay data," *Nucl. Phys.* **A687** (2001) 437–453, `arXiv:hep-ph/0010089`.

K. N. Zyablyuk, "V - A sum rules with D = 10 operators," *Eur. Phys. J.* **C38** (2004) 215–223, `arXiv:hep-ph/0404230`.

[39] R. A. Bertlmann, G. Launer, and E. de Rafael, "Gaussian Sum Rules in Quantum Chromodynamics and Local Duality," *Nucl. Phys.* **B250** (1985) 61.

[40] R. A. Bertlmann, C. A. Dominguez, M. Loewe, M. Perrottet, and E. de Rafael, "Determination of the Gluon Condensate and the Four Quark Condensate via FESR," *Z. Phys.* **C39** (1988) 231.

[41] J. Bijnens, E. Gámiz, and J. Prades, "Matching the electroweak penguins Q_7, Q_8 and spectral correlators," *JHEP* **10** (2001) 009, `arXiv:hep-ph/0108240`.

[42] **ALEPH** Collaboration, R. Barate *et al.*, "Measurement of the spectral functions of axial-vector hadronic tau decays and determination of $\alpha_S(M_\tau^2)$," *Eur. Phys. J.* **C4** (1998) 409–431.

[43] **ALEPH** Collaboration, R. Barate *et al.*, "Measurement of the spectral functions of vector current hadronic tau decays," *Z. Phys.* **C76** (1997) 15–33.

[44] **OPAL** Collaboration, K. Ackerstaff *et al.*, "Measurement of the strong coupling constant α_s and the vector and axial-vector spectral functions in hadronic τ decays," *Eur. Phys. J.* **C7** (1999) 571–593, `arXiv:hep-ex/9808019`.

[45] **CLEO** Collaboration, T. Coan *et al.*, "Measurement of α_S from tau decays," *Phys. Lett.* **B356** (1995) 580–588.

BABAR Collaboration, B. Aubert *et al.*, "Measurement of the $\tau^- \rightarrow K^-\pi^0\nu_\tau$ branching fraction," *Phys. Rev.* **D76** (2007) 051104, `arXiv:0707.2922 [hep-ex]`.

Belle Collaboration, K. Inami *et al.*, "First observation of the decay $\tau^- \rightarrow \phi K^-\nu/\tau$," *Phys. Lett.* **B643** (2006) 5–10, `arXiv:hep-ex/0609018`.

Belle Collaboration, M. Fujikawa *et al.*, "High-Statistics Study of the $\tau^- \rightarrow \pi^-\pi^0\nu_\tau$ Decay," *Phys. Rev.* **D78** (2008) 072006, `arXiv:0805.3773 [hep-ex]`.

[46] **BABAR** Collaboration, B. Aubert *et al.*, "Exclusive BR measurements of semileptonic tau decays into three charged hadrons, $\tau^- \rightarrow \phi\pi^-\nu_\tau$ and $\tau^- \rightarrow \phi K^-\nu_\tau$," *Phys. Rev. Lett.* **100** (2008) 011801, `arXiv:0707.2981 [hep-ex]`.

Belle Collaboration, D. Epifanov *et al.*, "Study of $\tau \rightarrow K_S\pi^-\nu_\tau$ decay at Belle," *Phys. Lett.* **B654** (2007) 65–73, `arXiv:0706.2231 [hep-ex]`.

S. Banerjee, "Measurement of $|V_{us}|$ using hadronic tau decays from BaBar & Belle," *PoS* **KAON** (2008) 009, `arXiv:0707.3058 [hep-ex]`.

[47] E. Braaten, "QCD Predictions for the Decay of the tau Lepton," *Phys. Rev. Lett.* **60** (1988) 1606–1609.

E. Braaten, "The Perturbative QCD Corrections to the Ratio R for tau Decay," *Phys. Rev.* **D39** (1989) 1458.

S. Narison and A. Pich, "QCD Formulation of the tau Decay and Determination of Lambda (MS)," *Phys. Lett.* **B211** (1988) 183.

[48] M. Davier, A. Hocker, and Z. Zhang, "The physics of hadronic tau decays," *Rev. Mod. Phys.* **78** (2006) 1043–1109, `arXiv:hep-ph/0507078`.

[49] A. Pich, "Tau physics: theory overview," *Nucl.Phys.Proc.Suppl.* **181-182** (2008) 300, `arXiv:0806.2793 [hep-ph]`.

[50] M. Davier *et al.*, "The Determination of α_s from τ Decays Revisited," *Eur. Phys. J.* **C56** (2008) 305–322, `arXiv:0803.0979 [hep-ph]`.

[51] E. Gámiz *et al.*, "Theoretical progress on the V_{us} determination from tau decays," *PoS* **KAON** (2008) 008, `arXiv:0709.0282 [hep-ph]`.

[52] J. F. Donoghue and E. Golowich, "Chiral sum rules and their phenomenology," *Phys. Rev.* **D49** (1994) 1513–1525, `arXiv:hep-ph/9307262`.

[53] M. Davier, L. Girlanda, A. Hocker, and J. Stern, "Finite energy chiral sum rules and tau spectral functions," *Phys. Rev.* **D58** (1998) 096014, `arXiv:hep-ph/9802447`.

[54] S. Narison, "New QCD-estimate of the kaon penguin matrix elements and ϵ'/ϵ," *Nucl. Phys.* **B593** (2001) 3–30, `arXiv:hep-ph/0004247`.

[55] J. F. Donoghue and E. Golowich, "Dispersive calculation of $B_7^{(3/2)}$ and $B_8^{(3/2)}$ in the chiral limit," *Phys. Lett.* **B478** (2000) 172–184, `arXiv:hep-ph/9911309`.

[56] M. Knecht, S. Peris, and E. de Rafael, "A critical reassessment of Q_7 and Q_8 matrix elements," *Phys. Lett.* **B508** (2001) 117–126, `arXiv:hep-ph/0102017`.

[57] V. Cirigliano, J. F. Donoghue, E. Golowich, and K. Maltman, "Determination of $\langle(\pi\pi)(I = 2)|Q_{7,8}|K^0\rangle$ in the chiral limit," *Phys. Lett.* **B522** (2001) 245–256, `arXiv:hep-ph/0109113`.

[58] S. Weinberg, "Phenomenological Lagrangians," *Physica* **A96** (1979) 327.

[59] J. Gasser and H. Leutwyler, "Chiral Perturbation Theory to One Loop," *Ann. Phys.* **158** (1984) 142.

[60] J. Gasser and H. Leutwyler, "Chiral Perturbation Theory: Expansions in the Mass of the Strange Quark," *Nucl. Phys.* **B250** (1985) 465.

[61] M. Knecht and E. de Rafael, "Patterns of spontaneous chiral symmetry breaking in the large N(c) limit of QCD-like theories," *Phys. Lett.* **B424** (1998) 335–342, `arXiv:hep-ph/9712457`.

[62] M. Knecht and A. Nyffeler, "Resonance estimates of O(p^6) low-energy constants and QCD short-distance constraints," *Eur. Phys. J.* **C21** (2001) 659–678, `arXiv:hep-ph/0106034`.

[63] V. Cirigliano *et al.*, "Towards a consistent estimate of the chiral low-energy constants," *Nucl. Phys.* **B753** (2006) 139–177, `arXiv:hep-ph/0603205`.

[64] V. Cirigliano, G. Ecker, M. Eidemuller, A. Pich, and J. Portoles, "The Green function in the resonance region," *Phys. Lett.* **B596** (2004) 96–106, `arXiv:hep-ph/0404004`.

[65] V. Cirigliano *et al.*, "The Green function and SU(3) breaking in K(l3) decays," *JHEP* **04** (2005) 006, `arXiv:hep-ph/0503108`.

[66] K. Kampf and B. Moussallam, "Tests of the naturalness of the coupling constants in ChPT at order p^6," *Eur. Phys. J.* **C47** (2006) 723–736, `arXiv:hep-ph/0604125`.

[67] S. Durr and J. Kambor, "Two-point function of strangeness-carrying vector-currents in two-loop chiral perturbation theory," *Phys. Rev.* **D61** (2000) 114025, `arXiv:hep-ph/9907539`.

[68] P. Masjuan and S. Peris, "A Rational Approach to Resonance Saturation in large-Nc QCD," *JHEP* **05** (2007) 040, `arXiv:0704.1247 [hep-ph]`.

[69] P. Masjuan and S. Peris, "A rational approximation to <VV-AA> and its O(p^6) low-energy constant," *Phys. Lett.* **B663** (2008) 61–65, `arXiv:0801.3558 [hep-ph]`.

[70] A. Pich, I. Rosell, and J. J. Sanz-Cillero, "Form-factors and current correlators: chiral couplings $L_{10}(\mu)$ and $C_{87}(\mu)$ at NLO in 1/N(C)," *JHEP* **07** (2008) 014, `arXiv:0803.1567 [hep-ph]`.

[71] M. Jamin, J. A. Oller, and A. Pich, "Order p^6 chiral couplings from the scalar $K\pi$ form-factor," *JHEP* **02** (2004) 047, `arXiv:hep-ph/0401080`.

[72] R. Unterdorfer and H. Pichl, "On the Radiative Pion Decay," *Eur. Phys. J.* **C55** (2008) 273–283, `arXiv:0801.2482 [hep-ph]`.

[73] J. Bijnens and P. Talavera, "$\pi \rightarrow l\nu\gamma$ form factors at two-loop," *Nucl. Phys.* **B489** (1997) 387–404, `arXiv:hep-ph/9610269`.

[74] J. Bijnens and P. Talavera, "Pion and kaon electromagnetic form factors," *JHEP* **03** (2002) 046, `arXiv:hep-ph/0203049`.

[75] J. Bijnens, G. Colangelo, and P. Talavera, "The vector and scalar form factors of the pion to 2 loops," *JHEP* **05** (1998) 014, `arXiv:hep-ph/9805389`.

[76] A. Pich, "Colourless mesons in a polychromatic world," `arXiv:hep-ph/0205030`.

[77] B. Moussallam, "A sum rule approach to the violation of Dashen's theorem," *Nucl. Phys.* **B504** (1997) 381–414, `arXiv:hep-ph/9701400`.

P. D. Ruiz-Femenia, A. Pich, and J. Portoles, "Odd-intrinsic-parity processes within the resonance effective theory of QCD," *JHEP* **07** (2003) 003, `arXiv:hep-ph/0306157`.

J. Bijnens, E. Gamiz, E. Lipartia, and J. Prades, "QCD short-distance constraints and hadronic approximations," *JHEP* **04** (2003) 055, `arXiv:hep-ph/0304222`.

I. Rosell, J. J. Sanz-Cillero, and A. Pich, "Towards a determination of the chiral couplings at NLO in $1/N_c$: $L_8^r(\mu)$," *JHEP* **01** (2007) 039, `arXiv:hep-ph/0610290`.

[78] M. González-Alonso, A. Pich, and J. Prades, "Determination of the Chiral Couplings L_{10} and C_{87} from Semileptonic Tau Decays," *Phys. Rev.* **D78** (2008) 116012, `arXiv:0810.0760 [hep-ph]`.

[79] M. González-Alonso, A. Pich, and J. Prades, "From hadronic tau decays to the chiral couplings L_{10} and C_{87}," *Nucl. Phys. Proc. Suppl.* **189** (2009) 90–95, `arXiv:0812.1943 [hep-ph]`.

M. González-Alonso, A. Pich, and J. Prades, "Chiral low-energy constants L_{10} and C_{87} from hadronic tau decays," *Nucl. Phys. Proc. Suppl.* **186** (2009) 171–174, `arXiv:0810.2459 [hep-ph]`.

M. González-Alonso, A. Pich, and J. Prades, "Chiral low-energy constants from tau data," `arXiv:0910.2264 [hep-ph]`.

[80] J. F. Donoghue and B. R. Holstein, "Components of a chiral coefficient," *Phys. Rev.* **D46** (1992) 4076–4081.

[81] G. Ecker, "Chiral perturbation theory," *Prog. Part. Nucl. Phys.* **35** (1995) 1–80, `arXiv:hep-ph/9501357`.

A. Pich, "Chiral perturbation theory," *Rept. Prog. Phys.* **58** (1995) 563–610, `arXiv:hep-ph/9502366`.

S. Scherer and M. R. Schindler, "A chiral perturbation theory primer," `arXiv:hep-ph/0505265`.

[82] S. Coleman, "The invariance of the vacuum is the invariance of the world," *Journal of Mathematical Physics* **7** (1966) no. 5, 787–787.

[83] J. Goldstone, "Field Theories with Superconductor Solutions," *Nuovo Cim.* **19** (1961) 154–164.

J. Goldstone, A. Salam, and S. Weinberg, "Broken Symmetries," *Phys. Rev.* **127** (1962) 965–970.

[84] H. W. Fearing and S. Scherer, "Extension of the ChPT meson Lagrangian to order p^6," *Phys. Rev.* **D53** (1996) 315–348, `arXiv:hep-ph/9408346`.

[85] J. Bijnens, G. Colangelo, and G. Ecker, "The mesonic chiral Lagrangian of order p^6," *JHEP* **02** (1999) 020, `arXiv:hep-ph/9902437`.

[86] J. Bijnens, G. Colangelo, and G. Ecker, "Renormalization of ChPT to order p^6," *Annals Phys.* **280** (2000) 100–139, `arXiv:hep-ph/9907333`.

[87] T. Ebertshauser, H. W. Fearing, and S. Scherer, "The anomalous ChPT meson Lagrangian to order p^6 revisited," *Phys. Rev.* **D65** (2002) 054033, `arXiv:hep-ph/0110261`.

J. Bijnens, L. Girlanda, and P. Talavera, "The anomalous chiral Lagrangian of order p^6," *Eur. Phys. J.* **C23** (2002) 539–544, `arXiv:hep-ph/0110400`.

[88] G. Ecker, "Chiral low-energy constants," *Acta Phys. Polon.* **B38** (2007) 2753–2762, `arXiv:hep-ph/0702263`.

[89] G. Amoros, J. Bijnens, and P. Talavera, "Two-point functions at two loops in three flavour ChPT," *Nucl. Phys.* **B568** (2000) 319–363, `arXiv:hep-ph/9907264`.

[90] G. 't Hooft, "A planar diagram theory for strong interactions," *Nucl. Phys.* **B72** (1974) 461.

[91] J. Gasser, C. Haefeli, M. A. Ivanov, and M. Schmid, "Integrating out strange quarks in ChPT," *Phys. Lett.* **B652** (2007) 21–26, arXiv:0706.0955 [hep-ph].

[92] J. Gasser, C. Haefeli, M. A. Ivanov, and M. Schmid, "Integrating out strange quarks in ChPT: terms at order p^6," *Phys. Lett.* **B675** (2009) 49–53, arXiv:0903.0801 [hep-ph].

[93] **ARGUS** Collaboration, H. Albrecht *et al.*, "Measurement of tau Decays Into Three Charged Pions," *Z. Phys.* **C33** (1986) 7.

[94] J. M. Yelton *et al.*, "Measurement of the branching fractions $\tau^- \to \rho^- \nu_\tau$ and $\tau^- \to K^{*-} \nu_\tau$," *Phys. Rev. Lett.* **56** (1986) 812.

[95] G. Ecker, J. Gasser, A. Pich, and E. de Rafael, "The Role of Resonances in Chiral Perturbation Theory," *Nucl. Phys.* **B321** (1989) 311.

G. Ecker *et al.*, "Chiral Lagrangians for Massive Spin 1 Fields," *Phys. Lett.* **B223** (1989) 425.

[96] **JLQCD** Collaboration, E. Shintani *et al.*, "S-parameter and pseudo-Nambu-Goldstone boson mass from lattice QCD," *Phys. Rev. Lett.* **101** (2008) 242001, arXiv:0806.4222 [hep-lat].

[97] **RBC** Collaboration, P. A. Boyle, L. Del Debbio, J. Wennekers, and J. M. Zanotti, "The S Parameter in QCD from Domain Wall Fermions," *Phys. Rev.* **D81** (2010) 014504, arXiv:0909.4931 [Unknown].

[98] R. Frezzotti, V. Lubicz, and S. Simula, "Electromagnetic form factor of the pion from twisted-mass lattice QCD at Nf=2," *Phys. Rev.* **D79** (2009) 074506, arXiv:0812.4042 [hep-lat].

[99] **JLQCD** Collaboration, S. Aoki *et al.*, "Pion form factors from two-flavor lattice QCD with exact chiral symmetry," *Phys. Rev.* **D80** (2009) 034508, arXiv:0905.2465 [hep-lat].

[100] M. E. Peskin and T. Takeuchi, "A New constraint on a strongly interacting Higgs sector," *Phys. Rev. Lett.* **65** (1990) 964–967.

M. E. Peskin and T. Takeuchi, "Estimation of oblique electroweak corrections," *Phys. Rev.* **D46** (1992) 381–409.

[101] J. A. Bagger, A. F. Falk, and M. Swartz, "Precision observables and electroweak theories," *Phys. Rev. Lett.* **84** (2000) 1385–1388, arXiv:hep-ph/9908327.

[102] S. Dutta, K. Hagiwara, Q.-S. Yan, and K. Yoshida, "Constraints on the electroweak chiral Lagrangian from the precision data," *Nucl. Phys.* **B790** (2008) 111–137, `arXiv:0705.2277 [hep-ph]`.

[103] S. Ciulli, C. Sebu, K. Schilcher, and H. Spiesberger, "QCD condensates from tau decay data: A functional approach," *Phys. Lett.* **B595** (2004) 359–367, `arXiv:hep-ph/0312212`.

[104] J. Rojo and J. I. Latorre, "Neural network parametrization of spectral functions from hadronic tau decays and determination of QCD vacuum condensates," *JHEP* **01** (2004) 055, `arXiv:hep-ph/0401047`.

[105] T. Das *et al.*, "Electromagnetic mass difference of pions," *Phys. Rev. Lett.* **18** (1967) 759–761.

[106] **MILC** Collaboration, A. Bazavov *et al.*, "MILC results for light pseudoscalars," *PoS* **CD09** (2009) 007, `arXiv:0910.2966 [Unknown]`.

[107] J. Bijnens, "ChPT in the meson sector," `arXiv:0909.4635 [hep-ph]`.

[108] E. Witten, "Some Inequalities Among Hadron Masses," *Phys. Rev. Lett.* **51** (1983) 2351.

[109] A. A. Almasy, K. Schilcher, and H. Spiesberger, "QCD condensates of dimension D = 6 and D = 8 from hadronic tau decays," *Phys. Lett.* **B650** (2007) 179–184, `arXiv:hep-ph/0612304`.

[110] B. L. Ioffe, "QCD at low energies," *Prog. Part. Nucl. Phys.* **56** (2006) 232–277, `arXiv:hep-ph/0502148`.

[111] A. A. Almasy, K. Schilcher, and H. Spiesberger, "Determination of QCD condensates from tau-decay data," *Eur. Phys. J.* **C55** (2008) 237–248, `arXiv:0802.0980 [hep-ph]`.

[112] S. Peris, B. Phily, and E. de Rafael, "Tests of large-N(c) QCD from hadronic tau decay," *Phys. Rev. Lett.* **86** (2001) 14–17, `arXiv:hep-ph/0007338`.

[113] S. Friot, D. Greynat, and E. de Rafael, "Chiral condensates, Q_7 and Q_8 matrix elements and large-N_c QCD," *JHEP* **10** (2004) 043, `arXiv:hep-ph/0408281`.

[114] O. Catà, "Relations between vacuum condensates and low energy parameters from a rational approach," *Phys. Rev.* **D81** (2010) 054011, `arXiv:0911.4736 [hep-ph]`.

[115] M. González-Alonso, A. Pich, and J. Prades. In preparation.

[116] C. N. Leung, S. T. Love, and S. Rao, "Low-Energy Manifestations of a New Interaction Scale: Operator Analysis," *Z. Phys.* **C31** (1986) 433.

[117] W. Buchmuller and D. Wyler, "Effective Lagrangian Analysis of New Interactions and Flavor Conservation," *Nucl. Phys.* **B268** (1986) 621.

[118] T. Appelquist and G.-H. Wu, "The EW chiral Lagrangian and new precision measurements," *Phys. Rev.* **D48** (1993) 3235–3241, `arXiv:hep-ph/9304240`.

A. C. Longhitano, "Heavy Higgs Bosons in the Weinberg-Salam Model," *Phys. Rev.* **D22** (1980) 1166.

F. Feruglio, "The Chiral approach to the electroweak interactions," *Int. J. Mod. Phys.* **A8** (1993) 4937–4972, `arXiv:hep-ph/9301281`.

J. Wudka, "Electroweak effective Lagrangians," *Int. J. Mod. Phys.* **A9** (1994) 2301–2362, `arXiv:hep-ph/9406205`.

[119] M. González-Alonso, G. Isidori, and J. F. Kamenik. In preparation.

[120] A. de Gouvea and J. Jenkins, "A survey of lepton number violation via eff. operators," *Phys. Rev.* **D77** (2008) 013008, `arXiv:0708.1344 [hep-ph]`.

[121] C. P. Burgess and J. A. Robinson, "Effective Lagrangians and CP violation from new physics,". Summer Study on CP Violation, Upton, N.Y., 1990.

[122] M. A. Abolins *et al.*, "Testing the Compositeness of Quarks and Leptons,". Proceedings of the 1982 DPF Summer Study on Elementary Particle Physics and Future Facilities, 28 June-16 July, 1982, Snowmass, Colorado.

[123] C. J. C. Burges and H. J. Schnitzer, "Vitual effects of excited quarks as probes of a possible new hadronic mass scale," *Nucl. Phys.* **B228** (1983) 464.

[124] Z. Han and W. Skiba, "Effective theory analysis of precision electroweak data," *Phys. Rev.* **D71** (2005) 075009, `arXiv:hep-ph/0412166`.

[125] V. Cirigliano, J. Jenkins, and M. González-Alonso, "Semileptonic decays of light quarks beyond the Standard Model," *Nucl. Phys.* **B830** (2010) 95–115, `arXiv:0908.1754 [hep-ph]`.

M. González-Alonso, "New Physics bounds from the combination of CKM-unitarity and high-energy data," *Acta Phys. Polon. Proc. Suppl.* (2010) , `arXiv:0910.3710 [hep-ph]`.

[126] R. S. Chivukula and H. Georgi, "Composite Technicolor Standard Model," *Phys. Lett.* **B188** (1987) 99.

L. J. Hall and L. Randall, "Weak scale effective supersymmetry," *Phys. Rev. Lett.* **65** (1990) 2939–2942.

A. J. Buras, P. Gambino, M. Gorbahn, S. Jager, and L. Silvestrini, "Universal unitarity triangle and physics beyond the standard model," *Phys. Lett.* **B500** (2001) 161–167, `arXiv:hep-ph/0007085`.

G. D'Ambrosio, G. F. Giudice, G. Isidori, and A. Strumia, "Minimal flavour violation: An effective field theory approach," *Nucl. Phys.* **B645** (2002) 155–187, `arXiv:hep-ph/0207036`.

[127] V. Cirigliano, B. Grinstein, G. Isidori, and M. B. Wise, "Minimal flavor violation in the lepton sector," *Nucl. Phys.* **B728** (2005) 121–134, `arXiv:hep-ph/0507001`.

[128] Z. Maki, M. Nakagawa, and S. Sakata, "Remarks on the unified model of elementary particles," *Prog. Theor. Phys.* **28** (1962) 870–880.

[129] **Particle Data Group** Collaboration, C. Amsler *et al.*, "Review of particle physics," *Phys. Lett.* **B667** (2008) 1.

[130] N. Cabibbo, "Unitary Symmetry and Leptonic Decays," *Phys. Rev. Lett.* **10** (1963) 531–533.

M. Kobayashi and T. Maskawa, "CP Violation in the Renormalizable Theory of Weak Interaction," *Prog. Theor. Phys.* **49** (1973) 652–657.

[131] R. Barbieri, C. Bouchiat, A. Georges, and P. Le Doussal, "Quark-lepton nonuniversality in Supersymmetric models," *Phys. Lett.* **B156** (1985) 348.

W. J. Marciano and A. Sirlin, "Constraint on additional neutral gauge bosons from electroweak radiative corrections," *Phys. Rev.* **D35** (1987) 1672–1676.

K. Hagiwara, S. Matsumoto, and Y. Yamada, "Supersymmetric contribution to the quark - lepton universality violation in charged currents," *Phys. Rev. Lett.* **75** (1995) 3605–3608, `arXiv:hep-ph/9507419`.

A. Kurylov and M. J. Ramsey-Musolf, "Charged current universality in the MSSM," *Phys. Rev. Lett.* **88** (2002) 071804, `arXiv:hep-ph/0109222`.

W. J. Marciano, "Implications of CKM unitarity," *PoS* **KAON** (2008) 003.

[132] **FlaviaNet Working Group on Kaon Decays** Collaboration, M. Antonelli *et al.*, "Precision tests of the Standard Model with leptonic and semileptonic kaon decays," `arXiv:0801.1817 [hep-ph]`.

[133] A. Filipuzzi and G. Isidori, "Violations of lepton-flavour universality in $P \rightarrow l\nu$ decays: a model-independent analysis," *Eur. Phys. J.* **C64** (2009) 55–62, `arXiv:0906.3024 [hep-ph]`.

[134] P. Herczeg, "Beta decay beyond the standard model," *Prog. Part. Nucl. Phys.* **46** (2001) 413–457.

[135] N. Severijns, M. Beck, and O. Naviliat-Cuncic, "Tests of the standard electroweak model in beta decay," *Rev. Mod. Phys.* **78** (2006) 991–1040, `arXiv:nucl-ex/0605029`.

[136] R. E. Behrends and A. Sirlin, "Effect of mass splittings on the conserved vector current," *Phys. Rev. Lett.* **4** (1960) 186–187.

M. Ademollo and R. Gatto, "Nonrenormalization Theorem for the Strangeness Violating Vector Currents," *Phys. Rev. Lett.* **13** (1964) 264–265.

[137] W. J. Marciano and A. Sirlin, "Radiative Corrections to beta Decay and the Possibility of a Fourth Generation," *Phys. Rev. Lett.* **56** (1986) 22.

V. Cirigliano *et al.*, "Radiative corrections to K_{l3} decays," *Eur. Phys. J.* **C23** (2002) 121–133, `arXiv:hep-ph/0110153`.

V. Cirigliano, H. Neufeld, and H. Pichl, "K_{e3} decays and CKM unitarity," *Eur. Phys. J.* **C35** (2004) 53–65, `arXiv:hep-ph/0401173`.

V. Cirigliano, M. Giannotti, and H. Neufeld, "Electromagnetic effects in Kl3 decays," *JHEP* **11** (2008) 006, `arXiv:0807.4507 [hep-ph]`.

[138] W. J. Marciano and A. Sirlin, "Improved calculation of electroweak radiative corrections and the value of $V_u d$," *Phys. Rev. Lett.* **96** (2006) 032002, `arXiv:hep-ph/0510099`.

[139] J. C. Hardy and I. S. Towner, "Superallowed 0+ to 0+ nuclear beta decays: A new survey with precision tests of the CVC hypothesis and the standard model," *Phys. Rev.* **C79** (2009) 055502, `arXiv:0812.1202 [nucl-ex]`.

[140] H. Leutwyler and M. Roos, "Determination of the Elements V(us) and V(ud) of the Kobayashi-Maskawa Matrix," *Z. Phys.* **C25** (1984) 91.

[141] J. Bijnens and P. Talavera, "K(l3) decays in chiral perturbation theory," *Nucl. Phys.* **B669** (2003) 341–362, `arXiv:hep-ph/0303103`.

[142] D. Becirevic *et al.*, "The $K \to \pi$ vector form factor at zero momentum transfer on the lattice," *Nucl. Phys.* **B705** (2005) 339–362, `arXiv:hep-ph/0403217`.

C. Dawson *et al.*, "Vector form factor in K_{l3} semileptonic decay with two flavors of dynamical domain-wall quarks," *Phys. Rev.* **D74** (2006) 114502, `arXiv:hep-ph/0607162`.

ETM Collaboration, V. Lubicz, F. Mescia, S. Simula, and C. Tarantino, "$K \to \pi\ell\nu$ Semileptonic Form Factors from Two-Flavor Lattice QCD," *Phys. Rev.* **D80** (2009) 111502, `arXiv:0906.4728 [hep-lat]`.

[143] P. A. Boyle *et al.*, "Kl3 semileptonic form factor from 2+1 flavour lattice QCD," *Phys. Rev. Lett.* **100** (2008) 141601, `arXiv:0710.5136 [hep-lat]`.

[144] N. Cabibbo, E. C. Swallow, and R. Winston, "Semileptonic hyperon decays," *Ann. Rev. Nucl. Part. Sci.* **53** (2003) 39–75, `arXiv:hep-ph/0307298`.

R. Flores-Mendieta, "V(us) from hyperon semileptonic decays," *Phys. Rev.* **D70** (2004) 114036, `arXiv:hep-ph/0410171`.

V. Mateu and A. Pich, "V(us) determination from hyperon semileptonic decays," *JHEP* **10** (2005) 041, `arXiv:hep-ph/0509045`.

[145] **MILC** Collaboration, C. Aubin *et al.*, "Light pseudoscalar decay constants, quark masses, and low energy constants from three-flavor lattice QCD," *Phys. Rev.* **D70** (2004) 114501, `arXiv:hep-lat/0407028`.

S. R. Beane, P. F. Bedaque, K. Orginos, and M. J. Savage, "f_K/f_π in Full QCD with Domain Wall Valence Quarks," *Phys. Rev.* **D75** (2007) 094501, `arXiv:hep-lat/0606023`.

B. Blossier *et al.*, "Pseudoscalar decay constants of kaon and D-mesons from Nf=2 twisted mass Lattice QCD," `arXiv:0904.0954 [hep-lat]`.

A. Bazavov *et al.*, "Full nonperturbative QCD simulations with 2+1 flavors of improved staggered quarks," `arXiv:0903.3598 [hep-lat]`.

[146] **HPQCD** Collaboration, E. Follana *et al.*, "High precision determination of the π, K, D and D_s decay constants from lattice QCD," *Phys. Rev. Lett.* **100** (2008) 062002, `arXiv:0706.1726 [hep-lat]`.

[147] W. J. Marciano, "Precise determination of $|V_{us}|$ from lattice calculations of pseudoscalar decay constants," *Phys. Rev. Lett.* **93** (2004) 231803, `arXiv:hep-ph/0402299`.

[148] R. Barbieri and A. Strumia, "What is the limit on the Higgs mass?," *Phys. Lett.* **B462** (1999) 144–149, `arXiv:hep-ph/9905281`.

[149] C. S. Wood *et al.*, "Measurement of parity nonconservation and an anapole moment in cesium," *Science* **275** (1997) 1759–1763.

[150] P. A. Vetter *et al.*, "Precise test of EW theory from a new measurement of parity nonconservation in atomic Tl," *Phys. Rev. Lett.* **74** (1995) 2658–2661.

[151] **NuTeV** Collaboration, G. P. Zeller *et al.*, "A precise determination of electroweak parameters in neutrino nucleon scattering," *Phys. Rev. Lett.* **88** (2002) 091802, `arXiv:hep-ex/0110059`.

[152] A. Blondel *et al.*, "Electroweak parameters from a high statistics neutrino nucleon scattering experiment," *Z. Phys.* **C45** (1990) 361–379.

CHARM Collaboration, J. V. Allaby *et al.*, "A Precise Determination of the Electroweak Mixing Angle from Semileptonic Neutrino Scattering," *Phys. Lett.* **B177** (1986) 446.

[153] **CCFR** Collaboration, K. S. McFarland *et al.*, "A precision measurement of electroweak parameters in neutrino nucleon scattering," *Eur. Phys. J.* **C1** (1998) 509–513, `arXiv:hep-ex/9701010`.

[154] **CHARM-II** Collaboration, P. Vilain *et al.*, "Precision measurement of electroweak parameters from the scattering of muon-neutrinos on electrons," *Phys. Lett.* **B335** (1994) 246–252.

[155] **LEP** Collaboration, Coll., "A Combination of preliminary electroweak measurements and constraints on the standard model," `arXiv:hep-ex/0312023`.

ALEPH Collaboration, Coll., "Precision electroweak measurements on the *Z* resonance," *Phys. Rept.* **427** (2006) 257, `arXiv:hep-ex/0509008`.

[156] **OPAL** Collaboration, G. Abbiendi *et al.*, "Tests of the SM and constraints on new physics from measurements of fermion pair production at 189-GeV to 209-GeV at LEP," *Eur. Phys. J.* **C33** (2004) 173–212, `arXiv:hep-ex/0309053`.

[157] **L3** Collaboration, P. Achard *et al.*, "Measurement of the cross section of W-boson pair production at LEP," *Phys. Lett.* **B600** (2004) 22–40, `arXiv:hep-ex/0409016`.

[158] **CDF** Collaboration, V. M. Abazov *et al.*, "Combination of CDF and DØ results on *W* boson mass and width," *Phys. Rev.* **D70** (2004) 092008, `arXiv:hep-ex/0311039`.

[159] M. Antonelli *et al.*, "Flavor Physics in the Quark Sector," `arXiv:0907.5386 [hep-ph]`.

[160] V. Cirigliano, A. Filipuzzi, and M. González-Alonso. In preparation.

[161] W. J. Marciano, "Fermi Constants and "New Physics"," *Phys. Rev.* **D60** (1999) 093006, `arXiv:hep-ph/9903451`.

J. Erler and P. Langacker, "Electroweak model and constraints on new physics," *Phys. Lett.* **B667** (2008) 125–144.

[162] **MuLan** Collaboration, D. B. Chitwood *et al.*, "Improved Measurement of the Positive Muon Lifetime and Determination of the Fermi Constant," *Phys. Rev. Lett.* **99** (2007) 032001, `arXiv:0704.1981 [hep-ex]`.

FAST Collaboration, A. Barczyk *et al.*, "Measurement of the Fermi constant by FAST," *Phys. Lett.* **B663** (2008) 172–180, `arXiv:0707.3904 [hep-ex]`.

[163] F. Scheck, "Muon Physics," *Phys. Rept.* **44** (1978) 187.

[164] C. Bouchiat and L. Michel, "Theory of mu-Meson Decay with the Hypothesis of Nonconservation of Parity," *Phys. Rev.* **106** (1957) 170–172.

T. Kinoshita and A. Sirlin, "Muon Decay with Parity Nonconserving Interactions and Radiative Corrections in the Two-Component Theory," *Phys. Rev.* **107** (1957) 593–599.

T. Kinoshita and A. Sirlin, "Polarization of Electrons in Muon Decay with General Parity-Nonconserving Interactions," *Phys. Rev.* **108** (1957) 844–850.

[165] L. Michel, "Interaction between four half spin particles and the decay of the mu meson," *Proc. Phys. Soc.* **A63** (1950) 514–531.

[166] A. Pich and J. P. Silva, "Constraining new interactions with leptonic τ decays," *Phys. Rev.* **D52** (1995) 4006–4018, `arXiv:hep-ph/9505327`.

[167] **TWIST** Collaboration, R. P. MacDonald *et al.*, "A Precision Measurement of the Muon Decay Parameters ρ and δ," *Phys. Rev.* **D78** (2008) 032010, `arXiv:0807.1125 [hep-ex]`.

[168] N. Danneberg *et al.*, "Muon decay: Measurement of the transverse polarization of the decay positrons and its implications for the Fermi coupling constant and time reversal invariance," *Phys. Rev. Lett.* **94** (2005) 021802.

[169] J. Portoles, "Analytical approaches to the calculation of $f^+_{K^0\pi^-}(0)$," `arXiv:hep-ph/0703093`.

[170] T. Kaneko, "Theoretical progress on V_{us} on lattice," *PoS* **KAON** (2008) 018, `arXiv:0710.0698 [hep-ph]`.

A. Juttner, "Progress in kaon physics on the lattice," *PoS* **LAT2007** (2007) 014, `arXiv:0711.1239 [hep-lat]`.

[171] **RBC and UKQCD** Collaboration, C. Allton *et al.*, "2+1 flavor domain wall QCD on a $(2fm)^3$ lattice: light meson spectroscopy with Ls = 16," *Phys. Rev.* **D76** (2007) 014504, `arXiv:hep-lat/0701013`.

[172] S. Durr *et al.*, "The ratio F_K/F_π in QCD," `arXiv:1001.4692 [Unknown]`.

[173] A. S. Kronfeld, "Non-Standard Physics in (Semi)leptonic Decays of Charmed Mesons," *PoS* **LAT2008** (2008) 282, `arXiv:0812.2030 [hep-lat]`.

[174] H. Primakoff and S. P. Rosen, "Double beta decay," *Rept. Prog. Phys.* **22** (1959) no. 1, 121–166.

[175] J. D. Jackson, S. B. Treiman, and H. W. Wyld, "Possible tests of time reversal invariance in Beta decay," *Phys. Rev.* **106** (1957) 517–521.

[176] D. H. Wilkinson, "Analysis of neutron beta decay," *Nucl. Phys.* **A377** (1982) 474–504.

S. Gardner and C. Zhang, "Sharpening low-energy, standard-model tests via correlation coefficients in neutron beta-decay," *Phys. Rev. Lett.* **86** (2001) 5666–5669, `arXiv:hep-ph/0012098`.

[177] A. Czarnecki, W. J. Marciano, and A. Sirlin, "Precision measurements and CKM unitarity," *Phys. Rev.* **D70** (2004) 093006, `arXiv:hep-ph/0406324`.

[178] H. Abele, "The neutron. Its properties and basic interactions," *Prog. Part. Nucl. Phys.* **60** (2008) 1–81.

[179] A. Serebrov *et al.*, "Measurement of the neutron lifetime using a gravitational trap and a low-temperature Fomblin coating," *Phys. Lett.* **B605** (2005) 72–78, `arXiv:nucl-ex/0408009`.

[180] M. Jamin, J. A. Oller, and A. Pich, "Scalar K pi form factor and light quark masses," *Phys. Rev.* **D74** (2006) 074009, `arXiv:hep-ph/0605095`.

[181] N. S. Craigie and J. Stern, "Sum rules for the spontaneous chiral symmetry breaking parameters of QCD," *Phys. Rev.* **D26** (1982) 2430.

Agradecimientos

Por las noches de vacío cuando te ibas a dormir
esperando que la suerte volviera a sonreír.
Amaral.

Tras casi cinco años en el IFIC y antes de dar el siguiente paso, me gustaría acordarme de todos los que me han acompañado en esta experiencia y me han ayudado a llegar hasta aquí.

Tengo que reconocer que nunca imaginé que realizar un doctorado mínimamente aceptable me fuera a costar tanto, ni tampoco que ante la dificultad me sacrificaría de la manera en que lo he hecho. Por tanto supongo que las primeras personas a las que debo nombrar en estos agradecimientos es a mis padres, que alguna culpa tendrán de que yo haya reaccionado de esta forma ante mi primer gran escollo. Gracias por la educación, la libertad y el cariño recibidos todos estos años.

Tengo que darle las gracias a Toni, por haber sido mi director de tesis, por haberme dado la oportunidad de unirme a este grupo de investigación y por apoyar mi carrera permitiéndome asistir a cursos y congresos. Gracias en particular por la atención prestada este último mes durante la redacción de esta tesis y por la eficiencia en las correcciones.

Quiero agradecerle especialmente a Jorge la ayuda prestada cada día de mi estancia en el IFIC. Por echarme una mano siempre que lo necesité, en cada detalle, en cada duda y en cada página de mi tesis. Y por sacarme de mi letargo cuando lo necesité, aunque fuera involuntariamente.

Un grazie particolare ai miei capi italiani, Vincenzo, Giancarlo e Gino, per l'ospitalità che mi hanno dimostrato e la pazienza che hanno avuto con me. Per non aver dimenticato che per affrontare un nuovo argomento è necessario tempo e un poco di aiuto. Posso dire con totale sincerità che è stato un onore e un piacere lavorare con loro.

Gracias por supuesto a los amigos del IFIC, por los buenos ratos pasados durante estos años, por tantas risas en las comidas y por esos cafés cuando uno ya no puede más. Gracias a Julia, Andreu, Diego, Paola, ... por los partidos de fútbol, por el salto en paracaídas, por el Wax y sus amigos, por aquellas tardes de Call of Duty, por las chinchetas, por los "preciosos alcantarillados verdes", por ganar una Eurocopa rodeado de italianos... Gracias a Alberto por las buenas discusiones de física en nuestro despacho, que se trasladan ahora a territorio americano.

I would like to thank the friends I have made in Los Alamos, Naples and Rome, for their hospitality and for the good moments. Thanks to Thanasis, Alex, Evsen, Celio, Enrico, Vita, Diego, ...

Y gracias a los amigos del mundo exterior. A mis queridas hermanitas, que siempre están ahí, a Mariano y Sole, a mis colegas de Murcia y a mis primos y tíos. Gracias a esos pocos profes del insti y de la uni que pusieron su granito de arena para que hoy esté yo aquí.

Gracias también al Ministerio de Ciencia e Innovación por la beca FPU. O lo que es lo mismo, gracias a esta sociedad por confiar en que el conocimiento es más barato que la ignorancia.

Y mil veces gracias a Luz María. No creo que pueda explicarse en unas pocas frases lo mucho que le agradezco todo lo que ella ha significado para mí en estos últimos cinco años. Ni tan siquiera un poco. Y prefiero no quedarme tan extremadamente corto. Ella lo sabe y a mí con eso me sobra. Nos vemos el 3 de Septiembre.

Estos años he viajado más de lo que pensé que haría en toda mi vida, pero puedo decir que ha sido un pequeño paseo comparado con lo recorrido a nivel personal. Ha sido, sin ningún tipo de dudas, el período más difícil de mi vida. Puedo decir que he hecho todo lo que ha estado en mi mano para hacer las cosas bien. Si lo he conseguido o no es una discusión más complicada. Ahora ha llegado el momento de marcharme y dar el siguiente paso.

Gracias otra vez a todos.

Valencia, 1 de Abril de 2010